Label-free proteomic analysis of *Xerophyta schlechteri* leaf tissue under dehydration stress

By

Hawwa Gabier

GBRHAW001

Thesis Presented for the Degree of
DOCTOR OF PHILOSOPHY

In the Department of Molecular and Cell Biology
UNIVERSITY OF CAPE TOWN

Supervisor:

Dr M.S. Rafudeen

Department of Molecular and Cell Biology

University of Cape Town

South Africa

Co-Supervisor:

Prof. Jill M. Farrant

Department of Molecular and Cell Biology

University of Cape Town

South Africa

August 2020

Table of Contents

Declaration

I, **Hawwa Gabier**, hereby declare that the work on which this thesis is based is my original work (except where acknowledgements indicate otherwise) and that neither the whole work nor any part of it has been, is being, or is to be submitted for another degree in this or any other university. I authorise the University to reproduce for the purpose of research either the whole or any portion of the contents in any manner whatsoever.

Signature: Signed by candidate **Date:** 27/07/2020

To my parents,

who taught me to live, love and seek knowledge.

Acknowledgements

In the name of Allah, the Most Gracious, the Most Merciful.

All praises to Allah for granting me this opportunity, the strength and support system to achieve my goals. It is a blessing to be able to achieve one's goals and an even greater blessing to have had the support and encouragement to do so, I therefore humbly take this opportunity to express my gratitude to the following people who have, in their own special way, enriched my journey.

To my supervisor, Dr Suhail Rafudeen, on my first day in the lab you asked me a very profound question; 'A PhD is a journey that can impact you mentally, physically, financially, emotionally and spiritually, are you ready?' I was taken by this question; and remembered it throughout this journey, as a source of motivation. This journey has no doubt been challenging and filled with difficulties. However, by the mercy of Allah, I overcame these challenges thanks to your supervision, patience, invaluable guidance, and constant encouragement. It has been an honour to be your student; you are always in my prayers.

To my co-supervisor, Prof Jill Farrant, you are an incredible woman who has been a constant encouragement and a wealth of knowledge. I thank you for your support and guidance. It has been an honour to be your student and you are always in my prayers.

Thank you to the Maize trust and NRF for the financial support through the years.

I wish to express my gratitude to Prof David Tabb, your guidance and invaluable input with the Proteomic data is greatly appreciated. To my friend Dr Imane Allali, I thank you for your guidance and support with the proteomic data. Dr Marlene du Preez, I thank you for being a part of my academic journey and always having an 'open door' policy for me even when I would just be venting. Thank you to the PSL lab past and present. Keren Cooper, thank you for your help and happy energy in the lab. Jean Ntuli, Thank you for your friendship and encouragement. Dr Christine Frances Madden, Chrissieeee, thank you for all your help and motivation. Dr Rizqah Kamies, thank you for your motivation, friendship and many great memories. Shakiera Sattar, thank you for your friendship and motivation always. Ali Elnaeim Elbasheir Ali, thank you for brainstorming my data with me. Dr Givemore Makonya I thank you for your encouragement and proof-reading my chapters.

Humaira Lambarey, one is lucky to find a kind and helpful person in a laboratory setting but finding friendship in that person too, is priceless. I thank you for proof-reading my chapters, your constant encouragement, motivation and friendship. The lab was not the same without you and the time spent with you will always be treasured. Amogelang Tshego Gill, thank you for your support and being an amazing friend. Your advice I will cherish always. Rudean Van Wyk, our friendship spans 'our UWC days', and true to those days I was once again able to call on you for help. Thank you for proof-reading my chapters and your encouragement. Luqmaan Rawoot, Thank you for all your support, motivation and advice over the years and for convincing me to not take legal action for knocking into my car, it was just the wind. Hendrik Els, thank you for proof-reading most of my chapters and always being there helping even before I ask. Ali Kiyaei, Sea point, UCT, Sea Point, our friendship spans many years, I thank you for your friendship and help through some challenging times and always being a source of motivation. Huda Abrahams, my travel buddy, your kind heart and warm nature is

something I treasure, you are a blessing in my life. Zaida Dalvie, our UWC days were filled with many adventures and dreams, I treasure the great memories in the lab and our coffee vent sessions, and you have been such a great support through my journey. Sana Chougle, wow, our friendship spans a lifetime, from school days through to University you have been my constant companion, confidant and motivator, you are very dear to me and I treasure your friendship. Abdul Halim Wise, I thank you for all the advice, wise words and navigating me out of some tough times. You have been a guide and inspiration to me and I am grateful to you for being a part of my life. Dr Mahjoubeh Jalali, my friendy, Firstly I miss you very much, we started the university journey together and you quickly became a very dear person to me. I thank you for all the amazing moments, the advice and care you have shown me. I treasure all the good memories and hope we are on the same continent again soon. Tasliem Omardien, I thank you for your support and friendship over the years, and treasure all the advice and support.

I thank you all for being my strength through my journey of life. Thank you for troubleshooting life with me, I am blessed to have you in my life.

Finally to my beloved family, my beloved father, Shaikh Fouad Gabier and beloved mother, Thuraya Gabier. Words cannot express my gratitude and love for you. Thank you for always standing by me, motivating me and being my strength. You have sacrificed so much for me. Through your love and guidance, I am able to face the challenges in life. To my eldest brother, Abdul Hafieth Gabier and wife, Dr Firzana, you are my greatest supporters and my strength, I thank you for your love and motivation. To my younger brother, Abdul Hakam Gabier, you are my biggest fan always cheering me on when I am facing any challenge. I thank you for your love and the vent sessions. To my nephews Ali and Azhar Fouad, and niecy, Sabah Thuraya, thank you for being my gaming buddies, you are love and joy!

To each and every one mentioned I pray your life is filled with peace, happiness and success.

Ameen

List of Figures

List of Tables

List of Supplementary Tables and Figures

List of Abbreviations

1-Cys Prx - 1-Cys-Peroxiredoxin

2DE - Two-dimensional electrophoresis

2DLC - Two-dimensional liquid chromatography

ABA - Abscisic acid

APEX - Absolute protein abundance

APX - Ascorbate peroxidase

ASC - Ascorbate

AWC - Absolute water content

CAT - Catalase

DW - Dry weight

ECs - Enzyme codes

ELIP - Early light-inducible protein

ERD -Early response to drying

FA - Formic Acid

GA - Gibberellic acid

GABA - Gamma aminobutyric acid

GC-MS - Gas chromatography-mass spectrometry

GDC - Glutamate decarboxylase

GO - Gene ontology

GS/GOGAT - Glutamine synthetase/glutamine oxoglutarate amidotransferase

GSH - Glutathione

GSSG - Oxidized glutathione

HCD -Higher collisional dissociation

HSP - Heat shock protein

IAA-Asp - Indole-3-acetic acid

IBA- Indole-3-butyric acid

ICA - Indole-3-carboxylic acid

ICAT - Isotope-coded affinity tags

iTRAQ - Isobaric tags for relative and absolute quantification

JA - Jasmonic acid

JA lle - Jasmonyl-l-isoleucine

KEGG -Kyoto Encyclopaedia of Genes and Genomes

LC-MS - Liquid chromatography-mass spectrometry

LEA - Late embryogenesis abundant protein

LFQ - Label-free quantification

LRD - Late response to drying

MMTS - Methylmethanethiosulphonate

MRD - Mid response to drying

MSTFA - N-Methyl-N-(trimethylsilyl) trifluoroacetamide

PAI - Protein abundance index

RFO - Raffinose family oligosaccharides

RNS - Reactive nitrogen species

ROS - Reactive oxygen species

RWC - Relative water content

SA - Salicylic acid

SD - Standard deviation

SDS - Sodium dodecyl sulfate

SOD - Superoxide dismutase

Suc/Fru - Sucrose to fructose ratio

UPR - Unfolded protein response

Abstract

Most higher plants cannot withstand severe water loss, except for a small group of angiosperms called resurrection plants. They can survive severe water loss without the loss of viability by employing mechanisms that aid them in desiccation tolerance. Desiccation tolerance in resurrection plants is a complex and multifaceted phenomenon and allows the plant to implement various strategies for survival.

The focus of this study was a label-free proteomic analysis of *Xerophyta schlechteri*, a monocotyledonous and poikilochlorophyllous resurrection plant, in response to desiccation. The study investigated some of the physiological, morphological and biochemical changes of *X. schlechteri* leaf tissue in response to dehydration followed by proteomic analyses using a spectral counting approach. The differentially expressed proteins were identified and quantified and then subjected to gene ontological analyses to identify relevant biological processes involved in desiccation tolerance. The proteomic data was finally correlated to and validated using metabolomic analyses.

X. schlechteri was subjected to a controlled dehydration stress treatment, in which changes in the relative water content (RWC) of leaf tissues, the associated changes in processes outlined above and further expanded on below, were determined. Three physiological stages were tentatively identified, namely, the early response to drying (ERD) which represents ~ 80 - 70% RWC (1.61 $gH_2O\ g^{-1}$ dwt -1.5 $gH_2O\ g^{-1}$ dwt), a mid-response to drying (MRD) represented by ~ 60 - 40% RWC (1.5 $gH_2O\ g^{-1}$ dwt -1.0 $gH2O\ g^{-1}$ dwt) and a late response to drying (LRD), represented by ~ 40 - 10% RWC (1.0 $gH_2O\ g^{-1}$ dwt - 0.5 $gH_2O\ g^{-1}$ dwt). Morphological changes in the late stages of drying were marked by loss of green chlorophyll, increased purple anthocyanin production and leaf folding along the midrib with the abaxial surface exposed to light. Chlorophyll content analyses showed a significant decrease in chlorophyll content in the dehydrated leaf tissue as compared to the fully hydrated state. Biochemical assays to measure the activity of enzymatic antioxidants, namely, ascorbate peroxidase (APX), catalase (CAT), glutathione reductase (GR) and superoxide dismutase (SOD) were done at selected RWC points. There was a significant increase in antioxidant enzyme activity for APX, CAT, GR and SOD in the dehydrated plant tissue.

The label-free proteomics approach utilized, identified a total of 3125 unique proteins in the *X. schlechteri* leaf tissue across the dehydration treatment of which a combined 517 proteins were significantly differentially expressed in response to drying. Amongst the differentially expressed proteins, 253 proteins were upregulated, and 264 proteins were downregulated. This was followed by functional analyses and classification of gene ontologies using bioinformatics tools such as Blast2GO, MapMan and KEGG. This allowed the identification of certain biological processes and pathways involved in the *X. schlechteri* desiccation response. Key biological processes and molecular processes were differentially expressed across the drying stages, these included photosynthesis, cellular respiration and antioxidant activity, respectively.

The proteomic analysis was complemented and validated using metabolomics approaches based on GC MS/MS and LC/MS. The abundance of specific sugars, sugar alcohols, fatty acids, organic acids, phytohormones and amino acids of *X. schlechteri* during desiccation were investigated. Sugars such as raffinose and sucrose are known to play a protective role in desiccation and were found to be abundant in MRD and LRD leaf tissue while, L-histidine, an amino acid which plays a critical role in plant growth, was found to be more abundant in LRD tissue as compared to MRD. The phytohormone abscisic acid, invoked in desiccation tolerance was found to be abundant at LRD and less abundant at ERD. The metabolomic data suggested that the regulation of metabolites was towards reducing possible toxic metabolites while increasing the expression of metabolites that help and protect plant cell integrity from the negative effects of desiccation.

The use of a label-free proteomics approach complemented with metabolomics allowed the identification and validation of biological processes and pathways potentially involved in establishing desiccation tolerance in *X. schlechteri*. As far as we are aware, this is the first label-free proteomic analysis of *X. schlechteri* in response to dehydration.

Chapter 1

Literature review

Introduction

Plants have to withstand unfavourable environmental conditions during their life cycle because of their sessile nature. These adverse environmental conditions affect plant growth, yield and long-term survival. Drought is an important abiotic stress factor for plants, especially with respect to crop plants as it directly impacts agricultural productivity and food security (UNDP, 2015). The increased prevalence of drought globally is also exacerbated by climate change (Voss-Fels *et al*., 2019).

Drought induces drastic physiological, morphological, biochemical and cellular changes in plants in order to survive the stress. Though these changes occur at both the level of the shoot and root, the severity and duration of the stress endured is dependent on the plant species and the respective eco-geography (Farooq *et al.,* 2009 a). There are three general overlapping adaptative mechanisms used by most plants in response to the severity of the water loss, namely 'avoidance', 'tolerance' and 'escape or recovery' (Laxa *et al*., 2019). According to those authors, avoidance is triggered at ~70 to 60% relative water content (RWC) where plant protection and adaption responses are activated to limit photosynthesis and reduce the generation of reactive oxygen species (ROS). Furthermore, water loss below 60% RWC results in activation of tolerance mechanisms which centre on biochemical changes that include osmo-protection, attenuation of metabolism with respect to reduced photosynthesis and activation of antioxidant systems. Most plants can withstand the loss of water to a certain extent, however, if water loss exceeds 40% RWC, it becomes detrimental to the plant and if this continues for an extended period, the cellular damage becomes irreversible and the plant eventually dies (Sharma and Zheng, *et al*., 2019). Plants that are very sensitive to drought will activate escape mechanisms whereby flowering and seed production is initiated before death.

Resurrection plants

There are, however, some species that do tolerate dehydration below 40% RWC, and indeed these species can tolerate loss of up to 95% of subcellular water and recover full metabolic activity within hours of rehydration (Gaff, 1977). This defines a category of plants that are

desiccation tolerant. Among angiosperms, this is a rare phenomenon, with only 135 species currently being reported to have vegetative desiccation tolerance (Gaff and Oliver, 2013). Tracheophytes with this ability are collectively called resurrection plants due to their ability to revive from a dead-like state. Resurrection plants are phylogenetically diverse, exhibit contrasting anatomy, drying and rehydration kinetics, but typically co-occur in specific habitat types in which there are frequent periods of extended drought. Over 90% of desiccation tolerant vascular plants inhabit rocky outcrops or inselbergs in Africa, Asia, and South America (Porembski and Barthlott, 2000). These habitats are characterized by shallow and nutrient poor soils, intense solar radiation and heat, sporadic water availability, and low relative humidity (Porembski and Barthlott, 2000; Porembski, 2007).

It has been proposed by Bewley (1979) that for plant tissue to survive severe water loss, three criteria should be met. Firstly, damage to tissue should be limited and it should be at a repairable level. Secondly, that the plant should be able to maintain its physiological integrity in the dried state. Lastly, the plant must be able to initiate repair and restoration of metabolism and growth upon rehydration in tissues affected by desiccation. All these criteria are variously met in resurrection plants and several comprehensive reviews on the mechanism, and their variations among species exist (Vicré *et al.,* 2004; Farrant *et al.,* 2007; Moore *et al.,* 2009; Dinakar *et al.,* 2012; Gechev *et al.,* 2012; Dinakar and Bartels, 2013; Zhang and Bartels, 2018; Oliver *et al.,* 2020). Some important features are outlined below.

The strategies employed by resurrection plants to overcome desiccation -

Morphological changes

Noticeable morphological changes occur among the different resurrection plant species in response to desiccation and are an important part of the adaption strategy to survive desiccation (Gaff, 1989; Scott, 2000; Farrant *et al*., 2003; Vander Willigen *et al*., 2003). Curling or folding of leaf blades is a common and more observable response upon dehydration. The C3 monocot species *Xerophyta humilis* and *Xerophyta schlechteri* fold leaves in half along the midrib exposing only the abaxial surfaces to direct sunlight, thus reducing light absorption by the leaf while in the desiccated state (Hallam and Luff, 1980; Sherwin and Farrant, 1998; Radermacher *et al.,* 2019). Similarly, the leaves of the dicot *Craterostigma* species curl inwards upon desiccation becoming tightly folded with only the abaxial surfaces of the older leaves exposed to sunlight (Sherwin and Farrant, 1998; Farrant, 2000; Vicré, 2001). The folding of

the leaves during drying allows the inner surface to be shaded from light and the surfaces that are exposed to light accumulate high levels of anthocyanins (Farrant, 2000; Radermacher *et al.*, 2019; Oliver *et al.*, 2020). The anthocyanins reflect photosynthetically active light and act as antioxidants (Larson, 1988; Smirnoff, 1993). The leaf folding and curling associated with dehydration also decrease the surface area which minimises the impact of UV radiation and consequent damage by oxidation stress (Gaff, 1989; Scott, 2000; Farrant *et al.*, 2003; Vander Willigen *et al.*, 2003; Bartels and Hussain, 2011).

Photosynthetic capacity and combating oxidative damage in resurrection plants

Water loss results in the disruption of photosynthesis leading to excessive generation of ROS which further damages the cell (Sharma *et al.*, 2012). Resurrection plants can be divided into two categories with regards to the manner in which photosynthesis is protected, namely, homoiochlorophyllous and poikilochlorophyllous plants (Farrant *et al.*, 2007; Figure 1.2, Laxa *et al*., 2019). During drying, homoiochlorophyllous species retain most or all the chlorophyll and preservation of their photosynthetic apparatus, this allowing rapid recovery of this metabolic processes upon rehydration. This contrasts with poikilochlorophyllous species that dismantles the photosynthetic apparatus and loses most of their chlorophyll during dehydration. Upon re-watering, poikilochlorophyllous plants resume photosynthesis slowly as all their photosynthetic components need to be re-synthesized (Beckett *et al.*, 2012).

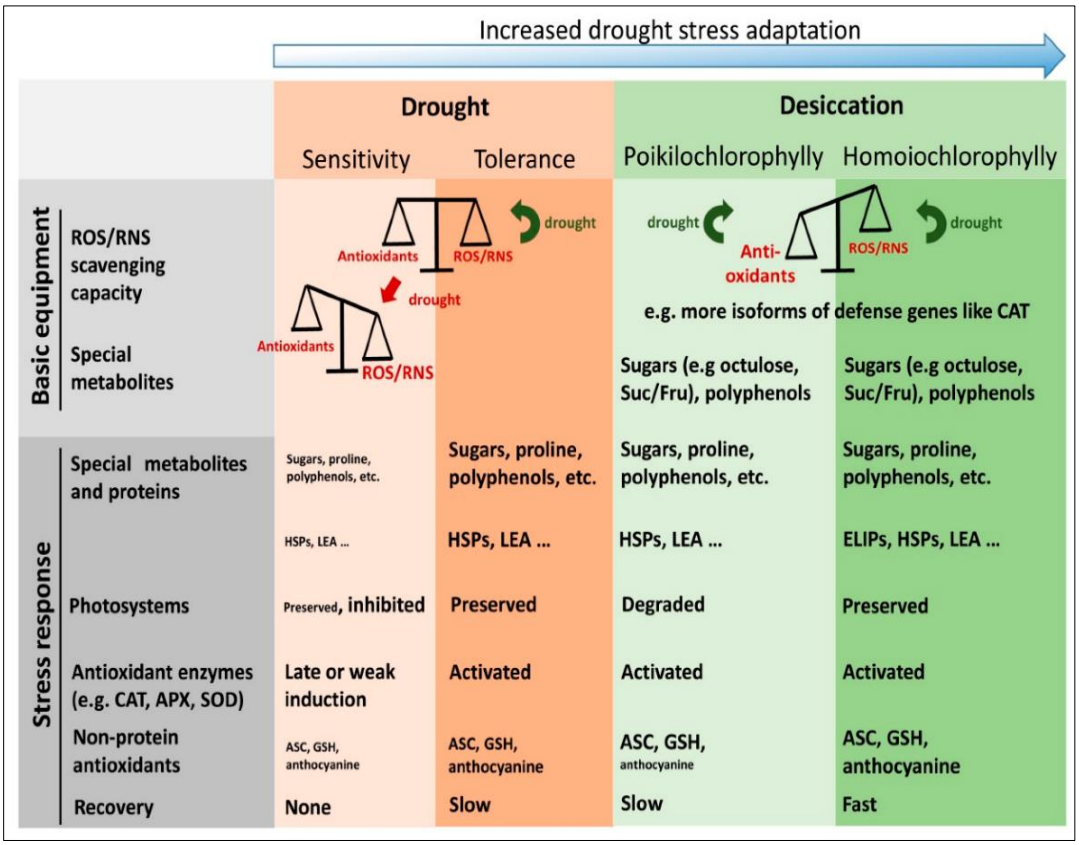

Figure 1.1: Representation of the characteristic features of drought (drought sensitive and drought tolerant) and desiccation (homoiochlorophyllous and poikilochlorophyllous) plants. The figure illustrates some of the properties related to physiological, metabolism, antioxidant and recovery that are associated with plants during drought. Green arrows represent the status that is preserved following drought. Red arrows represent reactive oxygen species (ROS/Reactive nitrogen species (RNS) prevalence. The strength of stressed measures is indicated by the font size. Abbreviations: GSH, glutathione. SOD, superoxide dismutase; ASC, ascorbate; CAT, catalase; APX, ascorbate peroxidase; Suc/Fru, sucrose to fructose ratio; ROS, reactive oxygen species; RNS, reactive nitrogen species; HSP, heat shock protein; LEA, late embryogenesis abundant protein; ELIP, early light-inducible protein. Image (Laxa *et al*., 2019).

Antioxidant protective mechanisms

ROS comprises of superoxide anion radical ($O_2 \cdot^-$), singlet oxygen ($^1O_2$), hydroxyl radical (OH) and perhydroxyl radical (HO_2) which, in excessive amounts, can cause damage to proteins, DNA and lipids affecting normal cellular functioning in plants (Foyer and Noctor, 2005). Under favourable conditions, ROS are continuously generated at basal levels in plants and are limited to the different cellular compartments such as the chloroplast, mitochondria and peroxisomes (Das and Roychoudhury, 2014). ROS do not cause damage during stress-free periods as there is a balance between ROS generation and ROS scavenging (Das and Roychoudhury, 2014). ROS produced in plants in response to abiotic and biotic stresses is part of the activation or modulation of signalling pathways involved in stress protection or pathogen

resistance. Severe water loss induces oxidative stress in plants by the generation of ROS and plants that can effectively mitigate the effects of ROS, are often drought tolerant (Farooq *et al.,* 2009; Foyer and Noctor 2003). The production of antioxidant enzymes such as ascorbate peroxidase (APX), superoxide dismutase (SOD), catalase (CAT) and glutathione reductase (GR) lower the levels of ROS and help avoid oxidative stress. Antioxidant protective mechanisms are important in resurrection plants in both establishing desiccation tolerance and subsequent recovery during rehydration (Kranner *et al.,* 2002; Challabathula *et al.,* 2016). It has also been reported that certain antioxidant systems are activated specifically in the vegetative tissue of resurrection plants. These include seed-specific 1-Cys-Peroxiredoxin (1-Cys Prx) (Mowla *et al*., 2002), 2-Cys Prx (Govender *et al.,* 2006), α-tocopherol (Kranner *et al.,* 2002) and a wide variety of polyphenols (Smirnoff, 1993; Moore *et al.,* 2005; Farrant *et al.,* 2007).

Protective properties of proteins

Protein synthesis ceases at mild levels of drought in desiccation sensitive plant species; while it continues until leaves are air-dry in desiccation tolerant species (Bartels *et al.,* 1990; Gaff *et al.,* 1997). Drought stress results in the transcription of various genes which produces proteins implicated in adaption or tolerance (Kavar *et al*., 2007). During desiccation, there is a change in protein expression, protein profile and turnover; all of which are essential; as it redirects protein synthesis to the production of proteins involved in protection (Blomstedt *et al.,* 1998). These stress protection proteins include late embryogenesis abundant (LEA) proteins (Feki and Brini, 2016), heat shock proteins (HSPs) (Griffiths *et al.,* 2014), glycine-rich proteins and antioxidant enzymes (Shivaraj *et al.,* 2018) among others.

There is a significant accumulation and response by LEA proteins to water loss (Rodriguez *et al.,* 2010). LEA proteins have been classified into several groups based on their amino acid sequence similarities and conserved motifs. LEA proteins are regulated by ABA-dependant and ABA-independent singling pathways (Vicré *et al.,* 2004; Farrant *et al.,* 2012). These proteins are also thought to act as osmo-protectants in the formation of the cytoplasmic glassy state formation (Vicré *et al*., 2004; Farrant *et al.,* 2012). Previous studies suggested that the protective activity which prevents damage of the various subcellular components during water loss could be attributed to the structural plasticity of LEAs (Artur *et al.,* 2019**).**

HSPs are a class of chaperones preventing aggregation of unfolded proteins and help maintain protein structure during denaturation conditions, such as desiccation (Jacob *et al.*, 2017). They are essential in many cellular processes such as protein synthesis and maturation induced by drought (Coca *et al*., 1994).

Previous studies in *Xerophyta* species found that upon desiccation there was a decrease in photosynthesis which corresponded with the decrease in several chloroplast proteins involved in photosynthetic activity (Collett, 2003; Dinakar and Bartels, 2013). These proteins include psbP, psbO (components of PSII complex), HCF136 which is a stability factor in PSII, Lhcb2 which is a component of the light-harvesting and the enzyme transketolase of the Calvin cycle (Collett, 2003; Dinakar and Bartels, 2013).

Studies conducted in various resurrection plants have revealed that other types of protection proteins are also induced upon dehydration and are present throughout the desiccation stress (Ingle *et al.,* 2007). The protection proteins are involved in a range of functions such as accumulation of sucrose (Ingram and Bartels,1996; Oliver *et al.,* 2010; Farrant *et al.,* 2007), scavenging ROS (Farrant *et al.*, 2007), cell wall protein remodelling (Shivaraj *et al.,* 2018) and while others have unknown functions.

Carbohydrate metabolism

Some carbohydrate metabolites drastically change in abundance during dehydration and play a vital role in cellular protection in resurrection plants. Previous studies have shown that during drying there is an accumulation of trehalose, sucrose and short-chain oligosaccharides such as raffinose (Bianchi *et al.*, 1991; Drennan *et al.*, 1993; Norwood *et al.,* 2000; Peters *et al.*, 2007). In resurrection plants, sucrose was found to be the major carbohydrate involved in protective functions against dehydration (Bianchi *et al.,* 1991; Ghasempour *et al.,* 1998; Norwood *et al.*, 2000; Scott, 2000; Whittaker *et al*., 2001; Cooper and Farrant, 2002; Zivkovic *et al.*, 2005). Comparative metabolic analyses between desiccation sensitive *Eragrostis* species and desiccation tolerant *Eragrostis nindensis* showed that *Eragrostis nindensis* accumulated sucrose in the desiccated leaves while there was no accumulation in the desiccation sensitive *Eragrostis* species (Illing *et al.,* 2005). The functions of sugars during dehydration include stabilisation of proteins and osmotic adjustments (Crowe *et al.,* 1998). Sugars such as sucrose and trehalose prevent protein denaturation and membrane fusions (Schiller *et al.,* 1997;

Ramanjulu and Bartels 2002). They are also believed to play a role in signalling and in subcellular vitrification (Farrant *et al.,* 2017; Oliver *et al.,* 2020)

I now focus on the resurrection plant *Xerophyta schlechteri* which has become a model plant to study the mechanism of desiccation tolerance (Mundree and Farrant, 2002; Farrant *et al.,* 2015; Costa *et al.,* 2017). As a side note, the populations upon which these authors worked were originally called *Xerophyta viscosa* (Coetzee, 1974). This species has now been classified as *Xerophyta schlechteri* by Behnke *et al.* (2013).

Xerophyta schlechteri

Xerophyta a plant genus within the Velloziaceae family is composed of 45 species of which 10 are known to be desiccation tolerant and are native to Africa, the Arabian Peninsula and Madagascar (Gaff and Oliver, 2013). *X. schlechteri* (Figure 1.3) is a poikilochlorophyllous monocot species distributed mainly in regions of Southern Africa (Farrant *et al.,* 2007; Farrant *et al.,* 2015). *X. schlechteri* is phylogenetically related to the Poaceae family, which include important grass crops such as maize (*Zea mays*) and therefore elucidating the mechanism of desiccation tolerance in *X. schlechteri* allows the potential for improvement of drought tolerance in cereal crops (Farrant *et al*., 2015; Costa *et al.,* 2017).

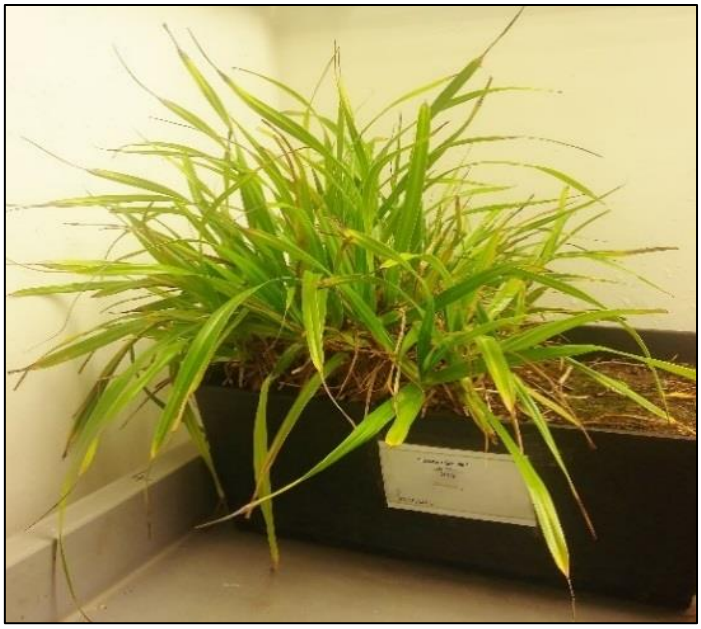

Figure 1.2: Matured fully hydrated *X. schlechteri* plant (in this study).

During desiccation there are morphological and anatomical changes that facilitate leaf folding, controlled regulation of photosynthesis (Sherwin and Farrant, 1998; Radermacher *et al.,* 2019) and a plethora of transcriptomic and metabolic changes that facilitate tolerance of extreme water loss in this species (Farrant *et al.,* 2015; Costa *et al.,* 2017; Radermacher *et al.,* 2019) Similar to other resurrection plants, *X. schlechteri* also activates antioxidant systems (Illing *et al*., 2005; Farrant *et al.,* 2007) and produces HSPs and LEAs to protect tissue against dehydration-induced cellular damage (Farrant *et al*., 2015; Artur *et al*., 2019).

A systems biology approach to elucidate the mechanisms involved in desiccation tolerance

Desiccation tolerance is controlled by many genes, proteins and the metabolite profile. A systems biology approach, which uses a combination of genomics, transcriptomics, proteomics and metabolomics, is an extremely useful and informative approach to understand the mechanisms involved in desiccation tolerance. The main advantage of this approach is that it also allows the identification of important biological, molecular and cellular processes which are associated with and crucial for the establishment of desiccation tolerance.

Transcriptomic analyses of desiccation tolerance

The genome and transcriptome of *X. schlechteri* was recently sequenced (Costa *et al.*, 2017), which allowed for a broader investigation into the mechanisms involved in desiccation tolerance. Desiccation sensitive plants experience metabolic stress when there is severe water loss and cessation of carbon gain. Resurrection plants, however, redirect their metabolism towards protection of their subcellular machinery and ultimately quiescence (Gaff, 1993; Farrant *et al.,* 2017). Costa *et al*. (2017) showed that the metabolic redirect in *X. schlechteri* upon desiccation was twofold based on differentially expressed genes. The two major changes in gene expression occurred at early response (between 60% RWC to 40% RWC) and late response (between 40% to 20% RWC). There is a higher number of differentially expressed genes being expressed at 40% RWC compared to other hydrated states. The study further showed that at 40% RWC, transcripts of genes related to chlorophyll degradation were significantly accumulated. Significantly, transcripts related to chlorophyll synthesis, thylakoid and chloroplast formation were also observed at 40% RWC. This reflects the poikilochloropyllous strategy adopted by *X. schlechteri*. The authors found that there was an

increase in accumulation of transcripts involved in protection, translation, protein folding and gene expression. The leaves were also found to be under control by both ABA-dependant and ABA-independent processes. A late response to drying showed accumulation of unfolded protein response (UPR) pathway (Reis *et al.*, 2011) in the endoplasmic reticulum (ER). This indicates that the UPR pathway is initiated during severe stress and activates the ER-located molecular chaperone binding protein. This prevents ER stress signalling, senescence and ultimately preventing activation of the UPR cell death response (Costa *et al.*, 2017).

Furthermore, transcripts promoting apoptosis decreased in abundance during dehydration and transcripts associated with autophagy increased. This supports the hypothesis that autophagy is a pro-survival strategy employed by resurrection plants (Williams *et al.*, 2015; Costa *et al.*, 2017).

Previous studies have shown that a common set of survival genes are recruited to confer desiccation tolerance to resurrection plants and seeds (Costa *et al.*, 2017; van Buren *et al*., 2018). The genes encoding for these proteins such as LEA proteins, exert a defence function, while others control carbohydrate metabolism resulting in raffinose and sucrose accumulation (Griffiths, *et al.*, 2016). The expression levels of protective genes probably contribute to the differences between desiccation tolerant and desiccation sensitive plants and ultimately survival and death of plants during drought (Illing *et al.*, 2005). The number of LEA genes present in desiccation tolerant and desiccation sensitive species are found to be similar, however more LEA genes are responsive to dehydration and the expression levels are seen to be higher in desiccation tolerant species (Giarola *et al.*, 2017).

Proteomic analysis of desiccation tolerance

The systematic analysis of the proteome is termed proteomics and is the active, epigenetic complement of the functional genome (Phizicky *et al.*, 2003). Proteomics allows the global analysis of proteins within various tissues and under different physiological states. Proteomics has become a crucial field of functional genomics for analysing large-scale identification of whole or specific proteins (Benkeblia, 2011). Plant proteome analysis has improved due to high-throughput techniques built on high-quality sample preparation, protein isolation, mass spectrometry sensitivity and robust protein searching algorithms (Benkeblia, 2011). This is further complemented by genome sequencing and annotation (Agrawal and Rakwal, 2006). Abiotic stress conditions such as drought, induces alterations in gene expression resulting in sequential effects in metabolic processes and changes in cellular protein abundance (Kosová *et*

al., 2011). Ultimately, the measurements of these changes in protein abundance and post-translational modifications elucidate key proteins and biological processes that can be used for further investigations (Vanderschuren *et al.*, 2013). Adapting this methodology for the examination of protein profile changes in response to drought allows for an understanding of the molecular mechanisms and drought tolerant phenotypes involved in stress tolerance or adaption (Nanjo *et al.*, 2011).

The high conservation of protein sequences sets it apart from transcriptomic based techniques (Carpentier *et al.*, 2008). In addition, although most biological processes within the plant cell are carried out by translated proteins rather than mRNA transcripts (with the exception of certain non-coding RNAs), the expressions of the transcripts do not necessarily result in protein expression (Carpentier *et al.*, 2008).

The whole proteome of resurrection plants namely *Boea hygrometrica* (Jiang *et al.*, 2007), *Sporobolus stapfianus* (Oliver *et al.*, 2007) and fern allies such as *Selaginella tamariscina* (Wang *et al.*, 2010) were previously investigated. Proteomic studies were also conducted on *X. viscosa* leaf tissue under dehydration stress and many proteins were implicated in different pathways of protective mechanisms as well as ROS scavenging, cellular, glycolytic and signalling pathways (Ingle *et al.*, 2007). Furthermore, proteomic studies were also done to investigate the *X. viscosa* nuclear proteome using two-dimensional gel electrophoresis (2-DE) (Abdalla *et al.*, 2010) and isobaric tags for relative and absolute quantification (iTRAQ) technology with two-dimensional liquid chromatography (2-DLC) approaches (Abdalla and Rafudeen, 2012). To date, there has been no published proteomic study on *X. schlechteri* with respect to desiccation.

Quantitative proteomics - An investigation of proteins using label-free quantification

The quantification of the proteome can be separated into two major approaches, namely, the use of labelling techniques and label-free techniques. There are a few common labelling methods such as 'isobaric tags for relative or absolute quantification' (iTRAQ) that involves the modification of peptides with isobaric tags (Ross *et al.*, 2004) or labelling of proteins using 'isotope-coded affinity tags' (ICAT) (Gygi *et al.*, 1999). Proteins can also be metabolically labelled by including a specific stable isotope labelling by amino acids in cell culture (SILAC) and which relies on the growing cell cultures to incorporate the isotopic amino acid in all its

proteins (Ong *et al.*, 2002). Although reliable, the labelling techniques require expensive tags and isotope labels, specialised licenced software to analyse the data, there is limited number of samples to label in a single experiment. Furthermore, some samples and proteins are not amenable to certain labelling techniques (Neilson *et al.*, 2011).

Label-free quantification (LFQ) utilises several techniques for the quantification and identification of differentially expressed proteins in complex biological samples. LFQ can be divided into two distinct strategies (Figure 1.4) namely; measurements of the peptide ion chromatogram peak intensity (Mortensen, 2009) and spectral counting which uses the number of peptides assigned to a protein in MS/MS stage as a measurement of relative protein abundance (Neilson *et al.*, 2011). The MS/MS stage is carried out by tandem mass spectrometry which separates peptide ions by molecular weight, allows fragmentation of these ions and subsequent protein identification based on fragment analyses (van Agthoven *et al.*, 2019).

LFQ techniques have been mainly applied to study biotic stress responses (Larrainzar *et al.*, 2007; Lee *et al.*, 2009; Poliakov *et al.*, 2011; Elmore *et al.*, 2012; Rodrigues *et al.*, 2012), and there are only a few reports on using such techniques in abiotic stresses, and to a lesser extent for crop plants such as maize (Gammulla *et al.*, 2011).

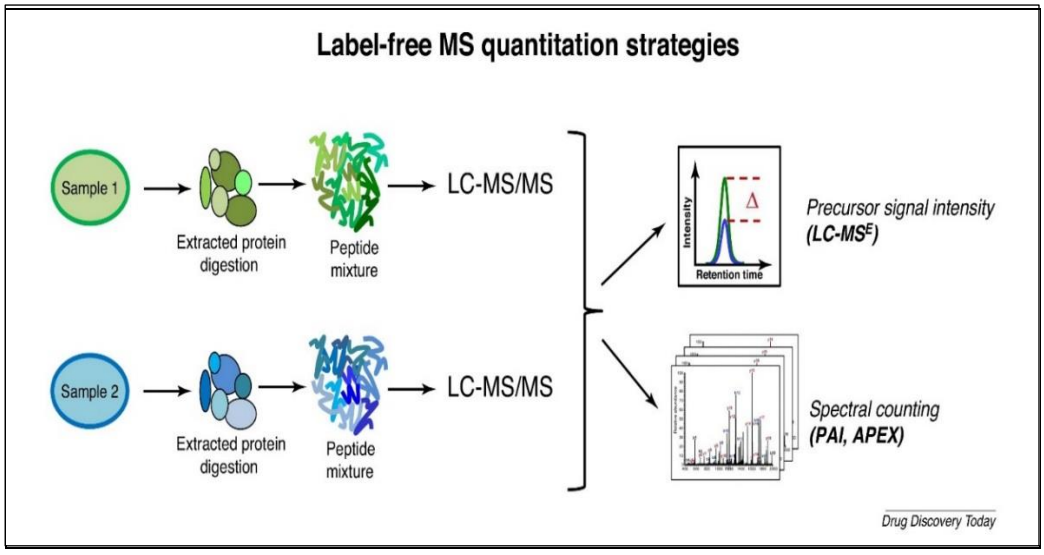

Figure 1.3: Label-free quantitation strategies are based on two types of measurements. Spectral counting and signal intensity. Spectral counting technique counts the number of tandem MS (MS/MS) spectra identified peptides then integrates the results for all the measured peptides of quantified proteins, such as PAI (protein abundance index) or APEX (absolute protein abundance). The signal intensity technique measures the relative abundance of the same peptide in various samples and is estimated by the signal intensity across multiple LC/MS runs (Banfi *et al.*, 2017).

For the purpose of this study, spectral counting was used and will be discussed further. The general concept of spectral counting is based on the observation that more abundant peptides will be selected for fragmentation producing a higher abundance of MS/MS spectra and thus is proportional to the protein amount (Lui *et al.,* 2004). Spectral counting has been reported not to be particularly sensitive to smaller changes of protein abundance (Hendrickson *et al.,* 2006; Trudgian *et al.,* 2011; Ahrné *et al.,* 2013). It was also reported that spectral counting techniques suffer from saturation effects when there are higher protein concentrations and more complex protein samples (Ishihama *et al.,* 2008; Grossmann *et al.,* 2010; Ahrné *et al.,* 2013). High abundance proteins reach maximum sequence coverage while low abundance proteins are under sampled. This, however, can be resolved by the optimization of dynamic exclusion settings in data dependant analysis increasing the quantification of high and low abundant proteins and increasing the reproducibility of spectral counting (Martins-de-Souza, 2014). Although these are a few of the drawbacks, spectral counting method is a valuable tool for the rapid screening of differences between samples resulting in a broad estimation of the concentration of proteins within the proteome (Martins-de-Souza, 2014).

Metabolomics

Metabolomics is a large-scale analysis of small molecules known as metabolites found within the cell, tissues or organisms (Jorge *et al.,* 2016). Metabolites are the end products of cellular processes and their occurrence and abundance reflect the adaptation of the biological system to the environmental changes. Metabolomics characterizes the small molecule complement and interrogates the metabolic networks in samples under different conditions. The metabolome reveals the metabolic state of a given cell, tissue or organism at a particular point in time. It is a complementary tool for understanding proteomic data by revealing biochemical pathways of interest (Kaddurah-Daouk and Krishnan, 2009) and has contribute to the study of desiccation tolerance in plants (Shulaev *et al.,* 2008). Several such studies have been conducted on various resurrection plants (Oliver *et al.,* 2011a; Moyankova *et al.,* 2014; Suguiyama *et al.,* 2014; Tshabuse *et al.,* 2018; Radermacher *et al.,* 2019). There are various metabolomic techniques used to track different compounds involved in stress responses. Gas chromatography-mass spectrometry (GC-MS) and Liquid chromatography-mass spectrometry (LC-MS) are commonly used for plant metabolite profiling (Fernie, 2007). These methods allow the

profiling of multiple compounds that belongs to different chemical classes such as amino acids, sugars, sugar alcohols and organic acids.

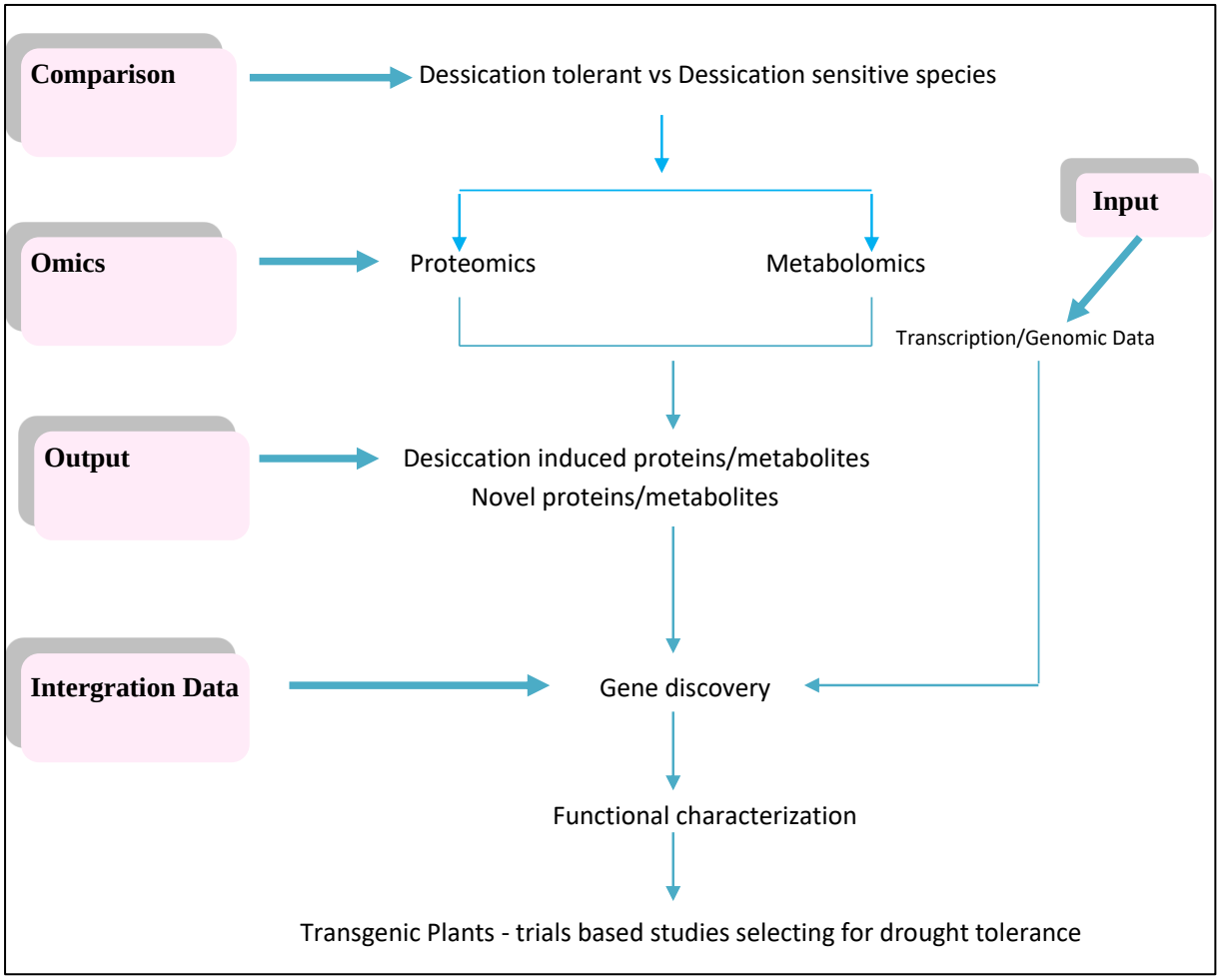

Figure 1.4: Elucidating desiccation tolerance and desiccation sensitivity in plant species studies using 'Omics' techniques, with the aim of identifying proteins and metabolites to complement transcriptomic and genomic data. This approach allows identification of target genes and stress tolerance mechanisms for generating drought tolerant crops (Adapted from Dinakar and Bartels, 2013).

The integration of data from proteomic and metabolomic studies allows for the decoding of important mechanisms such as desiccation tolerance in resurrection plants (Figure 1.5). The information on key biochemical pathways and biological processes associated with desiccation tolerance can be used to improve drought tolerance in crop plants such as maize. This would suggest that mature resurrection plants are prepared for the onset of dehydration stress, albeit it is not entirely true of the seedling stage (Gechev *et al.*, 2013). While dehydration rates in resurrection plants vary, they generally exhibit initial slow drying by accumulation of osmotically active substances affording time for synthesis of further protective metabolites and

proteins vital for the acquisition of desiccation tolerance (Yobi *et al.*, 2012; Radermacher *et al.*, 2019). In addition, resurrection plants accumulate metabolites that tend to extend protection during severe water loss and further reduce concentrations of metabolites that become toxic at higher concentrations (Hoekstra *et al.*, 2001; Dace, 2014).

The nature of many primary metabolites accumulated in resurrection plants contributes significantly to their ultimate survival, and the induction of metabolic quiescence on reaching the air-dry state. Previous studies have shown that upon drying, desiccation tolerant plants accumulate sugars such as sucrose and raffinose, which together with, LEA proteins for example, are thought to play a role in cytoplasmic vitrification in desiccated tissues (Vertucci and Farrant, 1995; Walters *et al.*, 2002; Hoekstra, 2005; Berjak and Pammenter, 2007). Furthermore, recent studies have invoked the role of Natural Deep Eutectic Solvents, which are comprised of combinations of sugars, organic acids and amino acids (Choi *et al.*, 2011; Dai *et al.*, 2013) in subcellular stabilization of the desiccated state (Oliver *et al.*, 2020). Studies have also shown crosstalk between sugars and hormones in regulating defence (Nishiyama, 2013). Hormones are also implicated in desiccation tolerance, this would include abscisic acid (ABA), reported as a central hormone that is involved in drought tolerance and the initiation of the ABA dependant pathway (Frank, 2000; Ullah *et al.*, 2018). In their study Ullah *et al.*, (2018) used metabolomics to validate proteomics and transcriptomic data.

Of the 'omics', the proteome is most closely related to the metabolome due to the fact that many metabolites that are directly regulated by enzymes/proteins involved in their metabolic pathways (Chu *et al.*, 2019). In fact, proteomic data mirrors modulations in the metabolomic data (Carrari *et al.*, 2006). Bioinformatics is a further essential component to integrate and manage the proteomic and metabolomic data and ultimately the link between the proteins and metabolic pathways.

The aim and objectives of this study

The aim of this study was twofold, firstly to use a label-free proteomic approach to investigate the proteome of *X. schlechteri* during desiccation in order to identify key biological, molecular and cellular processes involved in stress tolerance in this species. Secondly, to complement and validate the proteomic data using a metabolomics approach.

The specific objectives of this study (Figure 1.6) were firstly, to investigate the physiological and biochemical responses of *X. schlechteri* across selected drying stages. The changes in water content was monitored using relative water content (RWC) and absolute water content (AWC) measurements. The photosynthetic potential was monitored by chlorophyll content measurements. Biochemical analysis was conducted to observe the response of *X. schlechteri* across the drying stages and was achieved by enzyme assays for ascorbate peroxidase (APX), superoxide dismutase (SOD), catalase (CAT) and glutathione reductase (GR).

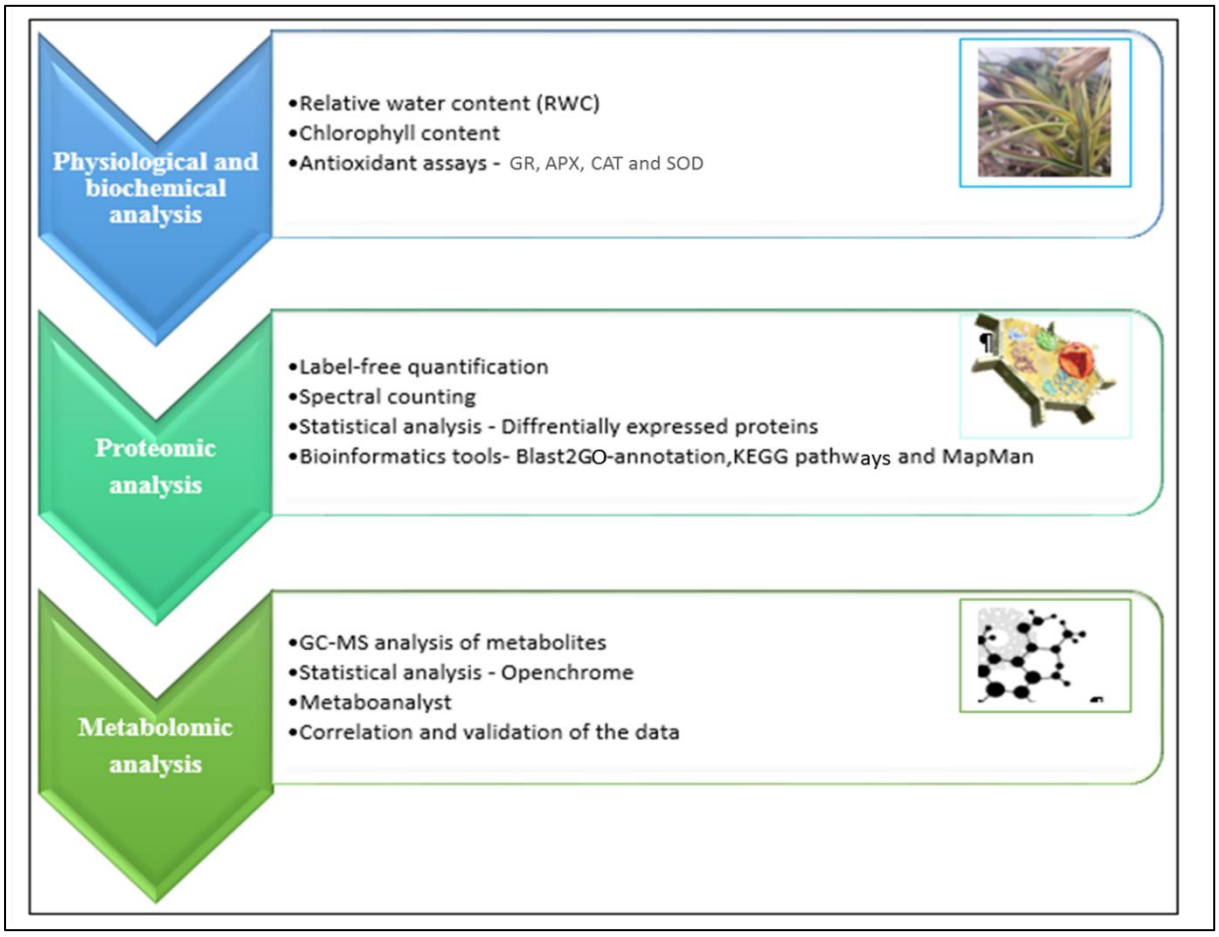

Figure 1.5: Schematic representation of the workflow employed in this study.

The second objective was to conduct an in-depth proteomic analysis of leaf tissues of *X. schlechteri* at various stages of dehydration. This was achieved using label-free quantification based on spectral counting and appropriate database searching and allowed for the quantification and identification of differentially expressed total proteins across the drying stages. Bioinformatics tools were used to achieve a comprehensive and visual representation of the responsive protein pathways to the different drying stages.

The final objective of this study was to confirm a subset of metabolites involved in *X. schlechteri* desiccation tolerance across the drying stages and thereby correlate and validate the data obtained from the biochemical and proteomic analysis.

Chapter 2

Analysis of the physiology, morphology and biochemical activity of *Xerophyta schlechteri* under dehydration stress

Introduction

Desiccation sensitive plants have multiple ways of retarding or regulating water loss, and exhibit varying levels of water loss (Taiz and Zeiger, 2006). However, when such plants are exposed to severe, extended droughts and severe water loss ensues, resulting in reduced rates of cell division, stem elongation and root proliferation, changes in leaf size as well as oxidative stress, among others (Avramova *et al.,* 2015).

In all plants, mitochondria and chloroplasts are major sites of ROS production as a consequence of metabolic processes involving electron transport system (Foyer and Noctor, 2005). Under severe water stress, disruption of the electron transport system occurs, resulting in excess ROS production (Farrant *et al.,* 2007; Oliver *et al.*, 2020). The excess production and accumulation of ROS is inadequately dealt with in desiccation sensitive plants which leads to irreversible damage of plant cells and ultimately their death (Cruz de Carvalho, 2008). The physiological and metabolomic changes that occur in plants during water loss depends on the plant species, growth stage, intensity and duration of the stress (Chaves, 2002). In crop plants such as maize (*Zea mays*), previous studies have shown that under severe and prolonged water loss, chlorophyll content decreases which leads to a reduced rate of photosynthesis (Castrillo and Calcagno, 1989; Alaei and Khabiri, 2012; Fani, 2012). Other studies have indicated that prolonged and severe water stress also leads to irreversible structural damage of the thylakoid membranes contributing to the decreased rate of photosynthesis (Cornic and Massacci, 1996; Farooq, 2009 b; Anjum, 2011). The degree of antioxidant activity is elevated under drought stress but are varied among plant species (Zhang and Kirkham, 1995) and cultivars (Bartoli *et al.,* 1999). Certain maize lines have been reported to increase in antioxidant activity when it experiences stress (Hernández *et al.,* 1999; Manchandia *et al*., 1999; Sairam *et al.,* 2002).

X. schlechteri can lose up to 95% of its total cellular water content and upon rehydration is able to regain its full metabolic potential (Sherwin and Farrant, 1998; Farrant *et al.,* 2015). As

indicated in Chapter 1, various protection mechanisms for drying are initiated to achieve the least possible stress damage associated with severe cellular water deficit. Being poikilochlorophyllous, *X. schlechteri* decreases ROS production and photo-oxidative stress by dismantling thylakoid membranes and chlorophyll degradation during dehydration along with increased antioxidant activity (Sherwin and Farrant, 1998; Mundree and Farrant, 2000; Farrant *et al.*, 2015). This is in line with all other resurrection plants studied (reviewed in Farrant *et al.*, 2007; Dinakar and Bartels, 2012; Giarola *et al.*, 2017). Furthermore, several resurrection plants accumulate enzymes like 1-cys-peroxiredoxin, which until recently have been considered to be antioxidants specific to seeds (Mowla *et al*., 2002; Illing *et al*., 2005).

The aims of this chapter

The aim of this chapter was to investigate some of the physiological, morphological and biochemical changes of *X. schlechteri* and Maize upon drying. Both species were subjected to dehydration treatment and their respective relative water contents were determined. This was followed by chlorophyll content analysis and antioxidant enzyme assays for both plants species. The rationale behind this chapter was to assess and confirm changes (relative to previous studies on *X. schlechteri*) in these values relative to the RWCs sampled at various stages of drying in *X. schlechteri* and furthermore to compare these with changes occurring upon water loss in a desiccation sensitive monocot such as maize.

Materials and methods

Plant material and growth conditions

X. schlechteri was collected from Buffelskloof Nature Reserve near Lydenberg (Mpumalanga Province, South Africa). The plants were maintained in soil under glasshouse conditions at the University of Cape Town (South Africa) until required for the dehydration experiment. The plants were then acclimated in an environmental chamber (Conviron Adaptis A350, Canada) where the environment was controlled at 16 hrs light, 300 $\mu molm^{-2}\ s^{-1}$, 25°C; 8 hrs dark, 20°C; 50 % relative humidity. Senescent leaf tips (Radermacher *et al.,* 2019) were removed and the plants were acclimated to these conditions for two weeks after which drought stress was applied. Five mature plants were utilized in this study.

Maize seeds (*Stowell's* Evergreen sweetcorn, South Africa) were sown in pots. The plants were grown in a growth room (temperature 26°C, humidity 36%, 12 hrs of day and 12 hrs of night). Soil moisture content was monitored at a 5 cm soil depth with a soil probe (WET-2 Sensor/HH2 Moisture Meter, Delta-T Devices, Cambridge, Great Britain). Soil moisture content was maintained with about 750 ml of tap water every second day. At 60 days after seed germination (stage V12), just before tussling the maize plants were subjected to dehydration treatments as described below. In total 40 plants were used for these studies.

Dehydration treatments

The five mature *X. schlechetri* plants that were chosen were of similar size to minimise plant to plant variation. Dehydration was achieved by withholding water and leaf sampling was conducted each day at the same time. Three leaves of the same length and size were excised from each replicate plant. Each leaf was split along the central vein and one half was flash frozen in liquid nitrogen and stored at -80°C for later use in biochemical studies. The other half was used to calculate the relative water content (RWC). The classic method of determination of plant RWC, as outlined by Barrs and Weatherley (1962) was followed with one exception. As the leaf tissues of *X. schlechteri* do not absorb water during the required overnight incubation, the turgid weight cannot be easily and accurately calculated. Thus in this study the absolute water content (AWC) was determined as outlined in Barrs and Weatherly (1962) in

that fresh weight (FW) of each leaf was determined immediately after it was excised and again after incubation at 70°C for 48 hrs for determination of dry weight (DW), using the formula AWC = (FW-DW)/DW and thus expressing water content as gH2O g^{-1} dwt. RWC was determined utilising the AWC of leaves at full turgor (AWC_{FT}) prior to initiation of dehydration and expressed as follows:

$$AWC/\ AWC_{FT}\ x\ 100.$$

For maize 5 of the 40 plants were kept fully hydrated by frequent watering and used as the hydrated control. The rest of the maize plants were subjected to dehydration by with holding water at the V12 stage. The soil water content was measured by using the volumetric soil probe (WET-2 Sensor/HH2 Moisture Meter, Delta-T Devices, Cambridge, Great Britain) in order to assess when plant dehydration might ensue. RWC was measured as described above for *X. schlechteri.* The leaf water content was determined on each of the five plants at each sampling point.

Chlorophyll content determination

The chlorophyll content of both fully hydrated and fully dehydrated *X. schlechteri* and maize leaves were determined according to Porra (2002) with some modifications. Approximately 300 mg of leaf tissues were ground to a fine powder and 5 ml of 80 % acetone was added. The tubes were mixed in the dark for 15 minutes and then centrifuged for 15 minutes at 4°C at 1000 *g*. The supernatant was transferred to a fresh tube and kept in the dark. The tubes were mixed thoroughly, and the absorbance of chlorophyll was measured using a MultiSkan EX microplate reader (Thermo Fisher Scientific, Inc., USA). Total chlorophyll content was determined by using the following equation of Lichtenthaler & Wellburn (1983).

[Chl a+b] = 17.76 x A 646.6 + 7.34 x A 663.6,

where A= absorbance

Chlorophyll content was normalized to the mass of the dry starting material. Three replicates were considered per treatment.

Antioxidant assays

A spectrophotometric approach was used to determine the antioxidant activity of ascorbate peroxidise (APX), catalase (CAT), glutathione reductase (GR) and superoxide dismutase (SOD). The method described in Bailly *et al.* (1996) was utilized for enzyme extraction and assessment of activity, with minor modifications. Dehydrated and hydrated leaf material of both plant species were ground with equal weights of insoluble polyvinylpyrrolidone (PVP) under liquid nitrogen. A volume of 3 ml of extraction buffer (0.1 M phosphate buffer, pH 7.8, 2 mM DTT, 0.1 mM EDTA, 1.25 mM PEG 4000) was added to 0.25 g of finely ground sample. Each sample was centrifuged at 14 812 *g* for 15 minutes at 4°C (Beckman Coulter, South Africa). The samples were run through PD 10 Sephadex columns (GE Healthcare, USA), which were first equilibrated with three washes of 3 ml of 0.1 M phosphate buffer (pH 7.8) as per manufacturer's instructions. Once the equilibration process was complete, samples were loaded onto these columns. The protein retained in the column was eluted with 3.5 ml of 0.1 M phosphate buffer (pH 7.8). The flow-through was collected and total protein quantified using the BCA (Bicinchoninic Acid) assay kit (Thermo Fisher Scientific, Inc., USA) method with BSA (Sigma, USA) as a standard. The standards were set up according to the instruction manual. The total protein absorbance was measured at 595 nm using the MultiSkan EX microplate reader (Thermo Fisher Scientific, Inc., USA) and then the analysis of the various antioxidant activities was conducted.

Catalase (CAT, EC: 1.11.1.6)

The measurement of CAT activity was carried out according to Claiborne (1985). CAT activity was measured at a wavelength of 240 nm for every second for 5 minutes. A UV plate was used and each well contained 50 mM phosphate buffer (pH 7.0), 37.5 mM H_2O_2 and 13.33 µl extract made up to a final volume of 200 µl with dH_2O. The results were calculated as µmol H_2O_2 catalysed per min per mg dry weight (mg protein. sec)$^{-1}$

Catalase activity was then **calculated using the following formula:**

Enzyme activity = $\frac{\text{(slope (dA/min) x final volume)}}{\text{(0.0436 x sample volume)}}$

Enzyme activity per gram = $\frac{\text{(Enzyme activity) x (Volume of buffer used for extraction)}}{\text{The weight of tissue used in the extraction}}$

- Extinction coefficient of H_2O_2 at 240 nm = 0.0436 Millimolar

Glutathione reductase (GR, EC: 1.6.4.2)

The measurement of GR activity was carried out according to Bailly *et al.* (1996). The reaction was conducted using a microplate at 25°C. Each well contained 0.1 M phosphate buffer (pH 7.8), 3 mM $MgCl_2$, 10 mM oxidized glutathione (GSSG), 0.5 mM NADPH, 100 µl extract and made up to a (dH_2O) final volume of 200 µl. Measurements were made at a wavelength of 340 nm and were taken every minute over a period of 20 minutes. The rate of NADPH oxidation was observed and the activity of GR was calculated as µmol NADPH oxidised

per mg protein **using the following formula:**

$$\text{Enzyme activity} = \frac{\text{(Rate) x (Volume of the buffer used for extraction)}}{\text{(Extract volume) x (Extinction coefficient of NADPH)}}$$

- Extinction coefficient of NADPH at 240 nm = 6.22 Millimolar

Superoxide Dismutase (SOD, EC: 1.15.1.1)

SOD activity was measured according to Bailly *et al.* (1996) with minor modifications. The SOD activity was measured at 560 nm in a microplate reader with volumes of each reaction per well containing 0.1 M phosphate buffer (pH 7.8), 1.3 µM riboflavin, 13 mM methionine, 63 µM nitro-blue tetrazolium (NBT), 50 µl extract and then made up to a final volume of 300 µl with dH_2O . The results were formulated as one unit of SOD (mg protein)$^{-1}$ representing one-unit enzyme activity which inhibited the photo-reduction of NBT to blue formazan by 50%.

Superoxide Dismutase was then **calculated using the following formula:**

$$\textbf{Enzyme \% inhibition} = \frac{[(\text{Abs control}) - (\text{Abs sample})]}{\text{Abs control}} \times 100$$

$$\textbf{Total enzyme activity} = \frac{\text{\% inhibition}}{50\% \times \text{protein concentration (mg)}}$$

Results and discussion

Physiological and morphological analyses

The relative water content of leaves of *X. schlechteri* was measured upon drying and is shown in Figure 2.1 along with representative images of plants at various stages of dehydration.

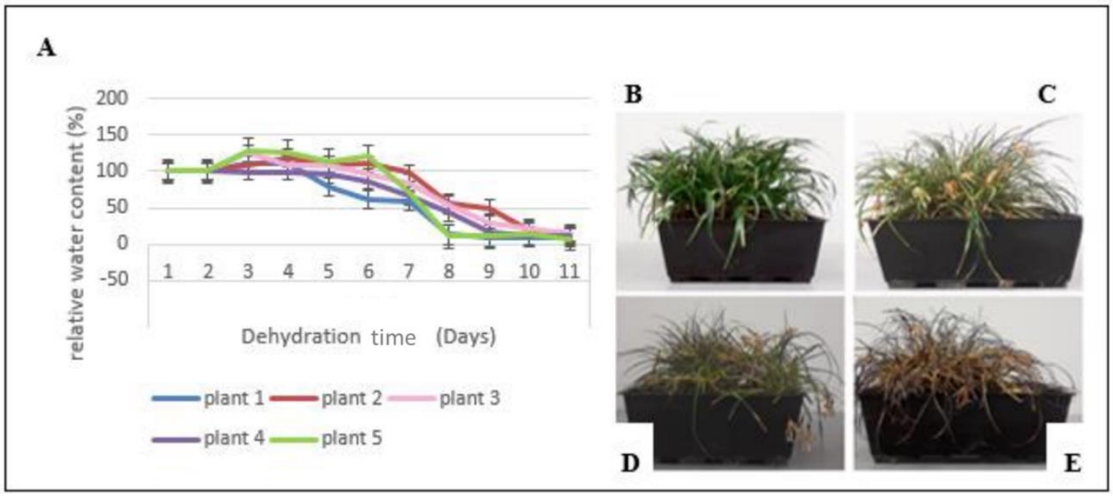

Figure 2.1: (A). Changes in relative water content of leaves of *X. schlechteri* under dehydration stress over a period of 11 days. Dehydration was performed on five biological replicates (n=5). (**p<0.01); error bars represent standard error between the technical replicates. **(B).** *X. schlechteri* representing hydrated (control) (~100 % relative water content, ~ 2.1 gH2O g^{-1} dwt; **(C).** *X. schlechteri* represented at early response to drying (~80 - 70% relative water content, ~1.61 gH2O g^{-1} dwt to ~1.5 gH2O g^{-1} dwt); **(D).** *X. schlechteri* at mid response to drying (~ 60 - 40% relative water content, ~ 1.5 gH2O g^{-1} dwt to ~1.0 gH2O g^{-1} dwt); **(E).** *X. schlechteri* represented at late response to drying (~ 40 - 10% relative water content, ~1.0 gH2O g^{-1} dwt to ~ 0.5 gH2O g^{-1} dwt).

At full turgor of 100% RWC, leaves contained 2.1 gH_2O g^{-1} dwt and in this experiment, it took 10 -11 days for all plants to reach an air-dry state of 10% RWC (0.5 gH_2O g^{-1} dwt). A previous study (Farrant.*et al.*, 2015) noted that *X. schlechteri* follows a reverse sigmoidal pattern upon drying, typical of most resurrection plants, and three stages can tentatively be identified, which correlate with distinct shifts in metabolic activity. These are the early response to drying which represents ~ 80 - 70% RWC (~1.61 gH_2O g^{-1} dwt to ~1.5 gH_2O g^{-1} dwt, a mid-response to drying represented by ~ 60 - 40% RWC (~1.5 gH_2O g^{-1} dwt to ~1.0 gH_2O g^{-1} dwt) and a late response to drying, represented by ~ 40 - 10% RWC (~1.0 gH_2O g^{-1} dwt to ~0.5 gH_2O g^{-1} dwt).

In Figure 2.1 A, the early response among all the *X. schlechteri* plants averaged between six to eight days before the decline into the mid phase. In the early response (Figure 2.1 C), the leaves maintained their green colour but at the mid response the leaves started losing their green colour

(Figure 2.1 D) which is indicative of poikilochlorophyllous resurrection plants that dismantle their photosynthetic apparatus upon drying (Sherwin and Farrant, 1998, Tuba and Lichtenthaler, 2011; Beckett *et al.*, 2012; Christ *et al.*, 2014). The mid response averaged between three to four days before entering the late response (Figure 2.1 E). During the late response (~ 40 - 10% RWC), the leaves were folded such that the abaxial surfaces only were exposed to light, with these becoming anthocyanin rich as seen by the dark shade of purple (Figure 2.1 E). The abaxial surface also protects the plant as it has a reflective sticky coating which serves to reduce light absorption (Sherwin and Farrant, 1998).

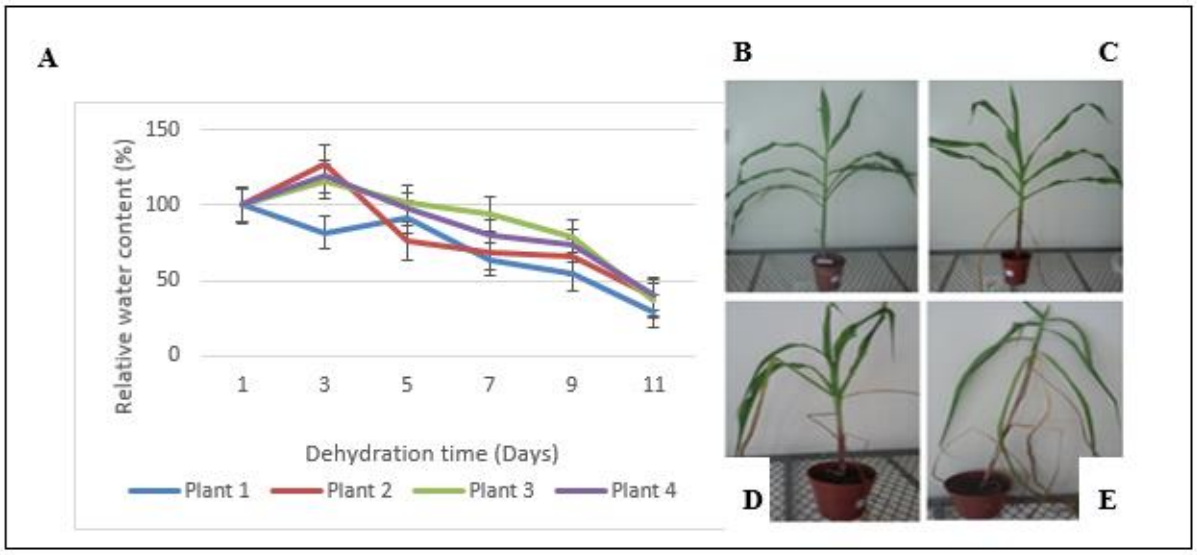

Figure 2.2: (A). Changes in relative water content of maize leaves under dehydration stress over a period of 11 days. Relative water content represented in percentage. Error bars specify standard error between technical repeats. Dehydration was performed on four biological replicates **(B).** Maize representing hydrated (control) (~100-90% relative water content ~5 $gH_2O\ g^{-1}$ dwt to 4.8 gH_2O); **(C).** Maize at early response to drying (~80-70%, ~ 4.4 $gH_2O\ g^{-1}$ dwt to 3.9 gH_2O); **(D).** Maize at mid response to drying (~70 - 60% relative water content, ~3.9 to 3.4 $gH_2O\ g^{-1}$ dwt); **(E).** Maize at late response to drying (~ 60 - 50%, ~3.4 gH_2O - 2 $gH_2O\ g^{-1}$ dwt).

A dehydration treatment of desiccation sensitive maize showed a gradual lowering of RWC over the dehydration period with a steep decline beginning on the ninth day (Figure 2.2 A). For comparative purposes, we have also defined early, mid and late stages of drying in maize. At full turgor, the absolute water content of leaves was 5 $gH_2O\ g^{-1}$ dwt (Figure 2.2 B). After three days of withholding water, maize leaves started showing signs of leaf wilting, (Figure 2.2 C) although the RWC of the leaves of most plants were elevated compared to the full turgor control (Figure 2.2 A). This feature is typical of plants that increase osmotic content of leaves during early stages of drought stress, thereby improving water transmission from roots (Farrant, 2007;

Kamies, Rafudeen and Farrant, 2010). By day 5, actual water loss was initiated with leaf tissues declining to ~ 70-60% RWC (Figure 2.2 D). Maize leaves showed wilting and rolling throughout the drought stress treatment. These morphological changes were observed within the first few days of drought stress treatment but as the dehydration treatment progressed, the degree of leaf rolling increased (Figure 2.2 E). These changes were noticeable when compared to the well-watered controls which had no rolling or wilting. In arid areas, many plants use leaf rolling as a drought avoidance mechanism as it decreases transpiration (Clarke, 1986; Fernandez and Castrillo, 1999). By day 11, the late stages of this drought experiment, the stem started turning deep red and leaves felt completely dry (Figure 2.2 E) although they were still at relatively high RWC of 60-50%.

Despite the similar trends in initial responses to withholding of water, in that both species initially maintained a high RWC for 6 days before obvious decline thereof, subsequent rates of water loss varied between the species. In *X. schlechteri* there was a rapid decline to 10% RWC, whereas in maize RWC remained above 50% during this time. This clearly points to different methods of water regulation between the two plant species. There were notable morphological differences between the two species. *X. schlechteri* had no obvious leaf drooping and the loss of chlorophyll and accumulation of purple anthocyanin was clearly visible. Maize leaves showed signs of drooping and leaf rolling, this likely slowing rate of water loss by reduction of transpiration, but some of the tissues remained green suggesting retention of chlorophyll.

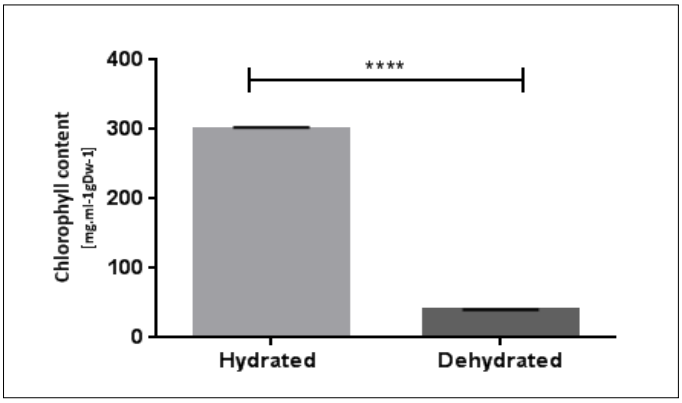

Figure 2.3: Chlorophyll content of *X. schlechteri* from hydrated and dehydrated leaf material performed on three biological replicates (n=3). The absorbance was read at 645 and 663 nm and calculated for total chlorophyll content. Data are represented by mean of ± SD (standard deviation). Asterisks indicates statistical differences as determined by the unpaired t-test (****, $p \leq 0.001$).

The morphological changes seen upon dehydration were also reflected in the chlorophyll content of leaves of the two species after 11 days of dehydration (Figures 2.3 and 2.4). In *X.*

schlechteri, there was a 90% reduction of chlorophyll from the fully hydrated to the desiccated state (Figure 2.3). This is similar to that reported by other researchers working on this species (Sherwin and Farrant, 1998; Radermacher *et al.,* 2019) and is typical of all poikilochlorophyllous resurrection plants (Dinakar *et al.,* 2012; Farrant *et al.,* 2012; Christ *et al.,* 2014).

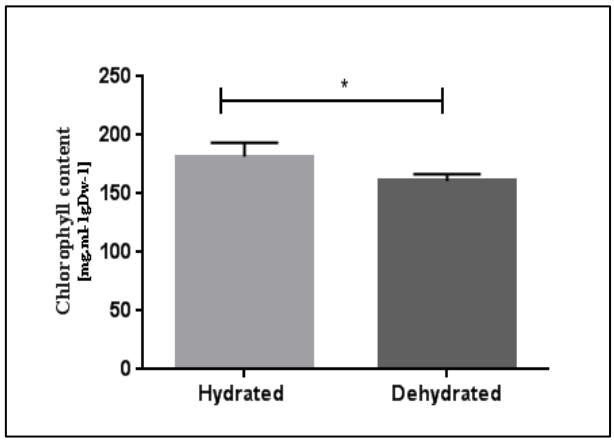

Figure: 2.4.: Chlorophyll content of maize from hydrated and dehydrated leaf material performed on three biological replicates (n=3). The absorbance was read at 645 and 663 nm and calculated for total chlorophyll content. Data are represented where error bars represent mean of ± SD (standard deviation). Asterisks indicates statistical differences as determined by the unpaired t-test (<0.05*).

The chlorophyll content in hydrated and dehydrated maize leaf material is shown in Figure 2.4. There was a small but significant decrease in chlorophyll content in the dehydrated samples which suggests that the 50% reduction in RWC had a negative impact on photosynthesis. During drought stress, the accumulation of ROS becomes excessive and this has been reported to cause reduction in chlorophyll content (Smirnoff, 1995). Furthermore, loss of chlorophyll is typical of the induction of senescence (Bresson *et al.,* 2018), which the maize plants in this study might have been entering.

When contrasting the chlorophyll assay results between *X. schlechteri* and maize, there is a massive reduction in chlorophyll content of ~90% in the former whereas in maize the reduction was only ~10%. This confirms previous studies that there is a structured downregulation of photosynthesis by *inter alia* chlorophyll breakdown in poikilochlorophyllous resurrection plants (Farrant *et al.*, 2015; Costa *et al.*, 2017), whereas desiccation sensitive plants such as maize, retain chlorophyll during water-loss, despite the risk of excessive ROS damaging the chloroplasts (Challabathula, *et al.,* 2018).

Antioxidant assays

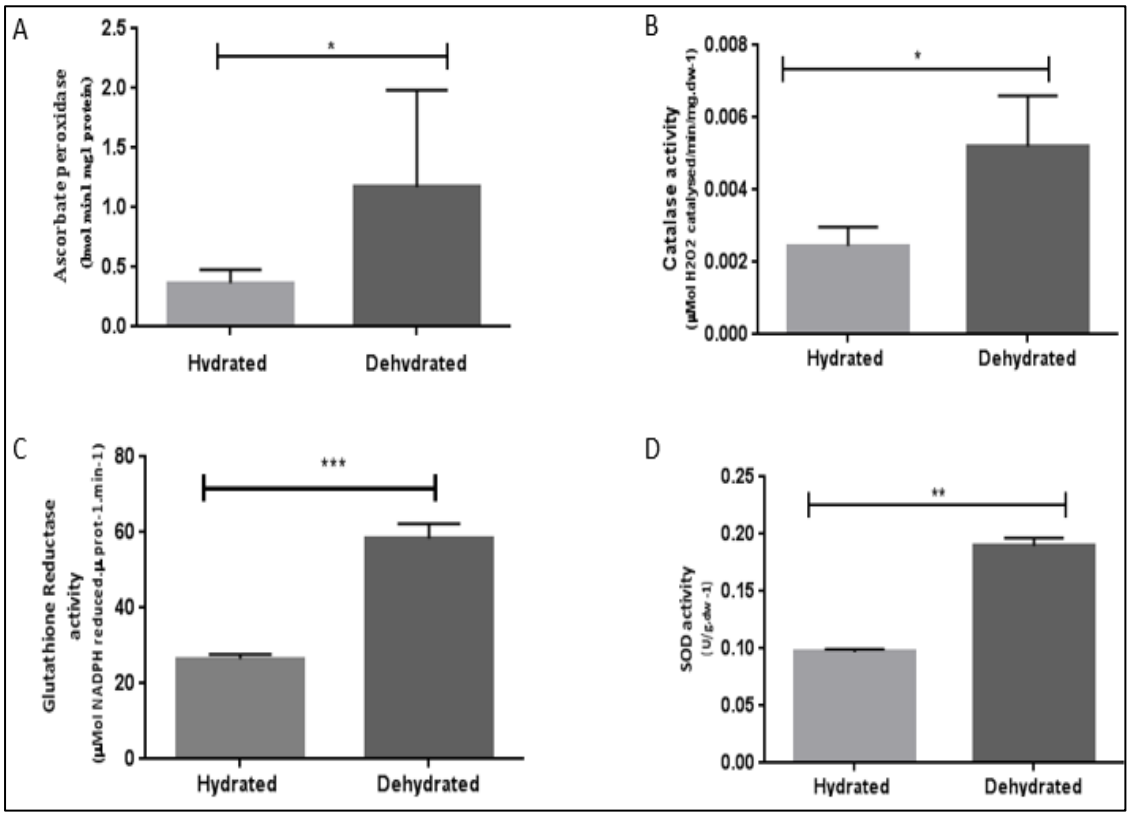

Figure 2.5: Activity of antioxidants in hydrated and dry leaves of *X. schlechteri*. **(A)**. Ascorbate peroxidase (APX) (µmol min^{-1} mg^{-1} of proteins), **(B).** Catalase (CAT) activity (µmol H_2O_2 catalysed/g/sec) and measured at a wavelength of 240nm, **(C).** Glutathione reductase (GR) (µmol NADPH reduced/g/min measured at a wavelength of 340nm and **(D).** Superoxide dismutase (SOD), units SOD/mg protein measured at a wavelength of 560nm in hydrated and dehydrated leaves of *X. schlechteri*. Error bars indicate standard deviation (n=3). Data are represented by mean of ± SD (standard deviation). Asterisks indicates statistical differences as determined by the unpaired t-test (*< 0.05; ** ≤ 0.01, *** ≤ 0.001).

The severity of the water loss can cause the production of ROS to exceed the capacity of antioxidants and antioxidant enzymes resulting in oxidative stress (Foyer and Noctor, 2005; Ajithkumar and Panneerselvam, 2014). The ROS must therefore be detoxified as efficiently as possible to prevent eventual damage to various cellular components (Gratão *et al.,* 2005).

Antioxidant assays were conducted to test enzymatic activities of ascorbate peroxidase (APX), catalase (CAT), glutathione reductase (GR) and superoxide dismutase (SOD) in *X. schlechteri* hydrated and dehydrated leaf material. There was a significant increase in antioxidant enzyme activity for APX, CAT, GR and SOD in the dehydrated plant tissue compared to the hydrated tissue (Figure 2.5). This confirms data of Sherwin and Farrant (1998) who found an increase in APX, GR and SOD activity during dehydration in *X.viscosa*, as well as that of several other

resurrection plants (Farrant *et al.*, 2007), including lower order desiccation tolerant species such as *Selaginella bryopteris* (Pandey *et al.*, 2010).

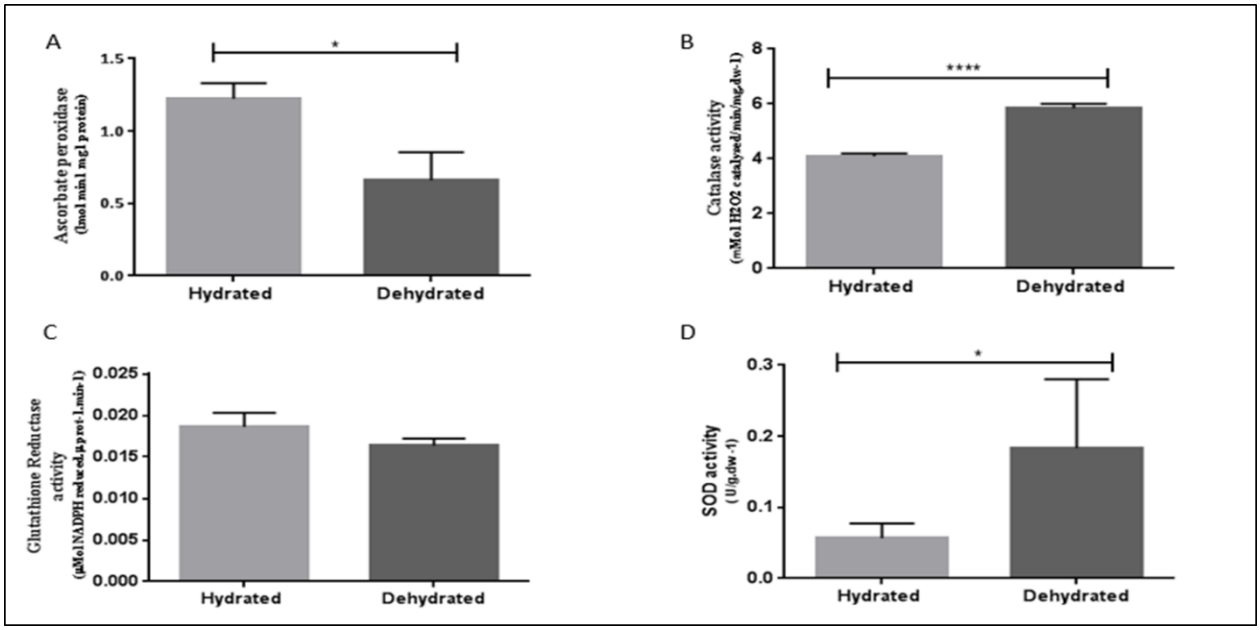

Figure 2.6: Activity of antioxidants in hydrated and dry leaves of maize, **(A)**. Ascorbate peroxidase (APX) (µmol min^{-1} mg^{-1} of proteins, **(B).** Catalase (CAT) (activity (µmol H_2O_2 catalysed/g/sec) and measured at a wavelength of 240nm, **(C).** Glutathione reductase (GR) (µmol NADPH reduced/g/min measured at a wavelength of 340nm and **(D).** Superoxide dismutase (SOD) (Units SOD/mg protein measured at a wavelength of 560nm in hydrated and dehydrated leaves of maize. Error bars indicate mean of ± SD (standard deviation) from three biologicals (n=3). Data are represented by Asterisks indicates statistical differences as determined by the unpaired t-test (*<0.05, **** ≤ 0.001).

Maize plants are also protected by an array of antioxidants such as APX, CAT, GR and SOD (Noctor & Foyer, 1998). In the current study, APX decreased significantly in dehydrated leaf tissues (Figure 2.6 A). Catalase and SOD increased significantly (*>0.05, **** ≤ 0.001) (Figure 2.6 B and D) respectively. While the APX and GR response contrasts with that observed in *X. schlechteri* (Figure 2.5 A and C) where the activity of these two antioxidant enzymes were significantly increased in dehydrated material, if one looks at the actual levels of activity between the two species, the data show that while both species utilise these antioxidants, they do so differently. In hydrated maize leaves APX and CAT activities were 3.25 µmol and 4 µmol respectively compared with 0.4 µmol and 0.002 µmol in *X. schlechteri*. In contrast GR and SOD activities were 10% lower in hydrated maize leaves compared with *X. schlechteri*. Dehydration resulted in lower overall activity of APX and GR in maize, but a higher CAT activity compared with *X. schlechteri*. Interestingly SOD activity was similar in

both species in the desiccated tissues. While these variations might suggest different regulation of these antioxidant activities in maize and *X. schlechteri* in response to drought, this is not uncommon among "housekeeping" antioxidants. Farrant *et al.* (2007) compared antioxidant activities of APX, GR, CAT and SOD in resurrection plants and desiccation sensitive species and that each species showed different trends in activity during initial water deficit stress, only the resurrection plants were able to retain activity below RWC of 50%. In the current study, the fact that all enzymes still retained some activity at 50% RWC in maize, suggests that these tissues had not yet succumbed due to excessive dehydration. This could also have been due to an accumulation of the enzymes. Further drying beyond this point however resulted in the maize not surviving and an attempt to rehydrate the maize was unsuccessful (data not shown).

Antioxidant activity is crucial in determining the drought tolerance of maize genotypes. It was found that, APX, SOD and CAT levels were upregulated in the drought tolerant CE704 maize genotype, while CAT and APX levels decreased in the drought sensitive genotype 2023 (Benešová *et al.*, 2012). The overall results from the antioxidant assays suggests that maize responds to excess ROS due to drought stress, however as water loss becomes more severe it is unable to withstand the stress and eventually dies.

Brief conclusion

This chapter presents some physiological, morphological and biochemical changes that occur in *X. schlechteri* and maize upon dehydration stress. Both plant species had changes in the morphology of their respective leaf tissue upon dehydration with loss of green chlorophyll and purple anthocyanin colour production evident in *X. schlechteri* in the late stages of drying. Chlorophyll content decreased by ~90% in *X. schlechteri* dehydrated tissue compared to hydrated, indicative of its poikilochlorophyllous nature. The systematic breakdown of chlorophyll and thylakoid membranes prevents damage by excess ROS and is complemented with efficient detoxification by various antioxidant systems. This prevents ROS damage to nucleic acid, protein and other cellular structures.

Maize initially used avoidance and protection mechanisms such as curling of the leaves and increasing the activity of certain antioxidant enzymes to cope with the loss of water. There was a slight decrease in chlorophyll content as dehydration proceeded which suggests perhaps the onset of senescence at 50% RWC. It is proposed that the maize antioxidant defence

mechanisms were unable to successfully detoxify the ROS possibly due to the decrease in APX and GR enzyme activity. The response observed for maize (Stowell's evergreen) is typical of desiccation sensitive plant species.

The basis for the observed physiological and biochemical changes is a consequence of molecular changes at the transcriptomic and proteomic level. This involves cellular adjustments more than just control of photosynthesis and modulation of antioxidant mechanisms and requires regulation of stress pathways and production of stress associated proteins. In the next chapter, we will explore the corresponding changes in the *X. schlechteri* proteome upon dehydration.

Chapter 3

Label-free quantitative analysis of the *X. schlechteri* leaf proteome in response to dehydration and gene ontology analyses

Introduction

As mentioned in chapter two, there are various physiological and biochemical changes in the *X. schlechteri* leaf tissue upon drying indicating changes at the level of the transcriptome and proteome across the drying curve. In this chapter, *X. schlechteri* proteins were quantified in response to dehydration stress using label-free quantification (LFQ) and appropriate database searching followed by gene ontology analyses.

LFQ is an LC-MS/MS based method that allows for the systematic analysis of differentially expressed proteins in complex biological samples (Tsai *et al.*, 2016). The fundamental steps to LFQ include protein extraction, protein reduction, alkylation and digestion followed by separation of the sample using liquid chromatography and identification of proteins using MS/MS and a relevant database search (Megger, 2013). The samples are then quantified on the basis of change in protein abundance for each protein identified in the treated sample compared to the control (Megger, 2013).

The measurement of the changes in protein abundance allows key biological processes and proteins to be highlighted for further investigation (Baginsky, 2009; Vanderschuren *et al.*, 2013). There are many bioinformatics tools that can be used for identifying biological processes, functional protein annotation and functional interpretation-based enrichment of gene ontology (GO) processes (Ashburner *et al.*, 2000). These programs depend on appropriate and well-curated plant databases which are often biased and tailored to well-known model plants such as Arabidopsis (*Arabidopsis thaliana*), maize (*Zea mays*) and rice (*Oryza sativa*) (Carpentier *et al.*, 2008).

Functional annotation and GO-term analyses are a challenge for non-model plant species such as *X. schlechteri* and requires suitable annotation tools and a bioinformatics pipeline for analyses. Although the genome of *X. schlechteri* was recently sequenced, it has not been fully

annotated (Costa *et al.*, 2017). This posed a significant challenge in the current study and a bioinformatics pipeline was followed using different software programs to overcome these hurdles and gain useful information about the dataset (summarised in Figure 3.1). The bioinformatics pipeline firstly used Blast2GO (Conesa *et al.*, 2005; Götz *et al.*, 2008) to retrieve gene ontology terms, classify and annotate proteins (Ashburner *et al.*, 2000) resulting in functional enrichment of *X. schlechteri* across the dehydration treatments. Secondly, MapMan analysis (Thimm *et al.*, 2004; Usadel *et al.*, 2005) was conducted in conjunction with Mercator (Lohse *et al.*, 2014) for profiling and mapping the differentially expressed proteins of *X. schlechteri* onto biological pathways and processes.

Lastly, as an addition, KEGG (Kyoto Encyclopaedia of Genes and Genomes) (Kanehisa and Goto, 2000) was conducted in Blast2GO to obtain information regarding stress-responsive pathways and the relevant enzymes associated with dehydration (presented in the supplementary material-KEGG pathways).

The aims of this chapter

The aims of this chapter were twofold, firstly, to identify and quantify differentially expressed *X. schlechteri* proteins in response to dehydration using label-free quantification. Secondly, to analyse the differentially regulated proteins with bioinformatic tools to find relevant functional processes in the context of the early response to drying (ERD), mid response to drying (MRD) and late response to drying (LRD).

Materials and methods

Proteomic analyses workflow

The proteomic analyses workflow consisted of wet lab, raw data processing and bioinformatic components respectively (summarised in Figure 3.1). Proteins extracted from *X. schlechteri* were subjected to LC-MS/MS analyses and raw data was processed to obtain protein identification and statistically significant differential expression of proteins during dehydration. These differentially expressed proteins were then functionally annotated using Blast2GO and Mercator pipelines for GO enrichment and pathway analyses. The details of the specific steps outlined in the workflow are as described below.

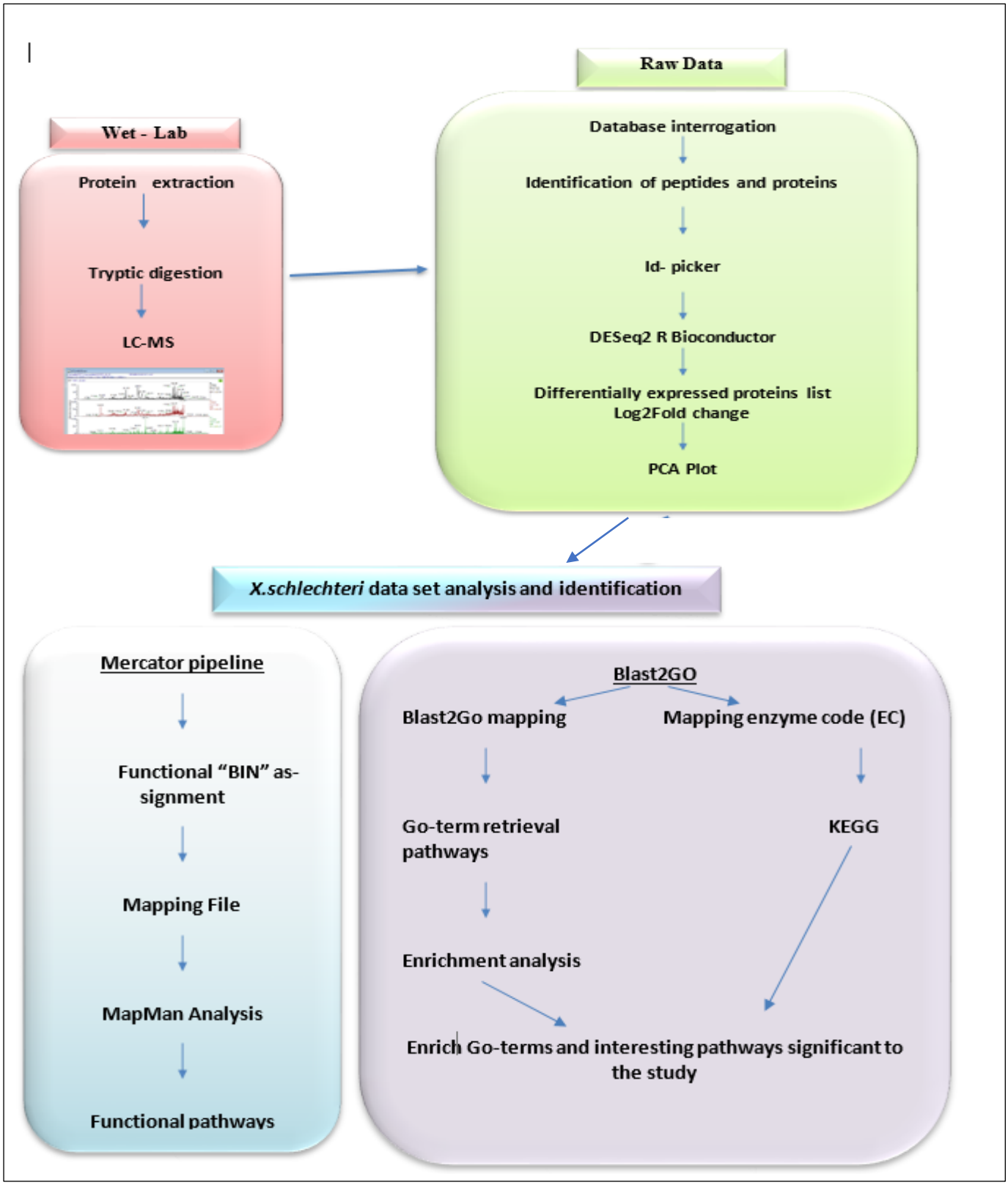

Figure 3.1: Workflow of the steps involved in obtaining functional classifications and pathways of proteins involved in the drying response of *X. schlechteri*. (Note: KEGG pathway analysis is presented in supplementary material. The biological pathways of interest were observed in KEGG (Kanehisa and Goto, 2000). The pathways showed the enzyme codes (ECs) for proteins within the *X. schlechteri* dataset and used for additional confirmation of the pathway analysis).

Plant material and sampling

X. schlechteri plants were maintained, dehydrated and sampled as described in Chapter 2. Five mature *X. schlechteri* plants and leaves of similar size were used as biological replicates and three leaves per biological replicate plants were sampled at each time point during the dehydration. Samples collected were utilized for water content determination as described in Chapter 2, with corresponding leaf tissues flash frozen in liquid nitrogen and stored at -80°C until used for protein extraction as described below.

Protein extraction

Tri-reagent (Sigma-Aldrich Corporation, St. Louis, MO, USA) was used for extracting proteins from leaf material. The leaf material was transferred from the -80°C storage to liquid nitrogen before performing the protein extraction. Leaf material was ground in a chilled mortar and pestle to a fine powder with liquid nitrogen and 1% (w/w) insoluble polyvinylpolypyrrolidone (PVP). Approximately 500 mg of ground material was aliquoted into 2 ml Eppendorf tubes, to which 750 µl of Tri Reagent was added. The tubes were gently inverted and vortexed at room temperature for 15 minutes followed by incubation for 5 minutes at room temperature. This allowed the complete dissociation of nucleoprotein complexes. The tubes were further incubated at room temperature for 3 minutes, this time with the addition of 200 µl of chloroform and inverted gently. Samples were then centrifuged for 15 minutes at 13 000 *g* at 4°C. The aqueous phase (RNA) was transferred to a fresh Eppendorf tube and stored. The organic phase containing total proteins were kept on ice for the rest of the steps unless indicated differently. Cold 100% ethanol was added to the protein extracts. The tubes were inverted and incubated at room temperature for 5 minutes. The tubes were then centrifuged for 15 minutes at 2500 *g*. The supernatant containing soluble proteins were transferred to a 2 ml low-bind Eppendorf tube containing 1.5 ml isopropanol. The tubes were incubated for 10 minutes at room temperature and centrifuged for 15 minutes at 10 250 *g* at 4°C. At this stage, a protein pellet was visible and was washed thrice with 2 ml of 0.1 M ammonium acetate (prepared in 100% methanol). The pellets were washed with cold acetone, thereafter, air-dried and stored at -80°C until further use.

Sample solubilisation and quantification

The protein pellets were resuspended in 50 mM triethylammonium bicarbonate (TEAB; Sigma, USA, T7408), 2% sodium dodecyl sulfate (SDS; Sigma, USA, 71736) and placed at 95°C for 5 minutes in order to solubilise. The samples were centrifuged at 13000 *g* for 5 minutes. Quantification was performed using the QuantiPro BCA assay kit (Sigma, USA, QPBCA) according to the manufacturer's instructions.

On-bead hydrophilic interaction liquid chromatography, (HILIC) digest

HILIC magnetic beads (ReSyn Biosciences, South Africa, HLC010,) were used in the workflow, beads were aliquoted into a fresh tube.The shipping solution removed. The beads were washed with 250 µl wash buffer (15% ACN, 100 mM ammonium acetate (Sigma, USA, 14267) pH 4.5) for one minute and repeated.

The beads were resuspended in loading buffer (30% ACN, 200 mM ammonium acetate, pH 4.5). The rest of the process described hereafter was performed using a Hamilton MassSTAR robotics liquid handler (Hamilton, Switzerland). A total of 50 µg of protein from each sample was transferred to a protein LoBind plate (Merck, USA, 0030504.100). Protein was reduced with tris (2-carboxyethyl) phosphine (TCEP; Sigma, USA, 646547) which was added to a final concentration of 10 mM TCEP and incubated at 60°C for 1 hour. Samples were cooled to room temperature and alkylated with methylmethanethiosulphonate (MMTS; Sigma, USA, 208795) (final concentration of 10 mM MMTS) and incubated at room temperature for 15 minutes. HILIC magnetic beads were added at an equal volume to that of the sample. The plate was then incubated on a shaker for 30 minutes at room temperature for binding of the protein to beads to take place. After binding, the beads were washed with 500 µl of 95% ACN for 1 minute, this was repeated 4 times.

Tryptic digestion

Trypsin (Promega, USA, PRV5111) was made up in 50 mM TEAB. It was added at a ratio of 1:10 total protein and was incubated for 4 hours on a shaker at 37°C. After digestion, the peptides (supernatant) was removed and dried down. The samples were then resuspended in LC loading buffer (0.1% Formic Acid (FA) and 2.5% ACN).

Liquid chromatography-mass spectrometry (LC-MS)

The LC-MS analysis was conducted with a Q-Exactive quadrupole-Orbitrap mass spectrometer (Thermo Fisher Scientific, USA) coupled with a Dionex Ultimate 3000 nano-HPLC system (Thermo Fisher Scientific, USA). The peptides were dissolved in 2% ACN, 0.1% FA (Sigma, USA, 56302), (Burdick & Jackson, USA, BJLC015CS) and loaded on a C18 trap column (PepMap100, 300 μm × 5 mm × 5 μm). Samples containing peptides were trapped onto the column and washed for 3 minutes after which the valve was switched, and peptides eluted onto the analytical column. The chromatographic separation was further performed using a Waters nanoEase (Zenfit) M/Z Peptide CSH C18 column (75 μm × 25 cm × 1.7 μm) as described below. There were two solvents (solvent A and B) employed in the system. Solvent A (1% FA) and solvent B (1% FA in ACN). The multi-step gradient for peptide separation was generated at 300 nL/minute as follows: time change 5 minutes, gradient change: 2-5% solvent B, time change 40 minutes, gradient change 5-18% Solvent B, time change 10 minutes, gradient change 18-30% solvent B, time change 2 minutes, gradient change 30-80% solvent B. The gradient was then held at 80% solvent B for 10 minutes before returning it to 2% solvent B and conditioning the column for 15 minutes. All data acquisition was obtained using Proxeon stainless steel emitters (Thermo Fisher, USA, TFES523). The mass spectrometer was operated with a capillary temperature of 320°C and operated in positive ion mode. The applied electrospray voltage was 1.95 kV.

Database interrogation

Relative quantification was conducted using Progenesis QI for Proteomics (Non-linear Dynamics, UK). Data processing included peak picking, run alignment and normalisation (singly charged spectra were removed from the processing pipeline). Database interrogation was performed with Byonic Software (Protein Metrics, USA) using a *Xerophyta schlechteri* database (August 2018 and version 3). The search parameters include 2 maximum number of missed cleavages with 1% false discovery rate (FDR) cut off.

Identification of peptides and proteins

The LC-MS/MS raw data (spectra) output was converted to mzML format. To determine the potential peptides, MS-GF+ search engine was used (Kim and Pevzner, 2014). A semi-tryptic specificity was used for the 52 *X. schlechteri* mzML files. The 52 *X. schlechteri* mzML files

were searched on the *Xerophyta* database (http://www.bioinformatics.nl/xerophyta/portal/data/). The data was processed using IDPICKER 3.1 (Ma *et al*., 2009) to yield a 2% peptide-spectrum match (PSM) FDR and required two distinct peptides sequences for each protein. A 4.44% empirical FDR was obtained with 2889 distinguishable protein groups matching 19,222 distinct peptide sequences and 152,912 peptide-spectrum matches (spectra).

DESeq2 in R-Bioconductor was used to analyse the data, detect differentially expressed proteins, normalize the counts and test for the significant differences between proteins according to their abundance in the samples using the Wald test and a p-value 0.05.

Gene ontology analysis pipeline

Protein annotation and GO-term retrieval

The protein identifications were further enriched by adding functional ontological information using Blast2GO v.5.2 (Götz *et al.,* 2008). The three common structured vocabularies used in systems biology for ontology are biological process, molecular function and cellular components. Investigation of the proteins were conducted using *X. schlechteri* FASTA database file (August 2018) searched against UNIPROTKB/SwissProt database using the BLASTP algorithm. The blast parameters were set at default, i.e. GO weight of 5, *e*-value filter if 1e-6, an hsp-hit coverage cut-off of 0 and an annotation cut-off of 55.

Mercator and MapMan analysis

Mercator workflow

Mercator v.3.6, is an online tool (https://plabipd.de/portal/home1) that assigns functional annotations to protein sequences using the MapMan (https://mapman.gabipd.org/home) "BIN" ontology. Mercator can be used to search unknown sequences against reference databases using protein domain searches or BLAST-based. Mercator then assigns BINs to the protein sequences based on the significant similarities to the reference protein domains or protein hits. The *X. schlechteri* input text file was uploaded to Mercator which mapped each input identifier to one or more BINs. The output file was then directly used as a mapping file for further high-throughput visualization using MapMan software (Lohse *et al.,* 2014).

MapMan workflow

MapMan (v.3.6) software was downloaded and used for the visualization of the differentially expressed *X. schlechteri* proteins using the 'scavenger' and 'imageAnnotator' modules. The scavenger modules create a non-redundant gene ontology. The image Annotator module allows for the visualization of the differentially expressed data on a schematic diagram showing various pathways associated with the proteins. The input folder contained Log2 fold changes and associated p-values of *X. schlechteri* obtained from Mercator as previously mentioned. MapMan software was configured to display upregulated proteins and downregulated proteins across the dehydration treatments, based on Log2 fold change with a p-value ≤ 0.05 statistical significance and further calculated using a Wilcoxon rank-sum test.

Results and discussion

Identification of differentially expressed proteins and quality control using bioinformatic tools

Differentially expressed proteins

The statistical design of R package DESeq 2 analyses was based on identifying the differentially expressed proteins and their differential expression across different treatments (Tables 3.1, 3.2 and 3.3). The differential expression was expressed as a Log2 fold change for p-values (≤ 0.05) and was complemented with *X. schlechteri* accession, protein description, InterPro and GO-term information. A total of 3125 unique proteins were identified in the *X. schlechteri* leaf material across the treatments (early, mid and late) of which a combined 517 proteins were differentially expressed in response to drying. Amongst the differentially expressed proteins, 253 proteins were upregulated and 264 proteins were downregulated. At ERD (Table 3.1) 29 proteins were found to be upregulated while 33 were downregulated. For MRD (Table 3.2), 56 proteins were upregulated and 128 were downregulated, while LRD (Table 3.3) had 168 proteins that were upregulated and 103 proteins that were downregulated.

Table 3.1: List of differentially expressed proteins involved early response to drying identified in *X. schlechteri* leaf samples.

Accession	Description	baseMean	log2FoldChange	p-value	InterPro	Go-term
Xvis03_221564-PA	processed-gene-12.109-mRNA-1protein Name:"Similar to Late embryogenesis abundant protein D-34 (Gossypium hirsutum)" AED:0.11 eAED:0.19 QI:0|0|0|1|1|1|2|0|254	2.208256511	2.07869733	0.003377706	IPR007011 (PFAM)	no GO terms
Xvis03_200886-PA	augustus-gene-6.42-mRNA-1 protein Name:"Similar to PLP1 Patatin-like protein 1 (Oryza sativa subsp. japonica)" AED:0.26 eAED:0.26 QI:72|0.4|0.16|1|1|1|6|0|314	2.889869909	1.552994529	0.004367183	IPR002641 (PFAM)	P:GO:0006629
Xvis03_220002-PA	augustus-gene-50.23-mRNA-1 protein Name:"Similar to Desiccation-related protein PCC3-06 (Craterostigma plantagineum)" AED:0.00 eAED:0.00 QI:100|1|1|1|1|1|2|285|218	8.3481686	1.709026897	0.007333848		no GO terms
Xvis03_225004-PA	processed-gene-0.29-mRNA-1 protein Name:"Similar to GLU Ferredoxin-dependent glutamate synthase, chloroplastic (Oryza sativa subsp. japonica)" AED:0.15 eAED:0.20 QI:0|0.82|0.86|0.94|1|1|36|0|1763	4.538397579	1.093872984	0.010961575	IPR017932 (PFAM)	
Xvis03_211917-PA	augustus-gene-8.2-mRNA-1 protein Name:"Similar to UGT78D2 UDP-glycosyltransferase 78D2 (Arabidopsis thaliana)" AED:0.00 eAED:0.00 QI:173|1|1|1|1|1|2|210|454	1.696612041	1.920989868	0.011244498	IPR002213 (PFAM)	F:GO:0016758
Xvis03_202087-PA	augustus-gene-8.14-mRNA-1 protein Name:"Similar to AAE3 Oxalate--CoA ligase (Arabidopsis thaliana)" AED:0.02 eAED:0.02 QI:521|1|1|1|1|1|4|258|517	2.212368933	1.706599422	0.01303	IPR000873 (PFAM)	F:GO:0003824
Xvis03_203578-PA	processed-gene-12.33-mRNA-1 protein Name:"Similar to Polyphenol oxidase, chloroplastic (Vitis vinifera)" AED:0.36 eAED:0.40 QI:797|0.5|0.33|1|1|1|3|0|273	4.551593209	0.950857782	0.016000633	IPR002227	F:GO:0004097;F:GO:0016491;P:GO:0055114
Xvis03_211325-PA	augustus-gene-1.70-mRNA-1 protein Name:"Similar to GDCSPA Glycine dehydrogenase	10.76576001	0.729163862	0.01618098	IPR002591 (PFAM);	F:GO:0003824;F:GO:0004375;P:GO:00

	(decarboxylating) A, mitochondrial (Flaveria pringlei)" AED:0.11 eAED:0.11 QI:248|0.76|0.85|1|1|1|14|321|903					06546; P:GO:005514
Xvis03_221126-PA	processed-gene-11.3-mRNA-1 protein Name:"Similar to Mavicyanin (Cucurbita pepo)" AED:0.03 eAED:0.03 QI:68|1|1|1|1|2|217|190	0.735849705	1.86719922	0.01686627	IPR008972	F:GO:000905
Xvis03_225456-PA	processed-gene-0.12-mRNA-1 protein Name:"Similar to Polyphenol oxidase, chloroplastic (Vitis vinifera)" AED:0.01 eAED:0.01 QI:289|1|1|1|1|2|284|597	3.953237343	0.91393486	0.026841309	IPR002227 (PFAM)	F:GO:0004097;F:GO:0016491;P:GO:0055114
Xvis03_222086-PA	processed-gene-4.0-mRNA-1 protein Name:"Similar to SBT3.3 Subtilisin-like protease SBT3.3 (Arabidopsis thaliana)" AED:0.15 eAED:0.15 QI:86|0.88|0.8|1|1|0.9|10|0|661	7.081485008	0.906750846	0.028952361	IPR037045	no GO terms
Xvis03_215744-PA	processed-gene-5.46-mRNA-1 protein Name:"Similar to CAL1 Calmodulin (Medicago sativa)" AED:0.17 eAED:0.17 QI:127|1|1|1|1|2|496|149	0.884696437	1.635472647	0.030612647	IPR002048 (PFAM)	F:GO:0005509;P:GO:0019722
Xvis03_210936-PA	augustus-gene-1.31-mRNA-1 protein Name:"Similar to At5g61250 Heparanase-like protein 2 (Arabidopsis thaliana)" AED:0.14 eAED:0.14 QI:264|0.22|0.2|1|0.88|0.9|10|0|512	4.241227829	0.954132089	0.034425962	IPR005199 (PFAM)	C:GO:0016020;F:GO:0016798
Xvis03_225004-PA	augustus-gene-8.38-mRNA-1 protein Name:"Similar to GLU Ferredoxin-dependent glutamate synthase, chloroplastic (Oryza sativa subsp. japonica)" AED:0.12 eAED:0.12 QI:225|0.96|1|1|0.96|1|32|887|1535	4.627647757	0.95110059	0.036775888	IPR036485	
Xvis03_207220-PA	augustus-gene-29.99-mRNA-1 protein Name:"Similar to Bowman-Birk type trypsin inhibitor (Triticum aestivum)" AED:0.14 eAED:0.14 QI:36|1|1|1|1|2|205|120	1.467485389	1.490311914	0.03752355	IPR000877 (PFAM)	F:GO:0004867;C:GO:0005576
Xvis03_225299-PA	processed-gene-0.7-mRNA-1 protein Name:"Similar to AGT1 Serine--glyoxylate aminotransferase (Arabidopsis thaliana)" AED:0.11 eAED:0.11 QI:101|1|1|1|0.8|0.66|6|208|401	5.458247752	0.795651548	0.042740279	IPR015421	F:GO:0003824
Xvis03_206589-PA	processed-gene-9.106-mRNA-1 protein	4.189543295	0.859536898	0.042986185	IPR001128 (PFAM)	F:GO:000556;F:GO:00165

	Name:"Similar to CYP74A2 Allene oxide synthase 2 (Oryza sativa subsp. japonica)" AED:0.00 eAED:0.00 QI:0|-1|0|1|-1|1|1|0|486					F:GO:0020037;P:GO:0055114
Xvis03_221325-PA	processed-gene-6.29-mRNA-1 protein Name:"Similar to B19.4 Late embryogenesis abundant protein B19.4 (Hordeum vulgare)" AED:0.16 eAED:0.16 QI:0|0.66|0.5|0.75|1|1|4|117|181	3.843070937	1.159483161	0.044432356	IPR038956 (PFAM)	no GO terms
Xvis03_223476-PA	augustus-gene-2.101-mRNA-1 protein Name:"Similar to Pyruvate kinase, cytosolic isozyme (Glycine max)" AED:0.04 eAED:0.04 QI:138|1|1|1|1|1|3|406|533	3.260231664	0.98750497	0.047705112	IPR001697	F:GO:0000287;F:GO:0003824;F:GO:0004743;P:GO:0006096;F:GO:0030955
Xvis03_223774-PA	processed-gene-15.13-mRNA-1 protein Name:"Similar to Late embryogenesis abundant protein 76 (Brassica napus)" AED:0.02 eAED:0.02 QI:314|1|1|1|1|1|3|870|266	3.830648677	1.533858234	0.047990256	IPR004864 (PFAM	no GO terms
Xvis03_221252-PA	processed-gene-1.52-mRNA-1 protein Name:"Similar to SPG20 Spartin (Homo sapiens)" AED:0.03 eAED:0.03 QI:113|1|1|1|1|1|4|834|401	2.614950623	1.383758686	0.049376875	IPR009686	no GO terms

Table 3.2: List of differentially expressed proteins involved mid response to drying identified in *X. schlechteri* leaf samples.

Accession	Description	baseMean	log2FoldChange	pvalue	InterPro	Go-Terms
Xvis03_220002-PA	processed-gene-8.116-mRNA-1 protein Name:"Similar to Desiccation-related protein PCC3-06 (Craterostigma plantagineum)" AED:0.00 eAED:0.00 QI:334|1|1|1|1|2|386|231	8.34817	2.74168	1.13E-05		no GO terms
Xvis03_202087-PA	augustus-gene-8.14-mRNA-1 protein Name:"Similar to AAE3 Oxalate--CoA ligase (Arabidopsis thaliana)" AED:0.02 eAED:0.02 QI:521|1|1|1|1|1|4|258|517	2.21237	2.3688	0.00046	IPR000873 (PFAM)	F:GO:0003824
Xvis03_204003-PA	augustus-gene-27.86-mRNA-1 protein Name:"Similar to Aldose reductase (Hordeum vulgare)" AED:0.09 eAED:0.09 QI:204|1|1|1|1|1|9|270|319	3.17441	1.94368	0.0005	IPR020471 (	F:GO:0016491;P:GO:0055114
Xvis03_211917-PA	augustus-gene-8.2-mRNA-1 protein Name:"Similar to UGT78D2 UDP-glycosyltransferase 78D2 (Arabidopsis thaliana)"	1.69661	2.56191	0.00066	IPR002213 (PFAM)	F:GO:0016758

	AED:0.00 eAED:0.00 QI:173|1|1|1|1|2|210|454					
Xvis03_215617-PA	late embryogenesis abundant protein D-29	3.29873	2.03005	0.0009		no GO terms
Xvis03_221325-PA	processed-gene-6.29-mRNA-1 protein Name:"Similar to B19.4 Late embryogenesis abundant protein B19.4 (Hordeum vulgare)" AED:0.16 eAED:0.16 QI:0|0.66|0.5|0.75|1|1|4|117|181	3.84307	1.81639	0.00126	IPR038956 (PFAM)	no GO terms
Xvis03_210802-PA	processed-gene-9.8-mRNA-1 protein Name:"Similar to LTI65 Low-temperature-induced 65 kDa protein (Arabidopsis thaliana)" AED:0.00 eAED:0.00 QI:247|1|1|1|1|5|289|574	3.50713	2.00575	0.00161		P:GO:0009737
Xvis03_216950-PA	augustus-gene-2.19-mRNA-1 protein Name:"Similar to 11 kDa late embryogenesis abundant protein (Helianthus annuus)" AED:0.13 eAED:0.13 QI:0|0.5|0.33|0.66|1|1|3|337|255	5.28524	1.65506	0.00189	IPR005513 (PFAM	P:GO:0009793
Xvis03_221252-PA	augustus-gene-6.27-mRNA-1 protein Name:"Similar to SPG20 Spartin (Homo sapiens)" AED:0.04 eAED:0.04 QI:93|1|1|1|0.75|0.6|5|21|403	2.61495	2.13635	0.00196	IPR009686 (PFAM);	no GO terms
Xvis03_219751-PA	augustus-gene-2.77-mRNA-1 protein Name:"Similar to GAPC3 Glyceraldehyde-3-phosphate dehydrogenase 3, cytosolic (Oryza sativa subsp. japonica)" AED:0.27 eAED:0.27 QI:255|0.9|1|1|1|1|11|366|288	12.4061	0.86947	0.00568	IPR020831	F:GO:0016620; P:GO:0055114
Xvis03_211956-PA	embryonic protein DC-8 isoform X2	10.5462	1.45642	0.00591		no GO terms
Xvis03_221252-PA	augustus-gene-6.27-mRNA-1 protein Name:"Similar to SPG20 Spartin (Homo sapiens)" AED:0.04 eAED:0.04 QI:93|1|1|1|0.75|0.6|5|21|403	1.18863	2.13471	0.00628	IPR009686 (PFAM);	no GO terms
Xvis03_205230-PA	processed-gene-22.97-mRNA-1 protein Name:"Similar to RAB18 Dehydrin Rab18 (Arabidopsis thaliana)" AED:0.00 eAED:0.00 QI:93|1|1|1|1|2|247|147	5.05544	1.4358	0.00704	IPR000167 (PFAM)	P:GO:0009415
Xvis03_220790-PA	augustus-gene-7.89-mRNA-1 protein Name:"Similar to SYNPCC7002_A1590 Uncharacterized protein SYNPCC7002_A1590 (Synechococcus sp. (strain ATCC 27264 / PCC 7002 / PR-6))" AED:0.04	1.30524	2.0387	0.00743	IPR018971 (PFAM)	no GO terms

	eAED:0.04 QI:148|1|1|1|1|6|744|229					
Xvis03_221564-PA	augustus-gene-1.8-mRNA-1 protein Name:"Similar to Late embryogenesis abundant protein D-34 (Gossypium hirsutum)" AED:0.08 eAED:0.23 QI:0|0|0.5|1|1|1|2|238|274	2.20826	1.93331	0.0076	IPR007011 (PFAM)	no GO terms
Xvis03_223774-PA	augustus-gene-3.64-mRNA-1 protein Name:"Similar to LEA14-A Late embryogenesis abundant protein Lea14-A (Gossypium hirsutum)" AED:0.40 eAED:0.40 QI:0|0|0|1|1|1|2|0|155	3.55628	1.5758	0.00796	IPR004864 (PFAM	no GO terms
Xvis03_205230-PA	processed-gene-22.97-mRNA-1 protein Name:"Similar to RAB18 Dehydrin Rab18 (Arabidopsis thaliana)" AED:0.00 eAED:0.00 QI:93|1|1|1|1|2|247|147	7.33068	1.1034	0.01074	IPR000167 (PFAM)	P:GO:0009415
Xvis03_208058-PA	processed-gene-23.43-mRNA-1 protein Name:"Similar to CML18 Probable calcium-binding protein CML18 (Oryza sativa subsp. japonica)" AED:0.02 eAED:0.02 QI:0|-1|0|1|-1|1|1|0|161	0.9707	1.97236	0.01121		F:GO:0005509
Xvis03_218200-PA	augustus-gene-6.42-mRNA-1 protein Name:"Similar to PLP1 Patatin-like protein 1 (Oryza sativa subsp. japonica)" AED:0.26 eAED:0.26 QI:72|0.4|0.16|1|1|1|6|0|314	2.88987	1.4167	0.01223	IPR002641 (PFAM)	P:GO:0006629
Xvis03_220002-PA	processed-gene-8.116-mRNA-1 protein Name:"Similar to Desiccation-related protein PCC3-06 (Craterostigma plantagineum)" AED:0.00 eAED:0.00 QI:334|1|1|1|1|2|386|231	8.7458	1.4657	0.01353		no GO terms
Xvis03_221512-PA	processed-gene-2.27-mRNA-1 protein Name:"Similar to Late embryogenesis abundant protein 76 (Brassica napus)" AED:0.12 eAED:0.12 QI:0|0.33|0.5|0.75|1|1|4|219|192	1.44462	1.87719	0.01396		no GO terms
Xvis03_202655-PA	processed-gene-53.13-mRNA-1 protein Name:"Similar to CCT2 Choline-phosphate cytidylyltransferase 2 (Arabidopsis thaliana)" AED:0.15 eAED:0.15 QI:50|1|1|1|1|8|392|291	0.98801	1.89108	0.01521	IPR004821 (PFAM	F:GO:0003824; P:GO:0009058
Xvis03_221512-PA	processed-gene-2.27-mRNA-1 protein Name:"Similar to Late	3.83065	1.86211	0.01641		no GO terms

	embryogenesis abundant protein 76 (Brassica napus)" AED:0.12 eAED:0.12 QI:0|0.33|0.5|0.75|1|1|4|219|192					
Xvis03_225532-PA	processed-gene-0.13-mRNA-1 protein Name:"Similar to DHN3 Dehydrin DHN3 (Hordeum vulgare)" AED:0.00 eAED:0.00 QI:270|1|1|1|1|2|257|183	6.48103	1.13443	0.01683	IPR000167 (PFAM);	P:GO:0009415
Xvis03_221564-PA	augustus-gene-1.8-mRNA-1 protein Name:"Similar to Late embryogenesis abundant protein D-34 (Gossypium hirsutum)" AED:0.08 eAED:0.23 QI:0|0|0.5|1|1|1|2|238|274	1.7858	1.70738	0.01734	IPR007011 (PFAM)	no GO terms
Xvis03_220240-PA	augustus-gene-8.38-mRNA-1 protein Name:"Similar to LEA3 Late embryogenesis abundant protein, group 3 (Oryza sativa subsp. indica)" AED:0.00 eAED:0.00 QI:193|1|1|1|1|2|266|174	13.1791	1.18885	0.01741		no GO terms
Xvis03_220597-PA	processed-gene-1.22-mRNA-1 protein Name:"Similar to RAB18 Dehydrin Rab18 (Arabidopsis thaliana)" AED:0.00 eAED:0.00 QI:228|1|1|1|1|2|308|136	4.64528	1.30412	0.01772	IPR000167 (PFAM	P:GO:0009415
Xvis03_223451-PA	processed-gene-3.71-mRNA-1 protein Name:"Similar to CSP1 Cold shock protein 1 (Arabidopsis thaliana)" AED:0.30 eAED:0.30 QI:0|-1|0|1|-1|1|1|0|215	1.65454	1.62548	0.01843	IPR002059	F:GO:0003676; F:GO:0008270
Xvis03_223476-PA	augustus-gene-2.101-mRNA-1 protein Name:"Similar to Pyruvate kinase, cytosolic isozyme (Glycine max)" AED:0.04 eAED:0.04 QI:138|1|1|1|1|3|406|533	3.02161	1.18192	0.02167	IPR001697	F:GO:0000287; F:GO:0003824; F:GO:0004743; P:GO:0006096; F:GO:0030955
Xvis03_222223-PA	processed-gene-2.73-mRNA-1 protein Name:"Similar to HSP70 Heat shock cognate 70 kDa protein (Petunia hybrida)" AED:0.11 eAED:0.11 QI:205|0.5|0.33|0.66|1|1|3|0|710	18.4419	0.60753	0.02505	IPR013126	no GO terms
Xvis03_210802-PA	processed-gene-9.8-mRNA-1 protein Name:"Similar to LTI65 Low-temperature-induced 65 kDa protein (Arabidopsis thaliana)" AED:0.00 eAED:0.00 QI:247|1|1|1|1|5|289|574	18.1056	1.16935	0.02542		P:GO:0009737
Xvis03_213342-PA	processed-gene-10.36-mRNA-1 protein Name:"Similar to Histone H4 (Glycine max)"	8.21874	0.81696	0.0291	IPR001951	F:GO:0003677; F:GO:0046982

	AED:0.00 eAED:0.01 QI:0|-1|0|1|-1|1|1|0|103					
Xvis03_223476-PA	augustus-gene-2.101-mRNA-1 protein Name:"Similar to Pyruvate kinase, cytosolic isozyme (Glycine max)" AED:0.04 eAED:0.04 QI:138|1|1|1|1|3|406|533	3.53294	1.06002	0.03324	IPR001697	F:GO:0000287;F:GO:0003824; F:GO:0004743; P:GO:0006096; F:GO:0030955
Xvis03_202976-PA	augustus-gene-30.2-mRNA-1 protein Name:"Similar to Blue copper protein (Pisum sativum)" AED:0.02 eAED:0.02 QI:94|1|1|1|1|2|158|189	0.91783	1.60444	0.03689	IPR008972	F:GO:0009055
Xvis03_221126-PA	augustus-gene-1.32-mRNA-1 protein Name:"Similar to Mavicyanin (Cucurbita pepo)" AED:0.01 eAED:0.01 QI:65|1|1|1|1|1|2|153|186	0.73585	1.63058	0.03825	IPR008972)	F:GO:0009055
Xvis03_220240-PA	augustus-gene-8.38-mRNA-1 protein Name:"Similar to LEA3 Late embryogenesis abundant protein, group 3 (Oryza sativa subsp. indica)" AED:0.00 eAED:0.00 QI:193|1|1|1|1|1|2|266|174	7.28924	1.13228	0.03889		no GO terms
Xvis03_221252-PA	augustus-gene-6.27-mRNA-1 protein Name:"Similar to SPG20 Spartin (Homo sapiens)" AED:0.04 eAED:0.04 QI:93|1|1|1|0.75|0.6|5|21|403	2.68011	1.34372	0.03974	IPR009686 (PFAM)	no GO terms
Xvis03_205813-PA	processed-gene-6.86-mRNA-1 protein Name:"Similar to RUB2 Ubiquitin-NEDD8-like protein RUB2 (Oryza sativa subsp. japonica)" AED:0.04 eAED:0.04 QI:73|1|1|1|1|1|3|301|153	7.62962	0.8021	0.04235	IPR019956 (PRINTS)	F:GO:0005515
Xvis03_209096-PA	processed-gene-16.57-mRNA-1 protein Name:"Similar to ABP20 Auxin-binding protein ABP20 (Prunus persica)" AED:0.02 eAED:0.02 QI:173|1|1|1|1|1|2|671|206	9.19049	0.7264	0.04322	IPR001929 (PRINTS)	F:GO:0030145; F:GO:0045735
Xvis03_202124-PA	processed-gene-11.0-mRNA-1 protein Name:"Similar to UGPA UTP--glucose-1-phosphate uridylyltransferase (Musa acuminata)" AED:0.18 eAED:0.18 QI:271|0.88|0.89|1|1|1|19|372|458	8.90801	0.65467	0.0444		F:GO:0003983; P:GO:0006011; F:GO:0070569
Xvis03_204659-PA	augustus-gene-39.13-mRNA-1 protein Name:"Similar to PHS2 Alpha-glucan phosphorylase 2, cytosolic (Arabidopsis thaliana)" AED:0.23	2.41403	1.37564	0.04789	IPR000811	F:GO:0004645; P:GO:0005975; F:GO:0008184; F:GO:0030170

	eAED:0.23 QI:181|0.92|0.93|1|0.92|0.86|15|169|732					
Xvis03_221564-PA	augustus-gene-1.8-mRNA-1 protein Name:"Similar to Late embryogenesis abundant protein D-34 (Gossypium hirsutum)" AED:0.08 eAED:0.23 QI:0|0|0.5|1|1|1|2|238|274	0.97016	1.55308	0.04808	IPR007011 (PFAM);	no GO terms
Xvis03_209643-PA	processed-gene-16.29-mRNA-1 protein Name:"Similar to ERF1-3 Eukaryotic peptide chain release factor subunit 1-3 (Arabidopsis thaliana)" AED:0.00 eAED:0.00 QI:0|-1|0|1|-1|1|1|0|43	0.91371	1.54312	0.04923		F:GO:0003747; C:GO:0005737; P:GO:0006415

Table 3.3: List of differentially expressed proteins involved Late response to drying identified in *X. schlechteri* leaf samples.

Accession	Description	baseMean	log2FoldChange	p-value	InterPro	Go-Terms
Xvis03_220002-PA	processed-gene-8.116-mRNA-1 protein Name:"Similar to Desiccation-related protein PCC3-06 (Craterostigma plantagineum)" AED:0.00 eAED:0.00 QI:334|1|1|1|1|1|2|386|231	8.7458046	3.31018732	3.45E-09		no GO terms
Xvis03_220597-PA	processed-gene-1.22-mRNA-1 protein Name:"Similar to RAB18 Dehydrin Rab18 (Arabidopsis thaliana)" AED:0.00 eAED:0.00 QI:228|1|1|1|1|1|2|308|136	5.0554445 4	2.6869117	3.86E-08	IPR000167 (PFAM	P:GO:0009415
Xvis03_210802-PA	processed-gene-9.8-mRNA-1 protein Name:"Similar to LTI65 Low-temperature-induced 65 kDa protein (Arabidopsis thaliana)" AED:0.00 eAED:0.00 QI:247|1|1|1|1|1|5|289|574	3.5071254 8	3.1803771	9.73E-08	IPR037491 (PANTHER)	P:GO:0009737
Xvis03_216950-PA	augustus-gene-2.19-mRNA-1 protein Name:"Similar to 11 kDa late embryogenesis abundant protein (Helianthus annuus)" AED:0.13 eAED:0.13 QI:0|0.5|0.33|0.66|1|1|3|337|255	5.2852439 6	2.55766398	3.13E-07	IPR005513 (PFAM)	P:GO:0009793
Xvis03_222911-PA	processed-gene-1.35-mRNA-1 protein Name:"Similar to CHLI Magnesium-chelatase subunit ChlI, chloroplastic (Oryza sativa subsp. japonica)" AED:0.00 eAED:0.00 QI:218|1|1|1|1|1|3|269|418	4.0856321 4	2.65244542	3.22E-07	IPR000523 (PFAM)	F:GO:0005524; P:GO:0015995; F:GO:0016851
Xvis03_221512-PA	processed-gene-2.27-mRNA-1 protein Name:"Similar to Late embryogenesis abundant	3.8306486 8	3.86180989	3.60E-07		no GO terms

	protein 76 (Brassica napus)" AED:0.12 eAED:0.12 QI:0|0.33|0.5|0.75|1|1|4|219|192					
Xvis03_220363-PA	augustus-gene-1.54-mRNA-1 protein Name:"Similar to ECU03_1610 Uncharacterized protein ECU03_1610 (Encephalitozoon cuniculi (strain GB-M1))" AED:0.03 eAED:0.03 QI:89|1|1|1|1|2|303|232	3.9401913	3.03913605	4.19E-07		no GO terms
Xvis03_200762-PA	processed-gene-88.24-mRNA-1 protein Name:"Similar to At4g13010 Putative quinone-oxidoreductase homolog, chloroplastic (Arabidopsis thaliana)" AED:0.26 eAED:0.26 QI:0|1|0.75|1|1|1|4|216|327	4.9709242 5	2.45863907	4.22E-07	IPR013154 (PFAM	P:GO:0055114
Xvis03_218117-PA	augustus-gene-11.3-mRNA-1 protein Name:"Similar to Embryonic protein DC-8 (Daucus carota)" AED:0.04 eAED:0.04 QI:0|1|0.66|1|1|1|3|517|510	10.546181 4	2.54581223	5.48E-07	PTHR33836:SF1	P:GO:0009737
Xvis03_221252-PA	augustus-gene-6.27-mRNA-1 protein Name:"Similar to SPG20 Spartin (Homo sapiens)" AED:0.04 eAED:0.04 QI:93|1|1|1|0.75|0.6|5|21|403	2.6149506 2	3.21616006	8.75E-07	IPR009686 (PFAM)	no GO terms
Xvis03_221564-PA	augustus-gene-1.8-mRNA-1 protein Name:"Similar to Late embryogenesis abundant protein D-34 (Gossypium hirsutum)" AED:0.08 eAED:0.23 QI:0|0|0.5|1|1|1|2|238|274	3.2987273 7	2.82360633	1.02E-06	IPR007011 (PFAM	no GO terms
Xvis03_222911-PA	processed-gene-1.35-mRNA-1 protein Name:"Similar to CHLI Magnesium-chelatase subunit ChlI, chloroplastic (Oryza sativa subsp. japonica)" AED:0.00 eAED:0.00 QI:218|1|1|1|1|1|3|269|418	2.7114771 3	2.66300275	1.80E-06	IPR000523 (PFAM);	F:GO:0005524; P:GO:0015995; F:GO:0016851
Xvis03_221325-PA	processed-gene-6.29-mRNA-1 protein Name:"Similar to B19.4 Late embryogenesis abundant protein B19.4 (Hordeum vulgare)" AED:0.16 eAED:0.16 QI:0|0.66|0.5|0.75|1|1|4|117|181	3.8430709 4	2.5169091	1.85E-06	IPR038956 (PFAM)	no GO terms
Xvis03_212894-PA	augustus-gene-2.1-mRNA-1 protein Name:"Similar to PORB Protochlorophyllide reductase B, chloroplastic (Hordeum vulgare)" AED:0.09 eAED:0.09 QI:162|1|1|1|1|1|5|457|393	3.0514899 9	2.11243109	2.74E-06	IPR002347 (PRINTS)	F:GO:0016630; P:GO:0055114
Xvis03_220239-PA	augustus-gene-8.37-mRNA-1 protein Name:"Similar to Late embryogenesis abundant protein Dc3 (Daucus carota)"	3.7055560 5	2.62485384	3.81E-06		no GO terms

	AED:0.00 eAED:0.00 QI:288|1|1|1|1|2|197|146					
Xvis03_220597-PA	processed-gene-1.22-mRNA-1 protein Name:"Similar to RAB18 Dehydrin Rab18 (Arabidopsis thaliana)" AED:0.00 eAED:0.00 QI:228|1|1|1|1|2|308|136	7.3306810 4	1.81808993	5.89E-06	IPR000167 (PFAM)	P:GO:0009415
Xvis03_221564-PA	augustus-gene-1.8-mRNA-1 protein Name:"Similar to Late embryogenesis abundant protein D-34 (Gossypium hirsutum)" AED:0.08 eAED:0.23 QI:0|0|0.5|1|1|1|2|238|274	2.2082565 1	3.08392405	6.38E-06	IPR007011 (PFAM)	no GO terms
Xvis03_220240-PA	augustus-gene-8.38-mRNA-1 protein Name:"Similar to LEA3 Late embryogenesis abundant protein, group 3 (Oryza sativa subsp. indica)" AED:0.00 eAED:0.00 QI:193|1|1|1|1|2|266|174	7.2892394 1	2.29795564	8.88E-06		no GO terms
Xvis03_220790-PA	augustus-gene-7.89-mRNA-1 protein Name:"Similar to SYNPCC7002_A1590 Uncharacterized protein SYNPCC7002_A1590 (Synechococcus sp. (strain ATCC 27264 / PCC 7002 / PR-6))" AED:0.04 eAED:0.04 QI:148|1|1|1|1|6|744|229	1.3052415 1	3.2089502	9.54E-06	IPR018971 (PFAM)	no GO terms
Xvis03_221252-PA	augustus-gene-6.27-mRNA-1 protein Name:"Similar to SPG20 Spartin (Homo sapiens)" AED:0.04 eAED:0.04 QI:93|1|1|0.75|0.6|5|21|403	2.6801088 5	2.63188195	1.13E-05	IPR009686 (PFAM)	no GO terms
Xvis03_221564-PA	augustus-gene-1.8-mRNA-1 protein Name:"Similar to Late embryogenesis abundant protein D-34 (Gossypium hirsutum)" AED:0.08 eAED:0.23 QI:0|0|0.5|1|1|1|2|238|274	1.7858015 6	2.88970967	1.70E-05	IPR007011 (PFAM)	no GO terms
Xvis03_218117-PA	augustus-gene-11.3-mRNA-1 protein Name:"Similar to Embryonic protein DC-8 (Daucus carota)" AED:0.04 eAED:0.04 QI:0|1|0.66|1|1|1|3|517|510	4.6698475 7	2.51898187	1.74E-05		P:GO:0009737
Xvis03_225532-PA	processed-gene-0.13-mRNA-1 protein Name:"Similar to DHN3 Dehydrin DHN3 (Hordeum vulgare)" AED:0.00 eAED:0.00 QI:270|1|1|1|1|2|257|183	6.4810301 9	1.88977715	2.04E-05	IPR000167 (PFAM)	P:GO:0009415
Xvis03_202087-PA	augustus-gene-8.14-mRNA-1 protein Name:"Similar to AAE3 Oxalate--CoA ligase (Arabidopsis thaliana)" AED:0.02 eAED:0.02 QI:521|1|1|1|1|1|4|258|517	2.2123689 3	2.65731454	5.13E-05	IPR000873 (PFAM)	F:GO:0003824
Xvis03_204003-PA	augustus-gene-27.86-mRNA-1 protein Name:"Similar to Aldose reductase (Hordeum vulgare)" AED:0.09	3.1744073	2.13724642	6.79E-05	IPR020471	F:GO:0016491; P:GO:0055114

	eAED:0.09 QI:204|1|1|1|1|1|9|270|319					
Xvis03_203592-PA	augustus-gene-31.41-mRNA-1 protein Name:"Similar to 1-Cys peroxiredoxin (Medicago truncatula)" AED:0.00 eAED:0.00 QI:253|1|1|1|1|1|2|509|219	9.7038722 4	1.3351265	7.04E-05	IPR000866	F:GO:0016209; F:GO:0016491; P:GO:0045454; F:GO:0051920; P:GO:0055114
Xvis03_205034-PA	late embryogenesis abundant protein D-34-like	1.1958591 4	3.0903517 3	7.65E-05	IPR007011 (PFAM)	no GO terms
Xvis03_220240-PA	augustus-gene-8.38-mRNA-1 protein Name:"Similar to LEA3 Late embryogenesis abundant protein, group 3 (Oryza sativa subsp. indica)" AED:0.00 eAED:0.00 QI:193|1|1|1|1|1|2|266|174	13.179127 6	1.9179068 9	7.91E-05		no GO terms
Xvis03_220597-PA	processed-gene-1.22-mRNA-1 protein Name:"Similar to RAB18 Dehydrin Rab18 (Arabidopsis thaliana)" AED:0.00 eAED:0.00 QI:228|1|1|1|1|1|2|308|136	4.6452791 6	2.0413783 3	8.67E-05	IPR000167 (PFAM)	P:GO:0009415
Xvis03_220002-PA	processed-gene-8.116-mRNA-1 protein Name:"Similar to Desiccation-related protein PCC3-06 (Craterostigma plantagineum)" AED:0.00 eAED:0.00 QI:334|1|1|1|1|1|2|386|231	25.904908 3	1.6696899 1	0.000135873		no GO terms
Xvis03_221720-PA	augustus-gene-5.43-mRNA-1 protein Name:"Similar to EIF-5A2 Eukaryotic translation initiation factor 5A-2 (Nicotiana plumbaginifolia)" AED:0.05 eAED:0.05 QI:177|1|1|1|0.8|0.66|6|330|160	2.1835228	2.0957290 1	0.000160339	IPR020189 (PFAM)	F:GO:0003723; F:GO:0003746; P:GO:0006452; F:GO:0043022; P:GO:0045901; P:GO:0045905
Xvis03_223454-PA	processed-gene-3.78-mRNA-1 protein Name:"Similar to PCKR1 Peptidyl-prolyl cis-trans isomerase (Catharanthus roseus)" AED:0.02 eAED:0.02 QI:0|-1|0|1|-1|1|1|0|173	7.4809848 9	1.2664219 9	0.000163465	IPR002130	P:GO:0000413; F:GO:0003755
Xvis03_211917-PA	augustus-gene-8.2-mRNA-1 protein Name:"Similar to UGT78D2 UDP-glycosyltransferase 78D2 (Arabidopsis thaliana)" AED:0.00 eAED:0.00 QI:173|1|1|1|1|1|2|210|454	1.6966120 4	2.7851324 4	0.000169236	IPR002213 (PFAM);	F:GO:0016758
Xvis03_221252-PA	augustus-gene-6.27-mRNA-1 protein Name:"Similar to SPG20 Spartin (Homo sapiens)" AED:0.04 eAED:0.04 QI:93|1|1|1|0.75|0.6|5|21|403	1.1886259	2.8708791 4	0.000184897	IPR009686 (PFAM)	no GO terms
Xvis03_210802-PA	processed-gene-9.8-mRNA-1 protein Name:"Similar to LTI65 Low-temperature-induced 65 kDa protein (Arabidopsis thaliana)" AED:0.00 eAED:0.00 QI:247|1|1|1|1|1|5|289|574	18.105578 8	1.9090698 6	0.000202692	IPR037491 (PANTHER)	P:GO:0009737

Xvis03_221564-PA	augustus-gene-1.8-mRNA-1 protein Name:"Similar to Late embryogenesis abundant protein D-34 (Gossypium hirsutum)" AED:0.08 eAED:0.23 QI:0|0|0.5|1|1|1|2|238|274	0.9701643 4	2.81667177	0.000227483	IPR007011 (PFAM)	no GO terms
Xvis03_225199-PA	processed-gene-0.101-mRNA-1 protein Name:"Similar to Aldose reductase (Hordeum vulgare)" AED:0.14 eAED:0.14 QI:154|0.87|0.88|1|0.62|0.55|9|25|337	6.8555564 5	1.61453776	0.000230193	IPR020471	F:GO:0016491; P:GO:0055114
Xvis03_220240-PA	augustus-gene-8.38-mRNA-1 protein Name:"Similar to LEA3 Late embryogenesis abundant protein, group 3 (Oryza sativa subsp. indica)" AED:0.00 eAED:0.00 QI:193|1|1|1|1|2|266|174	10.717152 8	2.54688193	0.000231897		no GO terms
Xvis03_209653-PA	processed-gene-17.23-mRNA-1 protein Name:"Similar to Os01g0270100 Cysteine proteinase inhibitor 12 (Oryza sativa subsp. japonica)" AED:0.07 eAED:0.07 QI:0|0|0|1|1|1|4|0|225	6.0337838 4	1.29142461	0.000294989		F:GO:0004869
Xvis03_214372-PA	processed-gene-6.62-mRNA-1 protein Name:"Similar to Eukaryotic translation initiation factor 5A (Manihot esculenta)" AED:0.20 eAED:0.20 QI:188|1|1|1|0.8|0.66|6|353|159	2.3676169 7	1.93495142	0.000335124	IPR020189 (PFAM	F:GO:0003723; F:GO:0003746; P:GO:0006452; F:GO:0043022; P:GO:0045901; P:GO:0045905
Xvis03_217638-PA	augustus-gene-2.63-mRNA-1 protein Name:"Similar to CCR1 Cinnamoyl-CoA reductase 1 (Arabidopsis thaliana)" AED:0.07 eAED:0.07 QI:0|0|0|1|1|1|6|0|324	1.4292214 2	2.60042155	0.000362868	IPR036291 (SUPERFAMILY)	F:GO:0003824; F:GO:0050662
Xvis03_201015-PA	augustus-gene-109.105-mRNA-1 protein Name:"Similar to MSRB5 Peptide methionine sulfoxide reductase B5 (Oryza sativa subsp. japonica)" AED:0.11 eAED:0.11 QI:31|0.33|0.5|1|1|1|4|790|250	1.0200315 3	2.59500971	0.000419649	IPR002579 (PFAM	P:GO:0006979; F:GO:0016671; P:GO:0030091; F:GO:0033743; P:GO:0055114
Xvis03_223774-PA	augustus-gene-3.64-mRNA-1 protein Name:"Similar to LEA14-A Late embryogenesis abundant protein Lea14-A (Gossypium hirsutum)" AED:0.40 eAED:0.40 QI:0|0|0|1|1|2|0|155	2.6095367 3	2.08462994	0.000431468	IPR004864 (PFAM);	no GO terms
Xvis03_209643-PA	processed-gene-16.29-mRNA-1 protein Name:"Similar to ERF1-3 Eukaryotic peptide chain release factor subunit 1-3 (Arabidopsis thaliana)" AED:0.00 eAED:0.00 QI:0|-1|0|1|-1|1|1|0|437	0.9953838 5	2.67709713	0.000456625	IPR005142 (PFAM);	F:GO:0003747; C:GO:0005737; P:GO:0006415

Xvis03_222292-PA	processed-gene-3.63-mRNA-1 protein Name:"Similar to CML18 Probable calcium-binding protein CML18 (Oryza sativa subsp. japonica)" AED:0.02 eAED:0.02 QI:0|-1|0|1|-1|1|1|0|161	0.9707048 7	2.64320394	0.000502823	IPR002048 (PFAM);	F:GO:0005509
Xvis03_206202-PA	processed-gene-9.17-mRNA-1 protein Name:"Similar to GMPM1 18 kDa seed maturation protein (Glycine max)" AED:0.23 eAED:0.23 QI:0|-1|0|1|-1|1|1|0|132	0.7758309 1	2.58855416	0.000767778	IPR005513 (PFAM)	P:GO:0009793
Xvis03_223451-PA	processed-gene-3.71-mRNA-1 protein Name:"Similar to CSP1 Cold shock protein 1 (Arabidopsis thaliana)" AED:0.30 eAED:0.30 QI:0|-1|0|1|-1|1|1|0|215	1.654539	2.16349653	0.000962503	IPR002059 (PFAM)	F:GO:0003676; F:GO:0008270
Xvis03_207466-PA	augustus-gene-21.70-mRNA-1 protein Name:"Similar to FLK Flowering locus K homology domain (Arabidopsis thaliana)" AED:0.22 eAED:0.22 QI:168|0.83|0.85|1|0.83|0.71|7|306|448	1.6807551 6	1.96005756	0.001155202		F:GO:0003723
Xvis03_202655-PA	processed-gene-53.13-mRNA-1 protein Name:"Similar to CCT2 Choline-phosphate cytidylyltransferase 2 (Arabidopsis thaliana)" AED:0.15 eAED:0.15 QI:50|1|1|1|1|8|392|291	0.9880117 4	2.43401057	0.001452068	IPR004821 (PFAM)	F:GO:0003824; P:GO:0009058
Xvis03_208182-PA	processed-gene-16.15-mRNA-1 protein Name:"Similar to EIF-5A2 Eukaryotic translation initiation factor 5A-2 (Nicotiana plumbaginifolia)" AED:0.11 eAED:0.11 QI:80|1|1|1|0.8|0.66|6|225|159	2.9786649 2	1.47675032	0.001520635	IPR001884	F:GO:0003723; F:GO:0003746; P:GO:0006452; F:GO:0043022; P:GO:0045901; P:GO:0045905
Xvis03_220599-PA	augustus-gene-1.77-mRNA-1 protein Name:"Similar to DHN1 Dehydrin DHN1 (Hordeum vulgare)" AED:0.00 eAED:0.00 QI:161|1|1|1|1|1|2|370|123	1.2881543 5	2.15460314	0.001607037	IPR000167 (PFAM)	P:GO:0009415
Xvis03_207220-PA	augustus-gene-29.99-mRNA-1 protein Name:"Similar to Bowman-Birk type trypsin inhibitor (Triticum aestivum)" AED:0.14 eAED:0.14 QI:36|1|1|1|1|1|2|205|120	1.3557005 2	2.18560715	0.001960747	IPR000877 (PFAM	F:GO:0004867; C:GO:0005576
Xvis03_222487-PA	processed-gene-2.59-mRNA-1 protein Name:"Similar to At4g22670 FAM10 family protein At4g22670 (Arabidopsis thaliana)" AED:0.11 eAED:0.11 QI:137|0.9|0.90|1|1|1|11|173|362	1.2118746	2.09622921	0.002077646	IPR034649 (PFAM)	F:GO:0005515; F:GO:0046983
Xvis03_218117-PA	augustus-gene-11.3-mRNA-1 protein Name:"Similar to Embryonic protein DC-8 (Daucus carota)" AED:0.04	11.156628 1	2.02192060	0.002120582		P:GO:0009737

	eAED:0.04 QI:0|1|0.66|1|1|1|3|517|510					
Xvis03_221354-PA	augustus-gene-2.78-mRNA-1 protein Name:"Similar to RPS12 40S ribosomal protein S12 (Hordeum vulgare)" AED:0.26 eAED:0.26 QI:0|1|0.75|1|1|1|4|274|184	0.9335730 1	2.33749638	0.002343013	IPR004038 (PFAM)	F:GO:0003735; C:GO:0005840; P:GO:0006412
Xvis03_207210-PA	augustus-gene-28.48-mRNA-1 protein Name:"Similar to CLPB3 Chaperone protein ClpB3, mitochondrial (Oryza sativa subsp. japonica)" AED:0.12 eAED:0.12 QI:139|1|1|1|1|10|182|968	3.1912218 2	1.71878718	0.002414538	IPR003959 (PFAM)	F:GO:0005524; C:GO:0005737; P:GO:0009408; P:GO:0019538; P:GO:0042026
Xvis03_213772-PA	processed-gene-11.46-mRNA-1 protein Name:"Similar to MT4A Metallothionein-like protein 4A (Oryza sativa subsp. japonica)" AED:0.00 eAED:0.00 QI:173|1|1|1|1|2|379|80	0.6676822	2.38067769	0.002496221	IPR000347 (PFAM)	F:GO:0046872
Xvis03_215569-PA	augustus-gene-5.91-mRNA-1 protein Name:"Similar to Carbonic anhydrase, chloroplastic (Hordeum vulgare)" AED:0.12 eAED:0.12 QI:674|1|1|1|1|8|205|260	12.652092 3	1.06362962	0.002688392	IPR001765 (PFAM	F:GO:0004089; F:GO:0008270
Xvis03_216330-PA	processed-gene-6.102-mRNA-1 protein Name:"Similar to PED1 3-ketoacyl-CoA thiolase 2, peroxisomal (Arabidopsis thaliana)" AED:0.14 eAED:0.14 QI:702|0.85|0.93|0.93|1|1|15|1904|479	2.1421563 1	1.71951601	0.003016808	IPR002155	F:GO:0003824; F:GO:0016747
Xvis03_200473-PA	processed-gene-61.44-mRNA-1 protein Name:"Similar to HOP3 Hsp70-Hsp90 organizing protein 3 (Arabidopsis thaliana)" AED:0.09 eAED:0.09 QI:150|1|1|1|1|1|7|289|574	1.3605723 6	2.19900046	0.002549607	IPR011990	F:GO:0005515
Xvis03_212894-PA	augustus-gene-2.1-mRNA-1 protein Name:"Similar to PORB Protochlorophyllide reductase B, chloroplastic (Hordeum vulgare)" AED:0.09 eAED:0.09 QI:162|1|1|1|1|1|5|457|393	0.8636714 2	2.28363271	0.002617543	IPR002347	F:GO:0016630; P:GO:0055114
Xvis03_219979-PA	processed-gene-5.16-mRNA-1 protein Name:"Similar to GMPM1 18 kDa seed maturation protein (Glycine max)" AED:0.00 eAED:0.00 QI:97|1|1|1|1|2|370|156	2.1927572 5	1.85844828	0.003530214	IPR005513 (PFAM)	P:GO:0009793
Xvis03_223144-PA	processed-gene-3.56-mRNA-1 protein Name:"Similar to RBCS1 Ribulose bisphosphate carboxylase small chain, chloroplastic (Musa acuminata)" AED:0.05 eAED:0.05 QI:145|1|1|1|1|3|356|174	11.937209	0.884589551	0.003578017	IPR024681	no GO terms

Xvis03_221236-PA	augustus-gene-4.54-mRNA-1 protein Name:"Similar to PXG Peroxygenase (Oryza sativa subsp. japonica)" AED:0.38 eAED:0.38 QI:85|0.66|0.85|0.85|1|1|7|299|316	2.1844627	1.63025003	0.003880978	IPR007736 (PFAM);	no GO terms
Xvis03_202954-PA	augustus-gene-28.13-mRNA-1 protein Name:"Similar to RPT1 26S protease regulatory subunit 7 (Prunus persica)" AED:0.05 eAED:0.05 QI:150|1|1|1|1|10|313|427	0.7858625	2.27520881	0.003897195	IPR041569 (PFAM)	F:GO:0005524; C:GO:0005737; F:GO:0016787; P:GO:0030163
Xvis03_205232-PA	processed-gene-22.101-mRNA-1 protein Name:"Similar to DHN1 Dehydrin DHN1 (Hordeum vulgare)" AED:0.36 eAED:0.36 QI:115|1|1|1|1|2|350|132	0.7488657	2.23928792	0.004190054	IPR000167 (PFAM)	P:GO:0009415
Xvis03_208328-PA	desiccation-related protein PCC13-62-like	14.197445 7	1.0339301	0.00423904	PF13668 (PFAM)	no GO terms
Xvis03_224660-PA	processed-gene-1.62-mRNA-1 protein Name:"Similar to FEN1 Flap endonuclease 1 (Zea mays)" AED:0.25 eAED:0.26 QI:20|0.7|0.71|0.95|1|1|21|362|621	0.7900292 6	2.17742296	0.004613511	IPR006084 (PRINTS)	F:GO:0003735; F:GO:0004518; C:GO:0005840; P:GO:0006281; P:GO:0006412; F:GO:0016788
Xvis03_205367-PA	augustus-gene-34.43-mRNA-1 protein Name:"Similar to MTA Metallothionein-like protein 1 (Pisum sativum)" AED:0.00 eAED:0.00 QI:175|1|1|1|1|2|359|83	0.7132959 4	2.14079999	0.005563873	IPR000347 (PFAM);	F:GO:0046872
Xvis03_219055-PA	augustus-gene-7.46-mRNA-1 protein Name:"Similar to TDX TPR repeat-containing thioredoxin TDX (Arabidopsis thaliana)" AED:0.04 eAED:0.04 QI:262|1|1|1|1|1|11|486|390	3.1299734 9	1.27228045	0.006235578	IPR034649 (PFAM)	F:GO:0005515; F:GO:0046983
Xvis03_220076-PA	augustus-gene-4.88-mRNA-1 protein Name:"Similar to GDCSH Glycine cleavage system H protein, mitochondrial (Oryza sativa subsp. japonica)" AED:0.04 eAED:0.04 QI:127|1|1|1|1|1|4|484|165	1.8467886 2	1.54574592	0.006344124	IPR017453	C:GO:0005960; P:GO:0019464
Xvis03_204022-PA	processed-gene-29.69-mRNA-1 protein Name:"Similar to RANBP1C Ran-binding protein 1 homolog c (Arabidopsis thaliana)" AED:0.01 eAED:0.01 QI:85|1|1|1|1|1|4|338|224	1.2867017 4	1.82668147	0.006795094	IPR000156 (PFAM)	P:GO:0046907
Xvis03_216515-PA	augustus-gene-8.70-mRNA-1 protein Name:"Similar to SAPK7 Serine/threonine-protein kinase SAPK7 (Oryza sativa subsp. japonica)" AED:0.12 eAED:0.12 QI:115|0.83|1|1|1|1|7|226|305	1.4089568 1	1.86595213	0.00701349	IPR011009	F:GO:0004672; F:GO:0005524; P:GO:0006468

Xvis03_205512-PA	processed-gene-10.28-mRNA-1 protein Name:"Similar to Hsp83 Heat shock protein 83 (Drosophila melanogaster)" AED:0.12 eAED:0.12 QI:147|1|1|1|1|19|333|803	5.9264619 8	1.09874135	0.007985264	IPR020575 (PRINTS	F:GO:0005524; P:GO:0006457; F:GO:0051082
Xvis03_215434-PA	augustus-gene-6.51-mRNA-1 protein Name:"Similar to Os01g0253300 Importin subunit alpha-1a (Oryza sativa subsp. japonica)" AED:0.21 eAED:0.21 QI:191|0.81|0.75|1|1|1|12|0|614	0.5923643 7	2.07947118	0.008324319	IPR011989 (	F:GO:0005515; C:GO:0005634; C:GO:0005737; P:GO:0006606; F:GO:0008565; F:GO:0061608
Xvis03_225042-PA	augustus-gene-0.56-mRNA-1 protein Name:"Similar to CSD2 Superoxide dismutase [Cu-Zn] 2, chloroplastic (Arabidopsis thaliana)" AED:0.13 eAED:0.13 QI:217|0.85|0.87|1|1|1|8|225|226	10.894930 1	0.77067073	0.008511462	IPR001424 (PRINTS)	P:GO:0006801; F:GO:0046872
Xvis03_221236-PA	augustus-gene-4.54-mRNA-1 protein Name:"Similar to PXG Peroxygenase (Oryza sativa subsp. japonica)" AED:0.38 eAED:0.38 QI:85|0.66|0.85|0.85|1|1|7|299|316	2.1381232 1	1.5111337	0.009316845	IPR007736 (PFAM)	no GO terms
Xvis03_224887-PA	augustus-gene-0.36-mRNA-1 protein Name:"Similar to At4g12130 Putative transferase At4g12130, mitochondrial (Arabidopsis thaliana)" AED:0.05 eAED:0.05 QI:50|1|1|1|1|5|427|411	1.7266701	1.545695	0.010231088	IPR017703	F:GO:0005515
Xvis03_210337-PA	augustus-gene-8.1-mRNA-1 protein Name:"Similar to RPS12 40S ribosomal protein S12 (Hordeum vulgare)" AED:0.38 eAED:0.38 QI:0|1|0.75|1|1|1|4|393|161	0.7889782 9	2.00466686	0.010436181	IPR000530 (PRINTS	F:GO:0003735; C:GO:0005840; P:GO:0006412
Xvis03_212520-PA	augustus-gene-6.14-mRNA-1 protein Name:"Similar to TUFB1 Elongation factor Tu, chloroplastic (Glycine max)" AED:0.04 eAED:0.16 QI:0|0|0.5|1|1|1|2|351|455	4.5985812	0.98459742	0.012595747	IPR000795 (PRINTS)	F:GO:0003746; F:GO:0003924; F:GO:0005525; P:GO:0006414
Xvis03_219784-PA	processed-gene-6.0-mRNA-1 protein Name:"Similar to MBF1B Multiprotein-bridging factor 1b (Arabidopsis thaliana)" AED:0.06 eAED:0.06 QI:115|1|1|1|1|1|4|351|141	1.0094991	1.86771964	0.013309481	IPR013729 (PFAM)	F:GO:0003677
Xvis03_202784-PA	processed-gene-9.6-mRNA-1 protein Name:"Similar to At5g12110 Elongation factor 1-beta 1 (Arabidopsis thaliana)" AED:0.07 eAED:0.07 QI:28|1|1|1|1|6|211|226	2.9260132 7	1.15718136	0.013874725	IPR014717	F:GO:0003746; P:GO:0006414
Xvis03_214871-PA	augustus-gene-0.9-mRNA-1 protein Name:"Similar to CYS6 Cysteine proteinase inhibitor 6 (Arabidopsis	3.3072269 5	1.09143226	0.013951824	IPR000010 (PFAM);	F:GO:0004869

	thaliana)" AED:0.25 eAED:0.25 QI:34|0.2|0.33|1|0.8|0.83|6|0|237					
Xvis03_217196-PA	augustus-gene-1.26-mRNA-1 protein Name:"Similar to AKR2 Ankyrin repeat domain-containing protein 2 (Arabidopsis thaliana)" AED:0.11 eAED:0.11 QI:0|0|0|1|1|1|6|0|276	0.9835682 7	1.77529497	0.014129423	IPR020683 (PFAM);	F:GO:0005515
Xvis03_215153-PA	augustus-gene-12.40-mRNA-1 protein Name:"Similar to RZ1B Glycine-rich RNA-binding protein RZ1B (Arabidopsis thaliana)" AED:0.25 eAED:0.25 QI:0|1|1|1|0.5|0.33|3|1599|326	0.7384757 5	1.83855001	0.01762934	IPR000504 (PFAM);	F:GO:0003676; F:GO:0008270
Xvis03_218200-PA	augustus-gene-6.42-mRNA-1 protein Name:"Similar to PLP1 Patatin-like protein 1 (Oryza sativa subsp. japonica)" AED:0.26 eAED:0.26 QI:72|0.4|0.16|1|1|1|6|0|314	2.8898699 1	1.30647099	0.01774307	IPR002641 (PFAM);	P:GO:0006629
Xvis03_225532-PA	processed-gene-0.13-mRNA-1 protein Name:"Similar to DHN3 Dehydrin DHN3 (Hordeum vulgare)" AED:0.00 eAED:0.00 QI:270|1|1|1|1|2|257|183	1.1125766 4	1.59920624	0.018250186	IPR000167 (PFA	P:GO:0009415
Xvis03_202929-PA	augustus-gene-26.5-mRNA-1 protein Name:"Similar to RPL23A 60S ribosomal protein L23 (Arabidopsis thaliana)" AED:0.39 eAED:0.40 QI:0|0|0|0.5|1|1|6|0|279	2.3983112 9	1.20009629	0.018286027	IPR000218 (PFAM)	F:GO:0003735; C:GO:0005840; P:GO:0006412
Xvis03_207625-PA	processed-gene-8.99-mRNA-1 protein Name:"Similar to COR47 Dehydrin COR47 (Arabidopsis thaliana)" AED:0.00 eAED:0.00 QI:100|1|1|1|1|1|2|435|268	1.8966244 9	1.72089728	0.018644009	IPR000167 (PFAM)	P:GO:0009415
Xvis03_221754-PA	augustus-gene-1.62-mRNA-1 protein Name:"Similar to MORF1 Multiple organellar RNA editing factor 1, mitochondrial (Arabidopsis thaliana)" AED:0.23 eAED:0.23 QI:47|1|1|1|0.75|0.6|5|384|406	0.9366691 8	1.72895072	0.01875143	IPR039206 (PANTHER);	P:GO:0016554
Xvis03_205232-PA	processed-gene-22.101-mRNA-1 protein Name:"Similar to DHN1 Dehydrin DHN1 (Hordeum vulgare)" AED:0.36 eAED:0.36 QI:115|1|1|1|1|1|2|350|132	1.4671627 6	1.58392948	0.018902918	IPR000167 (PFAM)	P:GO:0009415
Xvis03_218158-PA	augustus-gene-3.24-mRNA-1 protein Name:"Similar to Glutaredoxin (Ricinus communis)" AED:0.01 eAED:0.01 QI:220|1|1|1|1|1|4|501|106	2.8221512 7	1.16718112	0.019440464	IPR014025	F:GO:0009055; F:GO:0015035; P:GO:0045454

Xvis03_200250-PA	processed-gene-30.2-mRNA-1 protein Name:"Similar to HSP70 Stromal 70 kDa heat shock-related protein, chloroplastic (Pisum sativum)" AED:0.12 eAED:0.12 QI:46|0.75|0.88|0.88|1|1|9|437|741	19.813914	0.55487227	0.020900757	IPR013126 (PRINTS)	F:GO:0005524; P:GO:0006457; F:GO:0051082
Xvis03_205691-PA	processed-gene-31.124-mRNA-1 protein Name:"Similar to RuBisCO large subunit-binding protein subunit beta, chloroplastic (Pisum sativum)" AED:0.20 eAED:0.20 QI:97|0.8|0.81|0.87|0.93|0.87|16|0|678	13.019614	0.63729958	0.020957446	IPR001844	F:GO:0005524; P:GO:0042026
Xvis03_206458-PA	processed-gene-30.78-mRNA-1 protein Name:"Similar to PCKR1 Peptidyl-prolyl cis-trans isomerase (Catharanthus roseus)" AED:0.01 eAED:0.01 QI:0|-1|0|1|-1|1|1|0|173	4.5537958 2	0.88642056	0.0234936	IPR002130	P:GO:0000413; F:GO:0003755
Xvis03_209876-PA	augustus-gene-14.5-mRNA-1 protein Name:"Similar to RPS27B 40S ribosomal protein S27-2 (Arabidopsis thaliana)" AED:0.17 eAED:0.17 QI:86|1|1|1|0.66|0.75|4|47|86	0.7790348 2	1.76547852	0.021619681	IPR000592 (PFAM	F:GO:0003735; C:GO:0005840; P:GO:0006412
Xvis03_202103-PA	processed-gene-9.9-mRNA-1 protein Name:"Similar to Os02g0639900 Thioredoxin M1, chloroplastic (Oryza sativa subsp. japonica)" AED:0.00 eAED:0.00 QI:100|1|1|1|1|1|2|1208|190	1.7542165 8	1.35187505	0.021660558	PR00421	P:GO:0006662; F:GO:0015035; P:GO:0045454
Xvis03_221252-PA	augustus-gene-6.27-mRNA-1 protein Name:"Similar to SPG20 Spartin (Homo sapiens)" AED:0.04 eAED:0.04 QI:93|1|1|1|0.75|0.6|5|21|403	4.9004118 4	0.91443757	0.023504246	IPR009686 (PFAM)	no GO terms
Xvis03_212520-PA	augustus-gene-6.14-mRNA-1 protein Name:"Similar to TUFB1 Elongation factor Tu, chloroplastic (Glycine max)" AED:0.04 eAED:0.16 QI:0|0|0.5|1|1|1|2|351|455	6.5870721 9	0.7929123	0.028019252	IPR000795	F:GO:0003746; F:GO:0003924; F:GO:0005525; P:GO:0006414
Xvis03_211424-PA	augustus-gene-2.30-mRNA-1 protein Name:"Similar to GLX2-2 Hydroxyacylglutathione hydrolase cytoplasmic (Arabidopsis thaliana)" AED:0.23 eAED:0.23 QI:367|1|1|1|1|0.83|6|257|190	0.7837434 4	1.66394102	0.028671952	IPR032282 (PFAM)	F:GO:0004416; P:GO:0019243
Xvis03_221883-PA	processed-gene-4.16-mRNA-1 protein Name:"Similar to HVA22A HVA22-like protein a (Arabidopsis thaliana)" AED:0.26 eAED:0.26 QI:148|0.57|0.5|0.87|0.85|0.75|8|368|228	0.4564551 3	1.71820685	0.029354802	IPR004345 (PANTHER)	no GO terms

Xvis03_217585-PA	augustus-gene-6.44-mRNA-1 protein Name:"Similar to PAB8 Polyadenylate-binding protein 8 (Arabidopsis thaliana)" AED:0.09 eAED:0.09 QI:312|0.75|0.66|1|1|1|9|460|634	1.7435770 4	1.24665612	0.029518147	IPR012677	F:GO:0003676; F:GO:0003723
Xvis03_209548-PA	processed-gene-8.27-mRNA-1 protein Name:"Similar to AN3 Naringenin,2-oxoglutarate 3-dioxygenase (Fragment) (Petunia hybrida)" AED:0.02 eAED:0.02 QI:65|1|1|1|1|1|3|192|370	0.8835437 7	1.66413309	0.03067983	IPR027443	F:GO:0016491; P:GO:0055114
Xvis03_216135-PA	augustus-gene-2.5-mRNA-1 protein Name:"Similar to GSA Glutamate-1-semialdehyde 2,1-aminomutase, chloroplastic (Oryza sativa subsp. japonica)" AED:0.00 eAED:0.00 QI:90|1|1|1|1|1|3|296|478	3.3933298 2	0.93688668	0.033105684	IPR004639	F:GO:0003824; F:GO:0008483; F:GO:0030170; P:GO:0033014; F:GO:0042286
Xvis03_202562-PA	augustus-gene-46.31-mRNA-1 protein Name:"Similar to Major pollen allergen Cor a 1 isoforms 5, 6, 11 and 16 (Corylus avellana)" AED:0.26 eAED:0.26 QI:0|1|0.5|1|1|1|2|234|182	2.3364062 8	1.24519402	0.034320067	IPR000916 (PFAM)	P:GO:0006952
Xvis03_215759-PA	augustus-gene-6.67-mRNA-1 protein Name:"Similar to At5g39570 Uncharacterized protein At5g39570 (Arabidopsis thaliana)" AED:0.00 eAED:0.00 QI:88|1|1|1|1|1|2|401|452	0.8846234 4	1.65520634	0.035291239	IPR038943 (PANTHER)	F:GO:0070300
Xvis03_223860-PA	processed-gene-2.57-mRNA-1 protein Name:"Similar to v1g171563 Eukaryotic translation initiation factor 3 subunit G (Nematostella vectensis)" AED:0.02 eAED:0.02 QI:0|1|0.5|1|1|1|2|3401|289	1.2022400 2	1.37568463	0.037358344	IPR024675 (PFAM)	F:GO:0003676; F:GO:0003743; C:GO:0005737; C:GO:0005852
Xvis03_224754-PA	processed-gene-1.55-mRNA-1 protein Name:"Similar to At3g10130 Heme-binding-like protein At3g10130, chloroplastic (Arabidopsis thaliana)" AED:0.02 eAED:0.02 QI:0|-1|0|1|-1|1|1|0|209	0.5565459 9	1.62122527	0.039711403	IPR006917 (PFAM)	no GO terms
Xvis03_220719-PA	augustus-gene-6.9-mRNA-1 protein Name:"Similar to TSJT1 Stem-specific protein TSJT1 (Nicotiana tabacum)" AED:0.07 eAED:0.07 QI:59|0.5|0.8|0.8|1|1|5|232|256	0.5279493 4	1.61160659	0.041278577	IPR029055	no GO terms
Xvis03_208140-PA	processed-gene-11.6-mRNA-1 protein Name:"Similar to atad1a ATPase family AAA domain-containing protein 1-A (Danio rerio)" AED:0.12 eAED:0.12 QI:153|0.88|0.94|0.94|0.83|0.78|19|436|852	0.4586671 1	1.57057859	0.041779846	IPR003959 (PFAM)	F:GO:0005524

Xvis03_215764-PA	augustus-gene-6.61-mRNA-1 protein Name:"Similar to 29 kDa ribonucleoprotein B, chloroplastic (Nicotiana sylvestris)" AED:0.25 eAED:0.25 QI:94|0.75|0.6|0.8|1|1|5|0|355	3.0731014	0.95186173	0.042728409	IPR012677	F:GO:0003676
Xvis03_201416-PA	processed-gene-12.20-mRNA-1 protein Name:"Similar to Phosphoglycerate kinase, chloroplastic (Nicotiana tabacum)" AED:0.04 eAED:0.04 QI:190|1|1|1|1|6|289|477	21.548955	0.4267875	0.043273487	IPR001576	F:GO:0004618; P:GO:0006096
Xvis03_220549-PA	processed-gene-6.81-mRNA-1 protein Name:"Similar to NFS2 Cysteine desulfurase 1, chloroplastic (Arabidopsis thaliana)" AED:0.13 eAED:0.23 QI:55|0.77|0.8|1|1|1|10|0|498	0.5211484	1.58814569	0.043976028	IPR015421	F:GO:0003824; P:GO:0006534; F:GO:0030170; F:GO:0031071
Xvis03_203140-PA	processed-gene-45.24-mRNA-1 protein Name:"Similar to HSP81-1 Heat shock protein 81-1 (Oryza sativa subsp. japonica)" AED:0.48 eAED:0.48 QI:0|-1|0|1|-1|1|1|0|114	0.5419099	1.5849319	0.044355192	IPR001404 (PFAM)	F:GO:0005524; P:GO:0006457; F:GO:0051082
Xvis03_206453-PA	processed-gene-29.128-mRNA-1 protein Name:"Similar to CSP4 Cold shock domain-containing protein 4 (Arabidopsis thaliana)" AED:0.32 eAED:0.32 QI:0|-1|0|1|-1|1|1|0|231	1.3646643	1.28219745	0.044671688	PR01228	F:GO:0003676; F:GO:0008270
Xvis03_219977-PA	augustus-gene-5.85-mRNA-1 protein Name:"Similar to Os02g0194200 Zinc finger CCCH domain-containing protein 14 (Oryza sativa subsp. japonica)" AED:0.00 eAED:0.00 QI:185|1|1|1|1|1|3|411|290	0.5602625	1.55102977	0.045328627	IPR036612	F:GO:0003723; F:GO:0046872
Xvis03_222778-PA	processed-gene-2.13-mRNA-1 protein Name:"Similar to PR1 Pathogenesis-related protein 1 (Asparagus officinalis)" AED:0.28 eAED:0.28 QI:65|1|1|1|1|1|2|141|157	1.8705001	1.17876116	0.046245264	IPR000916 (PFAM)	P:GO:0006952
Xvis03_205594-PA	augustus-gene-17.68-mRNA-1 protein Name:"Similar to RPS27B 40S ribosomal protein S27-2 (Arabidopsis thaliana)" AED:0.09 eAED:0.09 QI:0|1|0.75|1|1|1|4|342|163	0.9846833	1.40368325	0.048067861	IPR000592 (PFAM)	F:GO:0003735; C:GO:0005840; P:GO:0006412
Xvis03_207368-PA	processed-gene-12.44-mRNA-1 protein Name:"Similar to Polyphenol oxidase, chloroplastic (Malus domestica)" AED:0.07 eAED:0.08 QI:0|-1|0|1|-1|1|1|0|578	8.3658069	0.72935219	0.049840164	IPR002227 (PFAM)	F:GO:0004097; F:GO:0016491; P:GO:0046148; P:GO:0055114
Xvis03_211532-PA	est_gff_Cufflinks-gene-11.15-mRNA-1 protein Name:"Similar to	3.15999	-2.188	0.00389	IPR000490 (PFAM)	

	Glucan endo-1,3-beta-glucosidase, acidic isoform (Zea mays)" AED:0.00 eAED:0.00 QI:59|1|1|1|1|2|102|335					
vis03_212894-PA	augustus-gene-2.1-mRNA-1 protein Name:"Similar to PORB Protochlorophyllide reductase B, chloroplastic (Hordeum vulgare)" AED:0.09 eAED:0.09 QI:162|1|1|1|1|5|457|393	3.05149	-1.8088	0.00687	IPR002347 (PFAM	
Xvis03_213363-PA	processed-gene-12.66-mRNA-1 protein Name:"Similar to Os09g0529100 Probable 6-phosphogluconolactonase 4, chloroplastic (Oryza sativa subsp. japonica)" AED:0.04 eAED:0.04 QI:89|1|1|1|1|3|259|276	0.91926	-1.9052	0.00974	IPR006148 (PFAM	F:GO:0004553; P:GO:0005975
Xvis03_224897-PA	augustus-gene-1.57-mRNA-1 protein Name:"Similar to HSP90 Endoplasmin homolog (Catharanthus roseus)" AED:0.10 eAED:0.10 QI:52|0.92|0.93|1|1|1|15|395|788	4.50708	-1.1669	0.00987	IPR003594 (PFAM);	F:GO:0016630; P:GO:0055114
Xvis03_224459-PA	augustus-gene-1.13-mRNA-1 protein Name:"Similar to RABA2A Ras-related protein RABA2a (Arabidopsis thaliana)" AED:0.02 eAED:0.02 QI:202|1|1|1|1|1|2|509|220	1.26609	-1.6274	0.01404	IPR001806 (PFAM)	P:GO:0005975; P:GO:0006098; F:GO:0017057
Xvis03_207311-PA	processed-gene-7.62-mRNA-1 protein Name:"Similar to ADK-B Adenylate kinase 4 (Oryza sativa subsp. japonica)" AED:0.05 eAED:0.05 QI:122|1|1|1|1|1|6|379|246	2.07578	-1.4418	0.01502	IPR007862 (PFAM)	F:GO:0005524; P:GO:0006457; F:GO:0051082
Xvis03_207665-PA	processed-gene-12.71-mRNA-1 protein Name:"Similar to HSP90 Endoplasmin homolog (Catharanthus roseus)" AED:0.12 eAED:0.12 QI:42|1|1|1|1|1|15|358|812	3.28464	-1.2209	0.01548	IPR003594 (PFAM	F:GO:0003924; F:GO:0005525
Xvis03_209992-PA	processed-gene-2.103-mRNA-1 protein Name:"Similar to Os06g0675700 Probable alpha-glucosidase Os06g0675700 (Oryza sativa subsp. japonica)" AED:0.08 eAED:0.08 QI:226|1|1|1|1|1|5|499|873	2.49202	-1.2614	0.01656	IPR025887 (PFAM)	F:GO:0004017; F:GO:0005524; P:GO:0006139; F:GO:0016776; F:GO:0019205
Xvis03_210350-PA	processed-gene-9.1-mRNA-1 protein Name:"Similar to TP53I3 Quinone oxidoreductase PIG3 (Homo sapiens)" AED:0.11 eAED:0.11 QI:0|0.44|0.5|0.7|1|1|10|268|486	1.93408	-1.5504	0.01721	IPR013149 (PFAM)	F:GO:0005524; P:GO:0006457; F:GO:0051082
Xvis03_216387-PA	augustus-gene-11.65-mRNA-1 protein Name:"Similar to Alpha-galactosidase (Coffea arabica)" AED:0.16 eAED:0.16 QI:81|1|1|1|0.92|0.92|14|139|642	3.48955	-1.0714	0.01845	IPR041233 (PFAM)	F:GO:0003824; F:GO:0004553; P:GO:0005975; F:GO:0030246
Xvis03_216480-PA	augustus-gene-6.109-mRNA-1 protein Name:"Similar to UVR8 Ultraviolet-B receptor UVR8 (Arabidopsis thaliana)" AED:0.10 eAED:0.10 QI:223|0.9|1|1|1|1|11|290|403	1.25457	-1.5671	0.02033	IPR000408	P:GO:0055114
Xvis03_207311-PA	processed-gene-7.62-mRNA-1 protein Name:"Similar to ADK-B Adenylate kinase 4 (Oryza sativa subsp. japonica)" AED:0.05 eAED:0.05 QI:122|1|1|1|1|1|6|379|246	2.07474	-1.3597	0.02359	IPR007862 (PFAM	F:GO:0003824; F:GO:0004553; P:GO:0005975

Xvis03_203608-PA	processed-gene-32.69-mRNA-1 protein Name:"Similar to PNSL1 Photosynthetic NDH subunit of lumenal location 1, chloroplastic (Arabidopsis thaliana)" AED:0.12 eAED:0.08 QI:81|1|0.85|1|1|1|7|565|263	0.923 83	-1.628 8	0.0251 9	IPR002683 (PFAM);	F:GO:0009881; P:GO:0010224; F:GO:0042803
Xvis03_206138-PA	processed-gene-3.62-mRNA-1 protein Name:"Similar to CHI4 Endochitinase PR4 (Phaseolus vulgaris)" AED:0.03 eAED:0.03 QI:30|1|1|1|1|1|2|158|277	1.246 83	-1.702 3	0.0271 2	IPR001002 (PFAM)	F:GO:0004017; F:GO:0005524; P:GO:0006139; F:GO:0016776; F:GO:0019205
Xvis03_219185-PA	processed-gene-8.51-mRNA-1 protein Name:"Similar to tal Transaldolase (Acidothermus cellulolyticus (strain ATCC 43068 / 11B))" AED:0.03 eAED:0.03 QI:60|0.83|0.85|1|1|1|7|483|446	0.544 74	-1.735 5	0.0277 7	IPR001585 (PFAM)	F:GO:0005509; C:GO:0009523; C:GO:0009654; P:GO:0015979; C:GO:0019898
Xvis03_202672-PA	processed-gene-54.103-mRNA-1 protein Name:"Similar to HEMC Porphobilinogen deaminase, chloroplastic (Oryza sativa subsp. japonica)" AED:0.01 eAED:0.01 QI:117|1|1|1|1|1|5|327|378	3.147 76	-1.086	0.0314	IPR022418 (PFAM)	F:GO:0004568; P:GO:0005975; P:GO:0006032; F:GO:0008061; P:GO:0016998
Xvis03_203714-PA	processed-gene-43.103-mRNA-1 protein Name:"Similar to At4g26910 Dihydrolipoyllysine-residue succinyltransferase component of 2-oxoglutarate dehydrogenase complex 2, mitochondrial (Arabidopsis thaliana)" AED:0.18 eAED:0.18 QI:18|1|1|1|0.85|0.8|15|384|475	4.416 19	-0.894 4	0.0325 4	IPR020828 (PFAM)	F:GO:0003824; F:GO:0004801; C:GO:0005737; P:GO:0005975; P:GO:0006098
Xvis03_207856-PA	augustus-gene-3.47-mRNA-1 protein Name:"Similar to GAPC2 Glyceraldehyde-3-phosphate dehydrogenase 2, cytosolic (Oryza sativa subsp. japonica)" AED:0.71 eAED:0.72 QI:0|0|0|0.66|1|1|6|0|224	7.893 22	-0.733	0.0328 8	IPR020828 (PFAM)	F:GO:0004418; P:GO:0033014
Xvis03_200416-PA	processed-gene-51.69-mRNA-1 protein Name:"Similar to CHLM Magnesium protoporphyrin IX methyltransferase, chloroplastic (Arabidopsis thaliana)" AED:0.34 eAED:0.34 QI:0|-1|0|1|-1|1|1|0|322	1.284 94	-1.548 5	0.0377 6	); IPR010940 (PFAM	F:GO:0004149; P:GO:0006099; F:GO:0016620; F:GO:0016746; C:GO:0045252; P:GO:0055114
Xvis03_220112-PA	augustus-gene-8.33-mRNA-1 protein Name:"Similar to RPL5 50S ribosomal protein L5, chloroplastic (Arabidopsis thaliana)" AED:0.02 eAED:0.03 QI:29|0.5|0.33|1|1|1|3|0|284	3.421 34	-0.937 8	0.0414 9	IPR031309 (PFAM)	F:GO:0016620; P:GO:0055114
Xvis03_215774-PA	augustus-gene-7.23-mRNA-1 protein Name:"Similar to CHLP Geranylgeranyl diphosphate reductase, chloroplastic (Nicotiana tabacum)" AED:0.00 eAED:0.00 QI:382|1|1|1|1|2|212|364	0.901 09	-1.542 3	0.0443 7	PTHR42685 (PANTHER)	P:GO:0015995; F:GO:0046406
Xvis03_213605-PA	processed-gene-14.84-mRNA-1 protein Name:"Similar to Os08g0288200 Probable adenylate kinase 5, chloroplastic (Oryza sativa subsp. japonica)" AED:0.22 eAED:0.22 QI:25|1|0.94|1|1|1|17|0|611	0.701 86	-1.537 1	0.0450 6	IPR018962 (PFAM)	F:GO:0003735; C:GO:0005840; P:GO:0006412
Xvis03_218927-PA	processed-gene-4.16-mRNA-1 protein Name:"Similar to PORB Protochlorophyllide reductase B,	2.115 55	-1.344 3	0.0478 4	IPR002347 (PFAM)	P:GO:0015979; P:GO:0015995; F:GO:0045550;

	chloroplastic (Hordeum vulgare)" AED:0.12 eAED:0.12 QI:128|0.75|0.6|1|1|1|5|341|353					P:GO:0051188; P:GO:0055114
Xvis03_212052-PA	augustus-gene-18.3-mRNA-1 protein Name:"Similar to RPN8A 26S proteasome non-ATPase regulatory subunit 7 homolog A (Arabidopsis thaliana)" AED:0.29 eAED:0.29 QI:0|0.9|0.81|0.90|1|1|11|444|363	0.87962	-1.4751	0.04822	IPR024969 (PFAM)	F:GO:0004017; F:GO:0005524; P:GO:0006139; F:GO:0016776; F:GO:0019205
Xvis03_211268-PA	processed-gene-9.25-mRNA-1 protein Name:"Similar to Vacuolar-processing enzyme (Citrus sinensis)" AED:0.07 eAED:0.07 QI:3|1|1|1|1|9|417|590	0.8108	-1.4811	0.04889	IPR001096	F:GO:0016630; P:GO:0055114
Xvis03_223095-PA	augustus-gene-3.96-mRNA-1 protein Name:"Similar to petC Cytochrome b6-f complex iron-sulfur subunit, chloroplastic (Oryza sativa subsp. japonica)" AED:0.11 eAED:0.11 QI:167|0.33|0.75|1|1|1|4|287|178	1.79206	-1.1934	0.04913	IPR005805	F:GO:0005515; C:GO:0005838
Xvis03_212113-PA	augustus-gene-6.61-mRNA-1 protein Name:"Similar to GGAT1 Glutamate--glyoxylate aminotransferase 1 (Arabidopsis thaliana)" AED:0.19 eAED:0.19 QI:107|0.85|0.93|0.93|0.85|0.93|15|450|533	3.88792	-2.4394	4.44E-05	IPR004839 (PFAM);	P:GO:0006508; F:GO:0008233
Xvis03_219859-PA	augustus-gene-3.73-mRNA-1 protein Name:"Similar to PSBO Oxygen-evolving enhancer protein 1, chloroplastic (Solanum lycopersicum)" AED:0.03 eAED:0.03 QI:216|1|1|1|1|2|224|332	18.7878	-1.2783	9.28E-05	IPR002628 (PFAM);	F:GO:0008121; F:GO:0009496; C:GO:0009507; C:GO:0016020; F:GO:0016491; F:GO:0016679; C:GO:0042651; F:GO:0045158; F:GO:0051537; P:GO:0055114
Xvis03_223853-PA	processed-gene-1.15-mRNA-1 protein Name:"Similar to RCA2 Ribulose bisphosphate carboxylase/oxygenase activase 2, chloroplastic (Larrea tridentata)" AED:0.12 eAED:0.12 QI:111|1|1|1|0.83|0.71|7|332|438	18.4585	-1.198	0.00026	IPR003959 (PFAM);	F:GO:0003824; P:GO:0009058; F:GO:0030170
Xvis03_204705-PA	processed-gene-11.1-mRNA-1 protein Name:"Similar to RPS17 40S ribosomal protein S17 (Solanum lycopersicum)" AED:0.06 eAED:0.06 QI:0|-1|0|1|-1|1|1|0|143	2.53029	-2.2506	0.0004	IPR001210 (PFAM);	C:GO:0009654; P:GO:0010207; F:GO:0010242; P:GO:0042549
Xvis03_214214-PA	processed-gene-11.33-mRNA-1 protein Name:"Similar to APX1 L-ascorbate peroxidase, cytosolic (Pisum sativum)" AED:0.17 eAED:0.17 QI:131|1|1|1|1|1|7|558|249	2.83113	-2.0161	0.00052	IPR002016	F:GO:0005524
Xvis03_223077-PA	processed-gene-1.89-mRNA-1 protein Name:"Similar to CAB13 Chlorophyll a-b binding protein 13, chloroplastic (Solanum lycopersicum)" AED:0.07 eAED:0.07 QI:182|1|1|1|1|1|4|188|263	2.97724	-1.9812	0.00056	IPR022796 (PFAM);	F:GO:0003735; C:GO:0005840; P:GO:0006412
Xvis03_223853-PA	processed-gene-1.15-mRNA-1 protein Name:"Similar to RCA2 Ribulose bisphosphate carboxylase/oxygenase activase 2, chloroplastic (Larrea tridentata)"	8.529	-1.4157	0.00061		F:GO:0004601; P:GO:0006979; F:GO:0020037; P:GO:0055114

	AED:0.12 eAED:0.12 QI:111|1|1|1|0.83|0.71|7|332|438					
Xvis03_204705-PA	processed-gene-11.1-mRNA-1 protein Name:"Similar to RPS17 40S ribosomal protein S17 (Solanum lycopersicum)" AED:0.06 eAED:0.06 QI:0|-1|0|1|-1|1|1|0|143	2.4569	-2.1525	0.00069	IPR001210 (PFAM);	P:GO:0009765; C:GO:0016020
Xvis03_220112-PA	augustus-gene-8.33-mRNA-1 protein Name:"Similar to RPL5 50S ribosomal protein L5, chloroplastic (Arabidopsis thaliana)" AED:0.02 eAED:0.03 QI:29|0.5|0.33|1|1|1|3|0|284	3.42134	-1.8424	0.00091	IPR031309 (PFAM)	F:GO:0005524
Xvis03_208337-PA	augustus-gene-6.16-mRNA-1 protein Name:"Similar to PSBO Oxygen-evolving enhancer protein 1, chloroplastic (Solanum lycopersicum)" AED:0.08 eAED:0.08 QI:229|1|1|1|0.5|0.33|3|86|332	20.0766	-1.0303	0.00095		F:GO:0003735; C:GO:0005840; P:GO:0006412
Xvis03_209988-PA	processed-gene-2.101-mRNA-1 protein Name:"Similar to PSBP Oxygen-evolving enhancer protein 2, chloroplastic (Cucumis sativus)" AED:0.32 eAED:0.32 QI:142|1|1|1|1|1|4|296|262	8.30561	-1.3232	0.00099	IPR002683 (PFAM);	F:GO:0003735; C:GO:0005840; P:GO:0006412
Xvis03_211060-PA	processed-gene-14.7-mRNA-1 protein Name:"Similar to Chlorophyll a-b binding protein, chloroplastic (Spinacia oleracea)" AED:0.01 eAED:0.01 QI:0|-1|0|1|-1|1|1|0|268	3.49088	-1.5912	0.00166	IPR023329	C:GO:0009654; P:GO:0010207; F:GO:0010242; P:GO:0042549
Xvis03_209992-PA	processed-gene-2.103-mRNA-1 protein Name:"Similar to Os06g0675700 Probable alpha-glucosidase Os06g0675700 (Oryza sativa subsp. japonica)" AED:0.08 eAED:0.08 QI:226|1|1|1|1|1|5|499|873	2.49202	-1.8609	0.00168	IPR025887 (PFAM)	F:GO:0005509; C:GO:0009523; C:GO:0009654; P:GO:0015979; C:GO:0019898
Xvis03_222105-PA	augustus-gene-5.53-mRNA-1 protein Name:"Similar to APXT L-ascorbate peroxidase T, chloroplastic (Arabidopsis thaliana)" AED:0.32 eAED:0.32 QI:0|0.5|0.45|0.72|0.9|0.81|11|0|364	1.93413	-2.1494	0.00227	IPR002016	P:GO:0009765; C:GO:0016020
Xvis03_219178-PA	processed-gene-7.19-mRNA-1 protein Name:"Similar to CNX1 Calnexin homolog 1 (Arabidopsis thaliana)" AED:0.09 eAED:0.09 QI:144|1|1|1|0.83|0.71|7|378|540	5.20508	-1.5791	0.00236	IPR001580	F:GO:0003824; F:GO:0004553; P:GO:0005975; F:GO:0030246
Xvis03_223899-PA	processed-gene-1.98-mRNA-1 protein Name:"Similar to RCA1 Ribulose bisphosphate carboxylase/oxygenase activase, chloroplastic (Zea mays)" AED:0.16 eAED:0.16 QI:463|0.90|0.91|1|0.81|0.66|12|225|280	20.31	-0.9016	0.00305	IPR003959 (PFAM);	F:GO:0004601; P:GO:0006979; F:GO:0020037; P:GO:0055114
Xvis03_201883-PA	augustus-gene-50.73-mRNA-1 protein Name:"Similar to APX1 L-ascorbate peroxidase, cytosolic (Pisum sativum)" AED:0.15 eAED:0.15 QI:0|0.85|0.75|1|1|0.87|8|414|307	2.25691	-1.8346	0.00312	IPR002207 (PRINTS);	F:GO:0005509; F:GO:0005515; C:GO:0005783; P:GO:0006457; F:GO:0051082
Xvis03_206991-PA	augustus-gene-10.52-mRNA-1 protein Name:"Similar to CPN21 20 kDa chaperonin, chloroplastic (Arabidopsis thaliana)" AED:0.07 eAED:0.07 QI:99|1|1|1|1|5|439|254	5.80316	-1.3029	0.00337	IPR020818	F:GO:0005524

Xvis03_207825-PA	processed-gene-26.31-mRNA-1 protein Name:"Similar to RPS17 40S ribosomal protein S17 (Solanum lycopersicum)" AED:0.03 eAED:0.03 QI:0|-1|0|1|-1|1|1|0|146	3.87617	-1.5202	0.00355	IPR036401	F:GO:0004601; P:GO:0006979; F:GO:0020037; P:GO:0055114
Xvis03_213217-PA	augustus-gene-16.1-mRNA-1 protein Name:"Similar to CSP41A Chloroplast stem-loop binding protein of 41 kDa a, chloroplastic (Arabidopsis thaliana)" AED:0.01 eAED:0.01 QI:41|1|1|1|1|1|6|52|409	9.28885	-1.198	0.00395		P:GO:0006457; F:GO:0046914; P:GO:1901671
Xvis03_221799-PA	processed-gene-5.86-mRNA-1 protein Name:"Similar to LHCB5 Chlorophyll a-b binding protein CP26, chloroplastic (Arabidopsis thaliana)" AED:0.06 eAED:0.06 QI:123|0.8|0.83|1|1|1|6|161|279	3.70776	-1.4652	0.00433	IPR022796 (PFAM);	F:GO:0003735; C:GO:0005840; P:GO:0006412
Xvis03_225066-PA	processed-gene-0.82-mRNA-1 protein Name:"Similar to Chlorophyll a-b binding protein, chloroplastic (Spinacia oleracea)" AED:0.00 eAED:0.00 QI:0|-1|0|1|-1|1|1|0|268	4.2432	-1.3049	0.00457	IPR022796 (PFAM);	F:GO:0003824; F:GO:0050662
Xvis03_203608-PA	processed-gene-32.69-mRNA-1 protein Name:"Similar to PNSL1 Photosynthetic NDH subunit of lumenal location 1, chloroplastic (Arabidopsis thaliana)" AED:0.12 eAED:0.08 QI:81|1|0.85|1|1|1|7|565|263	0.92383	-2.0582	0.0052	IPR002683 (PFAM);	P:GO:0009765; C:GO:0016020
Xvis03_218527-PA	augustus-gene-7.89-mRNA-1 protein Name:"Similar to FBPban1 Fructose-1,6-bisphosphatase, cytosolic (Musa acuminata)" AED:0.29 eAED:0.29 QI:151|0.63|0.75|1|0.54|0.66|12|242|350	2.84907	-1.5592	0.00612	IPR028343	P:GO:0009765; C:GO:0016020
Xvis03_224654-PA	processed-gene-1.9-mRNA-1 protein Name:"Similar to CAB21 Chlorophyll a-b binding protein 21, chloroplastic (Nicotiana tabacum)" AED:0.11 eAED:0.11 QI:0|0|0|0.5|1|1|2|0|328	2.58311	-1.5193	0.00684	IPR023329	F:GO:0005509; C:GO:0009523; C:GO:0009654; P:GO:0015979; C:GO:0019898
Xvis03_210597-PA	augustus-gene-8.18-mRNA-1 protein Name:"Similar to At1g67280 Probable lactoylglutathione lyase, chloroplast (Arabidopsis thaliana)" AED:0.06 eAED:0.06 QI:224|1|1|1|1|1|9|419|372	2.83797	-1.597	0.00703	IPR029068	P:GO:0005975; F:GO:0016791; F:GO:0042132
Xvis03_213652-PA	processed-gene-16.266-mRNA-1 protein Name:"Similar to RPL4 50S ribosomal protein L4, chloroplastic (Nicotiana tabacum)" AED:0.18 eAED:0.18 QI:0|-1|0|1|-1|1|1|0|272	2.15786	-1.7564	0.00707	IPR013005	P:GO:0009765; C:GO:0016020
Xvis03_202672-PA	processed-gene-54.103-mRNA-1 protein Name:"Similar to HEMC Porphobilinogen deaminase, chloroplastic (Oryza sativa subsp. japonica)" AED:0.01 eAED:0.01 QI:117|1|1|1|1|1|5|327|378	3.14577	-1.4667	0.00736	IPR000860	F:GO:0004462; F:GO:0046872
Xvis03_207337-PA	processed-gene-10.83-mRNA-1 protein Name:"Similar to rps5 30S ribosomal protein S5, chloroplastic (Arabidopsis thaliana)" AED:0.00 eAED:0.00 QI:186|1|1|1|1|1|2|216|309	3.17184	-1.4629	0.00756	IPR014721	F:GO:0003735; C:GO:0005840; P:GO:0006412
Xvis03_223438-PA	augustus-gene-1.2-mRNA-1 protein Name:"Similar to APX4 Probable L-ascorbate peroxidase 4 (Oryza sativa	3.41937	-1.4254	0.00828	IPR002207	F:GO:0004418; P:GO:0033014

	subsp. japonica)" AED:0.10 eAED:0.10 QI:188|1|1|1|1|9|226|284					
Xvis03_225066-PA	processed-gene-0.82-mRNA-1 protein Name:"Similar to Chlorophyll a-b binding protein, chloroplastic (Spinacia oleracea)" AED:0.00 eAED:0.00 QI:0|-1|0|1|-1|1|1|0|268	2.78397	-1.4164	0.00932	IPR022796 (PFAM);	F:GO:0003723; F:GO:0003735; C:GO:0005840; P:GO:0006412; C:GO:0015935
Xvis03_207668-PA	processed-gene-12.85-mRNA-1 protein Name:"Similar to PETH Ferredoxin--NADP reductase, leaf isozyme, chloroplastic (Pisum sativum)" AED:0.14 eAED:0.14 QI:231|1|1|1|1|1|9|392|366	9.06396	-0.9405	0.00942	IPR001709	F:GO:0004601; P:GO:0006979; F:GO:0020037; P:GO:0055114
Xvis03_211745-PA	augustus-gene-13.21-mRNA-1 protein Name:"Similar to TPIP1 Triosephosphate isomerase, cytosolic (Petunia hybrida)" AED:0.34 eAED:0.34 QI:46|0.88|0.8|0.9|1|1|10|0|326	5.56814	-1.1392	0.00977	IPR000652	P:GO:0009765; C:GO:0016020
Xvis03_219001-PA	processed-gene-2.79-mRNA-1 protein Name:"Similar to Transketolase, chloroplastic (Solanum tuberosum)" AED:0.04 eAED:0.04 QI:238|1|1|1|1|1|7|473|742	12.5651	-0.754	0.01109	IPR005475 (PFAM)	F:GO:0016491; P:GO:0055114
Xvis03_213345-PA	augustus-gene-10.80-mRNA-1 protein Name:"Similar to PGMP Phosphoglucomutase, chloroplastic (Solanum tuberosum)" AED:0.14 eAED:0.14 QI:0|0.88|0.94|1|0.88|0.89|19|523|691	3.1673	-1.3824	0.01219	IPR005841	F:GO:0003824; F:GO:0004807; P:GO:0006096
Xvis03_217041-PA	augustus-gene-12.20-mRNA-1 protein Name:"Similar to CPN21 20 kDa chaperonin, chloroplastic (Arabidopsis thaliana)" AED:0.12 eAED:0.12 QI:32|0.33|0.71|0.71|1|1|7|174|298	5.07952	-1.1018	0.0123	IPR020818	F:GO:0003824; F:GO:0004802
Xvis03_218722-PA	augustus-gene-3.37-mRNA-1 protein Name:"Similar to ATP synthase subunit delta', mitochondrial (Ipomoea batatas)" AED:0.20 eAED:0.20 QI:67|0|0.25|0.5|0.33|0.75|4|0|208	0.93503	-1.8597	0.01266	IPR036771	P:GO:0005975; F:GO:0016868; P:GO:0071704
Xvis03_200894-PA	augustus-gene-100.71-mRNA-1 protein Name:"Similar to CURT1D Protein CURVATURE THYLAKOID 1D, chloroplastic (Arabidopsis thaliana)" AED:0.11 eAED:0.11 QI:0|0.42|0.5|0.62|1|1|8|520|390	1.44097	-1.7823	0.01285	IPR025564 (PFAM	P:GO:0006457
Xvis03_220998-PA	augustus-gene-7.121-mRNA-1 protein Name:"Similar to ADG2 Glucose-1-phosphate adenylyltransferase large subunit 1, chloroplastic (Arabidopsis thaliana)" AED:0.11 eAED:0.11 QI:196|0.92|0.86|1|0.85|0.86|15|136|540	4.0113	-1.1797	0.01293	G3DSA:2.160.10.10 (GENE3D);)	P:GO:0015986; C:GO:0045261; F:GO:0046933
Xvis03_221570-PA	augustus-gene-2.10-mRNA-1 protein Name:"Similar to LSF1 Phosphoglucan phosphatase LSF1, chloroplastic (Arabidopsis thaliana)" AED:0.06 eAED:0.06 QI:233|0.83|0.71|1|0.5|0.42|7|831|301	4.03939	-1.3096	0.01298	G3DSA:2.30.42.10 (GENE3D);	C:GO:0009579
Xvis03_206281-PA	augustus-gene-15.74-mRNA-1 protein Name:"Similar to CYCL Cytochrome c1-1, heme protein,	1.35325	-1.6927	0.01317	IPR002326 (PRINTS);	P:GO:0009058; F:GO:0016779

	mitochondrial (Solanum tuberosum)" AED:0.28 eAED:0.28 QI:33|0.85|0.87|1|1|1|8|457|361					
Xvis03_211268-PA	processed-gene-9.25-mRNA-1 protein Name:"Similar to Vacuolar-processing enzyme (Citrus sinensis)" AED:0.07 eAED:0.07 QI:3|1|1|1|1|1|9|417|590	0.8108	-1.8733	0.01373	IPR001096 (PRINTS);	F:GO:0005515
Xvis03_215883-PA	processed-gene-4.2-mRNA-1 protein Name:"Similar to RPL8 60S ribosomal protein L8 (Solanum lycopersicum)" AED:0.00 eAED:0.00 QI:71|1|1|1|1|1|2|167|261	2.48107	-1.4888	0.01419	IPR014726	F:GO:0009055; F:GO:0020037
Xvis03_218222-PA	augustus-gene-8.105-mRNA-1 protein Name:"Similar to CURT1A Protein CURVATURE THYLAKOID 1A, chloroplastic (Arabidopsis thaliana)" AED:0.16 eAED:0.16 QI:215|1|1|1|0.8|0.66|6|98|167	2.17954	-1.5739	0.01442	IPR025564 (PFAM);	P:GO:0006508; F:GO:0008233
Xvis03_205605-PA	processed-gene-17.119-mRNA-1 protein Name:"Similar to At1g09760 U2 small nuclear ribonucleoprotein A' (Arabidopsis thaliana)" AED:0.23 eAED:0.27 QI:0|0.83|0.71|1|1|1|7|448|347	1.14694	-1.752	0.01459	PF14580 (PFAM);	F:GO:0003723; F:GO:0003735; C:GO:0005840; P:GO:0006412; C:GO:0015934
Xvis03_220187-PA	processed-gene-5.6-mRNA-1 protein Name:"Similar to HIR1 Hypersensitive-induced response protein 1 (Arabidopsis thaliana)" AED:0.13 eAED:0.13 QI:38|0.6|0.83|0.83|0.8|0.66|6|280|307	0.67439	-1.8741	0.01459	G3DSA:3.30.479.30 (GENE3D);	C:GO:0009579
Xvis03_220863-PA	processed-gene-0.82-mRNA-1 protein Name:"Similar to RPL3 60S ribosomal protein L3 (Oryza sativa subsp. japonica)" AED:0.08 eAED:0.08 QI:54|1|1|1|1|1|6|258|389	3.21493	-1.4162	0.01477	G3DSA:3.30.1430.10 ();	F:GO:0005515
Xvis03_224754-PA	processed-gene-1.55-mRNA-1 protein Name:"Similar to At3g10130 Heme-binding-like protein At3g10130, chloroplastic (Arabidopsis thaliana)" AED:0.02 eAED:0.02 QI:0|-1|0|1|-1|1|1|0|209	0.9696	-1.8449	0.01483	IPR006917 (PFAM);	no GO terms
Xvis03_208987-PA	augustus-gene-4.4-mRNA-1 protein Name:"Similar to BGAL9 Beta-galactosidase 9 (Arabidopsis thaliana)" AED:0.06 eAED:0.06 QI:63|1|1|1|0.94|0.94|19|309|904	4.0316	-1.1721	0.01497	IPR001944 (PRINTS);	F:GO:0003735; C:GO:0005840; P:GO:0006412
Xvis03_225829-PA	augustus-gene-0.17-mRNA-1 protein Name:"Similar to LHCA1 Chlorophyll a-b binding protein 6, chloroplastic (Arabidopsis thaliana)" AED:0.45 eAED:0.45 QI:0|0.44|0.4|0.5|1|1|10|334|459	2.89655	-1.3519	0.01499	PF02466 (PFAM);	no GO terms
Xvis03_207774-PA	processed-gene-21.50-mRNA-1 protein Name:"Similar to Transketolase, chloroplastic (Solanum tuberosum)" AED:0.17 eAED:0.17 QI:154|0.85|0.75|1|1|1|8|0|716	12.1963	-0.7238	0.01605	IPR005475 (PFAM)	F:GO:0004553; P:GO:0005975; F:GO:0030246
Xvis03_216387-PA	augustus-gene-11.65-mRNA-1 protein Name:"Similar to Alpha-galactosidase (Coffea arabica)" AED:0.16 eAED:0.16 QI:81|1|1|1|0.92|0.92|14|139|642	3.48955	-1.1722	0.0161	IPR002241 (PRINTS)	P:GO:0009765; C:GO:0016020

Xvis03_216480-PA	augustus-gene-6.109-mRNA-1 protein Name:"Similar to UVR8 Ultraviolet-B receptor UVR8 (Arabidopsis thaliana)" AED:0.10 eAED:0.10 QI:223|0.9|1|1|1|1|11|290|403	1.05463	-1.7793	0.01681	IPR000408 (PRINTS);	F:GO:0003824
Xvis03_224225-PA	augustus-gene-0.55-mRNA-1 protein Name:"Similar to TPIP1 Triosephosphate isomerase, chloroplastic (Spinacia oleracea)" AED:0.32 eAED:0.32 QI:0|0|0|0.55|0.87|1|9|0|311	5.33433	-1.0765	0.01687	IPR013785)	F:GO:0003824; F:GO:0004553; P:GO:0005975
Xvis03_212711-PA	processed-gene-16.130-mRNA-1 protein Name:"Similar to LHCB4.2 Chlorophyll a-b binding protein CP29.2, chloroplastic (Arabidopsis thaliana)" AED:0.05 eAED:0.05 QI:1875|1|1|1|0.5|0.33|3|204|289	5.22923	-1.0022	0.01704	IPR022796 (PFAM	F:GO:0009881; P:GO:0010224; F:GO:0042803
Xvis03_223588-PA	processed-gene-1.56-mRNA-1 protein Name:"Similar to VIT_19s0014g02480 Probable bifunctional methylthioribulose-1-phosphate dehydratase/enolase-phosphatase E1 1 (Vitis vinifera)" AED:0.24 eAED:0.24 QI:0|0.9|0.90|0.90|1|1|11|237|411	2.12507	-1.4509	0.01726	IPR036409	F:GO:0003824; F:GO:0004807; P:GO:0006096
Xvis03_224459-PA	augustus-gene-1.13-mRNA-1 protein Name:"Similar to RABA2A Ras-related protein RABA2a (Arabidopsis thaliana)" AED:0.02 eAED:0.02 QI:202|1|1|1|1|2|509|220	1.26609	-1.6123	0.01726	PR00449 (PRINTS	P:GO:0009765; C:GO:0016020
Xvis03_213988-PA	augustus-gene-11.18-mRNA-1 protein Name:"Similar to PAB1 Proteasome subunit alpha type-2 (Oryza sativa subsp. japonica)" AED:0.05 eAED:0.05 QI:70|1|1|1|1|1|10|615|222	2.8154	-1.3634	0.01778	IPR029055	F:GO:0000287; C:GO:0005737; F:GO:0016787; P:GO:0019509; F:GO:0043874; F:GO:0046872
Xvis03_215165-PA	augustus-gene-14.29-mRNA-1 protein Name:"Similar to EPHX2 Bifunctional epoxide hydrolase 2 (Sus scrofa)" AED:0.25 eAED:0.25 QI:33|1|1|1|0.75|0.6|5|416|321	1.40331	-1.6228	0.01858	IPR000073 (PRINTS);	F:GO:0003924; F:GO:0005525
Xvis03_216531-PA	augustus-gene-9.118-mRNA-1 protein Name:"Similar to RPL3 60S ribosomal protein L3 (Oryza sativa subsp. japonica)" AED:0.07 eAED:0.07 QI:0|1|0.83|1|1|0.83|6|237|407	3.43494	-1.266	0.02093	IPR000597 (PFAM);	F:GO:0004175; F:GO:0004298; C:GO:0005839; P:GO:0006511; C:GO:0019773; P:GO:0051603
Xvis03_215806-PA	processed-gene-9.114-mRNA-1 protein Name:"Similar to ANN1 Annexin D1 (Arabidopsis thaliana)" AED:0.04 eAED:0.04 QI:119|1|1|1|1|1|5|186|316	2.39682	-1.5174	0.02117	IPR001464 (PRINTS);	F:GO:0003824
Xvis03_224225-PA	augustus-gene-0.55-mRNA-1 protein Name:"Similar to TPIP1 Triosephosphate isomerase, chloroplastic (Spinacia oleracea)" AED:0.32 eAED:0.32 QI:0|0|0|0.55|0.87|1|9|0|311	1.62989	-1.5403	0.02134	IPR013785	F:GO:0003735; C:GO:0005840; P:GO:0006412
Xvis03_201588-PA	augustus-gene-28.7-mRNA-1 protein Name:"Similar to NAD-ME1 NAD-dependent malic enzyme 1, mitochondrial (Arabidopsis thaliana)" AED:0.22 eAED:0.22 QI:0|0.77|0.78|0.86|0.77|0.82|23|290|790	1.19584	-1.668	0.02134	IPR001891 (PRINTS);	F:GO:0005509; F:GO:0005544

Xvis03_219722-PA	augustus-gene-9.73-mRNA-1 protein Name:"Similar to CAB36 Chlorophyll a-b binding protein 36, chloroplastic (Nicotiana tabacum)" AED:0.36 eAED:0.36 QI:240|1|1|1|1|2|393|264	3.82232	-1.0662	0.02232	IPR022796 (PFAM	F:GO:0003824; F:GO:0004807; P:GO:0006096
Xvis03_221307-PA	processed-gene-5.33-mRNA-1 protein Name:"Similar to Peptide-N4-(N-acetyl-beta-glucosaminyl)asparagine amidase A (Prunus dulcis)" AED:0.04 eAED:0.04 QI:0|-1|0|1|-1|1|1|0|612	1.81413	-1.5359	0.0226	IPR021102 (PFAM)	F:GO:0004470; F:GO:0004471; F:GO:0051287; P:GO:0055114
Xvis03_205319-PA	processed-gene-30.54-mRNA-1 protein Name:"Similar to PSAH1 Photosystem I reaction center subunit VI-1, chloroplastic (Arabidopsis thaliana)" AED:0.09 eAED:0.09 QI:15|1|1|1|1|3|336|145	1.43339	-1.5556	0.02307	IPR004928 (PFAM);	P:GO:0009765; C:GO:0016020
Xvis03_209971-PA	augustus-gene-1.88-mRNA-1 protein Name:"Similar to IMPL1 Phosphatase IMPL1, chloroplastic (Arabidopsis thaliana)" AED:0.08 eAED:0.08 QI:62|1|1|1|0.9|0.81|11|343|347	0.84949	-1.7562	0.02329	IPR020552 (PRINTS);	no GO terms
Xvis03_223144-PA	processed-gene-3.56-mRNA-1 protein Name:"Similar to RBCS1 Ribulose bisphosphate carboxylase small chain, chloroplastic (Musa acuminata)" AED:0.05 eAED:0.05 QI:145|1|1|1|1|3|356|174	11.9372	-0.8436	0.025	IPR024681 (PRINTS)	C:GO:0009522; C:GO:0009538; P:GO:0015979
Xvis03_202356-PA	processed-gene-29.12-mRNA-1 protein Name:"Similar to PBG1 Proteasome subunit beta type-4 (Arabidopsis thaliana)" AED:0.13 eAED:0.13 QI:0|0.71|0.75|0.87|1|1|8|335|329	2.24439	-1.361	0.02579	IPR029055	F:GO:0008934; P:GO:0046854; P:GO:0046855
Xvis03_212711-PA	processed-gene-16.130-mRNA-1 protein Name:"Similar to LHCB4.2 Chlorophyll a-b binding protein CP29.2, chloroplastic (Arabidopsis thaliana)" AED:0.05 eAED:0.05 QI:1875|1|1|1|0.5|0.33|3|204|289	4.29118	-1.0098	0.02717	IPR022796 (PFAM	no GO terms
Xvis03_213887-PA	remorin-like isoform X2	3.12009	-1.2184	0.02722	IPR005516 (PFAM	F:GO:0004298; C:GO:0005839; P:GO:0051603
Xvis03_202061-PA	processed-gene-6.69-mRNA-1 protein Name:"Similar to RPL9 50S ribosomal protein L9, chloroplastic (Arabidopsis thaliana)" AED:0.06 eAED:0.06 QI:100|1|1|1|0.83|0.71|7|568|196	1.47336	-1.5557	0.02735	IPR020069 (PFAM)	P:GO:0009765; C:GO:0016020
Xvis03_202428-PA	augustus-gene-35.90-mRNA-1 protein Name:"Similar to CURT1A Protein CURVATURE THYLAKOID 1A, chloroplastic (Arabidopsis thaliana)" AED:0.22 eAED:0.42 QI:0|0.75|0.6|1|0.75|0.6|5|269|208	2.03114	-1.4203	0.02897	IPR025564 (PFAM)	no GO terms
Xvis03_203635-PA	augustus-gene-35.43-mRNA-1 protein Name:"Similar to CLPP5 ATP-dependent Clp protease proteolytic subunit 5, chloroplastic (Arabidopsis thaliana)" AED:0.40 eAED:0.40 QI:0|1|0.71|1|1|1|7|484|324	1.51163	-1.5248	0.02928	IPR001907 (PRINTS)	F:GO:0003735; C:GO:0005840; P:GO:0006412

Xvis03_208040-PA	processed-gene-21.10-mRNA-1 protein Name:"Similar to SHM4 Serine hydroxymethyltransferase 4 (Arabidopsis thaliana)" AED:0.05 eAED:0.05 QI:76|1|1|1|1|1|4|235|515	15.5743	-0.6129	0.02931	IPR015421	C:GO:0009579
Xvis03_217729-PA	processed-gene-11.5-mRNA-1 protein Name:"Similar to PETE Plastocyanin minor isoform, chloroplastic (Arabidopsis thaliana)" AED:0.37 eAED:0.37 QI:0|0|0|0.16|1|1|6|0|366	2.78506	-1.2689	0.03022	IPR002387 (PRINTS	F:GO:0004252; P:GO:0006508
Xvis03_225147-PA	augustus-gene-0.41-mRNA-1 protein Name:"Similar to CAB6A Chlorophyll a-b binding protein 6A, chloroplastic (Solanum lycopersicum)" AED:0.00 eAED:0.00 QI:106|1|1|1|1|1|3|75|204	3.86229	-1.0467	0.03095	IPR022796 (PFAM); SSF103511 (SUPERFAMILY)	F:GO:0003824; F:GO:0004372; P:GO:0019264; F:GO:0030170; P:GO:0035999
Xvis03_216230-PA	Basic secretory protease	1.58522	-1.482	0.03108	IPR007541 (PFAM)	F:GO:0005507; F:GO:0009055
Xvis03_217514-PA	processed-gene-7.97-mRNA-1 protein Name:"Similar to SPAC9E9.15 Uncharacterized protein C9E9.15 (Schizosaccharomyces pombe (strain 972 / ATCC 24843))" AED:0.14 eAED:0.14 QI:59|0.93|0.87|1|1|1|16|145|594	3.50708	-1.1035	0.03172	G3DSA:2.60.120.430	P:GO:0009765; C:GO:0016020
Xvis03_207968-PA	augustus-gene-15.42-mRNA-1 protein Name:"Similar to CAP10A Chlorophyll a-b binding protein CP24 10A, chloroplastic (Solanum lycopersicum)" AED:0.00 eAED:0.00 QI:218|1|1|1|1|1|2|259|254	0.64829	-1.688	0.03198	IPR023329	no GO terms
Xvis03_212120-PA	augustus-gene-8.8-mRNA-1 protein Name:"Similar to CEST Protein CHLOROPLAST ENHANCING STRESS TOLERANCE, chloroplastic (Oryza sativa subsp. japonica)" AED:0.04 eAED:0.04 QI:85|1|1|1|1|1|6|455|259	1.04313	-1.6193	0.03207	PTHR33672:SF3 (PANTHER);	P:GO:0032981
Xvis03_223438-PA	augustus-gene-1.2-mRNA-1 protein Name:"Similar to APX4 Probable L-ascorbate peroxidase 4 (Oryza sativa subsp. japonica)" AED:0.10 eAED:0.10 QI:188|1|1|1|1|1|9|226|284	2.60942	-1.2049	0.0321	IPR002207 (PRINTS);	P:GO:0009765; C:GO:0016020
Xvis03_211391-PA	processed-gene-20.57-mRNA-1 protein Name:"Similar to GGH2 Gamma-glutamyl hydrolase 2 (Arabidopsis thaliana)" AED:0.20 eAED:0.20 QI:39|1|0.85|1|1|1|7|0|302	2.25412	-1.3101	0.03222	IPR011697 (PFAM	C:GO:0009535; P:GO:0048564; P:GO:0080183
Xvis03_224849-PA	processed-gene-1.76-mRNA-1 protein Name:"Similar to FKBP19 Peptidyl-prolyl cis-trans isomerase FKBP19, chloroplastic (Arabidopsis thaliana)" AED:0.46 eAED:0.49 QI:0|0.72|0.83|0.91|0.90|0.83|12|203|320	0.70445	-1.6515	0.03297	IPR001179 (PFAM)	F:GO:0004601; P:GO:0006979; F:GO:0020037; P:GO:0055114
Xvis03_220733-PA	processed-gene-1.13-mRNA-1 protein Name:"Similar to CAT1 Catalase-1 (Triticum aestivum)" AED:0.19 eAED:0.19 QI:0|0|0|0.66|1|1|9|0|623	6.46283	-0.8621	0.03302	IPR018028 (PRINTS)	F:GO:0008242; F:GO:0016787
Xvis03_223095-PA	augustus-gene-3.96-mRNA-1 protein Name:"Similar to petC Cytochrome b6-f complex iron-sulfur subunit, chloroplastic (Oryza sativa subsp.	1.79206	-1.3542	0.03383	IPR005805 (PRINTS)	no GO terms

	japonica)" AED:0.11 eAED:0.11 QI:167|0.33|0.75|1|1|1|4|287|178					
Xvis03_216531-PA	augustus-gene-9.118-mRNA-1 protein Name:"Similar to RPL3 60S ribosomal protein L3 (Oryza sativa subsp. japonica)" AED:0.07 eAED:0.07 QI:0|1|0.83|1|1|0.83|6|237|407	3.11112	-1.2577	0.034	IPR000597 (PFAM)	F:GO:0004096; P:GO:0006979; F:GO:0020037; P:GO:0055114
Xvis03_220973-PA	augustus-gene-5.51-mRNA-1 protein Name:"Similar to RPS2C 40S ribosomal protein S2-3 (Arabidopsis thaliana)" AED:0.29 eAED:0.29 QI:54|1|1|1|0.5|0.33|3|154|274	3.11906	-1.1644	0.03495	IPR013810 (PFAM);	F:GO:0008121; F:GO:0009496; C:GO:0009507; C:GO:0016020; F:GO:0016491; F:GO:0016679; C:GO:0042651; F:GO:0045158; F:GO:0051537; P:GO:0055114
Xvis03_213605-PA	processed-gene-14.84-mRNA-1 protein Name:"Similar to Os08g0288200 Probable adenylate kinase 5, chloroplastic (Oryza sativa subsp. japonica)" AED:0.22 eAED:0.22 QI:25|1|0.94|1|1|1|17|0|611	0.70186	-1.6195	0.03534	IPR000850 (PRINTS);	F:GO:0003735; C:GO:0005840; P:GO:0006412
Xvis03_202672-PA	processed-gene-54.103-mRNA-1 protein Name:"Similar to HEMC Porphobilinogen deaminase, chloroplastic (Oryza sativa subsp. japonica)" AED:0.01 eAED:0.01 QI:117|1|1|1|1|1|5|327|378	4.01403	-1.0024	0.03547	IPR000860 (PRINTS)	F:GO:0003723; F:GO:0003735; C:GO:0005840; P:GO:0006412; C:GO:0015935
Xvis03_207337-PA	processed-gene-10.83-mRNA-1 protein Name:"Similar to rps5 30S ribosomal protein S5, chloroplastic (Arabidopsis thaliana)" AED:0.00 eAED:0.00 QI:186|1|1|1|1|1|2|216|309	0.96041	-1.5832	0.03649	IPR014721	F:GO:0004017; F:GO:0005524; P:GO:0006139; F:GO:0016776; F:GO:0019205
Xvis03_207968-PA	augustus-gene-15.42-mRNA-1 protein Name:"Similar to CAP10A Chlorophyll a-b binding protein CP24 10A, chloroplastic (Solanum lycopersicum)" AED:0.00 eAED:0.00 QI:218|1|1|1|1|1|2|259|254	0.92133	-1.5542	0.0365	IPR023329	F:GO:0004418; P:GO:0033014
Xvis03_212925-PA	processed-gene-5.93-mRNA-1 protein Name:"Similar to PETH Ferredoxin--NADP reductase, leaf-type isozyme, chloroplastic (Nicotiana tabacum)" AED:0.42 eAED:0.49 QI:0|0|0|0.8|1|1|5|0|177	1.71463	-1.4288	0.03651	IPR001433 (PFAM)	F:GO:0003723; F:GO:0003735; C:GO:0005840; P:GO:0006412; C:GO:0015935
Xvis03_211745-PA	augustus-gene-13.21-mRNA-1 protein Name:"Similar to TPIP1 Triosephosphate isomerase, cytosolic (Petunia hybrida)" AED:0.34 eAED:0.34 QI:46|0.88|0.8|0.9|1|1|10|0|326	4.98432	-0.9345	0.03734	IPR000652	P:GO:0009765; C:GO:0016020
Xvis03_212711-PA	processed-gene-16.130-mRNA-1 protein Name:"Similar to LHCB4.2 Chlorophyll a-b binding protein CP29.2, chloroplastic (Arabidopsis thaliana)" AED:0.05 eAED:0.05 QI:1875|1|1|1|0.5|0.33|3|204|289	3.26057	-1.0666	0.03818	IPR022796 (PFAM)	F:GO:0016491; P:GO:0055114
Xvis03_223588-PA	processed-gene-1.56-mRNA-1 protein Name:"Similar to VIT_19s0014g02480 Probable bifunctional methylthioribulose-1-phosphate dehydratase/enolase-phosphatase E1 1 (Vitis vinifera)"	9.12494	-0.9422	0.03981	IPR036409	F:GO:0003824; F:GO:0004807; P:GO:0006096

	AED:0.24 eAED:0.24 QI:0|0.9|0.90|0.90|1|1|11|237|411					
Xvis03_224459-PA	augustus-gene-1.13-mRNA-1 protein Name:"Similar to RABA2A Ras-related protein RABA2a (Arabidopsis thaliana)" AED:0.02 eAED:0.02 QI:202|1|1|1|1|1|2|509|220	2.84135	-1.1073	0.0404	PR00449 (PRINTS)	P:GO:0009765; C:GO:0016020
Xvis03_213988-PA	augustus-gene-11.18-mRNA-1 protein Name:"Similar to PAB1 Proteasome subunit alpha type-2 (Oryza sativa subsp. japonica)" AED:0.05 eAED:0.05 QI:70|1|1|1|1|1|10|615|222	1.45642	-1.4357	0.04396	IPR029055	F:GO:0000287; C:GO:0005737; F:GO:0016787; P:GO:0019509; F:GO:0043874; F:GO:0046872
Xvis03_207968-PA	augustus-gene-15.42-mRNA-1 protein Name:"Similar to CAP10A Chlorophyll a-b binding protein CP24 10A, chloroplastic (Solanum lycopersicum)" AED:0.00 eAED:0.00 QI:218|1|1|1|1|1|2|259|254	1.21025	-1.4563	0.04448	IPR023329	F:GO:0003924; F:GO:0005525
Xvis03_224672-PA	processed-gene-1.89-mRNA-1 protein Name:"Similar to ALATS Alanine--tRNA ligase (Arabidopsis thaliana)" AED:0.10 eAED:0.10 QI:33|1|1|0.90|0.90|22|389|993	5.12135	-0.9111	0.04584	IPR002318 (PRINTS)	F:GO:0004175; F:GO:0004298; C:GO:0005839; P:GO:0006511; C:GO:0019773; P:GO:0051603
Xvis03_208742-PA	augustus-gene-3.45-mRNA-1 protein Name:"Similar to At4g13360 3-hydroxyisobutyryl-CoA hydrolase-like protein 3, mitochondrial (Arabidopsis thaliana)" AED:0.08 eAED:0.08 QI:31|1|1|0.88|0.9|10|444|426	2.07578	-1.188	0.04736	IPR032259 (PFAM)	P:GO:0009765; C:GO:0016020
Xvis03_219507-PA	augustus-gene-9.55-mRNA-1 protein Name:"Similar to POPTRDRAFT_831870 Biotin carboxylase 1, chloroplastic (Populus trichocarpa)" AED:0.11 eAED:0.11 QI:0|1|0.94|1|0.93|0.76|17|386|550	1.25457	-1.3382	0.04879	IPR005481 (PFAM)	F:GO:0000166; F:GO:0003676; F:GO:0004812; F:GO:0004813; F:GO:0005524; C:GO:0005737; P:GO:0006419; P:GO:0043039
Xvis03_224372-PA	processed-gene-2.16-mRNA-1 protein Name:"Similar to UAM1 UDP-arabinopyranose mutase 1 (Oryza sativa subsp. japonica)" AED:0.08 eAED:0.08 QI:87|1|1|1|1|4|347|359	1.29159	-1.3747	0.0489	IPR037595 (PFAM)	F:GO:0003860
Xvis03_200047-PA	augustus-gene-4.43-mRNA-1 protein Name:"Similar to BGLU22 Beta-glucosidase 22 (Oryza sativa subsp. japonica)" AED:0.38 eAED:0.38 QI:56|0.9|0.81|1|1|1|11|40|465	0.95113	-1.505	0.04963	IPR001360	F:GO:0005524; F:GO:0016874; F:GO:0046872
	processed-gene-2.106-mRNA-1 protein Name:"Similar to Beta-galactosidase (Asparagus officinalis)" AED:0.13 eAED:0.13 QI:277|1|1|1|1|1|19|418|832	1.95118	-1.3412	0.04985	IPR001944	F:GO:0016866; P:GO:0071669
Xvis03_212711-PA		5.22923	-3.5991	1.84E-09	P:GO:0009765; C:GO:0016020	F:GO:0004553; P:GO:0005975
Xvis03_216014-PA	processed-gene-5.37-mRNA-1 protein Name:"Similar to PSAF Photosystem I reaction center subunit III, chloroplastic (Arabidopsis thaliana)" AED:0.24 eAED:0.24 QI:0|-1|0|1|-1|1|1|0|232	4.66208	-1.3266	0.00534		F:GO:0004553; P:GO:0005975; F:GO:0030246

Xvis03_220507-PA	Xvis03_220507-PA processed-gene-1.26-mRNA-1 protein Name:"Similar to PAP27 Probable inactive purple acid phosphatase 27 (Arabidopsis thaliana)" AED:0.08 eAED:0.08 QI:27|1|1|1|1|1|12|227|617	0.96041	-2.0796	0.00614		P:photosynthesis, light harvesting; C:membrane
Xvis03_219507-PA	augustus-gene-9.55-mRNA-1 protein Name:"Similar to POPTRDRAFT_831870 Biotin carboxylase 1, chloroplastic (Populus trichocarpa)" AED:0.11 eAED:0.11 QI:0|1|0.94|1|0.93|0.76|17|386|550	1.95077	-1.7797	0.00622	F:ATP binding; F:ligase activity; F:metal ion binding	
Xvis03_208742-PA	augustus-gene-3.45-mRNA-1 protein Name:"Similar to At4g13360 3-hydroxyisobutyryl-CoA hydrolase-like protein 3, mitochondrial (Arabidopsis thaliana)" AED:0.08 eAED:0.08 QI:31|1|1|1|0.88|0.9|10|444|426	1.92239	-1.4925	0.01126	F:3-hydroxyisobutyryl-CoA hydrolase activity	
Xvis03_224672-PA	processed-gene-1.89-mRNA-1 protein Name:"Similar to ALATS Alanine--tRNA ligase (Arabidopsis thaliana)" AED:0.10 eAED:0.10 QI:33|1|1|1|0.90|0.90|22|389|993	2.56021	-1.4947	0.01161	F:nucleic acidbinding; F:alanine tRNA ligase activity; F:ATP binding; C:cytoplasm; P:alanyl tRNAaminoacylation	
Xvis03_224372-PA	processed-gene-2.16-mRNA-1 protein Name:"Similar to UAM1 UDP-arabinopyranose mutase 1 (Oryza sativa subsp. japonica)" AED:0.08 eAED:0.08 QI:87|1|1|1|1|1|4|347|359	1.04109	-1.7951	0.01173	F:intramolecular transferase activity; P:plant-type cell wall organization or biogenesis	
Xvis03_200047-PA	augustus-gene-4.43-mRNA-1 protein Name:"Similar to BGLU22 Beta-glucosidase 22 (Oryza sativa subsp. japonica)" AED:0.38 eAED:0.38 QI:56|0.9|0.81|1|1|1|11|40|465	2.0106	-1.4771	0.01191	F:hydrolase activity, hydrolyzing O-glycosyl compounds; P:carbohydrate metabolic process	
Xvis03_223612-PA	augustus-gene-2.49-mRNA-1 protein Name:"Similar to CEBIP Chitin elicitor-binding protein (Oryza sativa subsp. japonica)" AED:0.27 eAED:0.27 QI:0|0.6|0.5|0.66|1|1|6|353|477	3.49938	-1.2764	0.01259	IPR036779	
Xvis03_213033-PA	processed-gene-15.37-mRNA-1 protein Name:"Similar to zta1 Probable quinone oxidoreductase (Schizosaccharomyces pombe (strain 972 / ATCC 24843))" AED:0.20 eAED:0.20 QI:0|0|0|0.8|1|1|5|0|292	0.90109	-1.882	0.01455	IPR013154 (PFAM);	
Xvis03_225238-PA	augustus-gene-0.18-mRNA-1 protein Name:"Similar to WAXY Granule-bound starch synthase 1, chloroplastic/amyloplastic (Antirrhinum majus)" AED:0.11 eAED:0.11 QI:73|1|1|1|0.92|0.85|14|142|611	0.87706	-1.8444	0.01633	IPR013534 (PFAM)	no GO terms
Xvis03_210933-PA	augustus-gene-1.32-mRNA-1 protein Name:"Similar to PAP2 Probable inactive purple acid phosphatase 2 (Arabidopsis thaliana)" AED:0.04	3.10401	-1.2006	0.01696	IPR015914 (PFAM)	P:GO:0055114

	eAED:0.04 QI:0|1|0.66|1|0.5|0.33|3|1759|658					
Xvis03_218675-PA	processed-gene-10.89-mRNA-1 protein Name:"Similar to AGD2 Probable LL-diaminopimelate aminotransferase, chloroplastic (Oryza sativa subsp. japonica)" AED:0.20 eAED:0.20 QI:0|0.85|0.75|1|1|1|8|209|407	0.98322	-1.7713	0.01755	IPR004839 (PFAM)	F:GO:0004373
Xvis03_212280-PA	processed-gene-6.79-mRNA-1 protein Name:"Similar to THI1-2 Thiamine thiazole synthase 2, chloroplastic (Vitis vinifera)" AED:0.02 eAED:0.02 QI:212|1|1|1|1|1|2|483|354	3.04448	-1.2108	0.0182	IPR002922	F:GO:0003993; F:GO:0016787; F:GO:0046872
Xvis03_205558-PA	augustus-gene-14.7-mRNA-1 protein Name:"Similar to CAB7 Chlorophyll a-b binding protein 7, chloroplastic (Solanum lycopersicum)" AED:0.16 eAED:0.16 QI:0|0.25|0.4|1|0.75|0.8|5|892|278	0.76517	-1.7151	0.02405	IPR022796	F:GO:0003824; F:GO:0008483; P:GO:0009058; F:GO:0030170
Xvis03_205102-PA	processed-gene-9.15-mRNA-1 protein Name:"Similar to GOR Glutathione reductase, chloroplastic (Fragment) (Nicotiana tabacum)" AED:0.14 eAED:0.14 QI:0|1|0.90|1|0.9|0.81|11|639|590	2.8642	-1.2104	0.02478	PR00411	P:GO:0009228
Xvis03_222506-PA	augustus-gene-4.97-mRNA-1 protein Name:"Similar to EDA2 Probable serine protease EDA2 (Arabidopsis thaliana)" AED:0.31 eAED:0.31 QI:159|0.92|0.92|1|1|1|14|279|488	1.7679	-1.4029	0.02497	IPR029058	P:GO:0009765; C:GO:0016020
Xvis03_225868-PA	augustus-gene-0.5-mRNA-1 protein Name:"Similar to caa43 2-haloacrylate reductase (Burkholderia sp.)" AED:0.18 eAED:0.18 QI:0|0.25|0|0.8|0.5|0.4|5|0|313	0.8474	-1.667	0.02744	IPR013149 (PFAM)	F:GO:0004362; P:GO:0006749; F:GO:0016491; P:GO:0045454; F:GO:0050660; F:GO:0050661; P:GO:0055114
Xvis03_204322-PA	processed-gene-9.15-mRNA-1 protein Name:"Similar to AFRR Monodehydroascorbate reductase (Solanum lycopersicum)" AED:0.13 eAED:0.13 QI:138|0.72|0.83|0.83|1|1|12|368|489	4.19782	-1.0042	0.02888	PR00368 (	P:GO:0006508; F:GO:0008236
Xvis03_211689-PA	processed-gene-6.93-mRNA-1 protein Name:"Similar to Proteasome subunit beta type-5 (Spinacia oleracea)" AED:0.07 eAED:0.07 QI:0|1|0.87|1|1|1|8|489|310	2.20452	-1.2707	0.02899	IPR000243	P:GO:0055114
Xvis03_217074-PA	processed-gene-2.49-mRNA-1 protein Name:"Similar to PME35 Probable pectinesterase/pectinesterase inhibitor 35 (Arabidopsis thaliana)" AED:0.36 eAED:0.36 QI:662|1|1|1|1|1|3|218|442	2.7986	-1.4097	0.03523	IPR035513	F:GO:0016491; F:GO:0050660; P:GO:0055114
Xvis03_201017-PA	processed-gene-109.26-mRNA-1 protein Name:"Similar to PPD Pyruvate, phosphate dikinase, chloroplastic (Mesembryanthemum crystallinum)" AED:0.09 eAED:0.09 QI:8|1|1|1|0.89|0.9|20|257|985	0.63176	-1.6375	0.03748		F:GO:0004175; F:GO:0004298; C:GO:0005839; P:GO:0051603
Xvis03_221989-PA	augustus-gene-2.19-mRNA-1 protein Name:"Similar to dapb3 Dipeptidyl aminopeptidase BIII (Pseudoxanthomonas mexicana)"	0.75018	-1.6281	0.03758	IPR011042	F:GO:0004857; F:GO:0030599; P:GO:0042545

	AED:0.29 eAED:0.29 QI:0|0.88|0.84|1|0.83|0.89|19|191|724					
Xvis03_200779-PA	processed-gene-89.11-mRNA-1 protein Name:"Similar to PSAL Photosystem I reaction center subunit XI, chloroplastic (Spinacia oleracea)" AED:0.06 eAED:0.06 QI:217|1|1|1|1|2|190|220	0.85247	-1.5768	0.03894	IPR036592	F:GO:0003824; F:GO:0005524; P:GO:0006090; F:GO:0016301; P:GO:0016310; F:GO:0016772; F:GO:0050242
Xvis03_217230-PA	processed-gene-4.43-mRNA-1 protein Name:"Similar to PREP1 Presequence protease 1, chloroplastic/mitochondrial (Arabidopsis thaliana)" AED:0.19 eAED:0.19 QI:1251|0.91|0.84|1|0.75|0.69|13|382|303	1.51292	-1.4476	0.03895		P:GO:0006508; F:GO:0008236
Xvis03_205724-PA	processed-gene-33.32-mRNA-1 protein Name:"Similar to IBI1 Aspartate--tRNA ligase 2, cytoplasmic (Arabidopsis thaliana)" AED:0.10 eAED:0.10 QI:60|0.77|0.8|1|1|1|10|190|552	0.94327	-1.5581	0.04086	IPR002312 (PRINTS)	C:GO:0009522; C:GO:0009538; P:GO:0015979
Xvis03_220977-PA	processed-gene-6.91-mRNA-1 protein Name:"Similar to CYP74B2 Linolenate hydroperoxide lyase, chloroplastic (Arabidopsis thaliana)" AED:0.02 eAED:0.17 QI:0|-1|0|1|-1|1|1|0|486	2.32482	-1.2537	0.04111	IPR002403 (PRINTS);	F:GO:0003824; P:GO:0006508; F:GO:0046872
Xvis03_210782-PA	augustus-gene-7.64-mRNA-1 protein Name:"Similar to Os08g0562700 Puromycin-sensitive aminopeptidase (Oryza sativa subsp. japonica)" AED:0.20 eAED:0.20 QI:160|0.75|0.81|0.90|0.84|0.84|33|284|1052	5.67678	-0.8996	0.04165	IPR024601 (PFAM)	F:GO:0000166; F:GO:0003676; F:GO:0004812; F:GO:0004815; F:GO:0005524; C:GO:0005737; P:GO:0006418; P:GO:0006422
Xvis03_219931-PA	processed-gene-8.160-mRNA-1 protein Name:"Similar to SAG12 Senescence-specific cysteine protease SAG12 (Arabidopsis thaliana)" AED:0.00 eAED:0.00 QI:0|1|0.5|1|1|1|2|268|331	1.17347	-1.4714	0.04335	IPR00066	F:GO:0004497; F:GO:0005506; F:GO:0016705; F:GO:0020037; P:GO:0055114
Xvis03_219642-PA	augustus-gene-3.70-mRNA-1 protein Name:"Similar to Serpin-Z1C (Triticum aestivum)" AED:0.04 eAED:0.04 QI:7|1|1|1|0.5|0.33|3|183|391	2.21959	-1.1341	0.04599	IPR023796 (PFAM)	F:GO:0008237; F:GO:0008270
Xvis03_221434-PA	processed-gene-2.106-mRNA-1 protein Name:"Similar to Beta-galactosidase (Asparagus officinalis)" AED:0.13 eAED:0.13 QI:277|1|1|1|1|1|19|418|832	2.43557	-1.2445	0.04617	F:hydrolase activity, hydrolyzing O-glycosyl compounds; P:carbohydrate metabolic process; F:carbohydrate binding	P:GO:0006508; F:GO:0008234
	processed-gene-9.114-mRNA-1 protein Name:"Similar to ANN1 Annexin D1 (Arabidopsis thaliana)" AED:0.04 eAED:0.04 QI:119|1|1|1|1|1|5|186|316	2.39682	-1.2301	0.04897	F:calcium ion binding; F:calcium-dependent phospholipid binding	C:GO:0005615

Quality control using principal component analysis on the differentially expressed proteins across the treatments

Principal component analysis (PCA) was used for multivariate analysis based on the differentially expressed proteins across the dehydration treatments (Figure 3.2). The PCA plot was used to eliminate sample outliers, reduce noisy data and differentiate between the stages of hydration sampled (control, early, mid and late). The distinct matches show that the replicates are reproducible and that there is a difference across the drying stages (Figure 3.2 C). The results indicated there is a significant difference at the protein groups at the adjusted p-value of 0.004 between early (80-70% RWC), mid (60-40% RWC) and late (40-10% RWC) (Figure 3.2 A). Overall this data shows that there was differential protein expression upon dehydration and provides confidence for further analyses of the differential proteins and functional enrichment.

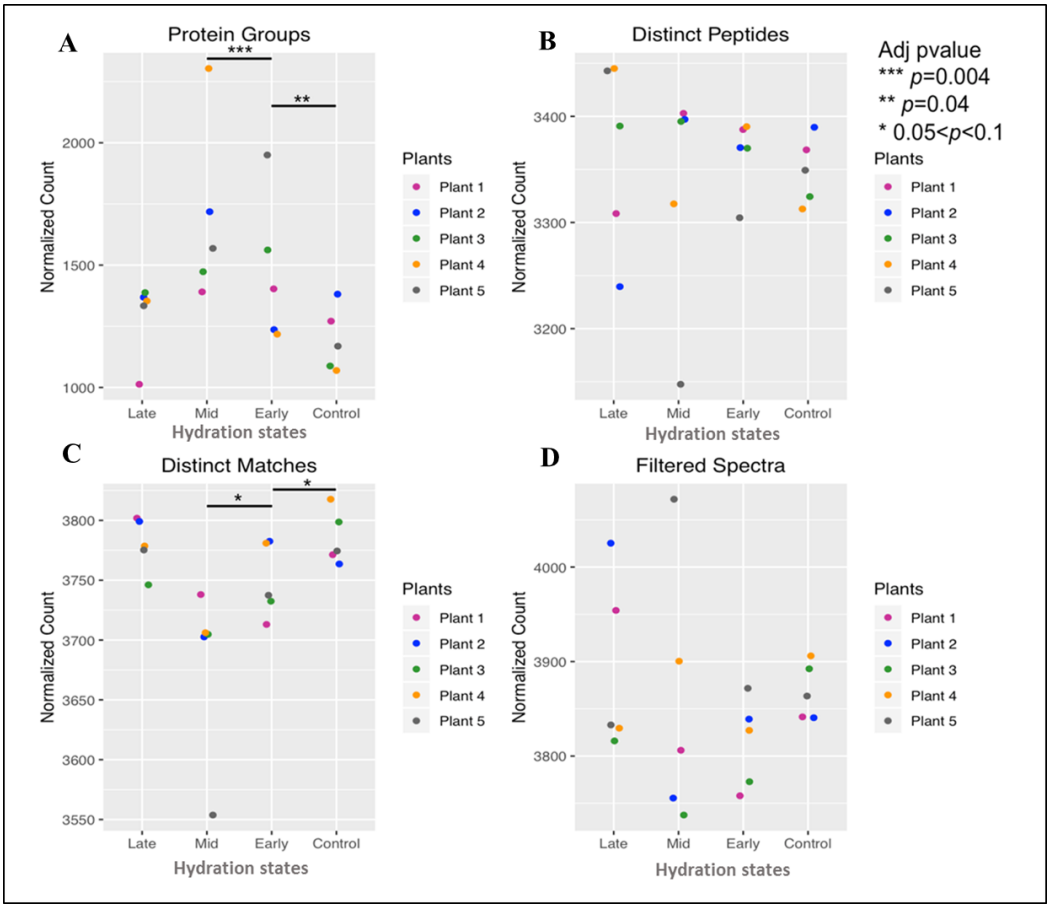

Figure 3.2: (A). PCA plot of protein groups were visualised, p-value = 0.004 and p-value = 0.04. Where a protein group consists of a master protein that is identified by sets of peptides. **(B).** and **(C).** Distinct peptides and distinct matches which determines the number of spectra that matches only that protein or peptide respectively. **(D).** Filtered spectra, 0.05 <p <0.1, describes the number of spectra that was found in each protein. Statistical significance was tested using the Wald test.

Protein annotation and functional interpretation of differentially expressed *X. schlechteri* proteins during dehydration using gene ontology

The proteomic data gave a myriad of protein identifications which requires annotation, biological context and visualisation in order to understand the key processes, networks and reactions that underly the drying responses of *X. schlechteri.* In order to gain this understanding, the *X. schlechteri* differentially expressed proteins were compared across the three stages of drying, including the up and down regulated proteins, using gene ontology tools such as Blast2GO and MapMan.

The Blast2GO program allows proteins to be assigned to three non-overlapping ontologies, namely, cellular component, molecular function and biological process (Figures 3.3, 3.4 and 3.5 respectively). The respective ontologies and proteins assigned to each process were examined according to the early (ERD), mid (MRD) and late (LRD) response to dehydration. MapMan provides a visual representation of the differentially expressed proteins and the processes they are involved in based on MapMan ontology (Usadel *et al.,* 2009). Mapman was used to assign the upregulated and downregulated proteins to specific BINs and visualise processes and stimuli.

Blast2GO analysis of cellular components, molecular functions and biological processes

The most highly represented cellular components at ERD (Figure 3.3 A) included the chloroplast (36%) and the cytosol (15%). Other cellular components that were observed were the cytoplasm (9%), nucleus (8%), mitochondria (8%), endoplasmic reticulum (6%), extracellular matrix (6%), peroxisome (4%), golgi apparatus (2%), lysosome (2%), vacuole (2%) and proteasome respectively. At MRD (Figure 3.3 B) as well as for the LRD (Figure 3.3 C) similar cellular compartments were observed, however, there was an increase in the chloroplast (47%) at MRD while for LRD, there was a decrease in chloroplast (35%). Furthermore, at MRD the cytoplasm (17%) and the nucleus (10%) increased while the cytosol (8%), decreased compared to ERD. The cell wall (1%) and plasma membrane (1%) continued to be represented at MRD and LRD and not at ERD.

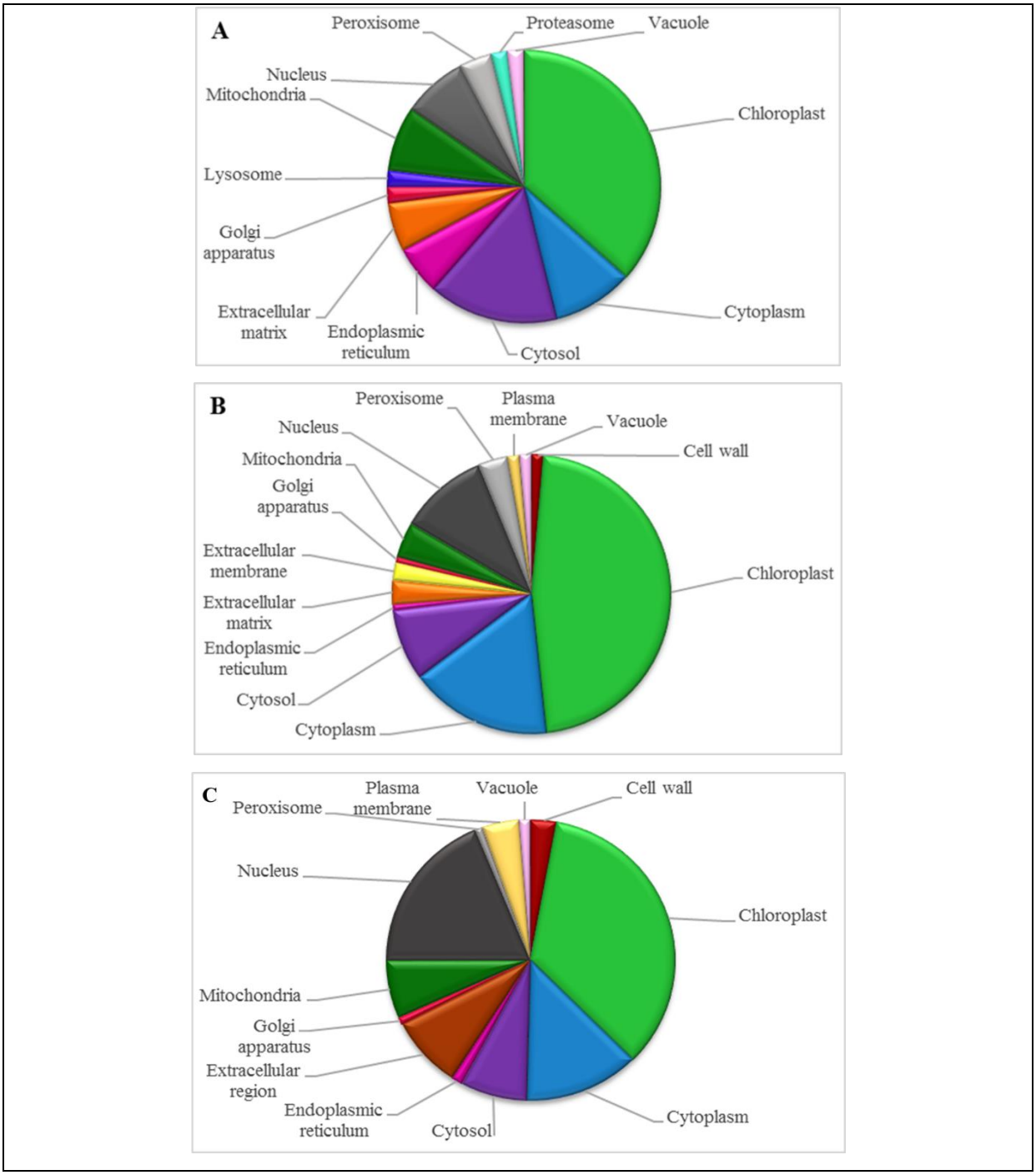

Figure 3.3: Cellular component prediction of the identified *X. schlechteri* differentially expressed proteins based on GO-annotation at the **(A).** Early response to drying; **(B).** Mid response to drying and **(C)**. Late response to drying.

The GO-terms allocated to the molecular functions of *X. schlechteri* were examined and the results showed that the ERD (80-70% RWC) is mostly associated with antioxidants (4%), binding (6%) and catalytic activity (1%) (Figure 3.4 A). As the drying progressed and reached the MRD (60-40% RWC) (Figure 3.4 B), proteins belonging to antioxidants (9%), binding activity (13%) and catalytic activity (3%) increased compared to the ERD. In addition, proteins

belonging to transport (1%) and translation regulation (3%) became associated with MRD. A significant increase in proteins belonging to binding (47%), antioxidants (24%) and catalytic activity (7%) was observed at the LRD (Figure 3.4 C). Transcription (2%) and translation (5%) also became associated with LRD while proteins belonging to electron carriers and molecular transducers decreased compared to the ERD.

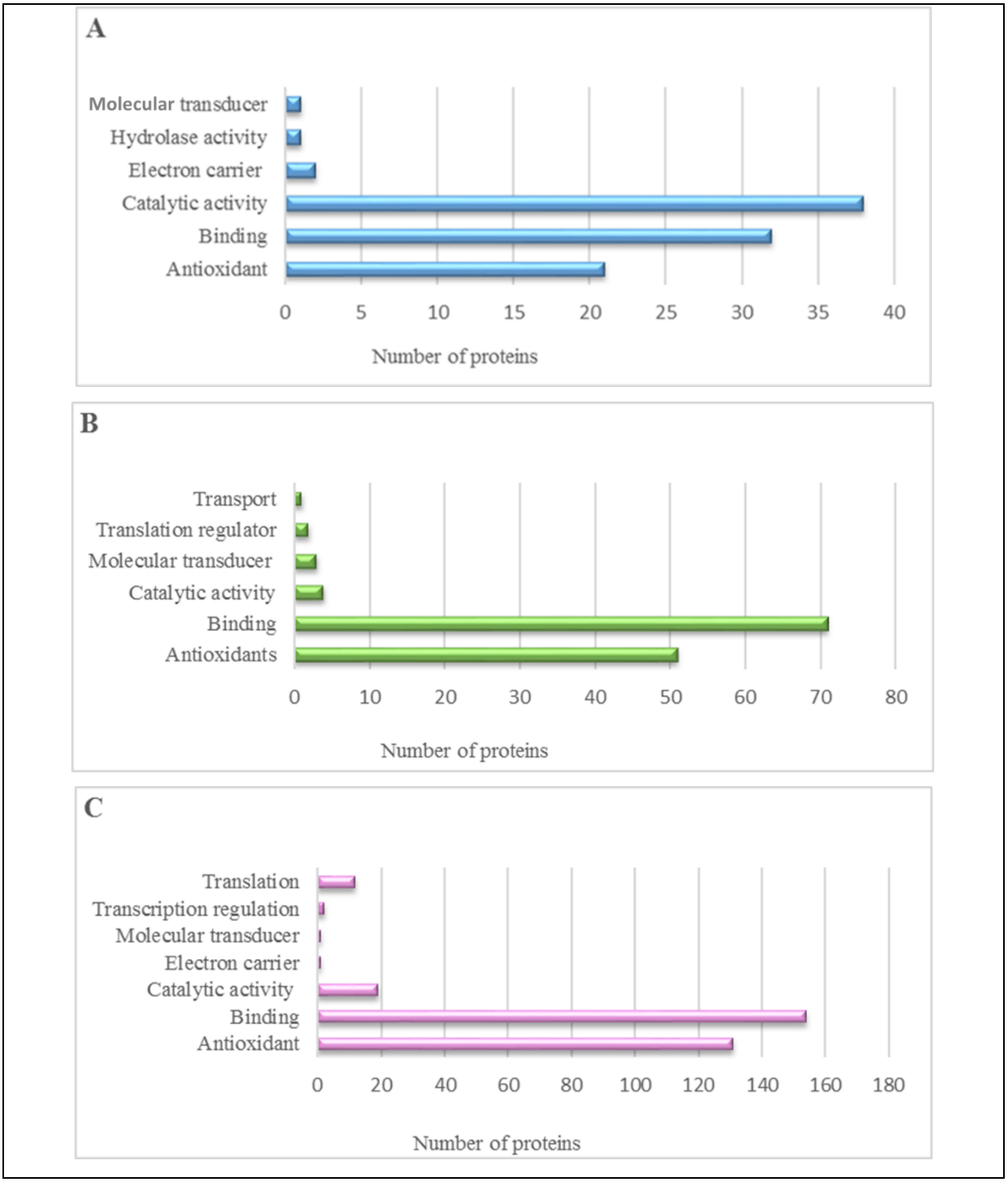

Figure 3.4: Molecular process predictions of the identified *X. schlechteri* differentially expressed proteins based on GO-annotation. **(A).** Early response to drying; **(B).** Mid response to drying and **(C).** Late response to drying.

The GO-terms allocated to the biological processes of *X. schlechteri* indicated that proteins belonging to biochemical processes were increased at LRD when compared to ERD and MRD (Figure 3.5). Similarly, this increase at LRD can be seen for the biosynthesis pathway, catabolic pathways, cellular and defence response. Proteins belonging to translation increased at MRD and continued through to LRD.

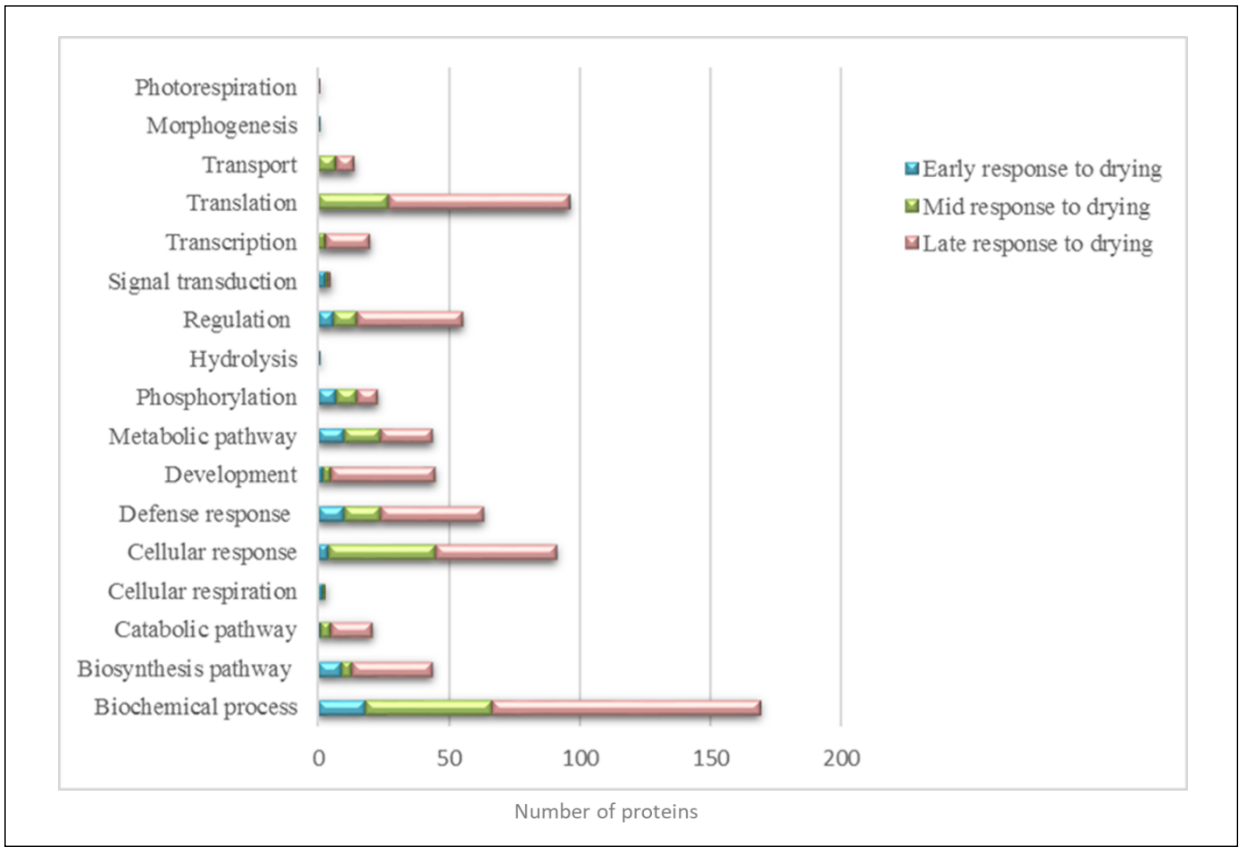

Figure 3.5: Biological process predictions of *X. schlechteri* differentially expressed proteins across treatments.

MapMan analysis, molecular functions and biological processes

MapMan was also used to obtain functional information of the dehydration responsive *X. schlechteri* proteins where the differentially expressed proteins were assigned to various BINs based on MapMan ontology (Table 3.4 A, B and C). A total of 253 proteins of 269 were mapped to 25 functional BINs across the dehydration treatments (ERD, MRD and LRD). The tables display BIN numbers, BIN names, number of elements which are the proteins allocated to each BIN along with the associated probabilities (p-value ≤ 0.05). Significance was tested through Wilcoxon Rank Sum, this test is similar to a student's t-test, where significance is

tested based on whether changes within a BIN are more extreme than the changes in all the proteins.

Table 3.4 A: Representing upregulated and downregulated *X. schlechteri* proteins at early response to drying.

Bin	Name Upregulated proteins at ERD	Elements (no.of proteins allocated)	p-value
35	Not assigned	11	0.676053
9	Secondary metabolism	2	0.791296
1	Photosynthesis	1	0.140458
4	Amino acid metabolism	1	0.140458
11	Phytohormone action	1	0.259640
25	Nutrient uptake	1	0.259640
5	Lipid metabolism	1	0.435156
2	Cellular respiration	1	0.664612
Bin	**Name Downregulated proteins at ERD**	**Elements (no.of proteins allocated)**	**p-value**
7	Co-enzyme metabolism	5	0.785817
19	Protein homeostasis	4	0.335234
35	Not assigned	3	0.276986
3	Carbohydrate metabolism	2	0.045141
1	Photosynthesis	2	0.920212
6	Nucleotide metabolism	2	0.920212
2	Cellular respiration	1	0.127153
17	Protein biosynthesis	1	0.165518
22	Vesicle trafficking	1	0.405381
26	External stimuli response	1	0.488074
27	Multi-process regulation	1	1

Table 3.4 B: Representing upregulated and downregulated *X. schlechteri* proteins at mid response to drying.

Bin	Name Upregulated proteins at MRD	Elements (no.of proteins allocated)	p-value
35	Not assigned	2	0.029297
19	Protein homeostasis	2	0.028108
3	Carbohydrate metabolism	2	0.107347
5	Lipid metabolism	2	0.941653
9	Secondary metabolism	1	0.114128
12	Chromatin organisation	1	0.202622
2	Cellular respiration	1	0.332880
17	Protein biosynthesis	1	0.798859
16	RNA processing	1	0.878482
26	External stimuli response	1	0.878482

Bin	Name Downregulated proteins at MRD	Elements (no.of proteins allocated)	p-value
1	Photosynthesis	27	2.71E-04
35	Not assigned	16	0.481927
17	Protein biosynthesis	11	0.297923
19	Protein homeostasis	6	0.855506
3	Carbohydrate metabolism	5	0.002388
2	Cellular respiration	5	0.185229
10	Redox homeostasis	5	0.210305
4	Amino acid metabolism	2	0.207697
21	Cell wall organisation	2	0.287358
18	Protein modification	2	0.575503
16	RNA processing	2	0.910829
6	Nucleotide metabolism	2	0.933061
27	Multi-process regulation	1	0.150744
26	External stimuli response	1	0.245505
22	Vesicle trafficking	1	0.442687
7	Co-enzyme metabolism	1	0.921600

Table 3.4 C: Representing upregulated and downregulated *X. schlechteri* proteins at late response to drying.

Bin	Name Upregulated proteins at LRD	Elements (no.of proteins allocated)	p-value
35	Not assigned	48	3.66E-04
17	Protein biosynthesis	14	0.350356
7	Co-enzyme metabolism	5	0.701357
1	Photosynthesis	4	0.004989
18	Protein modification	4	0.067196
5	Lipid metabolism	4	0.776159
16	RNA processing	4	0.845021
10	Redox homeostasis	3	0.060389
19	Protein homeostasis	3	0.213074
26	External stimuli response	3	0.775051
9	Secondary metabolism	3	0.806496
23	Protein translocation	3	0.854240
2	Cellular respiration	2	0.156297
3	Carbohydrate metabolism	1	0.086411
13	Cell cycle organisation	1	0.506139
14	DNA damage response	1	0.506139
15	RNA biosynthesis	1	0.551926
Bin	**Name Downregulated proteins at LRD**	**Elements (no.of proteins allocated)**	**p-value**
1	Photosynthesis	16	0.021967
35	Not assigned	14	0.335041

3	Carbohydrate metabolism	6	0.241955
19	Protein homeostasis	4	0.364960
10	Redox homeostasis	3	0.497135
21	Cell wall organisation	2	0.340023
7	Co-enzyme metabolism	2	0.896482
17	Protein biosynthesis	2	0.965407
27	Multi-process regulation	1	0.273913
26	External stimuli response	1	0.465759
4	Amino acid metabolism	1	0.584346
2	Cellular respiration	1	0.715337
22	Vesicle trafficking	1	0.761192

Similar biological processes to the Blast2GO results were also observed using MapMan. There was a number of differentially expressed proteins placed in the "not assigned" BIN (BIN 35). This suggested that a considerable amount of *X. schlechteri* proteins were under represented. This could be due to the fact that *X. schlechteri* has only recently been sequenced (Costa *et al.*, 2017) and there is insufficient annotated information compared to that available for model-plant organisms such as Arabidopsis thaliana. Nevertheless, a significant amount of proteins were identified within the *X. schlechteri* dataset that had protein annotation information for further bioinformatic analyses. Proteins that were successfully mapped to BIN classes showed differentially regulated proteins involved in the various biological processes of *X. schlechteri.*

To obtain a holistic view of the response of *X. schlechteri* across the dehydration stages (ERD, MRD and LRD) and based on the results from the MapMan gene ontology outline above, a visual representation of the responses is given in Figure 3.6. Some of these responses, and their role in mitigating the effects of dehydration, will be discussed in context below.

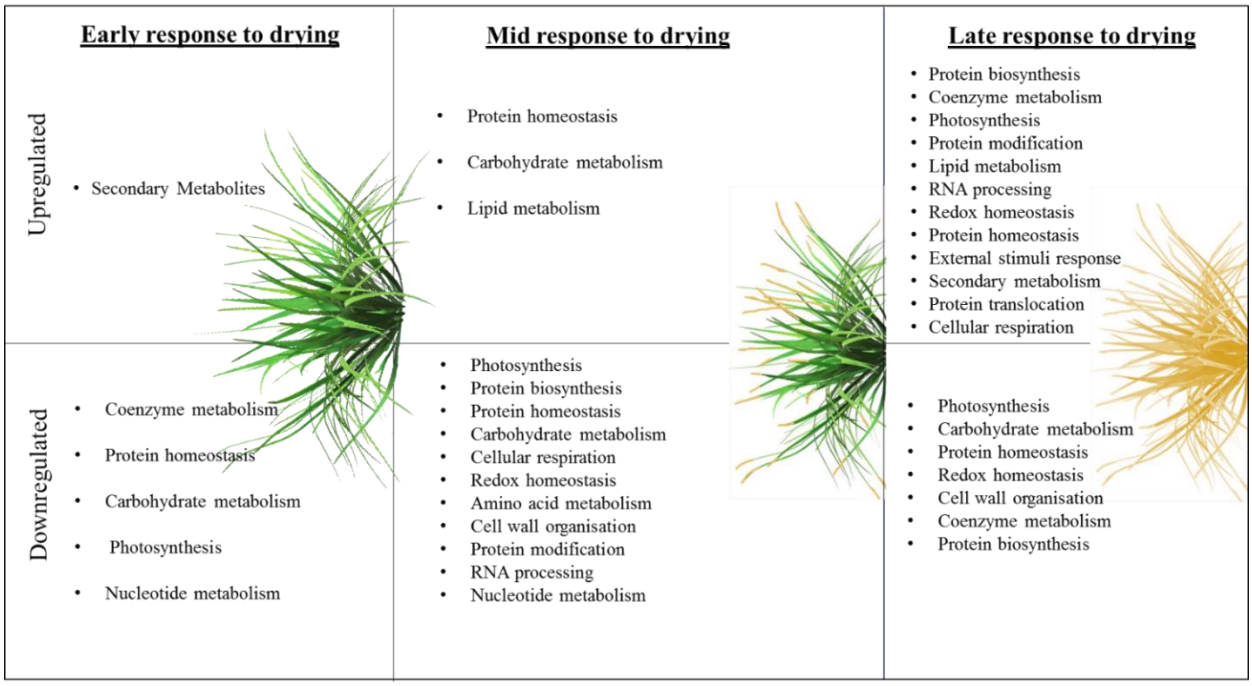

Figure 3.6: Visual representation of *X. schlechteri* response to dehydration based on MapMan gene ontology. The figure is a visual representation of the gene ontologies associated with the differentially expressed *X. schlechteri* proteins that were mapped to BIN's in MapMan (see Table 3.4 A, B and C). The upregulated and downregulated proteins were mapped across the drying stages, early response to drying, mid response to drying and late response to drying.

While proteins associated with cellular processes are variously upregulated and downregulated during the various stages of rehydration, the following discussion will concentrate on the predominant trends and highlight the relevance of some of these components in the acquisition of desiccation tolerance, in the light of existing literature on drought and particularly vegetative desiccation tolerance.

Early response to drying

At ERD several of the upregulated proteins were involved in secondary metabolism. Resurrection plants utilise their secondary metabolites for protection against severe water loss and stress caused by UV-light damage (Moore *et al.*, 2005; Farrant *et al.*, 2007). Such protection enables resurrection plants to gain an advantage over other plant species within their particular ecological niche in response to water loss (Gechev *et al*., 2014). The proteins involved in secondary metabolism (Supplementary Table S3.1) were UDP-glycosyltransferase (GO:0016758) and chloroplastic polyphenol oxidase (PPO)(GO: 0004097) both which are thought to be involved in plant defence against drought (Li *et al.*, 2017; Boeckx *et al.*, 2015).

While other roles for UDP glycosyltransferases have been suggested, its role in secondary metabolism has been linked to anthocyanin production (Li *et al.*, 2017). Supporting this role in *X. schlechteri*, Sherwin and Farrant (1998) report an increase in anthocyanin production during this stage of dehydration, which continues throughout dehydration in this species. Here, anthocyanins play a role both in protection against excess light and in an antioxidant capacity. Li *et al.* (2017) found that UDP- glycosyltransferases belongs to the glycosyltransferase family in plants and are responsible for controlling many metabolic processes and transferring sugar moieties onto small molecules. The researchers also found that overexpression of UDP-glycosyltransferase enhanced the tolerance to drought, low temperatures and salt stress in *Arabidopsis thaliana*. PPO catalyses the oxidation of monophenols and/or o-diphenols to o-quinones with the concomitant reduction of oxygen to water. Several roles for PPO have been proposed, including defence against herbivory, pathogens and abiotic stresses, particularly those affecting photosynthesis (Boeckx *et al*., 2015). However, the exact role they might play remains equivocal, and may vary among species.

Our study also shows that certain proteins associated with metabolic processes were downregulated at ERD (Figure 3.6) and these processes include co-enzyme, carbohydrate and nucleotide metabolism. Proteins involved in protein homeostasis and photosynthesis were also downregulated. Co-enzyme metabolism had the most number of proteins allocated to this processes (Supplementary Table S3.2) and included HEMC Porphobilinogen deaminase (GO:0004568), CHLM Magnesium protoporphyrin IX methyltransferase (GO:0004149), PORB Protochlorophyllide reductase B (GO:0016630) and CHLP Geranylgeranyl diphosphate reductase (GO:0046406), all of which are involved in photosynthesis and chlorophyll synthesis.

CHLP Geranylgeranyl diphosphate reductase (GO:0046406) catalyzes the reduction of geranylgeranyl diphosphate to phytyl diphosphate, providing phytol for both tocopherol and/or chlorophyll synthesis (Tanaka *et al.*, 1999). Its downregulation thus implies declined synthesis of either or both of these molecules. Downregulation of chlorpohyll biosynthesis is consistent with the poikilochlorophyllous nature of *X. schlechteri*. Collett *et al.*(2003) reported a decline in transcription of CHLP geranylgeranyl diphosphate reductase in the poikilochlorophyllous sister species *Xerophyta humilis*, although this occurred only in the MRD at RWC below 60%. PORB Protochlorophyllide reductase B is another co-enzyme that was downregulated at ERD. This enzyme is involved in the pathway chlorophyll biosynthesis (Garrone *et al*., 2015) and

thus its downregulation, along with CHLP geranylgeranyl diphosphate reductase is further in keeping with the poikilochlorophyllous nature of *X. schlechteri*.

Less proteins were associated with carbohydrate metabolism and nucleotide metabolism compared to co-enzyme metabolism (Supplementary Table S3.2). Carbohydrate metabolism showed downregulation of the 6-phosphogluconolactonase (GO: 0005975) and transaldolase (GO: 0015979) which are enzymes that are involved in the pentose phosphate pathway (PPP). This pathway is central to plant metabolism in that it parallels or can serve as an alternative to glycolysis (Kruger and von Schaewen, 2003). It has two distinct connected phases, namely, an oxidative phase and a non-oxidative phase. The non-oxidative phase serves as a precursor for nucleotide biosynthesis (Xiong *et al.,* 2009), while the oxidative phase results in conversion of hexose phosphates to glyceraldehyde-3-phosphate and CO_2 and thus via its role in photosynthesis, can in turn affect various aspects of plant growth, chloroplast development and stem elongation which ultimately affects the amount of biomass (Dubouzet *et al.,* 2013). Modulation of its activity during the ERD in *X. schlechteri* could possibly slow down photosynthesis.

The protein homeostasis process involved HSP 90 (GO: 0003924) which plays an important role in stress response, plant development and disease resistance (Lindquist and Jarosz, 2010). HSP 90 is the most abundant HSP, with multiple proposed functions and has been shown to be accumulated during the LRD in *X. schlechteri*, where it has been proposed to predominantly play a chaperonin role (Walford *et al*., 2003; Farrant *et al.*, 2015). The reason for its initial decline observed in this study could be due to the fact that it is at ERD, and *X. schlechteri* is in the initial stages of dehydration and does not require this protection.

Another protein involved in protein homeostasis was RPN8A 26S proteasome non-ATPase regulatory subunit 7 homolog A (GO:0004017) which plays a role in the determination of leaf polarity (Huang *et al.*, 2006). Asparaginyl endopeptidase (GO:0016630) has a significant role in plant defence and seed storage protein maturation (Jackson *et al*., 2018).

Typical to *X. schlechteri,* there were photosynthesis-related proteins that were downregulated specific to the photosynthesis process. These were Rieske iron-sulfur (GO: 0005515) and PNSL1 Photosynthetic NDH subunit of lumenal (GO: 0009765). Studies conducted on Rieske iron-sulfur found that it belongs to a complex through which electrons flow allowing energy to be used by the carbon source of the plant and was also found to increase photosynthesis by 10% (Ermakova *et al.,* 2019). PNSL1 Photosynthetic NDH subunit of lumenal is believed to be PsbP- like proteins that is involved in photosystem II repair in *A. thaliana* (Ishihara *et al.*,

2007). Interestingly, Collett *et al.,* (2003) showed a decline in PsbP transcripts below 60% RWC in *X. humilis*, confirming the finding here.

Mid response to drying

As drying continued and *X. schlechteri* shifted into the MRD, the upregulated proteins (Supplementary Table S 3.3) were seen to be predominantly involved in protein homeostasis and included HSP70 (Heat shock cognate 70 kDa protein) (GO:0006457) and RUB2 (Ubiquitin-NEDD8-like protein RUB2) (GO:0005515). Protein homeostasis is the ability of the cell to properly manufacture, fold, and deactivate protein molecules, so that the cell can respond to both internal and external environments (Díaz-Villanueva, *et al.,* 2015). When stress occurs, the co-ordinated synthesis of heat shock proteins (HSP) is brought upon in order to combat the damaging effects of protein denaturation (Ellis and van der Vies, 1991, Gething and Sambrook, 1992; Parsell and Lindquist, 1993; Morimoto *et al.,* 1994; Netzer and Hartl, 1998; Miernyk, 1999; Abdalla and Rafudeen, 2012). HSP 70 is known to protect organisms from stress by providing cytoprotection against macromolecular damage (Morano and Thiele, 1999) and have been shown to accumulate during the MRD to LRD in *Xerophyta viscosa* (Ingel *et al.*, 2008; Abdalla and Rafudeen, 2012).

Carbohydrate metabolism is crucial for cellular protection in resurrection plants (Dinakar and Bartels, 2013). This study also showed an upregulation in carbohydrate metabolism at MRD and involved UDP-glucose pyrophosphorylase (GO:0006011) and PHS2 Alpha-glucan phosphorylase 2 (GO:0005975). Carbohydrate content (sugars) changes drastically and is abundant during the different drying stages. Sugars have many roles such as being substrates in reactions, having a structural role in many biochemical processes and are transporters as well as being storage substances (Fernandez *et al.,* 2017). In resurrection plants, the universal presence of high levels of sucrose at the late stages of dehydration have been invoked to act inter alia in vitrification of the cytosol and cytoplasm (reviewed in Farrant *et al*., 2017; Oliver *et al.,* 2020). Carbohydrate metabolism brought about the upregulation of UDP-glucose pyrophosphorylase (UGPase) which is a key enzyme in sucrose metabolism and carbohydrate biosynthesis (Coleman *et al.*, 2006). UGPase is believed to be involved in sucrose metabolism where it works in co-ordination with sucrolytic enzymes (namely, SuSy, fructokinase, and SPS/SPP) and hexose phosphates (Kleczkowski, 1994). UGPase is an ubiquitous enzyme that produces UDP-glucose which is vital for sucrose and polysaccharide synthesis (Meng *et al.,* 2009).

Lipid metabolism was also upregulated at MRD which involved phospholipase A2 (GO:0004623) and PLP1 Patatin-like protein 1 (GO:0006629). Phospholipase A2 proteins are involved in pathways which ultimately results in the production of jasmonic acid and related compounds (Narvaez-Vasquez and Florin-Christensen *et al.,* 1999). Jasmonic acid is an important hormone for the regulation of plant development and mediator of abiotic stress (Ruan *et al.,* 2019). The rapid activation of phospholipase A2 activity are thought to be involved in plant defence related processes (Narváez-Vásquez *et al.,* 1999).

A large number of proteins were downregulated at MRD (Supplementary Table S3.4), these included proteins associated with photosynthesis, protein biosynthesis, protein homeostasis, carbohydrate metabolism, cellular respiration, redox homeostasis, cell wall organisation, protein modification, RNA processing and nucleotide metabolism.

The largest number of proteins were found to be downregulated in photosynthesis.This is attributed to the poikiolochlorophyllous nature of this plant. Upon closer inspection of the photosynthetic proteins (Supplementary Figure S3.1 and Table S3.5 A), it can be seen that there is a large number of proteins associated with the photosystem II complex (PSII) that are downregulated at MRD. Similarly, a host of proteins involved in the Calvin cycle were also downregulated (Supplementary Figure S3.1 and Table S.3.5 B-Calvin cycle) all corroborating results from a previous transcriptomic study on this species (Costa *et al.,* 2017). When the drying of plants occurs, there is a huge decrease in yield which is a result of inhibition of photosynthesis (Kalaji *et al.,* 2016). In this condition the plant absorbs more light energy than it can consume and the excess energy increases ROS accumulation (as discussed in Chapter 2). To survive these changes, plants initiate a series of regulatory mechanisms such as photorespiration and the downregulation of photosystem II complex (PS-II) activity (Li and Ma, 2012). Thus, examining how *X. schlechteri* avoids oxidative damage will help future drought tolerant plants

The correlation between photosynthesis, Calvin cycle and cellular respiration is that the product of the one process serves as the reactants of the other.

Protein biosynthesis-related proteins were also downregulated, possibly suggesting a general slowing down of translation. These proteins included RPL5 50S ribosomal protein L5 (GO: 0016620), which is responsible for the synthesis of proteins involved in photosynthetic apparatus (Yamaguchi and Subramanian, 2000; Bieri *et al.,* 2016.). Plant serine-threonine proteins are known to regulate signal transduction pathways via phosphorylation (Dudek *et al.,* 1997; Roth *et al.,* 2018).

Late response to drying

Upregulated proteins at the LRD included those involved in processes such as protein biosynthesis, co-enzyme metabolism, photosynthesis, protein modification, lipid metabolism, RNA processing, redox homeostasis, protein homeostasis, external stimuli response, secondary metabolism, protein translocation and cellular respiration (Table 3.4 C, Supplementary Table S3.6). The process with the highest number of proteins was protein biosynthesis (14 according to Table 3.4 C). Abdalla and Rafudeen, (2012) similarly reported an extensive upregulation of such processes in *X. viscosa*. In desiccation sensitive plants protein biosynthesis ceases at even mild levels of drought stress while desiccation tolerant plants are capable of continuing protein synthesis until leaves are almost air-dry (Bartels *et al.*, 1990; Gaff *et al*., 1997). A common feature in desiccation tolerant leaf tissue is the upregulation of LEA proteins. A large number of LEA proteins were identified at LRD (Table 3.3). It has been reported that LEA proteins have a protective role and thus accumulate abundantly in resurrection plants (Michel *et al.*, 1994; Velasco *et al*., 1994; Alamillo and Bartels, 1996; Ingram and Bartels, 1996; Ndima *et al.*, 2001). Upregulation also included EF-Tu translation elongation factor which are reported to be involved in abiotic stress response in plants (Fu *et al.*, 2012). Cellular respiration was also found to be upregulated at LRD with an increase in protein (phosphoglycerate kinase-GO:0006096) involved in glycolysis. Protein modification and protein translocation were also seen to be upregulated at LRD, where protein modification involved S-glutathionylation and protein folding. An aqueous environment has been noted to be an essential requirement for correct protein folding and that as water is lost. Resurrection plants have an adaptation mechanism such as the role of chaperones, to prevent protein degradation and misfolding of proteins. (Farrant *et al*., 2007). This may confer the upregulation of protein translocation and RNA processing (Supplementary Table S3.6) which involves a number of chaperone proteins. RNA processing may also be upregulated at LRD as *X. schlechteri* stores RNA required for recovery in rehydration particularly for photosynthesis.

At the LRD stage, several proteins involved in photosynthesis, carbohydrate metabolism, protein homeostasis, redox homeostasis, cell wall organisation, coenzyme metabolism and protein biosynthesis were downregulated. With respect to the proteins downregulated in photosynthesis, they included LHCb1/2/3 of LHC-II complex, PsbO and PsaD and their downregulation help further minimize potential ROS generation from photosynthetic activity.

The redox enzymes (Supplementary Table S3.7) that are present do not denature during drying and thus are possibly able to detoxify ROS during LRD (Sherwin and Farrant, 1996; Mundree and Farrant, 2000; Farrant *et al.*, 2007).

The co-enzymes that were downregulated at LRD (Supplementary Table S 3.7) were involved in the thiamine pathway (THI1-2 Thiamine thiazole synthase 2) (GO:0003993). Thiamine biosynthesis was previously linked to oxidative stress responses (Tunc-Ozdemir *et al.*, 2009). Thiamine metabolism also plays a protective role against stresses (Settembre *et al.*, 2003). The results obtained from the KEGG analysis also showed thiamine metabolism to be represented (Supplementary Table S3.8). Previous studies (Tunc-Ozdemir *et al.*, 2009) have found the accumulation of thiamine upon stress plays a role in combating ROS induced damage. At this stage of the dehydration it can be proposed that *X. schlechteri* mostly has ROS under control and oxidative damage is no longer a threat.

X. schlechteri undergoes an array of distinct changes in metabolic and biological activity in response to each drying stage. There seems to be certain biological processes and differentially expressed proteins that are involved across the different drying stages. The overall changes observed across the drying stages are most likely not only to facilitate drying in *X. schlechteri*, but also to prepare for reconstitution of the biological and metabolic processes upon rehydration.

Brief Conclusion

The aims set out for this chapter wer to identify and quantify the differentially expressed proteins in *X. schlechteri* across the three drying stages and to find biological processes that play a role in its desiccation response. The process was initiated by a label-free quantification approach which helped identify and quantify the differentially expressed proteins. It was established that the *X. schlechteri* differentially expressed datasets were well-represented with usable protein descriptions and annotations. A combined number of 517 proteins were differentially expressed in response to drying. This was followed by further functional analyses using bioinformatics tools that allowed functional classifications for biological processes, molecular functions and cellular compartments that were involved in the *X. schlechteri* drying response. These results supported the physiological results (Chapter 2, those reported in previous studies on *X. schlechteri* (Mundree and Farrant 2000; Farrant *et al.*, 2015; Costa *et*

al., 2017) and other resurrection plants (reviewed in Dinakar and Bartels, 2013; Zhang *et al.*, 2016).

The gene ontology analyses of the differentially expressed proteins allowed for a visual representation of the overall *X. schlechteri* proteome response at the different drying stages (Figure 3.6). Specific *X. schlechteri* proteins and biological processes that may play a role in withstanding the various drying stages were also highlighted. *X. schlechteri* appears to employ and adopt many strategies to withstand drying.

The aforementioned proteomic and bioinformatic workflow successfully identified and quantified differentially expressed proteins and their subsequent functional classification allowed certain biological processes and pathways involved in the *X. schlechteri* desiccation reponse to be highlighted. The next chapter will focus on the corresponding metabolome at the three drying stages in order to correlate and validate the data obtained in this chapter.

Chapter 4

A metabolomic approach to investigating the drying response of *X. schlechteri* and maize to dehydration

Introduction

Metabolomics has been used to study the response of plants to environmental stresses such as drought as it allows the quantification and identification of metabolites which may play an important role in drought tolerance (llakhverdiev *et al.,* 2008; Arbona *et al.*, 2013). With respect to crop plants and their stress responses, metabolomics also allows key biological processes to be identified and serves as a tool for biomarker discovery (Oikawa *et al*., 2008; Simó *et al.,* 2014). These potential biomarkers could be integrated into marker-assisted breeding strategies in order to enhance the selection of plants with desired traits (Tuberosa and Salvi, 2006). Metabolomics ultimately plays an important role in bridging the gap between phenotype-genotype studies and for enriching and complementing data of functional ontological analyses obtained from genomics, transcriptomics and proteomics (Parida, 2018). Importantly, metabolomics can also be used to validate proteomic data in order to confirm the differential expression of the proteins or support the role of identified biological processes and pathways (Chagoyen and Pazos, 2013).

Traditionally, validation of proteomic data was done using Western blots, biochemical assays or measuring the corresponding mRNA abundance of selected differentially expressed proteins in the proteome dataset (Vogel and Marcotte, 2012; Payne, 2015). Metabolomics offer several advantages compared to the traditional approaches of validation. A metabolite, be it a sugar, amino acid or hormone, that is identified and quantified in parallel with a proteomic study, is the functional product of a pathway as a result of specific differentially expressed proteins. The epigenetic nature of the proteome is also reflected in the metabolome (Mhlongo, *et al.*, 2018). This is not the case where mRNA abundance is used for validation due to mRNA degradation or differences in translational efficiency (Vogel and Marcotte, 2012; Payne, 2015). Lastly, metabolomics allows the identification of many metabolites compared to biochemical assays which are often specific for a selected enzyme or metabolite.

Label-free quantification analysis (LFQ) is becoming a common and established technique for analysing the proteome. The amount of data obtained from LFQ is very large compared to traditional proteomic approaches such as two-dimensional MS proteomics and it is therefore more suitable to validate subsets of the LFQ data using metabolomics.

The rationale behind this chapter was to use a metabolomics approach to investigate specific phytohormones, amino acids, sugars, sugar alcohols, fatty acids and/or organic acids in *X. schlechteri* in response to dehydration. Investigating the abundance or presence of these metabolites will help validate data from the proteomic study and may shed further light on the biological processes involved in the adaptations of *X. schlechteri* to dehydration.

The aim of this chapter

The aim of this chapter was to employ the GC-MS and LC-MS methods to observe the abundance of sugars, sugar alcohols, fatty acids, organic acids, phytohormones and amino acids of *X. schlechteri* in response to drying across ERD (~80-70% RWC), MRD (~60-40% RWC) and LRD (~40-10% RWC) compared to the hydrated (100% RWC) control. As indicated above, this is, in part, to validate the proteome study outlined in Chapter 3.
The metabolomic analyses were also conducted in parallel on maize plants subjected to dehydration to ~ 60-50% RWC compared to hydrated control, in order to contrast the response of a desiccation sensitive plant species with a desiccation tolerant one at these RWC points. The RWC threshold in the range of 60-50% was selected because according to Chapter 2, the antioxidant enzymes retained some activity at 50% RWC in maize, suggesting that tissues had not succumbed to excessive dehydration.

Materials and method

Plant material and sampling

X. schlechteri and maize were maintained and dehydrated as described in Chapter 2. In the case of *X. schlechteri,* five plants and leaf tissue of similar size were used as biologicals and three leaves per biological were sampled at each time point during the dehydration. In the case of maize, 5 of the 40 plants were kept aside, were kept fully hydrated by frequent watering and

served as the hydrated control. As previously determined (Chapter 2) the rest of the maize plants were subjected to dehydration by withholding water at the V12 stage. The leaf water content was determined on each of the five plants at each sampling point.

Extraction and derivatization of metabolites

Extraction and derivatization of metabolites were conducted according to Lisec *et al.,* 2006. Leaf material from the different stages of dehydration were ground into a fine powder in liquid nitrogen using a mortar and pestle. Samples were accurately weighed, and 100 mg of finely ground material was placed in a 2 ml round bottom tube with a cap and rapidly placed in liquid nitrogen. Pre-cooled 1.4 ml of methanol was added. The samples were vortexed for 10 seconds, after which 60 µl of ribitol (0.2 mg/ml^{-1} stock in dH_2O) was used. The ribitol served as an internal quantitative standard. The samples were vortexed once again for 10 seconds and then shaken for 10 minutes at 70°C in a thermomixer. The samples were centrifuged for 10 minutes at 11 000 *g*, transferred to a Schott GL 14 vial followed by the addition of 750 µl of chloroform. Approximately 1.5 ml of dH_2O was added and vortexed for 10 seconds. The samples were then centrifuged for 15 minutes at 2200 *g* and 150 µl from the upper phase (polar phase) was transferred into a fresh 1.5 ml tube. The sample was then vacuumed concentrated. The tubes were filled with argon gas, to prevent oxidation and placed in a plastic bag containing silica bead desiccant and frozen at -80°C. Before derivatization, samples were freeze-dried for 30 minutes. The derivatization process begins with the addition of 40 µl methoxyamination reagent to the aliquots. One empty tube was used as a derivatization control. The samples were shaken for 2 hours at 37°C, while N-Methyl-N-(trimethylsilyl) trifluoroacetamide (MSTFA) was prepared with 20 µl of retention standard mixture. Approximately 70 µl of MSTFA prepared solution was added to the aliquots. The aliquots were then shaken for 30 minutes at 37°C and transferred to glass vials suitable for GC-MS analysis. The library of standards used in this study was prepared in the same manner, using a mixture of amino acids, sugars, phytohormones, organic acids and fatty acids. Amino acids (alanine, 5-oxoproline, L-serine, aspartic acid, serine, L-histidine, glycine, L-phenylalanine, valine, proline, norleucine, tyrosine, methionine, asparagine, lysine and tryptophan); sugars (galactose, fructose, glucose, erythritol , raffinose, sucrose and cellobiose); sugar alcohols (myo-inositol, sorbitol , mannitol and arabitol); organic acids (malic acid, citric acid and lactic acid); fatty acids (quininic acid, palmitic acid and stearic acid) and phytohormones (Gibberellic acid (GA), jasmonyl-l-

isoleucine (JA lle), salicylic acid (SA), indole-3-carboxylic acid (ICA), jasmonate (JA), indole-3-acetic acid (IAA-Asp), abscisic acid (ABA) and indole-3-butyric acid (IBA)) were run individually.

GC MS/MS metabolite profiling of amino acids and sugars, sugar alcohols, organic acids and fatty acids

Experiments were performed on a model 7000C gas chromatograph equipped with a 7693 autosampler and interfaced to a 7000A Triple Quadrupole mass spectrometer (Agilent Technologies, Santa Clara, CA, USA). The GC injection port temperature was set at 230°C and 1 µl of sample was injected using the autosampler setup which was in split-less mode with helium carrier gas flow set to 2 ml per minute. The electronic pressure control was enabled to keep the flow rate constant. The split ratio was adjusted to 1:25. The initial oven temperature was 80°C isothermal for 2 minutes followed by 15°C per minute ramp to 330°C and the temperature was held for 6 minutes. Analytes were separated on an Agilent HP-5ms column of 30 m length and 250 µm internal diameter. The HP5-ms is a low-polarity column with a (5%-Phenyl)-methylpolysiloxane stationary phase suitable for high-resolution separation of TMS-derivatised compounds (Agilent, Germany). The remaining monitored chromatography time proceeded with a 170-s solvent delay with filaments turned off. The mass spectrometer was configured for Electron Impact (EI) ionisation at -70 eV with the recorded mass range of m/z 70 to m/z 600 at 20 scans per second, manual mass defect was set to 0 and the detector voltage was ~1700-1850 V. MassHunter B.05 GC MS/MS software (Agilent, Germany) was used to identify and quantify metabolites from the spectrum using Acquired spectrum data identifying metabolites using known standards given above and the internal standard, ribitol.

LC/MS metabolite profiling of phytohormones

The phytohormones were run on AB sciex Qtrap 4000 LC-MSMS system coupled to an ACQUITY UPLC Waters. The column temperature was set to 40°C and an injection volume of 2 µl. The flow rate was 0.4ml/min and MS mode set at all ion fragmentation (AIF) with maximum injection time of 100 ms. Automatic gain control value was set at 1.00E+06. The Q-Exactive mass spectrometer features HCD (higher collisional dissociation) with an energy scale set at 30.0 eV. The recorded scan range MS was 100-1500 *m/z* with a capillary voltage of 3 kV. Auxiliary gas flow was 20 au with a capillary temperature of 200°C.The drying gas

temperature was 350°C and skimmer voltage 25 V and tube lens 130 V. Samples were analysed in positive ionization mode, followed by the same samples analysed in negative ionization mode.

Data processing

The chromatogram data obtained from both the GC MS/MS and LCMS was analysed in Openchrom 1.3 (https://www.openchrom.net/download) with Savitsky-Golay smoothing using the AMDIS and NIST MS (https://chemdata.nist.gov/mass-spc/ms-search/) libraries to identify specific metabolites. MetaboAnalyst version 4 (https://www.metaboanalyst.ca/) (Chong *et al.,* 2019) was used to do comparative statistics using ANOVA with Fisher's PLS-DA method and t-test to compare relative abundance across samples. The statistical tests generated dimension reduction which results in a score plot which distinguish variances in the dataset (Szymanska *et al.,* 2012). These results were further validated by performing heatmap hierarchical clusters based on difference in the respective metabolites across the drying stages. The hierarchical cluster is represented as a heat map with dendrograms using Euclidean distance.

Results and discussion

The changes in the metabolic profiles of the leaf samples of *X. schlechteri* and maize respectively were analysed during dehydration. The metabolites that changed significantly in abundance were used to validate and correlate the previous proteomic data (Chapter 3).

Variance of metabolites across the drying stages in *X. schlechteri*

It was important to first determine whether there was a difference in the metabolites during dehydration. Score plots were therefore conducted to investigate the variance of the metabolites (amino acids, sugars, sugar alcohols, organic acids, fatty acids and phytohormones) and the relationship amongst the samples across the drying treatments.

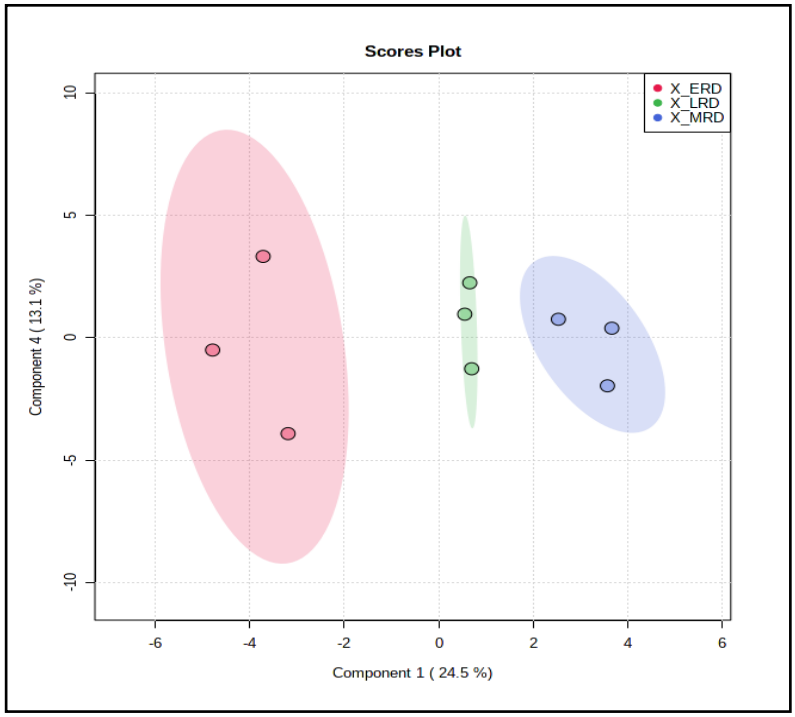

Figure 4.1: Scores plot based on principal components analyses of selected metabolites in *X. schlechteri* leaf material across the dehydration. Each circle represents a biological repeat while each colour represents the different drying stages. The variance with component 1 at 24.5 % and component 2 at 13.1%. The red circle represents early response to drying (ERD), blue circles represents mid response to drying (MRD) and green represents late response to drying (LRD).

The score plots for the metabolites (Figure 4.1) clustered separately for the different drying stages with component 1 at 24.5 % and component 2 at 13.1% of variance. In summary, these plots show that the respective metabolites in *X. schlechteri* leaf material varied between the three drying stages. Amino acid, sugar, sugar alcohol, organic acid, fatty acid and phytohormone analyses in *X. schlechteri* leaf tissue.

Heatmap hierarchical clusters were used to illustrate the abundance of the different metabolites across the three drying stages in *X. schlechteri* leaf tissue based on standards.

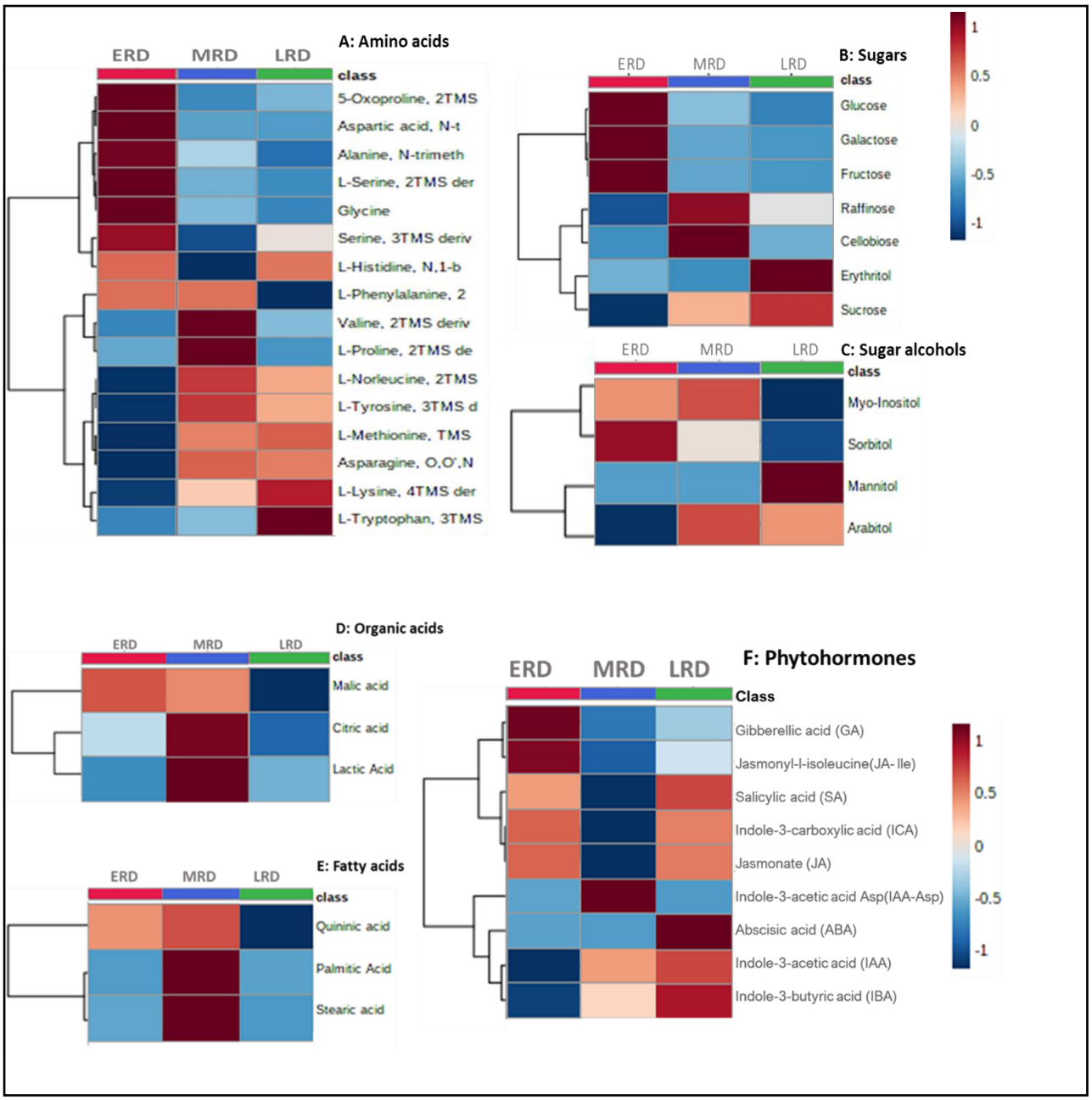

Figure 4.2: Heatmap of differentially abundant selected metabolites in *X. schlechteri*. Heatmap of **(A).** Amino acids across drying stages; **(B).** Sugars across drying stages; **(C).** Sugar alcohols across drying stages; **(D).** Organic acids across drying stages; **(E).** Fatty acids across drying stages and **(F).** Phytohormones across drying stages. The 'class' shown on the right side of the heatmap lists the metabolites. The drying stages represented are early response to drying (ERD), mid response to drying (MRD) and late response to drying (LRD). Shades of maroon represent high abundance of metabolites and shades of blue represent low abundance of metabolites.

All 16 amino acids for which standards were used showed significant changes in their abundance in *X. schlechteri* across the drying stages (Figure 4.2 A).

Alanine, 5-oxoproline, L-serine, aspartic acid, glycine and serine were shown to be highly abundant at ERD. Both L-alanine and β-alanine are involved in multiple stress responses in plants (Parthasarathy *et al.,* 2019) and are associated with replication, recombination and repair, transcription, signal transduction mechanism, amino acid transport, ribosomal structure and biogenesis, translation, coenzyme transport and metabolism. Previous studies (Parthasarathy *et al*., 2019) found that alanine plays important roles in plant physiology, metabolism and defence. High and increased levels of alanine during ERD in *X. schlechteri* have been reported by Radermacher *et al.,* (2019) and have been proposed by those to play a role in osmoprotection (Oliver *et al.,* 2011a). Alanine is thought to link Gamma aminobutyric acid (GABA) metabolism with glycolysis (Igamberdiev and Kleczkowski, 2018) and is the third most important anaerobic metabolism product (Sousa and Sodek, 2002).

The glutamate pathway (Supplementary Figure S 4.1) seems to be significant at the ERD stage in *X. schlechteri.* Glutamate and glutamine are derived from the assimilation of nitrate and ammonium in plants. Ammonium is assimilated into glutamine and glutamate via the glutamine synthetase (GS)/glutamine-oxoglutarate aminotransferase (GOGAT) cycle (Lea and Miflin, 1974, Tabuchi, 2007). Glutamine and glutamate can be derived from other amino acids such as arginine and proline (Forde and Lea, 2007). Glutamate has many functions such as in protein synthesis and is a major amino acid donor for the synthesis of nitrogen compounds and amino acids (Forde and Lea, 2007). It is also required for the synthesis of glutathione (GSH), a tripeptide of cysteine and glycine and an intracellular antioxidant in plants (Lu, 2013). It can be converted into GABA via glutamate decarboxylase (GDC). GABA and alanine rapidly accumulate in response to abiotic stress in order to modulate plant growth (Shelp, 1999; Bouche and Fromm, 2004; Bown *et al*., 2006; Reggiani *et al.,* 2000). In addition, glutamate has been implicated in root architecture (Walch-Liu *et al*., 2006; Forde and Walch-Liu, 2009) and calcium signalling (Dennison and Spalding, 2000). In *Arabidopsis thaliana* glutamate was found to inhibit primary root growth while stimulating the outgrowth of lateral roots (Walch-Liu *et al*., 2006). Previous studies have shown that 5-oxoproline, also known as pyroglutamic acid, is involved in the glutamine pathway (Mazelis and Pratt, 1976). Recently it has been shown that when this metabolite is applied as a treatment to lettuce under water deficit stress it can increase the yield by 31% through enhancing photosynthesis and plant stress defence responses (Jiménez-Arias *et al.,* 2019). The increase of 5-oxoproline at ERD in *X. schlechteri*

could therefore have contributed in enhancing the stress defence responses before the subsequent decrease observed at MRD and LRD.

The other amino acids that were also found to be abundnat at ERD were L-histidine and L-phenylalanine. L-histidine plays a critical role in plant growth and development (Ingle, 2011), while L-phenylalanine is involved in the synthesis of flavanoids and plays a role in plant defense (Ishihara *et al.,* 2008). The importance of L-phenylalanine is further emphasised by the fact that 20-30% of photosynthetically fixed carbon is directed towards its synthesis (Yoo *et al.,* 2013). Glycine was also seen to be abundant at ERD and this was also noted previously in the proteomics analyses where the glycine, serine and threonine KEGG pathways were highlighted (Chapter 3, Supplementary Table S3.10 and Figure S3.4). Previous studies have shown glycine to accumulate in the cytoplasm serving to stabilize and protect membranes and enzymes during stressful conditions (Winzor *et al.,* 1992).

As *X. schlechteri* shifted into MRD the accumulation pattern of amino acids changed as well, where alanine, 5-oxoproline, L-serine, aspartic acid, serine and L-histidine were shown to be less abundant. Alanine as mentioned before is associated with many processes including transcription and translation and it was previously observed that alanine-tRNA ligase was also downregulated in the proteomic data (Chapter 3, Table 3.2 and 3.3). L-phenylalanine, valine, proline, norleucine, tyrosine, methionine, asparagine and lysine were seen to be highly accumulated at MRD when compared to ERD. Tryptophan continued to be less abundant at MRD.

There was also a change in amino acid abundance and pattern as *X. schlechteri* shifted into LRD. Alanine, 5-oxoproline, L-serine and aspartic acid were seen to be less abundant while serine and L-histidine have increased in abundance from MRD to LRD. L-phenylalanine, valine and proline became less abundant at LRD compared to MRD. Norleucine, tyrosine, methionine, asparagine and lysine continued to be present in higher levels than ERD. Tryptophan however became highly abundant at LRD, confirming the observation of Radermacher *et al.,* (2019) on *X. schlechteri* during drought stress. Previous studies have shown that tryptophan plays a key role in defence response and the regulation of plant development (Ishihara *et al.,* 2008).

Amino acid accumulation during drying stages has been reported to play a key role in tolerance to drought stress (Joshi *et al*., 2010) and desiccation tolerance (Yobi *et al.,* 2019). Amino acids

either serves as osmotic adjusters or mobilize the formation of new proteins which are used to improve the plants response to drought (Campalans *et al.,* 1999). In the case of resurrection plants, they are also proposed to act as osmoprotectants and as nitrogen stores required for recovery on rehydration (Oliver *et al.,* 2020).

There was a change in the sugar profile across the dehydration stages (Figure 4.2 B) with galactose, fructose and glucose being abundant at ERD. The other sugars that were relatively abundant at ERD were the sugar alcohols - myo-inositol, sorbitol and erythritol. Malic acid the cyclitol quinic acid, were also relatively high at the ERD. Raffinose, sucrose, cellobiose and the sugar alcohols, mannitol and arabitol were less abundant at ERD, as were the organic acids citric and lactic acid and the fatty acids stearic and palmitic acids. As *X. schlechteri* shifted into MRD, galactose, fructose, glucose and erythritol were seen to be less abundant. Mannitol was less abundant at ERD and MRD compared to LRD. Sucrose, raffinose, arabitol, palmitic acid, cellobiose and the organic acids citric, malic and lactic acid, together with quinic and stearic acids became abundant at MRD. The increase in sucrose at this stage of dehydration has been previously reported for *X. schlechteri* (Radermacher *et al.,* 2019) and the present study suggests that this correlates with the decline in fructose and glucose. Interestingly, raffinose peaks at this stage of dehydration (Figure 4.2 B). This sugar, together with sucrose, has been proposed to play a role in vitrification of the cytosol at the LRD (Berjak *et al.,* 2007; Farrant *et al.,* 2007; 2017) and accumulation of this sugar in the mid to late stages of drying has been reported for some (e.g. Peters *et al.,* 2007; Liu *et al.,* 2019) but not all resurrection plants, this often being substituted for other Raffinose Oligosaccharides (RFO's) (Farrant *et al.,* 2017).

With respect to increase in the organic acids at this stage of dehydration, citrate accumulation has been shown to occur in *X. schlechteri* (Radermacher *et al.,* 2019) and in several other resurrection plants examined (Mundree and Farrant, 2000). It has been proposed that such accumulation could be the result of the shutdown of the tricarboxylic acid (TCA) cycle (Oliver *et al.,* 2020). Furthermore, together with sucrose and some amino acids, citric acid has been proposed to form Natural Deep Eutectic Solvents (Choi *et al.,* 2011, Dai *et al.,* 2013) which in turn have been proposed to stabilize the subcellular milieu in the desiccated state (Farrant *et al.,* 2017). There was a temporary increase in malic acid, lactic acid and quinic levels at the MRD.

However, it has been noted that the reasons for malic acid accumulation in the apoplast may not be due to drought stress per se, but rather as part of the stomatal regulatory system that works synergically with ABA (Wilkinson and Davies, 2002). A decrease in the accumulation of malic acid at LRD could be due to the TCA cycle shutdown. The other organic acid, lactic

acid is the product of anaerobic respiration and its accumulation here is not a commonly observed phenomenon in plants, but its production in bacteria has been shown to act as an antioxidant (Ding *et al.*, 2017).

Galactose, fructose and glucose continued to be less abundant at LRD, and there was a decline in cellobiose and the sugar alcohols, sorbitol and myo-inositol, as has been previously reported (Radermacher *et al.*, 2019). Similarly, the organic acids and fatty acids were also less abundant at LRD. There was an increase in abundance in mannitol, erythritol, raffinose, arabitol and sucrose at LRD. In previous studies myo-inositol was implicated as a precursor of many metabolites with regards to abiotic stress tolerance (Obata *et al.*, 2015) and functioning as an osmolyte and signalling molecule (Cote and Crain, 1993; Kaur *et al.*, 2013). Myo-inositol is a key component of the RFO pathway where together with UDP-galactose it forms galactinol through the galactinol synthase activity (Elsayed *et al.*, 2014). Galactinol in turn serves as a galactosyl residue to sucrose via different enzymes such as raffinose synthase and stachyose synthase to form raffinose and stachyose. Use of these pathways in production of RFOs has been demonstrated in the resurrection plant *Xerophyta viscosa* and the decline in myo-inositol in the current study is proposed to be as a consequence of the increased levels of raffinose in the later stages of drying (Peters *et al.*, 2007; Lehner *et al.*, 2008). These RFOs in turn have several functions such as serving as compatible solutes involved in stress tolerance, antioxidants, and help in carbon partitioning in response to stress (ElSayed *et al.*, 2014). Myo-inositol is also thought to play an important role in controlling the hormone auxin where it can bind to auxin and temporarily form an inactive conjugate (Bandurski, 1979). It is thought that these inactive conjugates allow for safe storage and transport of auxins thereby regulating its availability during stress or other physiological responses (Bandurski, 1979). Our results show an increase of myo-inositol and raffinose at MRD and a decrease at LRD (Figure 4.2 B and C) suggesting that the protection afforded to *X. schlechteri* via myo-inositol and RFOs occurs early in the desiccation tolerance response. The increase in mannitol can also be seen, previous studies have reported mannitol to be possibly playing a role in both abiotic and biotic stresses (Stoop *et al.*, 1996).

As previously reported, a common response to plant desiccation tolerance in the late drying stage is the high accumulation of certain sugars (reviewed in Berjak *et al*., 2007; Bartels and Hussain, 2011; Farrant *et al.*, 2015; Dinakar and Bartels, 2013, Elsayed *et al*., 2014). The sugars that accumulated at LRD are proposed to have protective mechanisms such as anhydrous glass formation (Crowe *et al.*, 1998; Hoekstra *et al.*, 2001), cytoplasm vitrification (Leopold

and Vertucci, 1986; Vertucci and Farrant, 1995) and stabilizing membrane proteins (Hartung *et al*., 1998; Oliver *et al.,* 1998). Raffinose which were found to be accumulated at MRD and LRD, is synthesised via galactose and myo-inositol being linked in the activated galactinol molecule. Raffinose are thought to be part of the stress tolerance mechanisms by protecting plant cells from oxidative damage caused by stress (Nishizawa, 2008; Peshev, 2013). However, it was also observed that certain sugars were also less abundant at LRD and more abundant at MRD (Figure 4.2 B).

Phytohormones, play a vital role in response to drought and other abiotic stresses (Wani *et al.,* 2016). A total of nine phytohormones were investigated across the drying stages in *X. schlechteri* (Figure 4.2 F). It was observed that at ERD, five phytohormones were found to be abundant and four less abundant. Gibberellic acid (GA), Jasmonyl-l-isoleucine (JA-lle), salicylic acid (SA), indole-3-carboxylic acid (ICA) and jasmonate (JA) were found to be abundant at ERD. GAs functions throughout the plant life cycle and is a growth hormone involved in cell elongation and enhancing cell division (Wang *et al*., 2008; Colebrook *et al.,* 2014). JA has been reported as being a central pathway to regulating plant defence and consists of a cascade of jasmonic acid derivatives collectively known as jasmonates (Erb *et al.,* 2012; Wasternack and Strnad, 2016). Indole-3-acetic acid Asp (IAA-Asp), abscisic acid (ABA), Indole-3-acetic acid (IAA) and Indole-3-butyric acid (IBA) were less abundant in *X. schlechteri* at ERD. As *X. schlechteri* shifted into MRD the GA, JA-lle, SA, ICA, JA and ABA were less abundant while all the auxin conjugates became abundant.

GA, JA-lle and IAA-Asp were less abundant at LRD while SA, ICA, JA, ABA, IAA and Indole-3-butyric acid (IBA) were abundant. SA was previously reported as a signalling molecule, playing a vital role in development, plant growth, flowering and defence during abiotic stress (Chen *et al.,* 2009; Khan *et al.,* 2015; Miura and Tada, 2014). ABA has also been reported as a central hormone in abiotic stress and is involved in drought tolerance, root development, stomatal regulation and the initiation of the ABA dependant pathway (Ullah *et al.,* 2018) and has been invoked in desiccation tolerance in all studies in which this hormone was measured (Vicré *et al.,* 2004). Though abiotic stress is mediated mostly by ABA, SA and JA, the overall stress response is not restricted to these phytohormones and there is crosstalk between phytohormones and other second messengers in regulating the defence response (Nakashima and Yamaguchi-Shinozaki, 2013; Nishiyama, 2013). The increase in auxins during late stages of drying is of note and in the only other study on auxins in resurrection

plants by Vicre *et al.* (2004), *Craterostigma wilmsii* similarly showed an increased presence in the late stages of drying. Those authors have invoked a role for the need for root regeneration on rehydration.

Validation and comparison of selected *X. schlechteri* proteins from proteomic dataset with metabolomic data

The *X. schlechteri* proteomic dataset from Chapter 3 provided a list of differentially regulated proteins in response to dehydration. Gene ontological analyses of some of these proteins showed their involvement in biological processes or in pathways linked to plant stress responses. The proteome in many instances give rise to the metabolome and therefore the role of selected proteins in a biological process can be validated or supported by corresponding metabolomic data. The metabolomic profile is influenced by proteins through enzymatic activities, pathways and transport while changes in protein expression may be affected by metabolite concentrations (Ghoumari *et al.,* 2003). A combination of these 'omic' approaches may provide a more comprehensive understanding of the biological function (Kitano, 2002). In addition, the benefit of comparing proteomic and metabolomic data under the same stress is often the similarity of the metabolic pathways and metabolites identified in each approach (Peng *et al*., 2015).

In the present study we integrated the *X. schlechteri* proteomic and metabolomic data in response to dehydration for validation and comparison. An overview of the corresponding *X. schlechteri* metabolites and proteins together with the functional category, molecular function and biological process across the drying stages can be seen in Tables 4.1 A, B and C. The abundance and decrease of metabolites were compared to the *X. schlechteri* protein expression obtained in the proteomic dataset (Chapter 3, Table 3.1). In addition, Supplementary Table S4.2 shows the pathways that were important in *X. schlechteri* stress response obtained with KEGG.

Table 4.1 A: Early response to drying and the corresponding metabolites and proteins.

Metabolites	Protein	Functional category	Molecular function	Biological process	Proteome/ metabolome
Serine	AGT1 Serine--glyoxylate	Amino acid transport and metabolism	catalytic activity transferase activity	Photorespiration glycine biosynthetic	Upregulated/ abundant

	aminotransferase (Xvis03_225299-PA)	Nucleotide transport and metabolism Coenzyme transport and metabolism Translation, ribosomal structure and biogene	transaminase activity	process, by trans-amination of glyoxylate	
Raffinose	RFS Galactinol--sucrose galactosyltransferase (Xvis03_210699-pa)	Signal transduction mechanisms Carbohydrate transport and metabolism Translation, ribosomal structure and biogenesis Cell wall/membrane/envelope biogenesis	Glycosyltransferase, Transferase	Carbohydrate metabolism raffinose family oligosaccharide biosynthetic process	Downregulated/ less abundant

Table 4.1 B: Mid response to drying and the corresponding metabolites and proteins.

Metabolites	Protein	Functional category	Molecular function	Biological process	Proteome/ metabolome
Alanine	GGAT1 Glutamate--glyoxylate aminotransferase 1 (Arabidopsis thaliana (Xvis03_212113-PA)	Amino acid transport and metabolism Transcription Coenzyme transport and metabolism	catalytic activity pyridoxal phosphate binding glycine:2-oxoglutarate aminotransferase activity transaminase activity alanine-glyoxylate transaminase activity L-alanine:2-oxoglutarate aminotransferase activity transferase activity	glycine biosynthetic process L-alanine catabolic process Photorespiration response to hypoxia	Downregulated/ less abundant
Serine	CLPP5 ATP-dependent Clp protease proteolytic subunit 5 (Xvis03_203635-PA)	Posttranslational modification, protein turnover, chaperones Signal transduction mechanisms Energy production and conversion	serine-type endopeptidase activity peptidase activity hydrolase activity serine-type peptidase activity	proteolysis	Downregulated/ less abundant
Serine	Serine hydroxymethyltransferase	Amino acid transport and metabolism Carbohydrate	glycine hydro-xymethyltrans-ferase activity	Tetra-hydrofolate inter-conversion	Downregulated/ less abundant

	(Xvis03_208040-PA)	transport and metabolism Signal transduction mechanisms	catalytic activity pyridoxal phosphate binding transferase activity	glycine biosynthetic process from serine glycine biosynthetic process cellular amino acid biosynthetic process methylation	
Serine	CLPP5 ATP-dependent Clp protease proteolytic subunit 5(Xvis03_211565-pa)	Posttranslational modification protein turnover, chaperones Signal transduction mechanisms Energy production and conversion	peptidase activity hydrolase activity serine-type peptidase activity ATPase binding,	proteolysis, protein quality control for misfolded or incompletely synthesized proteins	Downregulated/ less abundant
Tryptophan	At2g04400 Indole-3-glycerol phosphate synthase (Xvis03_219386-pa)	Amino acid transport and metabolism Carbohydrate transport and metabolism Translation, ribosomal structure and biogenesis	catalytic activity indole-3-glycerol-phosphate synthase activity	GO:0006568: tryptophan metabolic process	Downregulated/ less abundant
Galactose	RFS Galactinol--sucrose galactosyltransferase (Xvis03_210699-pa)	Signal transduction mechanisms Carbohydrate transport and metabolism Inorganic ion transport and metabolism	Transferase. raffinose family oligosaccharide biosynthetic process	galactose metabolic process	Downregulated/ less abundant
Fructose	FBPban1 Fructose-1,6-bisphosphatase (Xvis03_218527-pa)	Carbohydrate transport and metabolism Inorganic ion transport and metabolism Amino acid transport and metabolism	fructose 1,6-bisphosphate 1-phosphatase activity phosphoric ester hydrolase activity	dephosphorylation	Downregulated/\ less abundant
Glucose	ADG2 Glucose-1-phosphate adenylyltransferase large subunit 1 (Xvis03_220998-PA)	Carbohydrate transport and metabolism Signal transduction mechanisms Cell wall/membrane/envelope biogenesis	nucleotidyltransferase activity transferase activity		Downregulated/ less abundant

Sucrose	UDP-glucose pyrophosphorylase (UGPase) (Xvis03_202124-pa)	Sucrose metabolism Carbohydrate metabolism			Upregulated/ abundant

Table 4.1 C: Late response to drying and the corresponding metabolites and proteins.

Metabolites	**Protein**	**Functional category**	**Molecular function**	**Biological process**	**Proteome / metabolome**
Alanine	ALATS Alanine--tRNA ligase (Xvis03_224672-PA)	Translation, ribosomal structure and biogenesis Replication, recombination and repair Transcription Signal transduction mechanisms	alanine-tRNA ligase activity nucleotide binding ATP binding nucleic acid binding ligase activity tRNA binding zinc ion binding metal ion binding	alanyl-tRNA aminoacylation tRNA aminoacylation mitochondrial alanyl-tRNA aminoacylation	Downregulated/ less abundant
Serine	SAPK7 Serine/threonine-protein kinase SAPK7 (Xvis03_216515-PA)	protein serine/threonine kinase activity protein kinase activity ATP binding nucleotide binding transferase activity kinase activity ATP binding	defence response to bacterium intracellular signal transduction protein phosphorylation, abscisic acid-activated signalling pathway		Upregulated/ abundant
Glucose	ADG2 Glucose-1-phosphate adenylyltransferase large subunit 1 (Xvis03_220998-PA)				Downregulated/ less abundant

The metabolome and proteome are a direct reflection of the functional status of the cells and associated biological profile as it changes in response to stress at a given point in time (Zhang *et al.*, 2014; Patel and Ahmed, 2015). The inter-connectedness between the proteome and metabolome involves numerous pathways and biological processes which can help identify key

stress tolerance mechanisms. In addition, differentially regulated proteins or metabolites obtained from proteomic or metabolomic datasets from the same experiment can be cross validated between each dataset to confirm their regulation. It can be noted in our study that the metabolomic abundance profile complements the differential expression of the selected *X. schlechteri* proteins across the drying stages (Table 4.1 A, B and C) and provides further confirmation of pathways associated with *X. schlechteri* upon drying (Supplementary Table S4.2).

Variance of metabolites across two drying stages in maize

As mentioned previously in Chapter 2, it is important to contrast and compare the overall changes in *X. schlechteri* with a desiccation sensitive plant such as maize.

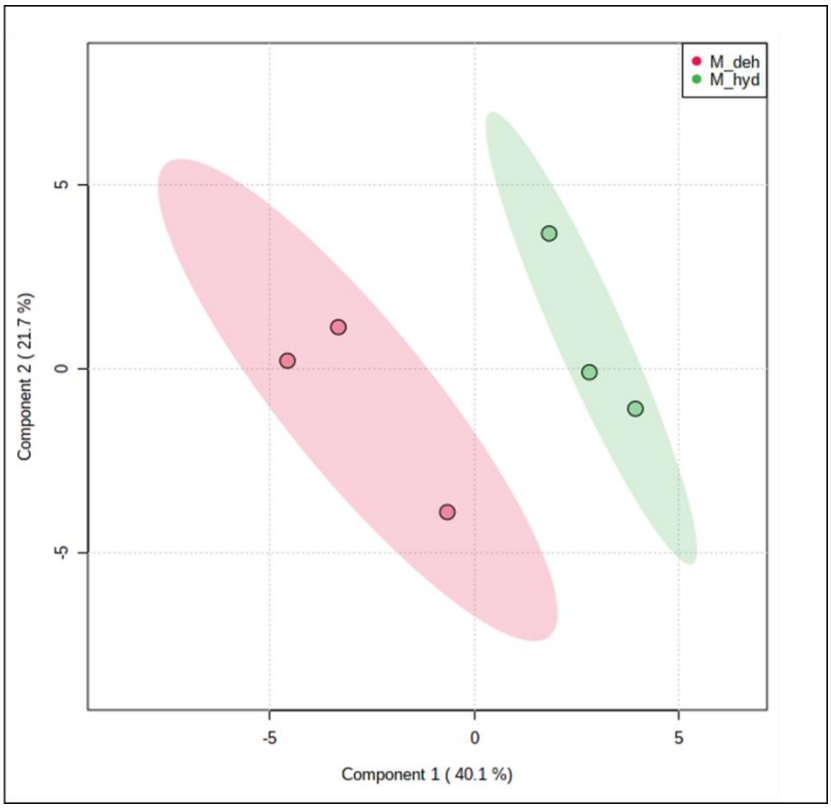

Figure 4.3: Scores plot based on Principal Components Analyses (PCA) of select metabolites in maize leaf material across hydrated and dehydrated points. Each circle represents a biological repeat while each colour represents the hydrated and dehydrated points respectively with green circle indicating hydration and the red circle indicating dehydration. Metabolite variance with component 1at 40.1% and component 2 at 21.7%.

We performed a parallel metabolomic investigation; focussing only on amino acids, sugars, sugar alcohols, organic acids and fatty acids; using maize leaf samples at two drying stages,

hydrated (100% RWC) and dehydrated ~ 60-50% RWC. The score plots for the metabolites (Figure 4.3) had the hydrated and dehydrated samples cluster very far from each with component 1 at 40.1 % and component 2 at 21.7 % of variance. In summary, these plots show that the respective metabolites in maize leaf tissue varied between the hydrated and dehydrated samples.

Amino acid, sugars, sugar alcohols, organic acid and fatty acid analyses in maize leaf tissue

A total of 17 amino acids were analysed in maize in hydrated and dehydrated samples using heatmap hierarchical clustering (Figure 4.4). In the hydrated samples, 7 amino acids were abundant and 10 were less abundant. The dehydrated samples showed a total of 10 abundant amino acids and 7 were less abundant. L-tryptophan, 5-oxoproline, L-norleucine, L-methionine, serine, isoleucine and L-proline were found to be abundant in the hydrated samples and less abundant as maize shifted into the dehydrated state. Asparagine, L-serine, alanine, valine, L-tyrosine, L-histidine, L-phenylalanine, aspartic acid and tryptophan were less abundant in the hydrated samples and abundant in dehydrated samples. Our results indicate that there was a larger accumulation of amino acids in dehydrated compared to the hydrated samples. This is supported by previous studies which show that many amino acids accumulate under drought stress (Rai, 2002). The accumulation could be due to metabolic distress initiating the increase in osmolality by holding onto water thus changing protein synthesis.

Though previous studies have shown an accumulation of proline to be associated with stress in plants (Lui and Zhu, 1997), our results show less abundance of proline in the dehydrated tissue. Previous studies have also shown proline accumulation was higher in drought tolerant then drought sensitive plants (Yoshiba *et al*., 1997) and it has been suggested that proline accumulation may be an adaption process to withstand water stress but only over short periods (Jäger and Meyer, 1977). The decline in proline observed in the current study is counter to these proposals of its role. However, the maize in the present study did not survive beyond ~60-50% RWC, which is also the only drying stage at which proline was measured. It is possible that an earlier accumulation did occur.

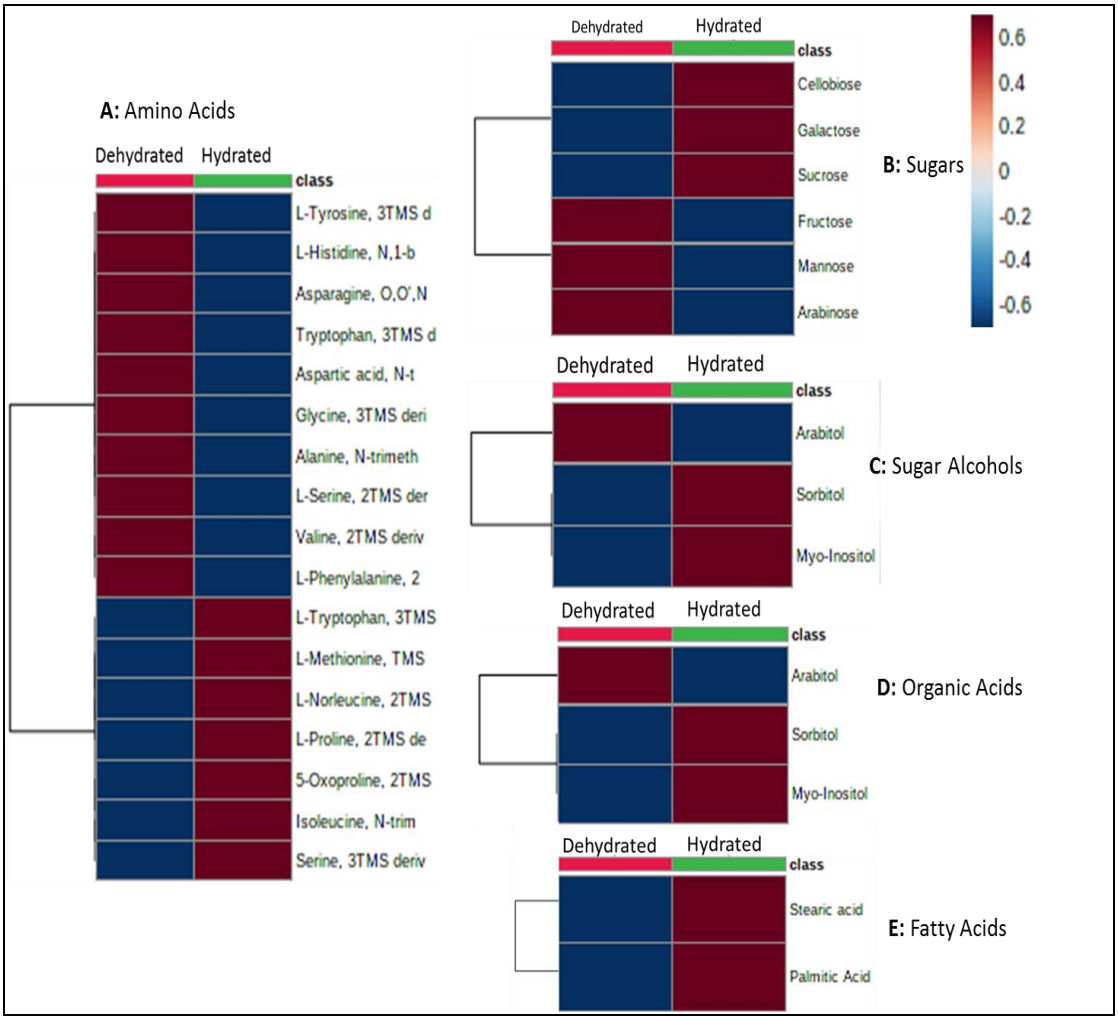

Figure 4.4: Heatmap of differentially abundant selected metabolites in maize across hydrated and dehydrated states, the 'class' shown on the right side of the cluster lists the metabolites. **(A)**. Amino acids of dehydrated and hydrated samples, **(B)**. Sugars of dehydrated and hydrated samples, **(C).** Sugar alcohols of dehydrated and hydrated samples **(D).** Organic acids of dehydrated and hydrated samples **(E).** Fatty acids of dehydrated and hydrated samples. Maroon representing high abundance metabolites and blue representing low abundance metabolites.

The abundance of selected sugars were also measured in hydrated and dehydrated samples of maize leaf tissue (Figure 4.4). A total of 6 sugars, 3 sugar alcohols, 4 organic acids and 2 fatty acids were examined, and in the hydrated samples, 7 of these metabolites were abundant and 12 were less abundant and the opposite was seen in dehydrated samples. Mannose, malic acid, lactic acid, arabitol and fructose were abundant at the hydrated samples and less abundant in dehydration. Our results indicate galactose, myo-inositol, sorbitol, sucrose, palmitic acid and stearic acid were more abundant in hydrated maize leaf tissue.

An overview of the metabolite accumulation differences in *X. schlechteri* and maize

The differences or similarities of metabolite accumulation between the desiccation tolerant *X. schlechteri* and desiccation sensitive maize may provide insight into strategies to survive drought. Although absolute values of metabolites were not determined, this would refer to changes in trends in abundance during a dehydration time course in this study. The key differences in the level of accumulation between maize to *X. schlechteri* are summarized in Figure 4.5 below.

In general, plants respond to severe water loss depending on the genotype, species, the severity of the drought and the developmental stage of the plant. Previous studies have shown that amino acids play an important role in protein synthesis, signalling processes and stress tolerance in plants (Hildebrandt *et al.,* 2015; Rai *et al.,* 2002). In addition, the accumulation of amino acids differs and changes depending on the physiological and developmental state of the plant. A decrease in accumulation of amino acids contributes to the energy state of the plant and is often a reflection of its physiological conditions where it could for example be experiencing severe water loss (Rosa *et al.,* 2009). Under severe water deficit stress, plants tend to generally decrease protein synthesis and enzyme regulation (Good and Zaplachinski, 1994) and increase protein degradation (Huang and Jander, 2017). However, there is a regulated shut down of these processes in resurrection plants, whereas in desiccation sensitive plants, such processes are associated with senescence and/or unregulated metabolism due to the consequences of severe water loss (Moore *et al.,* 2008; Farrant *et al.,* 2017; Oliver *et al.,* 2020). Amino acid accumulation has been observed in many resurrection plants during severe water loss (Tymms and Gaff, 1978; Gaff and McGregor, 1979).

Amino acids such as alanine were in high abundance at ERD in *X. schlechteri* and as drying continued and *X. schlechteri* shifted into MRD the accumulation of alanine decreased. In contrast, in maize leaf tissue, alanine was at low abundance in hydrated samples and in high abundance in dehydrated samples. Methionine and proline were abundant in hydrated maize tissue but less abundant in dehydrated maize tissue while methionine increased in both MRD for *X. schlechteri* while proline increased in MRD (Figure 4.5). These observations and difference in amino acid abundance between the two plant species indicate that there are differences in the drying strategies between these two plant species. Previous studies have found methionine to be important in human food and animal feed leading to many efforts being made to produce plants having higher methionine content (Amir, 2008). Apart from the

nutritional importance, methionine is also important in plant cells as it plays a role in protein constitution, initiation of mRNA translation and regulating a number of cellular processes (Amir, 2008). In addition, methionine is also thought to be involved in the protection of cells against ROS-induced stress (Le *et al*., 2013). This could be the reason of the accumulation of methionine in *X. schlechteri*. L-proline was observed to be abundant in hydrated samples and then less abundant in the dehydrated samples of maize. In *X. schlechteri*, L-proline was less abundant at ERD, and as the shift occurred into MRD, L-proline became abundant. Previous studies have shown that proline accumulation occurs as a result of water loss and are thought to play a role in drought tolerance (Verbruggen and Hermans, 2008; Yang *et al*., 2010; Sharma *et al*., 2011). As previously mentioned the lack of proline accumulation seems to be a feature of some drought sensitive plants and was also observed in previous studies (Yang *et al.*, 2018). Drought sensitive maize line, B73, showed low levels of glutathione metabolites for example, proline, glutamate and 5-oxoproline upon drought. Both proline and 5-oxoproline (pyroglutamic acid) were less abundant in the maize leaf tissues in the current study. The pattern of amino acid accumulation in maize might indicate onset of senescence (Watanabe *et al.*, 2013).

In plants, sugars play a key role in respiration, numerous biochemical processes, act as transporters and storage substances (Ciereszko, 2009; Ruan, 2014; Sami *et al.*, 2016; Łukaszuk *et al.*, 2017). Sugars also play a pivotal role in plant defence against stress factors (Ciereszko, 2018). Identifying the accumulation and regulation of sugars under stress treatments such as drought will elucidate the key strategies employed by different plants for defence (Ruan, 2014; Łukaszuk *et al.*, 2017). Based on the results in Figure 4.5, the sugar accumulation between *X. schlechteri* and maize varied with regards to fructose which was abundant in dehydrated maize tissue but less abundant at MRD in *X. schlechteri*. Two fatty acids, Stearic acid and palmitic acid, sugar and sugar alcohol, cellobiose, sucrose and sorbitol accumulated at MRD in *X. schlechteri* but less abundant in dehydrated maize tissue. Water loss results in a decrease in the efficiency of photosynthesis in source tissues that synthesize and export sugars thereby reducing their supply to sink tissues and in turn disrupts respiration, growth, and development. This results in major physiological and biochemical changes in order to sustain respiration and other metabolic processes (Journet *et al.*, 1986; Yu, 1999). The observed increase in abundance of the other sugars in dehydrated maize was therefore most likely as a response to sugar starvation and the plant trying to maintain respiration and key metabolic processes. In addition there is also crosstalk between sugar and hormonal networks which ultimately affects growth

and development and a disruption of the sugar network can therefore negatively impact hormone regulation (Matsoukas, 2014). The observation that important sugars and sugar alcohol such as sucrose and myo-inositol were decreased in dehydrated maize tissue and the absence of raffinose while these same sugars were abundant at MRD in *X. schlechteri* points to the importance of these sugars in providing and maintaining tolerance to severe water loss. As mentioned previously these sugars are important in the formation of RFOs while myo-inositol also serves to modulate auxin levels. The regulation in *X. schlechteri* of specific sugar levels across the drying stages together with the shutdown of photosynthesis prevents sugar starvation and establishes desiccation tolerance.

The observed differences in the metabolomic profile between *X. schlechteri* and maize in response to dehydration can explain in part the desiccation tolerance of *X. schlechteri* and maize sensitivity to water loss.

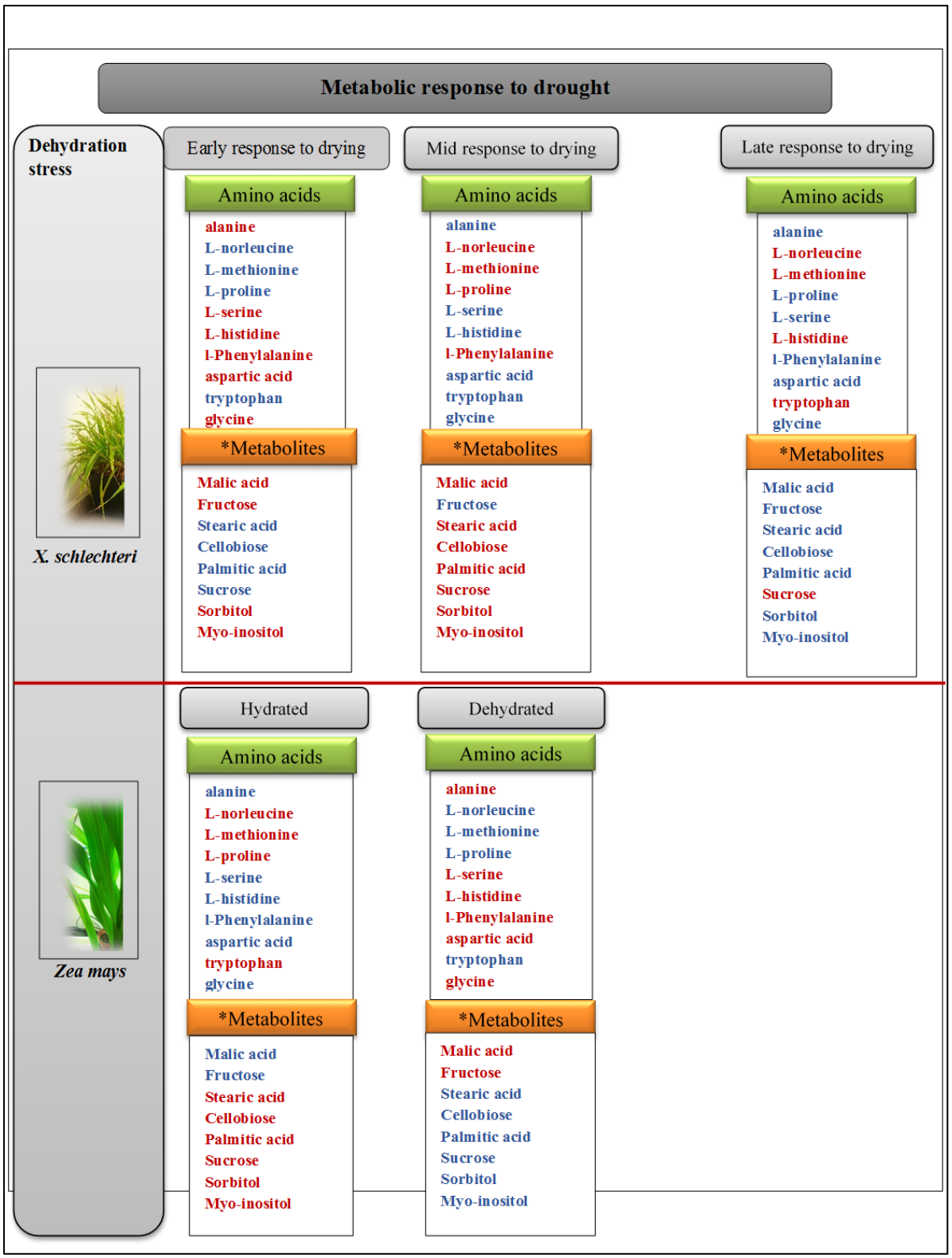

Figure 4.5: Overview of the metabolomic response of *X. schlechteri* and *Zea mays* to water loss. The amino acids, sugars, sugar alcohols, organic acids and fatty acids are a selection that were noticeably different between *X. schlechteri* and *Zea mays* across the different stress treatments. Amino acids, sugars, sugar alcohols, organic acids and fatty acids represented in red font indicates high abundance and blue font represents low abundance. *Metabolites labelled in the overview collectively refers to sugars, sugar alcohols, organic acids and fatty acids.

Brief Conclusion

The validation and confirmation of selected data from the label-free proteomic study was achieved by using a metabolomic approach based on GC MS/MS and LCMS techniques. The changes in abundance of amino acids, sugars, sugar alcohols, fatty acids, organic acids and phytohormones across the drying stages in *X. schlechteri* were examined and inferences drawn to their role in desiccation tolerance. This was related to the proteomic dataset from Chapter 3, in which proteins were associated with pathways linked to or involved in response to plant stress. These *X. schlechteri* proteins showed differential expression across the drying stages and associated metabolites were also quantified for abundance across the same stages. We observed that selected differentially expressed proteins had a similar expression profile to the abundance profile of the corresponding metabolite at the respective drying stages. The results obtained in the metabolomics approach supported the proteomic analyses and validated previously identified differentially expressed proteins and pathways (Table 4.1 A, B and C).

The change in metabolomic profile across the dehydration stages was important in establishing dessication tolerance and key sugars, organic acids and amino acids were identified that could be playing a role in its establishment. A parallel metabolomic approach was performed on the dessication sensitive maize, with the exception of phytohormones, to show the contrasting metabolite profile in response to intermediate levels of water loss (60-50% RWC) and ultimately what might be contributing to tolerance of extreme water loss in *X. schlechteri*. Sugars and sugar alcohols such as sucrose, raffinose and myo-inositol appear to have important roles in dehydration tolerance. Diffrences in the accumulation of amino acids were also observed between *X. schlechteri* and maize such as alanine and proline.

The intergration of proteomic and metabolomic approaches allowed important strategies in establishing dessication tolerance to be highlighted in *X. schlechteri* and this information could be used in future to improve drought tolerance of crop plants. Observations of different metabolite responses of *X. schlechteri* and maize to loss of between 50-40% water content gave insight to the differences in physiological responses of these two species, and thus also insight as to how this could be utilized to improve water deficit tolerance in maize.

Chapter 5

Conclusion

The monocotyledonous resurrection species *X. schlechteri* can survive extreme water loss, down to 5% RWC, in its vegetative tissue and, remain in this state for extended periods and then resume full physiological and metabolic activity within 72 hr of re-watering (Sherwin and Farrant, 1998; Farrant, 2000; Farrant *et al.*, 2015). A thorough understanding of this vegetative desiccation-tolerance phenomenon by the identification of key biological processes and pathways together with information on the associated genes, proteins and metabolites, could be used to improve drought-tolerance of cereal crops of agronomic importance. Though *X. schlechteri* is a non-model plant species, a combination of different systems biological approaches such as genomics, transcriptomics, proteomics and metabolomics complemented with bioinformatics can help identify these key biological processes during dehydration.

The aim of this study was two-fold (Summarized in Figure 5.1). Firstly, to use a label-free proteomics approach to investigate the *X. schlechteri* proteome in response to dehydration, and secondly, to validate and correlate the data obtained with a metabolomic approach. While genomic, transcriptomic (Costa *et al.*, 2107) and some metabolomic (Radermacher *et al.*, 2019) data is available for this species, to date there has been no proteomic study conducted that would add the missing link between these "omics" studies, and so more convincingly demonstrate its power as a new "model organism" for extreme drought tolerance. My study has also provided information that could be used to improve the drought tolerance of maize. The survival strategies employed by *X. schlechteri* compared to maize differ in some regard and the genes that are over expressed in *X. schlechteri* may be used to conduct transgenic studies in maize.

Prior to conducting the proteomic workflow, it was important to establish the characteristic features during drying of *X. schlechteri* plants used and under the environmental conditions used, in the current study. The first objective of the study was to physiologically, morphologically and biochemically characterise *X. schlechteri* in response to a controlled dehydration (Chapter 2). Relative water content (RWC) and absolute water content (AWC) was used to monitor the changes in water loss. The establishment of three stages of drying were identified; early response to drying (~ 80 – 70% RWC ; ~1.61 $gH_2O\ g^{-1}$ dwt -~1.5 $gH_2O\ g^{-1}$ dwt), a mid-response to drying (~ 60 - 40% RWC ;~1.5 $gH_2O\ g^{-1}$ dwt - ~1.0 $gH_2O\ g^{-1}$ dwt) and

a late response to drying (~ 40 - 10% RWC ; ~1.0 gH_2O g^{-1} dwt -~0.5 gH_2O g^{-1} dwt), (Figure 2.1- Chapter 2). In the first few days of the dehydration stress, the *X. schlechteri* steadily started drying down, with the observation of leaves folding along the midrib and loss of green chlorophyll with concomitant purple anthocyanin production. The *X. schlechteri* plants took an average of six to eight days before the decline from ERD to MRD. Additionally, biochemical assays were conducted on *X. schlechteri* at the hydrated and dehydrated stages. Photosynthetic potential was monitored using chlorophyll content measurements (Figure 2.3-Chapter 2) where chlorophyll content was seen to decrease upon dehydration. This result was supported by data obtained in Chapter 3 and Chapter 4 where there was a downregulation of proteins involved in chlorophyll synthesis (Figure 3.6; Table 3.4). This confirms the poikilochlorophyllous nature of *X. schlechteri* (Sherwin and Farrant, 1998) and its importance in establishing desiccation-tolerance in this species. Antioxidant enzyme assays for ascorbate peroxidase (APX), superoxide dismutase (SOD), catalase (CAT) and glutathione reductase (GR) indicated an increase in antioxidant enzyme activity in dehydrated tissue of *X. schlechteri* (Figure 2.5-Chapter 2).

Physiological, morphological and biochemical studies were also conducted on maize in response to water loss. In the first three days of withholding water, slight drooping of the maize leaves was observed. The loss of water became more apparent as the dehydration proceeded to 60% -70% RWC (Figure 2.2-Chapter 2). The stem eventually started turning deep red as the maize entered the later stages of drying. The photosynthetic potential was monitored using chlorophyll content measurements (Figure 2.4-Chapter 2) and the chlorophyll content was seen to decrease upon dehydration but not as significantly as *X. schlechteri.* This, together with obvious anthocyanin production in stems suggests that maize was experiencing drought induced senescence (Close, and Beadle, 2003). The antioxidant assays (Figure 2.6-Chapter 2) conducted on dehydrating maize leaves suggests that the enzymes APX, SOD, CAT and GR showed increased activity due to excess ROS production during early drought stress but as water loss became more severe, maize was unable to withstand the stress and eventually died after drying below 50% RWC. In a comparative study on 5 resurrection species with 3 desiccation sensitive *Eragrostis* species, Farrant *et al.*(2007) showed similar findings and proposed that these antioxidant enzymes were protected in resurrection plant species but became denatured during drying of the desiccation sensitive species.

***X. schlechteri* exposed to dehydration**

A

Physiological and biochemical analysis

Relative water content

- Early response to drying
- Mid response to drying
- Late response to drying

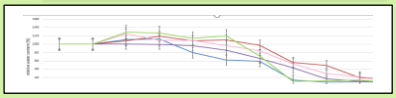

Assays

Chlorophyll content - decreased at dehydrated
Ascorbate peroxidase - increase at dehydrated
Catalase activity - increase at dehydrated
Glutathione reductase - increase at dehydrated
Superoxide dismutase - increase at dehydrated

B

Proteomic analysis: Label-free quantification

Functional analysis and Pathway analysis

Drying stages

ERD

- antioxidants
- binding activity
- catalytic activity
- cellular response
- metabolic pathway
- defence response

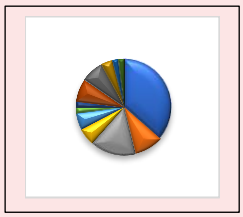

MRD

- antioxidants
- binding activity
- catalytic activity
- transport
- translation
- regulation

LRD

- antioxidants
- binding activity
- catalytic activity
- transcription
- translation
- regulation
- development
- defence response
- cellular process
- catabolic process
- biosynthesis pathways
- biochemical pathways

C

Metabolomic analysis: Validation

Metabolite analysis

Amino acid

- alanine
- 5-oxoproline
- L-histadine
- L-phenylalanine
- L-proline
- L-serine
- aspartic acid

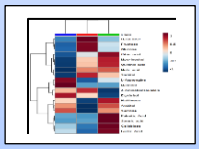

Phytohormones

- gibberellic acid
- iso-jasmonyl-l-isoleucine
- salicylic acid
- indole-3-carboxylic acid
- jasmonic acid
- indole-3-acetic acid
- Abscisic acid

Indole-3-butyricacid

Sugars/Sugar alcohols/fatty acids and organic acids

- galactose
- glucose
- fructose
- raffinose
- sucrose
- myo-inositol
- arabitol
- citric acid
- malic acid

Figure 5.1: Summary of the key changes in *X. schlechteri* during dehydration **(A).** Physiological changes representing the identified drying stages of *X. schlechteri* in this study. Key antioxidant changes in *X. schlechteri* from hydrated to dehydrated stages. **(B).** Proteomic analysis of *X. schlechteri* showing the key biological processes across the drying stages (ERD, MRD, and LRD), and **(C).** Associated metabolomic analysis representing key metabolites that were differentially expressed across the drying stages.

The second objective of the study was to conduct an in-depth proteomic analysis of *X. schlechteri* across the drying stages. A label-free quantification method was employed using spectral counting and a total of 3125 unique proteins were identified in the *X. schlechteri* leaf material across the drying treatments, of which 65 proteins had unknown prediction. These unassigned proteins need further characterisation as they may contain useful information on desiccation tolerance. The proteins were quantified, and 517 unique proteins were found to be differentially expressed in response to drying. Amongst the differentially expressed proteins, 253 proteins were upregulated and 264 were downregulated proteins.

The gene ontologies were then identified and assigned GO-terms for functional classification using bioinformatics tools. This allowed for the categorization of the proteins into molecular functions, biological processes and cellular compartments. The response to drying employed by *X. schlechteri* across the selected drying stages, ERD, MRD, and LRD is evident from the data presented in Chapter 3. The key findings are outlined in Figure 5.2. During the ERD (Figure 5.2 A) upregulation of secondary metabolites specifically UDP-glycosyltransferases and ultimately the synthesis of anthocyanins and an upregulation in phenylalanine which is involved in the synthesis of flavonoids were seen. Proteins associated with photosynthesis were seen to be downregulated. As *X. schlechteri* shifted into MRD (Figure 5.2 B), an upregulation of carbohydrate metabolism and protein homeostasis were seen. The co-ordinated synthesis of heat shock proteins (HSPs), chaperones and RUB2-ubiquitin also occurred. A notable downregulation of photosynthesis was evident. Figure 5.2 B also suggests a generation of more vacuoles at MRD. Oliver *et al.,* 2020 suggests the generation of more numerous and smaller vacuoles arises and is associated with desiccation. This may be formed de novo or by division of the original water-filled vacuoles which may result in temporary storage organelles which contains by-products generated during desiccation or becoming autophagosomes.

As the drying continued into the LRD (Figure 5.2 C), the molecular functions at the late response to drying showed an increase in antioxidants which correlated to data shown in Chapter 2. Upregulation of protein biosynthesis, protein homeostasis and cellular respiration was evident, and a downregulation of co-enzymes and photosynthesis occurred.

The cellular compartments such as the chloroplast was highly presented supporting the results shown in the molecular functions and biological processes, with a notable increase at the mid response to drying and a decrease at late response to drying. MapMan analysis was conducted to further investigate the roles of the proteins in biological processes involved in the different stages of drying. MapMan analysis revealed an abundance of proteins that were involved in

photosynthesis and supports the previously mentioned importance of poikilochlorophylly. Further protein abundance was found in carbohydrate metabolism, redox homeostasis, protein homeostasis, cellular respiration, co-enzyme metabolism and protein biosynthesis. These results for protein abundance in redox homeostasis were consistent with results obtained in Chapter 2. Similarly, with protein abundance for carbohydrate metabolism, protein homeostasis and co-enzyme metabolism supported the observations with respect to the metabolomic data (Chapter 4). An additional analysis was conducted (data represented in Supplementary material-KEGG pathways) which further confirmed the results obtained in Chapter 3 and 4 where a number of the pathways involved in amino acid metabolism and sugar metabolism were observed to increase during desiccation (Figure S3.2-Supplementary material Chapter 3).

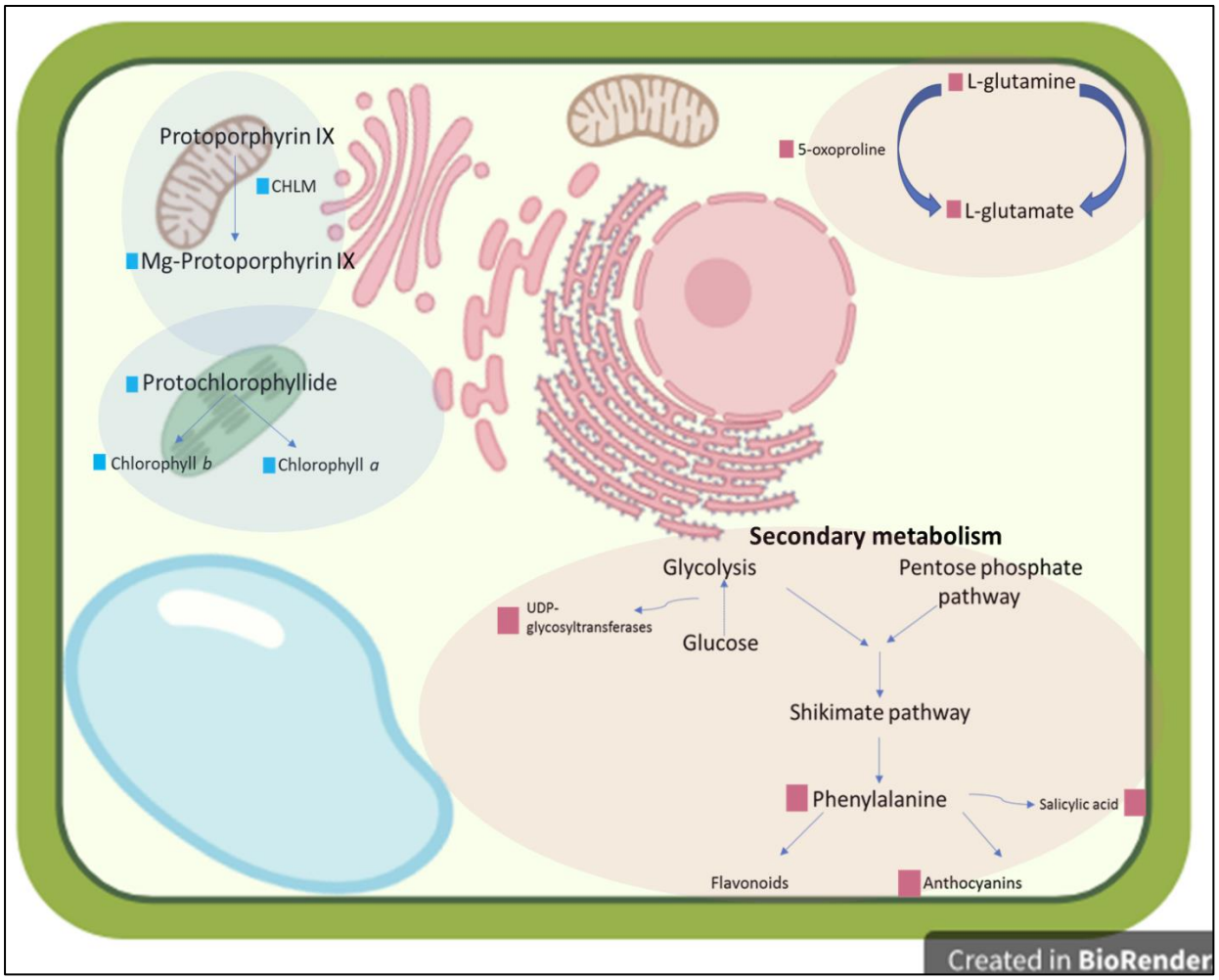

Figure 5.2 A: Proposed model of key responses of *X. schlechteri* at ERD. Pink squares represent upregulation and blue squares represent downregulation.

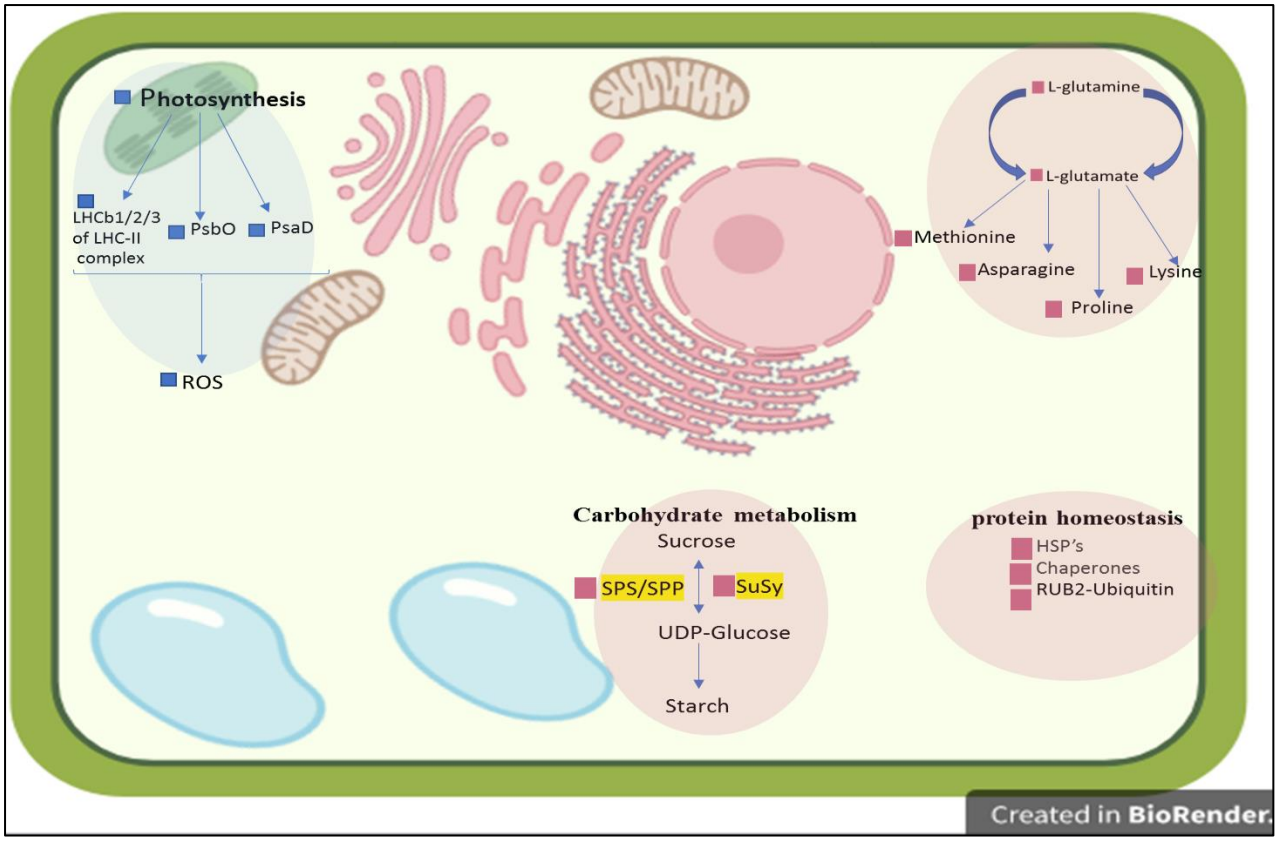

Figure 5.2 B: Proposed model of key responses of *X. schlechteri* at MRD. Pink squares represent upregulation and blue squares represent downregulation.

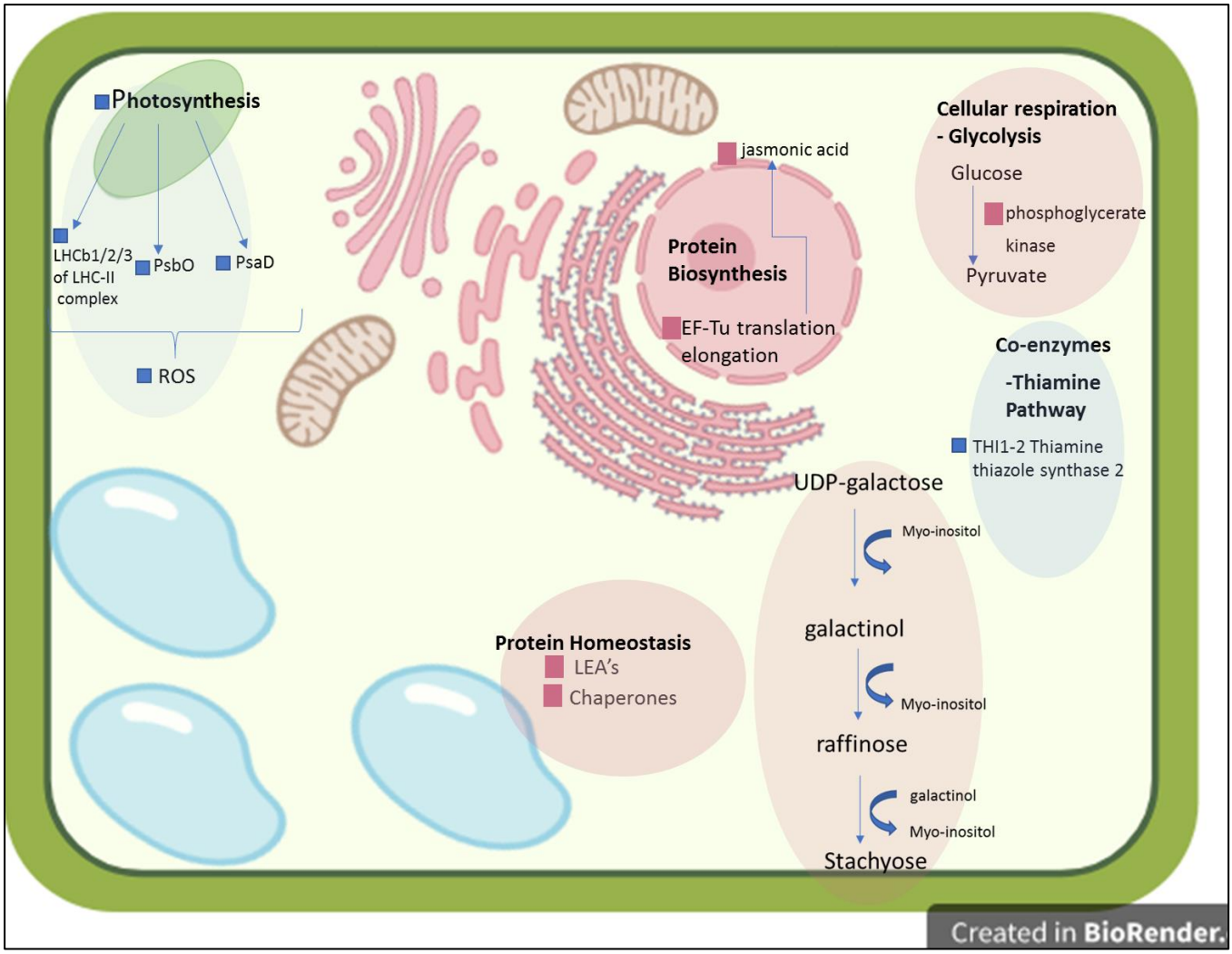

Figure 5.2 C: Proposed model of key responses of *X. schlechteri* at LRD. Pink squares represent upregulation and blue squares represent downregulation.

The final objective of the study was to validate the proteomic data by investigating a subset of metabolites involved in the drying stages in *X. schlechteri.* This was achieved by the metabolomic investigation of the abundance of 16 standard amino acids, 9 standard phytohormones and standard 7 sugars, 4 sugar alcohol, 3 fatty acids and 3 organic acids at the different responses to drying. The amino acids showed (Figure 4.2 A-Chapter 4) a pattern of accumulation of alanine, 5-oxoproline, L-serine, aspartic acid and serine, L-histidine and L-phenylalanine at ERD (Figure 5.2 A). At MRD and LRD, alanine, 5-oxoproline, L-serine, aspartic acid and serine were seen to be less abundant. At MRD and LRD, however, norleucine, tyrosine, methionine, asparagine and lysine continued to be abundant, while tryptophan was accumulated only at LRD. Previous studies (Ishihara *et al.*, 2008) have shown that tryptophan

plays a key role in defence response. Analysis of the sugars and sugar alcohols (Figure 4.2 B and C) showed that raffinose, arabitol and sucrose were observed in dehydration samples which correlated with the proteomic results (Chapter 3). Previous studies indicated that these sugars are implicated as protection metabolites in resurrection plants (Bianchi *et al.*, 1991; Ghasempour *et al.*, 1998; Norwood *et al.*, 2000; Scott, 2000; Whittaker *et al.*, 2001; Cooper and Farrant, 2002; Zivkovic *et al.*, 2005; Farrant *et al.*, 2015).

This study further provides insight into and elucidates the role of a selection of phytohormones of *X. schlechteri* in response to drought. The phytohormone investigation (Figure 4.2 C) showed abscisic acid (ABA) and the auxin conjugates, Indole-3-acetic acid Asp (IAA-Asp), Indole-3-acetic acid (IAA) and Indole-3-butyric acid (IBA) were less abundant in *X. schlechteri* at ERD. As *X. schlechteri* shifted into MRD, ABA, jasmonate, GA and SA were less abundant. Jasmonate and ABA were however accumulated at LRD, the same pattern as seen in the proteomic data (Chapter 3). Previous studies (Erb *et al.*, 2012; Ullah *et al.*, 2018) reported JA and ABA to be involved in drought tolerance. Although hormonal crosstalk during drought is complex, this study does shed light on key changes occurring in *X. schlechetri* during the drying stages. These phytohormones and their associated metabolic pathways can be considered as metabolic targets for drought tolerance in crop plants.

The metabolomic profile of maize was also examined using similar metabolite standards as *X. schlechteri* so as to ascertain similarities or differences (Figure 4.5) between the two plants (*X. schlechteri*, desiccation tolerant and maize desiccation sensitive). L-methionine, that has been reported (Le *et al*., 2013) to be involved in the protection of cells against H_2O_2-induced stress, was less abundant in the dehydrated samples of maize. Metabolite accumulation of maize also varied compared to *X. schlechteri* with regards to stearic acid, cellobiose, palmitic acid, sucrose, sorbitol being less accumulated in maize. Previous research (Journet *et al.*, 1986; Yu, 1999) has found that plants that decrease sugar levels undergo lots of physiological and biochemical change in order to sustain respiration. An overview of the two species (Figure 4.5, Chapter 4) further showed the metabolites employed by *X. schlechteri* in the LRD a drying point beyond which maize could survive. Perhaps if maize expressed the metabolites such as L-norleucine, L-methionine, L-proline, L-serine, L-histidine and glycine similar to *X. schlechteri* this would improve its chances of survival as drying progressed.

The main advantage of the label-free proteomic approach complemented with metabolomics used in this study is that it reflects the actual outcome of the corresponding transcriptomic and epigenetic regulation in response to desiccation. This allows for a more holistic overview and

perspective of the biological processes and mechanisms involved in *X. schlechteri* desiccation tolerance. The main disadvantage of the label-free proteomic approach is the biological variation among stress treated plants which reduces the number of possible protein identifications and complicates quantification of differential expression. Although this can be remedied by increasing biological replicates, it is not feasible with species such as *X. schlechteri* where there is a limited number of plants allowed for collection and study. The other weakness of this study was the lack of a fully annotated *X. schlechteri* genome which would have allowed more biological processes to be identified and analysed using bioinformatics tools. Despite these challenges useful data was obtained and future studies should concentrate on subcellular proteomics using the label-free approach and metabolomics.

Recently, in mammalian models, it was found that key metabolites play an important role in transcriptional responses by regulating chromatin modifying enzymes and therefore implicated in epigenetic control (Mohammed *et al.,* 2020). Many of these metabolites are involved in energy homeostasis and can enter the nucleus to affect gene regulation (Lempradl *et al.,* 2015). Therefore, understanding the role of specific proteins and metabolites in the nucleus, chloroplast and mitochondria of resurrection plants during dehydration stress may shed light on other important regulatory mechanisms involved in desiccation tolerance.

Based on this study and the results obtained, the label-free proteomic workflow should also be conducted on rehydrated *X. schlechteri* leaf samples. This would further elucidate the differentially expressed proteins employed by *X. schlechteri* after dehydration and upon rehydration. This could provide key strategies and pathways employed by a desiccation tolerant plant after surviving drought conditions. Studies on poikilochlorophyllous species have shown that genes transcribed during late stages of desiccation, particularly those associated with re-establishment of photosynthetic potential, are not translated until rehydration (Dace *et al.,* 1998; Costa *et al.,* 2017; Madden, 2019), introducing other regulatory processes that need investigation.

The objectives of this study were achieved, making this study, to our knowledge, the first reported label-free proteomic analysis of the *X. schlechteri* leaf proteome in response to dehydration.

Supplementary material - Chapter 3

Table S3.1: List of the Bin names, id and description of the upregulated proteins at ERD

BinName	id	Description
Secondary metabolism. phenolics.flavonoid biosynthesis.flavonol glycosides.flavonol-3-O-rhamnosyltransferase'	xvis03_211917-pa	flavonol-3-O-rhamnosyltransferase (original description: augustus-gene-8.2-mRNA-1 protein Name:Similar to UGT78D2 UDP-glycosyltransferase 78D2 (Arabidopsis thaliana) AED:0.00 eAED:0.00 QI:173|1|1|1|1|1|2|210|454)'
Secondary metabolism. phenolics.flavonoid biosynthesis.aurones.aureusidin synthase'	xvis03_203578-pa	aureusidin synthase (original description: augustus-gene-30.42-mRNA-1 protein Name:Similar to Polyphenol oxidase, chloroplastic (Vitis vinifera) AED:0.01 eAED:0.01 QI:30|1|1|1|1|1|2|191|591)'

Table S3.2: List of the Bin names, id and description of the downregulated proteins at ERD

BinName	id	Description
Coenzyme metabolism.tetrapyrrol biosynthesis.uroporphyrinogen III formation.porphobilinogen deaminase'	xvis03_202672-pa	porphobilinogen deaminase (original description: processed-gene-54.103-mRNA-1 protein Name:Similar to HEMC Porphobilinogen deaminase, chloroplastic (Oryza sativa subsp. japonica) AED:0.01 eAED:0.01 QI:117|1|1|1|1|1|5|327|378)'
Coenzyme metabolism.tetrapyrrol biosynthesis.chlorophyll metabolism.Mg-protoporphyrin IX O-methyltransferase'	xvis03_200416-pa	Mg-protoporphyrin IX O-methyltransferase (original description: processed-gene-51.69-mRNA-1 protein Name:Similar to CHLM Magnesium protoporphyrin IX methyltransferase, chloroplastic (Arabidopsis thaliana) AED:0.34 eAED:0.34 QI:0|-1|0|1|-1|1|1|0|322)'
Coenzyme metabolism.tetrapyrrol biosynthesis.chlorophyll metabolism.protochlorophyllide oxidoreductase (pOR) activities.light-dependent pOR'	xvis03_212894-pa	light-dependent protochlorophyllide oxidoreductase (original description: augustus-gene-2.1-mRNA-1 protein Name:Similar to PORB Protochlorophyllide reductase B, chloroplastic (Hordeum vulgare) AED:0.09 eAED:0.09 QI:162|1|1|1|1|1|5|457|393)'
Coenzyme metabolism.tetrapyrrol biosynthesis.chlorophyll	xvis03_218927-pa	light-dependent protochlorophyllide oxidoreductase (original description: processed-gene-

metabolism.protochlorophyllide oxidoreductase (pOR) activities.light-dependent pOR'		4.16-mRNA-1 protein Name:Similar to PORB Protochlorophyllide reductase B, chloroplastic (Hordeum vulgare) AED:0.12 eAED:0.12 QI:128|0.75|0.6|1|1|1|5|341|353)'
Coenzyme metabolism.tetrapyrrol biosynthesis.chlorophyll metabolism.chlorophyll(ide) interconversions.geranylgeranyl reductase (Chlp)'	xvis03_215774-pa	geranylgeranyl reductase (ChlP) (original description: augustus-gene-7.23-mRNA-1 protein Name:Similar to CHLP Geranylgeranyl diphosphate reductase, chloroplastic (Nicotiana tabacum) AED:0.00 eAED:0.00 QI:382|1|1|1|1|1|2|212|364)'
protein homeostasis.protein quality control.Hsp90 chaperone system.chaperone (Hsp90)'	xvis03_207665-pa	chaperone (Hsp90) (original description: processed-gene-12.71-mRNA-1 protein Name:Similar to HSP90 Endoplasmin homolog (Catharanthus roseus) AED:0.12 eAED:0.12 QI:42|1|1|1|1|1|15|358|812)'
protein homeostasis.protein quality control.Hsp90 chaperone system.chaperone (Hsp90)'	xvis03_224897-pa	chaperone (Hsp90) (original description: augustus-gene-1.57-mRNA-1 protein Name:Similar to HSP90 Endoplasmin homolog (Catharanthus roseus) AED:0.10 eAED:0.10 QI:52|0.92|0.93|1|1|1|15|395|78 8)'
protein homeostasis.ubiquitin-proteasome system.26S proteasome.19S regulatory particle.non-ATpase components.regulatory component RpN8'	xvis03_212052-pa	regulatory component RPN8 of 26S proteasome (original description: augustus-gene-18.3-mRNA-1 protein Name:Similar to RPN8A 26S proteasome non-ATPase regulatory subunit 7 homolog A (Arabidopsis thaliana) AED:0.29 eAED:0.29 QI:0|0.9|0.81|0.90|1|1|11|444|3 63)'
protein homeostasis.proteolysis.cysteine-type peptidase activities.C13-class asparaginyl endopeptidase (Legumain)'	xvis03_211268-pa	asparaginyl endopeptidase (Legumain) (original description: processed-gene-9.25-mRNA-1 protein Name:Similar to Vacuolar-processing enzyme (Citrus sinensis) AED:0.07 eAED:0.07 QI:3|1|1|1|1|9|417|590)'
Carbohydrate metabolism.oxidative pentose phosphate pathway.oxidative phase.6-phosphogluconolactonase'	xvis03_213363-pa	6-phosphogluconolactonase (original description: processed-gene-12.66-mRNA-1 protein Name:Similar to Os09g0529100 Probable 6-

		phosphogluconolactonase 4, chloroplastic (Oryza sativa subsp. japonica) AED:0.04 eAED:0.04 QI:89|1|1|1|1|1|3|259|276)'
Carbohydrate metabolism.oxidative pentose phosphate pathway.non-oxidative phase.transaldolase'	xvis03_219185-pa	transaldolase (original description: processed-gene-8.51-mRNA-1 protein Name:Similar to tal Transaldolase (Acidothermus cellulolyticus (strain ATCC 43068 / 11B)) AED:0.03 eAED:0.03 QI:60|0.83|0.85|1|1|1|7|483|446)'
photosynthesis.photophosphorylation.cytochrome b6/f complex.Rieske iron-sulfur component petC'	xvis03_223095-pa	Rieske iron-sulfur component PetC of cytochrome b6/f complex (original description: augustus-gene-3.96-mRNA-1 protein Name:Similar to petC Cytochrome b6-f complex iron-sulfur subunit, chloroplastic (Oryza sativa subsp. japonica) AED:0.11 eAED:0.11 QI:167|0.33|0.75|1|1|1|4|287|178)'
photosynthesis.photophosphorylation.chlororespiration.NADH dehydrogenase-like (NDH) complex.lumen subcomplex L.component pnsL1'	xvis03_203608-pa	component PnsL1 of NDH lumen subcomplex L (original description: processed-gene-32.69-mRNA-1 protein Name:Similar to PNSL1 Photosynthetic NDH subunit of lumenal location 1, chloroplastic (Arabidopsis thaliana) AED:0.12 eAED:0.08 QI:81|1|0.85|1|1|1|7|565|263)'
Nucleotide metabolism.purines.phosphotransfers.adenylate kinase'	xvis03_207311-pa	adenylate kinase (original description: processed-gene-7.62-mRNA-1 protein Name:Similar to ADK-B Adenylate kinase 4 (Oryza sativa subsp. japonica) AED:0.05 eAED:0.05 QI:122|1|1|1|1|1|6|379|246)'
Nucleotide metabolism.purines.phosphotransfers.adenylate kinase'	xvis03_213605-pa	adenylate kinase (original description: processed-gene-14.84-mRNA-1 protein Name:Similar to Os08g0288200 Probable adenylate kinase 5, chloroplastic (Oryza sativa subsp. japonica) AED:0.22 eAED:0.22 QI:25|1|0.94|1|1|1|17|0|611)'

Table S3.3: List of the Bin names, id and description of the upregulated proteins at MRD

BinName	id	Description
protein homeostasis.protein quality control.cytosolic Hsp70 chaperone system.chaperone (Hsp70)'	xvis03_222223-pa	chaperone (Hsp70) (original description: processed-gene-2.73-mRNA-1 protein Name: Similar to HSP70 Heat shock cognate 70 kDa protein (Petunia hybrida) AED:0.11 eAED:0.11 QI:205|0.5|0.33|0.66|1|1|3|0|710)'
protein homeostasis.ubiquitin-proteasome system.ubiquitin-fold protein conjugation.RUB/NEDD8 conjugation (neddylation).ubiquitin-fold protein (RUB)'	xvis03_205813-pa	ubiquitin-fold protein (RUB) (original description: processed-gene-6.86-mRNA-1 protein Name: Similar to RUB2 Ubiquitin-NEDD8-like protein RUB2 (Oryza sativa subsp. japonica) AED:0.04 eAED:0.04 QI:73|1|1|1|1|1|3|301|153)'
Carbohydrate metabolism.sucrose metabolism.biosynthesis.cytosolic UDp-glucose pyrophosphorylase'	xvis03_202124-pa	cytosolic UDP-glucose pyrophosphorylase (original description: processed-gene-11.0-mRNA-1 protein Name:Similar to UGPA UTP--glucose-1-phosphate uridylyltransferase (Musa acuminata) AED:0.18 eAED:0.18 QI:271|0.88|0.89|1|1|1|19|372|458)'
Carbohydrate metabolism.starch metabolism.degradation.maltose metabolism.cytosolic alpha-glucan phosphorylase'	xvis03_204659-pa	cytosolic alpha-glucan phosphorylase (original description: augustus-gene-39.13-mRNA-1 protein Name:Similar to PHS2 Alpha-glucan phosphorylase 2, cytosolic (Arabidopsis thaliana) AED:0.23 eAED:0.23 QI:181|0.92|0.93|1|0.92|0.86|15|169|732)'
Lipid metabolism.glycerolipid biosynthesis.phosphatidylcholine.CTp:phosphorylcholine cytidylyltransferase'	xvis03_202655-pa	CTP:phosphorylcholine cytidylyltransferase (original description: processed-gene-53.13-mRNA-1 protein Name:Similar to CCT2 Choline-phosphate cytidylyltransferase 2 (Arabidopsis thaliana) AED:0.15 eAED:0.15 QI:50|1|1|1|1|8|392|291)'
Lipid metabolism.lipid degradation.phospholipase activities.phospholipase A2 activities.phospholipase A2 (ppLA2-II)'	xvis03_218200-pa	phospholipase A2 (pPLA2-II) (original description: augustus-gene-6.42-mRNA-1 protein Name:Similar to PLP1 Patatin-like protein 1 (Oryza sativa subsp. japonica) AED:0.26 eAED:0.26 QI:72|0.4|0.16|1|1|1|6|0|314)'

Table S3.4: List of the Bin names, id and description of the downregulated proteins at MRD

BinName	id	Description
photosynthesis.photophosphorylation.photosystem II.LHC-II complex.component LHCb1/2/3'	xvis03_211060-pa	component LHCb1/2/3 of LHC-II complex (original description: processed-gene-14.7-mRNA-1 protein Name:Similar to Chlorophyll a-b binding protein, chloroplastic (Spinacia oleracea) AED:0.01 eAED:0.01 QI:0|-1|0|1|-1|1|1|0|268)'
photosynthesis.photophosphorylation.photosystem II.LHC-II complex.component LHCb1/2/3'	xvis03_219722-pa	component LHCb1/2/3 of LHC-II complex (original description: augustus-gene-9.73-mRNA-1 protein Name:Similar to CAB36 Chlorophyll a-b binding protein 36, chloroplastic (Nicotiana tabacum) AED:0.36 eAED:0.36 QI:240|1|1|1|1|1|2|393|264)'
photosynthesis.photophosphorylation.photosystem II.LHC-II complex.component LHCb1/2/3'	xvis03_223077-pa	component LHCb1/2/3 of LHC-II complex (original description: processed-gene-1.89-mRNA-1 protein Name:Similar to CAB13 Chlorophyll a-b binding protein 13, chloroplastic (Solanum lycopersicum) AED:0.07 eAED:0.07 QI:182|1|1|1|1|1|4|188|263)'
photosynthesis.photophosphorylation.photosystem II.LHC-II complex.component LHCb1/2/3'	xvis03_224654-pa	component LHCb1/2/3 of LHC-II complex (original description: processed-gene-1.9-mRNA-1 protein Name:Similar to CAB21 Chlorophyll a-b binding protein 21, chloroplastic (Nicotiana tabacum) AED:0.11 eAED:0.11 QI:0|0|0|0.5|1|1|2|0|328)'
photosynthesis.photophosphorylation.photosystem II.LHC-II complex.component LHCb1/2/3'	xvis03_225066-pa	component LHCb1/2/3 of LHC-II complex (original description: processed-gene-0.82-mRNA-1 protein Name:Similar to Chlorophyll a-b binding protein, chloroplastic (Spinacia oleracea) AED:0.00 eAED:0.00 QI:0|-1|0|1|-1|1|1|0|268)'
photosynthesis.photophosphorylation.photosystem II.LHC-II complex.component LHCb4'	xvis03_212711-pa	component LHCb4 of LHC-II complex (original description: processed-gene-16.130-mRNA-1 protein Name:Similar to LHCB4.2 Chlorophyll a-b binding protein CP29.2, chloroplastic (Arabidopsis thaliana) AED:0.05 eAED:0.05 QI:1875|1|1|1|0.5|0.33|3|204|289)'

photosynthesis.photophosphorylation.photosystem II.LHC-II complex.component LHCb5'	xvis03_221799-pa	component LHCb5 of LHC-II complex (original description: processed-gene-5.86-mRNA-1 protein Name:Similar to LHCB5 Chlorophyll a-b binding protein CP26, chloroplastic (Arabidopsis thaliana) AED:0.06 eAED:0.06 QI:123|0.8|0.83|1|1|1|6|161|279)'
photosynthesis.photophosphorylation.photosystem II.LHC-II complex.component LHCb6'	xvis03_207968-pa	component LHCb6 of LHC-II complex (original description: augustus-gene-15.42-mRNA-1 protein Name:Similar to CAP10A Chlorophyll a-b binding protein CP24 10A, chloroplastic (Solanum lycopersicum) AED:0.00 eAED:0.00 QI:218|1|1|1|1|2|259|254)'
photosynthesis.photophosphorylation.photosystem II.pS-II complex.oxygen-evolving center (OEC) extrinsic proteins.component OEC33/psbO'	xvis03_208337-pa	component PsbO/OEC33 of PS-II oxygen-evolving center (original description: augustus-gene-6.16-mRNA-1 protein Name:Similar to PSBO Oxygen-evolving enhancer protein 1, chloroplastic (Solanum lycopersicum) AED:0.08 eAED:0.08 QI:229|1|1|1|0.5|0.33|3|86|332)'
photosynthesis.photophosphorylation.photosystem II.pS-II complex.oxygen-evolving center (OEC) extrinsic proteins.component OEC33/psbO'	xvis03_219859-pa	component PsbO/OEC33 of PS-II oxygen-evolving center (original description: augustus-gene-3.73-mRNA-1 protein Name:Similar to PSBO Oxygen-evolving enhancer protein 1, chloroplastic (Solanum lycopersicum) AED:0.03 eAED:0.03 QI:216|1|1|1|1|2|224|332)'
photosynthesis.photophosphorylation.photosystem II.pS-II complex.oxygen-evolving center (OEC) extrinsic proteins.Viridiplantae-specific components.component OEC23/psbp'	xvis03_209988-pa	component PsbP of PS-II oxygen-evolving center (original description: processed-gene-2.101-mRNA-1 protein Name:Similar to PSBP Oxygen-evolving enhancer protein 2, chloroplastic (Cucumis sativus) AED:0.32 eAED:0.32 QI:142|1|1|1|1|4|296|262)'
photosynthesis.photophosphorylation.photosystem II.assembly and maintenance.assembly factor (MET1)'	xvis03_221570-pa	MET1 protein involved in PS-II assembly (original description: augustus-gene-2.10-mRNA-1 protein Name:Similar to LSF1 Phosphoglucan phosphatase LSF1, chloroplastic (Arabidopsis thaliana) AED:0.06 eAED:0.06 QI:233|0.83|0.71|1|0.5|0.42|7|831|301)'
photosynthesis.photophosphorylation.cytochrome b6/f complex.Rieske iron-sulfur component petC'	xvis03_223095-pa	Rieske iron-sulfur component PetC of cytochrome b6/f complex (original description: augustus-

		gene-3.96-mRNA-1 protein Name:Similar to petC Cytochrome b6-f complex iron-sulfur subunit, chloroplastic (Oryza sativa subsp. japonica) AED:0.11 eAED:0.11 QI:167|0.33|0.75|1|1|1|4|287|178)'
photosynthesis. photophosphorylation. Cytb6/f to pS-I electron carriers.plastocyanin'	xvis03_217729-pa	plastocyanin electron carrier (original description: processed-gene-11.5-mRNA-1 protein Name:Similar to PETE Plastocyanin minor isoform, chloroplastic (Arabidopsis thaliana) AED:0.37 eAED:0.37 QI:0|0|0|0.16|1|1|6|0|366)'
photosynthesis.photophosphorylation.photosystem I.LHC-I complex.component LHCa1'	xvis03_225147-pa	component LHCa1 of LHC-I complex (original description: augustus-gene-0.41-mRNA-1 protein Name:Similar to CAB6A Chlorophyll a-b binding protein 6A, chloroplastic (Solanum lycopersicum) AED:0.00 eAED:0.00 QI:106|1|1|1|1|1|3|75|204)'
photosynthesis.photophosphorylation.photosystem I.LHC-I complex.component LHCa1'	xvis03_225829-pa	component LHCa1 of LHC-I complex (original description: augustus-gene-0.17-mRNA-1 protein Name:Similar to LHCA1 Chlorophyll a-b binding protein 6, chloroplastic (Arabidopsis thaliana) AED:0.45 eAED:0.45 QI:0|0.44|0.4|0.5|1|1|10|334|459)'
photosynthesis.photophosphorylation.photosystem I.pS-I complex.component psaH'	xvis03_205319-pa	component PsaH of PS-I complex (original description: processed-gene-30.54-mRNA-1 protein Name:Similar to PSAH1 Photosystem I reaction center subunit VI-1, chloroplastic (Arabidopsis thaliana) AED:0.09 eAED:0.09 QI:15|1|1|1|1|1|3|336|145)'
photosynthesis.photophosphorylation.linear electron flow.ferredoxin-NADp reductase (FNR) activity.ferredoxin-NADp oxidoreductase'	xvis03_207668-pa	ferredoxin-NADP oxidoreductase (original description: processed-gene-12.85-mRNA-1 protein Name:Similar to PETH Ferredoxin--NADP reductase, leaf isozyme, chloroplastic (Pisum sativum) AED:0.14 eAED:0.14 QI:231|1|1|1|1|1|9|392|366)'
photosynthesis.photophosphorylation.chlororespiration.NADH dehydrogenase-like (NDH) complex.lumen subcomplex L.component pnsL1'	xvis03_203608-pa	component PnsL1 of NDH lumen subcomplex L (original description: processed-gene-32.69-mRNA-1 protein Name:Similar to PNSL1 Photosynthetic NDH subunit of lumenal location 1, chloroplastic (Arabidopsis thaliana)

		AED:0.12 eAED:0.08 QI:81|1|0.85|1|1|1|7|565|263)'
photosynthesis.calvin cycle.ribulose-1,5-bisphosphat carboxylase/oxygenase (RuBisCo) activity.RuBisCo heterodimer.small subunit'	xvis03_223144-pa	small subunit of ribulose-1,5-bisphosphat carboxylase/oxygenase heterodimer (original description: processed-gene-3.56-mRNA-1 protein Name:Similar to RBCS1 Ribulose bisphosphate carboxylase small chain, chloroplastic (Musa acuminata) AED:0.05 eAED:0.05 QI:145|1|1|1|1|3|356|174)'
photosynthesis.calvin cycle.ribulose-1,5-bisphosphat carboxylase/oxygenase (RuBisCo) activity.RuBisCo assembly.auxiliary co-chaperone (CpN20)'	xvis03_206991-pa	CPN20 auxiliary co-chaperone involved in RuBisCo assembly (original description: augustus-gene-10.52-mRNA-1 protein Name:Similar to CPN21 20 kDa chaperonin, chloroplastic (Arabidopsis thaliana) AED:0.07 eAED:0.07 QI:99|1|1|1|1|5|439|254)'
photosynthesis.calvin cycle.ribulose-1,5-bisphosphat carboxylase/oxygenase (RuBisCo) activity.RuBisCo assembly.auxiliary co-chaperone (CpN20)'	xvis03_217041-pa	CPN20 auxiliary co-chaperone involved in RuBisCo assembly (original description: augustus-gene-12.20-mRNA-1 protein Name:Similar to CPN21 20 kDa chaperonin, chloroplastic (Arabidopsis thaliana) AED:0.12 eAED:0.12 QI:32|0.33|0.71|0.71|1|1|7|174|298)'
photosynthesis.calvin cycle.ribulose-1,5-bisphosphat carboxylase/oxygenase (RuBisCo) activity.RuBisCo regulation.ATp-dependent activase (RCA)'	xvis03_223853-pa	ATP-dependent activase involved in RuBisCo regulation (original description: processed-gene-1.15-mRNA-1 protein Name:Similar to RCA2 Ribulose bisphosphate carboxylase/oxygenase activase 2, chloroplastic (Larrea tridentata) AED:0.12 eAED:0.12 QI:111|1|1|1|0.83|0.71|7|332|438)'
photosynthesis.calvin cycle.triosephosphate isomerase'	xvis03_224225-pa	triosephosphate isomerase (original description: augustus-gene-0.55-mRNA-1 protein Name:Similar to TPIP1 Triosephosphate isomerase, chloroplastic (Spinacia oleracea) AED:0.32 eAED:0.32 QI:0|0|0|0.55|0.87|1|9|0|311)'
photosynthesis.calvin cycle.transketolase'	xvis03_207774-pa	transketolase (original description: processed-gene-21.50-mRNA-1 protein Name:Similar to Transketolase, chloroplastic (Solanum tuberosum) AED:0.17 eAED:0.17 QI:154|0.85|0.75|1|1|1|8|0|716)'

photosynthesis.calvin cycle.transketolase'	xvis03_219001-pa	transketolase (original description: processed-gene-2.79-mRNA-1 protein Name:Similar to Transketolase, chloroplastic (Solanum tuberosum) AED:0.04 eAED:0.04 QI:238|1|1|1|1|1|7|473|742)'
photosynthesis.photorespiration.serine hydroxymethyltransferase (SHM)'	xvis03_208040-pa	serine hydroxymethyltransferase (original description: processed-gene-21.10-mRNA-1 protein Name:Similar to SHM4 Serine hydroxymethyltransferase 4 (Arabidopsis thaliana) AED:0.05 eAED:0.05 QI:76|1|1|1|1|1|4|235|515)'
protein biosynthesis.ribosome biogenesis.large ribosomal subunit (LSU).LSU proteome.component RpL3'	xvis03_216531-pa	component RPL3 of LSU proteome component (original description: augustus-gene-9.118-mRNA-1 protein Name:Similar to RPL3 60S ribosomal protein L3 (Oryza sativa subsp. japonica) AED:0.07 eAED:0.07 QI:0|1|0.83|1|1|0.83|6|237|407)'
protein biosynthesis.ribosome biogenesis.large ribosomal subunit (LSU).LSU proteome.component RpL3'	xvis03_220863-pa	component RPL3 of LSU proteome component (original description: processed-gene-0.82-mRNA-1 protein Name:Similar to RPL3 60S ribosomal protein L3 (Oryza sativa subsp. japonica) AED:0.08 eAED:0.08 QI:54|1|1|1|1|1|6|258|389)'
protein biosynthesis.ribosome biogenesis.large ribosomal subunit (LSU).LSU proteome.component RpL8'	xvis03_215883-pa	component RPL8 of LSU proteome component (original description: processed-gene-4.2-mRNA-1 protein Name:Similar to RPL8 60S ribosomal protein L8 (Solanum lycopersicum) AED:0.00 eAED:0.00 QI:71|1|1|1|1|1|2|167|261)'
protein biosynthesis.ribosome biogenesis.small ribosomal subunit (SSU).SSU proteome.component RpS2'	xvis03_220973-pa	component RPS2 of SSU proteome (original description: augustus-gene-5.51-mRNA-1 protein Name:Similar to RPS2C 40S ribosomal protein S2-3 (Arabidopsis thaliana) AED:0.29 eAED:0.29 QI:54|1|1|1|0.5|0.33|3|154|274)'
protein biosynthesis.ribosome biogenesis.small ribosomal subunit (SSU).SSU proteome.component RpS17'	xvis03_204705-pa	component RPS17 of SSU proteome (original description: processed-gene-11.1-mRNA-1 protein Name:Similar to RPS17 40S ribosomal protein S17 (Solanum lycopersicum) AED:0.06

		eAED:0.06 QI:0|-1|0|1|-1|1|1|0|143)'
protein biosynthesis.ribosome biogenesis.small ribosomal subunit (SSU).SSU proteome.component RpS17'	xvis03_207825-pa	component RPS17 of SSU proteome (original description: processed-gene-26.31-mRNA-1 protein Name:Similar to RPS17 40S ribosomal protein S17 (Solanum lycopersicum) AED:0.03 eAED:0.03 QI:0|-1|0|1|-1|1|1|0|146)'
protein biosynthesis.organelle machinery.plastidial ribosome.large ribosomal subunit proteome.component psRpL4'	xvis03_213652-pa	component psRPL4 of large ribosomal subunit proteome (original description: processed-gene-16.266-mRNA-1 protein Name:Similar to RPL4 50S ribosomal protein L4, chloroplastic (Nicotiana tabacum) AED:0.18 eAED:0.18 QI:0|-1|0|1|-1|1|1|0|272)'
protein biosynthesis.organelle machinery.plastidial ribosome.large ribosomal subunit proteome.component psRpL5'	xvis03_220112-pa	component psRPL5 of large ribosomal subunit proteome (original description: augustus-gene-8.33-mRNA-1 protein Name:Similar to RPL5 50S ribosomal protein L5, chloroplastic (Arabidopsis thaliana) AED:0.02 eAED:0.03 QI:29|0.5|0.33|1|1|1|3|0|284)'
protein biosynthesis.organelle machinery.plastidial ribosome.large ribosomal subunit proteome.component psRpL9'	xvis03_202061-pa	component psRPL9 of large ribosomal subunit proteome (original description: processed-gene-6.69-mRNA-1 protein Name:Similar to RPL9 50S ribosomal protein L9, chloroplastic (Arabidopsis thaliana) AED:0.06 eAED:0.06 QI:100|1|1|1|0.83|0.71|7|568|196)'
protein biosynthesis.organelle machinery.plastidial ribosome.small ribosomal subunit proteome.component psRpS5'	xvis03_207337-pa	component psRPS5 of small ribosomal subunit proteome (original description: processed-gene-10.83-mRNA-1 protein Name:Similar to rps5 30S ribosomal protein S5, chloroplastic (Arabidopsis thaliana) AED:0.00 eAED:0.00 QI:186|1|1|1|1|1|2|216|309)'
protein biosynthesis.organelle machinery.translation initiation.initiation factor (IF-3)'	xvis03_224254-pa	IF-3 translation initiation factor (original description: augustus-gene-0.0-mRNA-1 protein Name:Similar to infC Translation initiation factor IF-3 (Nostoc sp. (strain PCC 7120 / UTEX 2576)) AED:0.11 eAED:0.11 QI:31|1|1|1|0.55|0.5|10|360|276)'

protein homeostasis.protein quality control.ER Quality Control (ERQC) machinery.calnexin/calreticulin chaperone system.CNX-CRT cycle.lectin chaperone (CNX)'	xvis03_219178-pa	lectin chaperone (CNX) (original description: processed-gene-7.19-mRNA-1 protein Name:Similar to CNX1 Calnexin homolog 1 (Arabidopsis thaliana) AED:0.09 eAED:0.09 QI:144|1|1|1|0.83|0.71|7|378|540)'
protein homeostasis.protein quality control.Hsp60 chaperone system.Hsp60-co-chaperone (Hsp20)'	xvis03_206991-pa	Hsp60-co-chaperone (Hsp20) (original description: augustus-gene-10.52-mRNA-1 protein Name:Similar to CPN21 20 kDa chaperonin, chloroplastic (Arabidopsis thaliana) AED:0.07 eAED:0.07 QI:99|1|1|1|1|5|439|254)'
protein homeostasis.protein quality control.Hsp60 chaperone system.Hsp60-co-chaperone (Hsp20)'	xvis03_217041-pa	Hsp60-co-chaperone (Hsp20) (original description: augustus-gene-12.20-mRNA-1 protein Name:Similar to CPN21 20 kDa chaperonin, chloroplastic (Arabidopsis thaliana) AED:0.12 eAED:0.12 QI:32|0.33|0.71|0.71|1|1|7|174|298)'
protein homeostasis.ubiquitin-proteasome system.26S proteasome.20S core particle.alpha-type components.component alpha type-2'	xvis03_213988-pa	component alpha type-2 of 26S proteasome (original description: augustus-gene-11.18-mRNA-1 protein Name:Similar to PAB1 Proteasome subunit alpha type-2 (Oryza sativa subsp. japonica) AED:0.05 eAED:0.05 QI:70|1|1|1|1|10|615|222)'
protein homeostasis.ubiquitin-proteasome system.26S proteasome.20S core particle.beta-type components.component beta type-7'	xvis03_202356-pa	component beta type-7 of 26S proteasome (original description: processed-gene-29.12-mRNA-1 protein Name:Similar to PBG1 Proteasome subunit beta type-4 (Arabidopsis thaliana) AED:0.13 eAED:0.13 QI:0|0.71|0.75|0.87|1|1|8|335|329)'
protein homeostasis.proteolysis.cysteine-type peptidase activities.C13-class asparaginyl endopeptidase (Legumain)'	xvis03_211268-pa	asparaginyl endopeptidase (Legumain) (original description: processed-gene-9.25-mRNA-1 protein Name:Similar to Vacuolar-processing enzyme (Citrus sinensis) AED:0.07 eAED:0.07 QI:3|1|1|1|1|9|417|590)'
Carbohydrate metabolism.sucrose metabolism.biosynthesis.cytosolic triose-phosphate isomerase'	xvis03_211745-pa	cytosolic triose-phosphate isomerase (original description: augustus-gene-13.21-mRNA-1 protein Name:Similar to TPIP1 Triosephosphate isomerase, cytosolic (Petunia hybrida) AED:0.34 eAED:0.34 QI:46|0.88|0.8|0.9|1|1|10|0|326)'

Carbohydrate metabolism.starch metabolism.biosynthesis.ADp-glucose pyrophosphorylase'	xvis03_220998-pa	ADP-glucose pyrophosphorylase (original description: augustus-gene-7.121-mRNA-1 protein Name:Similar to ADG2 Glucose-1-phosphate adenylyltransferase large subunit 1, chloroplastic (Arabidopsis thaliana) AED:0.11 eAED:0.11 QI:196|0.92|0.86|1|0.85|0.86|15|136|540)'
Carbohydrate metabolism.oxidative pentose phosphate pathway.non-oxidative phase.transketolase'	xvis03_207774-pa	transketolase (original description: processed-gene-21.50-mRNA-1 protein Name:Similar to Transketolase, chloroplastic (Solanum tuberosum) AED:0.17 eAED:0.17 QI:154|0.85|0.75|1|1|1|8|0|716)'
Carbohydrate metabolism.oxidative pentose phosphate pathway.non-oxidative phase.transketolase'	xvis03_219001-pa	transketolase (original description: processed-gene-2.79-mRNA-1 protein Name:Similar to Transketolase, chloroplastic (Solanum tuberosum) AED:0.04 eAED:0.04 QI:238|1|1|1|1|1|7|473|742)'
Carbohydrate metabolism.plastidial glycolysis.triosephosphate isomerase'	xvis03_224225-pa	triosephosphate isomerase (original description: augustus-gene-0.55-mRNA-1 protein Name:Similar to TPIP1 Triosephosphate isomerase, chloroplastic (Spinacia oleracea) AED:0.32 eAED:0.32 QI:0|0|0|0.55|0.87|1|9|0|311)'
Cellular respiration.glycolysis.cytosolic glycolysis.triosephosphate isomerase'	xvis03_211745-pa	triosephosphate isomerase (original description: augustus-gene-13.21-mRNA-1 protein Name:Similar to TPIP1 Triosephosphate isomerase, cytosolic (Petunia hybrida) AED:0.34 eAED:0.34 QI:46|0.88|0.8|0.9|1|1|10|0|326)'
Cellular respiration.glycolysis.methylglyoxal degradation.lactoyl-glutathione lyase (GLX1)'	xvis03_210597-pa	lactoyl-glutathione lyase (GLX1) (original description: augustus-gene-8.18-mRNA-1 protein Name:Similar to At1g67280 Probable lactoylglutathione lyase, chloroplast (Arabidopsis thaliana) AED:0.06 eAED:0.06 QI:224|1|1|1|1|1|9|419|372)'
Cellular respiration.tricarboxylic acid cycle.mitochondrial NAD-dependent malic enzyme'	xvis03_201588-pa	mitochondrial NAD-dependent malic enzyme (original description: augustus-gene-28.7-mRNA-1 protein Name:Similar to NAD-ME1 NAD-dependent malic enzyme 1, mitochondrial (Arabidopsis thaliana) AED:0.22 eAED:0.22

		QI:0|0.77|0.78|0.86|0.77|0.82|23|290|790)'
Cellular respiration.oxidative phosphorylation.cytochrome c reductase complex.component cytochrome c1'	xvis03_206281-pa	cytochrome c1 component of cytochrome c reductase complex (original description: augustus-gene-15.74-mRNA-1 protein Name:Similar to CYCL Cytochrome c1-1, heme protein, mitochondrial (Solanum tuberosum) AED:0.28 eAED:0.28 QI:33|0.85|0.87|1|1|1|8|457|361)'
Cellular respiration.oxidative phosphorylation.ATp synthase complex.peripheral MF1 subcomplex.subunit delta_'	xvis03_218722-pa	subunit delta_ of ATP synthase peripheral MF1 subcomplex (original description: augustus-gene-3.37-mRNA-1 protein Name:Similar to ATP synthase subunit delta', mitochondrial (Ipomoea batatas) AED:0.20 eAED:0.20 QI:67|0|0.25|0.5|0.33|0.75|4|0|208)'
Redox homeostasis.enzymatic reactive oxygen species scavengers.catalase'	xvis03_220733-pa	catalase (original description: processed-gene-1.13-mRNA-1 protein Name:Similar to CAT1 Catalase-1 (Triticum aestivum) AED:0.19 eAED:0.19 QI:0|0|0|0.66|1|1|9|0|623)'
Redox homeostasis.hydrogen peroxide removal.ascorbate-glutathione cycle.ascorbate peroxidase (ApX)'	xvis03_201883-pa	ascorbate peroxidase (APX) (original description: augustus-gene-50.73-mRNA-1 protein Name:Similar to APX1 L-ascorbate peroxidase, cytosolic (Pisum sativum) AED:0.15 eAED:0.15 QI:0|0.85|0.75|1|1|0.87|8|414|307)'
Redox homeostasis.hydrogen peroxide removal.ascorbate-glutathione cycle.ascorbate peroxidase (ApX)'	xvis03_214214-pa	ascorbate peroxidase (APX) (original description: processed-gene-11.33-mRNA-1 protein Name:Similar to APX1 L-ascorbate peroxidase, cytosolic (Pisum sativum) AED:0.17 eAED:0.17 QI:131|1|1|1|1|1|7|558|249)'
Redox homeostasis.hydrogen peroxide removal.ascorbate-glutathione cycle.ascorbate peroxidase (ApX)'	xvis03_222105-pa	ascorbate peroxidase (APX) (original description: augustus-gene-5.53-mRNA-1 protein Name:Similar to APXT L-ascorbate peroxidase T, chloroplastic (Arabidopsis thaliana) AED:0.32 eAED:0.32 QI:0|0.5|0.45|0.72|0.9|0.81|11|0|364)'

Redox homeostasis.hydrogen peroxide removal.ascorbate-glutathione cycle.ascorbate peroxidase (ApX)'	xvis03_223438-pa	ascorbate peroxidase (APX) (original description: augustus-gene-1.2-mRNA-1 protein Name:Similar to APX4 Probable L-ascorbate peroxidase 4 (Oryza sativa subsp. japonica) AED:0.10 eAED:0.10 QI:188|1|1|1|1|9|226|284)'
Amino acid metabolism.biosynthesis.aspartate family.aspartate-derived amino acids.methionine.salvage pathway.bifunctional methylthioribulose-1-phosphate dehydratase and enolase-phosphatase'	xvis03_223588-pa	bifunctional methylthioribulose-1-phosphate dehydratase and enolase-phosphatase (original description: processed-gene-1.56-mRNA-1 protein Name:Similar to VIT_19s0014g02480 Probable bifunctional methylthioribulose-1-phosphate dehydratase/enolase-phosphatase E1 1 (Vitis vinifera) AED:0.24 eAED:0.24 QI:0|0.9|0.90|0.90|1|1|11|237|411)'
Amino acid metabolism.biosynthesis.serine family.glycine.serine hydroxymethyltransferase	xvis03_208040-pa	serine hydroxymethyltransferase (original description: processed-gene-21.10-mRNA-1 protein Name:Similar to SHM4 Serine hydroxymethyltransferase 4 (Arabidopsis thaliana) AED:0.05 eAED:0.05 QI:76|1|1|1|1|1|4|235|515)'
Nucleotide metabolism.purines.phosphotransfers.adenylate kinase'	xvis03_207311-pa	adenylate kinase (original description: processed-gene-7.62-mRNA-1 protein Name:Similar to ADK-B Adenylate kinase 4 (Oryza sativa subsp. japonica) AED:0.05 eAED:0.05 QI:122|1|1|1|1|1|6|379|246)'
Nucleotide metabolism.purines.phosphotransfers.adenylate kinase'	xvis03_213605-pa	adenylate kinase (original description: processed-gene-14.84-mRNA-1 protein Name:Similar to Os08g0288200 Probable adenylate kinase 5, chloroplastic (Oryza sativa subsp. japonica) AED:0.22 eAED:0.22 QI:25|1|0.94|1|1|1|17|0|611)'
RNA processing.pre-mRNA splicing. U2-type-intron-specific major spliceosome. U2 small nuclear ribonucleoprotein particle (snRNp).protein factor (U2A)'	xvis03_205605-pa	protein factor U2A of U2 small nuclear ribonucleoprotein particle (snRNP) (original description: processed-gene-17.119-mRNA-1 protein Name:Similar to At1g09760 U2 small nuclear ribonucleoprotein A' (Arabidopsis thaliana) AED:0.23 eAED:0.27 QI:0|0.83|0.71|1|1|1|7|448|347)'
RNA processing.organelle machinery.ribonuclease activities.endoribonuclease (CSp41)'	xvis03_213217-pa	endoribonuclease (CSP41) (original description: augustus-gene-16.1-mRNA-1 protein Name:Similar to CSP41A

		Chloroplast stem-loop binding protein of 41 kDa a, chloroplastic (Arabidopsis thaliana) AED:0.01 eAED:0.01 QI:41|1|1|1|1|1|6|52|409)'
protein modification.protein folding.protein folding catalyst (FKBp)'	xvis03_208652-pa	protein folding catalyst (FKBP) (original description: processed-gene-19.48-mRNA-1 protein Name:Similar to FKBP62 Peptidyl-prolyl cis-trans isomerase FKBP62 (Arabidopsis thaliana) AED:0.12 eAED:0.12 QI:105|0.91|0.92|1|1|1|13|323|570)'
protein modification.protein folding.protein folding catalyst (FKBp)'	xvis03_224849-pa	protein folding catalyst (FKBP) (original description: processed-gene-1.76-mRNA-1 protein Name:Similar to FKBP19 Peptidyl-prolyl cis-trans isomerase FKBP19, chloroplastic (Arabidopsis thaliana) AED:0.46 eAED:0.49 QI:0|0.72|0.83|0.91|0.90|0.83|12|203|320)'
Cell wall organisation.pectin.rhamnogalacturonan I.modification and degradation.beta-galactosidase (BGAL)'	xvis03_208987-pa	beta-galactosidase (BGAL) (original description: augustus-gene-4.4-mRNA-1 protein Name:Similar to BGAL9 Beta-galactosidase 9 (Arabidopsis thaliana) AED:0.06 eAED:0.06 QI:63|1|1|1|0.94|0.94|19|309|904)'
Cell wall organisation.pectin.rhamnogalacturonan I.modification and degradation.beta-galactosidase (BGAL)'	xvis03_221434-pa	beta-galactosidase (BGAL) (original description: processed-gene-2.106-mRNA-1 protein Name:Similar to Beta-galactosidase (Asparagus officinalis) AED:0.13 eAED:0.13 QI:277|1|1|1|1|1|19|418|832)'

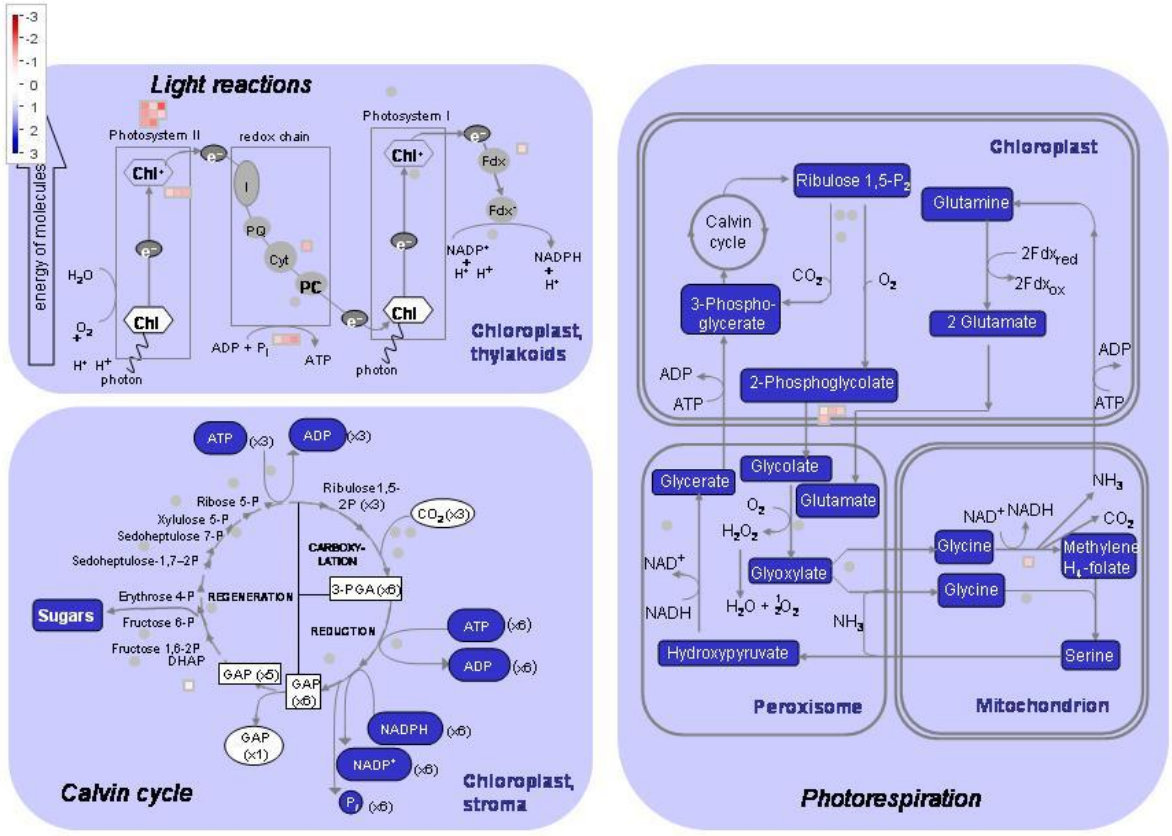

Figure S3.1: Representing downregulated proteins at MRD involved in photorespiration, Calvin cycle and light reaction (Supplementary Table S3.3). The pink squares indicated downregulated proteins.

Table S3.5 A: Representing light reaction, Calvin cycle and photorespiration:

Light reaction:

BinName	id	Description	Log2Fold change
photosynthesis.photophosphorylation.photosystem II.LHC-II complex.component LHCb1/2/3'	xvis03_211060-pa	component LHCb1/2/3 of LHC-II complex (original description: processed-gene-14.7-mRNA-1 protein Name:Similar to Chlorophyll a-b binding protein, chloroplastic (Spinacia oleracea) AED:0.01 eAED:0.01 QI:0|-1|0|1|-1|1|1|0|268)'	-1.59118
photosynthesis.photophosphorylation.photosystem II.LHC-II complex.component LHCb1/2/3'	xvis03_219722-pa	component LHCb1/2/3 of LHC-II complex (original description: augustus-gene-9.73-mRNA-1 protein Name:Similar to CAB36	-2.82067

		Chlorophyll a-b binding protein 36, chloroplastic (Nicotiana tabacum) AED:0.36 eAED:0.36 QI:240|1|1|1|1|2|393|264)'	
photosynthesis.photophosphorylation.photosystem II.LHC-II complex.component LHCb1/2/3'	xvis03_223077-pa	component LHCb1/2/3 of LHC-II complex (original description: processed-gene-1.89-mRNA-1 protein Name:Similar to CAB13 Chlorophyll a-b binding protein 13, chloroplastic (Solanum lycopersicum) AED:0.07 eAED:0.07 QI:182|1|1|1|1|4|188|263)'	-3.54613
photosynthesis.photophosphorylation.photosystem II.LHC-II complex.component LHCb1/2/3'	xvis03_224654-pa	component LHCb1/2/3 of LHC-II complex (original description: processed-gene-1.9-mRNA-1 protein Name:Similar to CAB21 Chlorophyll a-b binding protein 21, chloroplastic (Nicotiana tabacum) AED:0.11 eAED:0.11 QI:0|0|0|0.5|1|1|2|0|328)'	-2.68394
photosynthesis.photophosphorylation.photosystem II.LHC-II complex.component LHCb1/2/3'	xvis03_225066-pa	component LHCb1/2/3 of LHC-II complex (original description: processed-gene-0.82-mRNA-1 protein Name:Similar to Chlorophyll a-b binding protein, chloroplastic (Spinacia oleracea) AED:0.00 eAED:0.00 QI:0|-1|0|1|-1|1|1|0|268)'	-1.30492
photosynthesis.photophosphorylation.photosystem II.LHC-II complex.component LHCb4'	xvis03_212711-pa	component LHCb4 of LHC-II complex (original description: processed-gene-16.130-mRNA-1 protein Name:Similar to LHCB4.2 Chlorophyll a-b binding protein CP29.2, chloroplastic (Arabidopsis thaliana) AED:0.05 eAED:0.05 QI:1875|1|1|1|0.5|0.33|3|204|289)'	-3.59907

photosynthesis.photophosphorylation.photosystem II.LHC-II complex.component LHCb5'	xvis03_202336-pa	component LHCb5 of LHC-II complex (original description: augustus-gene-27.98-mRNA-1 protein Name:Similar to LHCB5 Chlorophyll a-b binding protein CP26, chloroplastic (Arabidopsis thaliana) AED:0.08 eAED:0.08 QI:26|1|1|1|1|6|330|363)'	-3.18151
photosynthesis.photophosphorylation.photosystem II.LHC-II complex.component LHCb5'	xvis03_221799-pa	component LHCb5 of LHC-II complex (original description: processed-gene-5.86-mRNA-1 protein Name:Similar to LHCB5 Chlorophyll a-b binding protein CP26, chloroplastic (Arabidopsis thaliana) AED:0.06 eAED:0.06 QI:123|0.8|0.83|1|1|1|6|161|279)'	-1.46518
photosynthesis.photophosphorylation.photosystem II.LHC-II complex.component LHCb6'	xvis03_207968-pa	component LHCb6 of LHC-II complex (original description: augustus-gene-15.42-mRNA-1 protein Name:Similar to CAP10A Chlorophyll a-b binding protein CP24 10A, chloroplastic (Solanum lycopersicum) AED:0.00 eAED:0.00 QI:218|1|1|1|1|1|2|259|254)'	-1.68796
photosynthesis.photophosphorylation.photosystem II.LHC-II complex.component LHCb6'	xvis03_217301-pa	component LHCb6 of LHC-II complex (original description: augustus-gene-11.85-mRNA-1 protein Name:Similar to CAP10A Chlorophyll a-b binding protein CP24 10A, chloroplastic (Solanum lycopersicum) AED:0.00 eAED:0.00 QI:77|1|1|1|1|1|2|315|254)'	-1.89943
photosynthesis.photophosphorylation.photosystem II.pS-II complex.oxygen-	xvis03_208337-pa	component PsbO/OEC33 of PS-II oxygen-evolving center (original description: augustus-gene-6.16-mRNA-	-1.03026

evolving center (OEC) extrinsic proteins.component OEC33/psbO'		1 protein Name:Similar to PSBO Oxygen-evolving enhancer protein 1, chloroplastic (Solanum lycopersicum) AED:0.08 eAED:0.08 QI:229|1|1|1|0.5|0.33|3|86|332)'	
photosynthesis.photophosphorylation.photosystem II.pS-II complex.oxygen-evolving center (OEC) extrinsic proteins.component OEC33/psbO'	xvis03_219859-pa	component PsbO/OEC33 of PS-II oxygen-evolving center (original description: augustus-gene-3.73-mRNA-1 protein Name:Similar to PSBO Oxygen-evolving enhancer protein 1, chloroplastic (Solanum lycopersicum) AED:0.03 eAED:0.03 QI:216|1|1|1|1|1|2|224|332)'	-1.27835
photosynthesis.photophosphorylation.photosystem II.pS-II complex.oxygen-evolving center (OEC) extrinsic proteins.Viridiplantae-specific components.component OEC23/psbp'	xvis03_209988-pa	component PsbP of PS-II oxygen-evolving center (original description: processed-gene-2.101-mRNA-1 protein Name:Similar to PSBP Oxygen-evolving enhancer protein 2, chloroplastic (Cucumis sativus) AED:0.32 eAED:0.32 QI:142|1|1|1|1|1|4|296|262)'	-1.3232
photosynthesis.photophosphorylation.photosystem I.LHC-I complex.component LHCa1'	xvis03_225147-pa	component LHCa1 of LHC-I complex (original description: augustus-gene-0.41-mRNA-1 protein Name:Similar to CAB6A Chlorophyll a-b binding protein 6A, chloroplastic (Solanum lycopersicum) AED:0.00 eAED:0.00 QI:106|1|1|1|1|1|3|75|204)'	-3.1886
photosynthesis.photophosphorylation.photosystem I.LHC-I complex.component LHCa1'	xvis03_225829-pa	component LHCa1 of LHC-I complex (original description: augustus-gene-0.17-mRNA-1 protein Name:Similar to LHCA1 Chlorophyll a-b binding protein 6, chloroplastic	-2.65519

		(Arabidopsis thaliana) AED:0.45 eAED:0.45 QI:0|0.44|0.4|0.5|1|1|10|334|459)'	
photosynthesis.photophosphorylation.photosystem I.LHC-I complex.component LHCa2'	xvis03_205558-pa	component LHCa2 of LHC-I complex (original description: augustus-gene-14.7-mRNA-1 protein Name:Similar to CAB7 Chlorophyll a-b binding protein 7, chloroplastic (Solanum lycopersicum) AED:0.16 eAED:0.16 QI:0|0.25|0.4|1|0.75|0.8|5|892|278)'	-2.75709
photosynthesis.photophosphorylation.photosystem I.pS-I complex.component psaD'	xvis03_207379-pa	component PsaD of PS-I complex (original description: processed-gene-13.65-mRNA-1 protein Name:Similar to psaD Photosystem I reaction center subunit II, chloroplastic (Cucumis sativus) AED:0.32 eAED:0.32 QI:0|-1|0|1|-1|1|1|0|274)'	-1.34089
photosynthesis.photophosphorylation.photosystem I.pS-I complex.component psaF'	xvis03_216014-pa	component PsaF of PS-I complex (original description: processed-gene-5.37-mRNA-1 protein Name:Similar to PSAF Photosystem I reaction center subunit III, chloroplastic (Arabidopsis thaliana) AED:0.24 eAED:0.24 QI:0|-1|0|1|-1|1|1|0|232)'	-1.32661
photosynthesis.photophosphorylation.photosystem I.pS-I complex.component psaH'	xvis03_205319-pa	component PsaH of PS-I complex (original description: processed-gene-30.54-mRNA-1 protein Name:Similar to PSAH1 Photosystem I reaction center subunit VI-1, chloroplastic (Arabidopsis thaliana) AED:0.09 eAED:0.09 QI:15|1|1|1|1|1|3|336|145)'	-2.7504

photosynthesis.photophosphorylation.photosystem I.pS-I complex.component psaL'	xvis03_200779-pa	component PsaL of PS-I complex (original description: processed-gene-89.11-mRNA-1 protein Name:Similar to PSAL Photosystem I reaction center subunit XI, chloroplastic (Spinacia oleracea) AED:0.06 eAED:0.06 QI:217|1|1|1|1|1|2|190|220)'	-1.57683
photosynthesis.photophosphorylation.Cytb6/f to pS-I electron carriers.plastocyanin'	xvis03_217729-pa	plastocyanin electron carrier (original description: processed-gene-11.5-mRNA-1 protein Name:Similar to PETE Plastocyanin minor isoform, chloroplastic (Arabidopsis thaliana) AED:0.37 eAED:0.37 QI:0|0|0|0.16|1|1|6|0|366)'	-1.26885
BinName	id	description	up and downregulation across treatments for mapman attempt 2 duplicate removed.txt
photosynthesis.photophosphorylation.linear electron flow.ferredoxin-NADp reductase (FNR) activity.ferredoxin-NADp oxidoreductase'	xvis03_207668-pa	ferredoxin-NADP oxidoreductase (original description: processed-gene-12.85-mRNA-1 protein Name:Similar to PETH Ferredoxin--NADP reductase, leaf isozyme, chloroplastic (Pisum sativum) AED:0.14 eAED:0.14 QI:231|1|1|1|1|1|9|392|366)'	-0.9405

S3.5 B - Calvin cycle:

BinName	id	description	Log2Fold change
photosynthesis.photorespiration.serine hydroxymethyltransferase (SHM)'	xvis03_208040-pa	serine hydroxymethyltransferase (original description: processed-gene-21.10-mRNA-1 protein Name:Similar to SHM4 Serine hydroxymethyltransferase 4 (Arabidopsis thaliana) AED:0.05 eAED:0.05 QI:76|1|1|1|1|1|4|235|515)'	-0.61287
photosynthesis.photorespiration.glycine decarboxylase complex.lipoamide-containing component H-protein'	xvis03_220076-pa	lipoamide-containing component H-protein of glycine cleavage system (original description: augustus-gene-4.88-mRNA-1 protein Name:Similar to GDCSH Glycine cleavage system H protein, mitochondrial (Oryza sativa subsp. japonica) AED:0.04 eAED:0.04 QI:127|1|1|1|1|1|4|484|165)'	1.545746
photosynthesis.photorespiration.aminotransferase activities.serine-glyoxylate transaminase'	xvis03_225299-pa	serine-glyoxylate transaminase (original description: processed-gene-0.7-mRNA-1 protein Name:Similar to AGT1 Serine--glyoxylate aminotransferase (Arabidopsis thaliana) AED:0.11 eAED:0.11 QI:101|1|1|1|0.8|0.66|6|208|401)'	5.458248

Table S3.5 C-Photorespiration:

BinName	id	Description	Log2Fold change
photosynthesis.calvin cycle.ribulose-1,5-bisphosphat carboxylase/oxygenase (RuBisCo) activity.RuBisCo heterodimer.small subunit'	xvis03_223144-pa	small subunit of ribulose-1,5-bisphosphat carboxylase/oxygenase heterodimer (original description: processed-gene-3.56-mRNA-1 protein Name:Similar to RBCS1 Ribulose bisphosphate carboxylase small chain, chloroplastic (Musa acuminata) AED:0.05 eAED:0.05 QI:145|1|1|1|1|1|3|356|174)'	0.88459
photosynthesis.calvin cycle.ribulose-1,5-bisphosphat carboxylase/oxygenase (RuBisCo) activity.RuBisCo assembly.CpN60 assembly chaperone complex.component CpN60b'	xvis03_205691-pa	component CPN60b of CPN60 assembly chaperone complex (original description: processed-gene-31.124-mRNA-1 protein Name:Similar to RuBisCO large subunit-binding protein subunit beta, chloroplastic (Pisum sativum) AED:0.20 eAED:0.20 QI:97|0.8|0.81|0.87|0.93|0.87|16|0|678)'	0.6373
photosynthesis.calvin cycle.ribulose-1,5-bisphosphat carboxylase/oxygenase (RuBisCo) activity.RuBisCo assembly.auxiliary co-chaperone (CpN20)'	xvis03_206991-pa	CPN20 auxiliary co-chaperone involved in RuBisCo assembly (original description: augustus-gene-10.52-mRNA-1 protein Name:Similar to CPN21 20 kDa chaperonin, chloroplastic (Arabidopsis thaliana) AED:0.07 eAED:0.07 QI:99|1|1|1|1|1|5|439|254)'	-1.30291
photosynthesis.calvin cycle.ribulose-1,5-bisphosphat carboxylase/oxygenase (RuBisCo) activity.RuBisCo assembly.auxiliary co-chaperone (CpN20)'	xvis03_217041-pa	CPN20 auxiliary co-chaperone involved in RuBisCo assembly (original description: augustus-gene-12.20-mRNA-1 protein Name:Similar to CPN21 20 kDa chaperonin, chloroplastic (Arabidopsis thaliana) AED:0.12 eAED:0.12 QI:32|0.33|0.71|0.71|1|1|7|174|298)'	-1.10176
photosynthesis.calvin cycle.ribulose-1,5-bisphosphat carboxylase/oxygenase (RuBisCo) activity.RuBisCo regulation.ATp-dependent activase (RCA)'	xvis03_223853-pa	ATP-dependent activase involved in RuBisCo regulation (original description: processed-gene-1.15-mRNA-1 protein Name:Similar to RCA2 Ribulose bisphosphate carboxylase/oxygenase activase 2, chloroplastic (Larrea tridentata) AED:0.12 eAED:0.12 QI:111|1|1|1|0.83|0.71|7|332|438)'	-1.19803
photosynthesis.calvin cycle.phosphoglycerate kinase'	xvis03_201416-pa	phosphoglycerate kinase (original description: processed-gene-12.20-mRNA-1 protein Name:Similar to Phosphoglycerate kinase, chloroplastic (Nicotiana tabacum)	0.426788

		AED:0.04 eAED:0.04 QI:190|1|1|1|1|1|6|289|477)'	
photosynthesis.calvin cycle.triosephosphate isomerase'	xvis03_224225-pa	triosephosphate isomerase (original description: augustus-gene-0.55-mRNA-1 protein Name:Similar to TPIP1 Triosephosphate isomerase, chloroplastic (Spinacia oleracea) AED:0.32 eAED:0.32 QI:0|0|0|0.55|0.87|1|9|0|311)'	-1.07647

Table S3.6: List of the Bin names, id and description of the upregulated proteins at LRD

BinName	id	Description
protein biosynthesis.ribosome biogenesis.large ribosomal subunit (LSU).LSU proteome.component RpL23'	xvis03_202929-pa	component RPL23 of LSU proteome component (original description: augustus-gene-26.5-mRNA-1 protein Name:Similar to RPL23A 60S ribosomal protein L23 (Arabidopsis thaliana) AED:0.39 eAED:0.40 QI:0|0|0|0.5|1|1|6|0|279)'
protein biosynthesis.ribosome biogenesis.small ribosomal subunit (SSU).SSU proteome.component RpS12'	xvis03_210337-pa	component RPS12 of SSU proteome (original description: augustus-gene-8.1-mRNA-1 protein Name:Similar to RPS12 40S ribosomal protein S12 (Hordeum vulgare) AED:0.38 eAED:0.38 QI:0|1|0.75|1|1|1|4|393|161)'
protein biosynthesis.ribosome biogenesis.small ribosomal subunit (SSU).SSU proteome.component RpS12'	xvis03_221354-pa	component RPS12 of SSU proteome (original description: augustus-gene-2.78-mRNA-1 protein Name:Similar to RPS12 40S ribosomal protein S12 (Hordeum vulgare) AED:0.26 eAED:0.26 QI:0|1|0.75|1|1|1|4|274|184)'
protein biosynthesis.ribosome biogenesis.small ribosomal subunit (SSU).SSU proteome.component RpS27'	xvis03_205594-pa	component RPS27 of SSU proteome (original description: augustus-gene-17.68-mRNA-1 protein Name:Similar to RPS27B 40S ribosomal protein S27-2 (Arabidopsis thaliana) AED:0.09 eAED:0.09 QI:0|1|0.75|1|1|1|4|342|163)'
protein biosynthesis.ribosome biogenesis.small ribosomal subunit (SSU).SSU proteome.component RpS27'	xvis03_209876-pa	component RPS27 of SSU proteome (original description: augustus-gene-14.5-mRNA-1 protein

		Name:Similar to RPS27B 40S ribosomal protein S27-2 (Arabidopsis thaliana) AED:0.17 eAED:0.17 QI:86|1|1|1|0.66|0.75|4|47|86)'
protein biosynthesis.mRNA quality control.NMD Nonsense-Mediated Decay.eRF1-eRF3 aberrant mRNA detection complex.component eRF1'	xvis03_209643-pa	eRF1 peptide release factor (original description: processed-gene-16.29-mRNA-1 protein Name:Similar to ERF1-3 Eukaryotic peptide chain release factor subunit 1-3 (Arabidopsis thaliana) AED:0.00 eAED:0.00 QI:0|-1|0|1|-1|1|1|0|437)'
protein biosynthesis.translation initiation.pre-Initiation Complex (pIC) module.eIF3 mRNA-to-pIC binding complex.component eIF3g'	xvis03_223860-pa	component eIF3g of eIF3 mRNA-to-PIC binding complex (original description: processed-gene-2.57-mRNA-1 protein Name:Similar to v1g171563 Eukaryotic translation initiation factor 3 subunit G (Nematostella vectensis) AED:0.02 eAED:0.02 QI:0|1|0.5|1|1|1|2|3401|289)'
protein biosynthesis.translation initiation.mRNA loading.mRNA poly-A-tail binding factor (pABp)'	xvis03_217585-pa	mRNA poly-A-tail binding factor (PABP) (original description: augustus-gene-6.44-mRNA-1 protein Name:Similar to PAB8 Polyadenylate-binding protein 8 (Arabidopsis thaliana) AED:0.09 eAED:0.09 QI:312|0.75|0.66|1|1|1|9|460|634)'
protein biosynthesis.translation elongation.eEF1 aminoacyl-tRNA binding factor activity.eEF1B eEF1A-GDp-recycling complex.component eEF1B-beta/-delta'	xvis03_202784-pa	component eEF1B-beta/-delta of eEF1B eEF1A-GDP-recycling complex (original description: processed-gene-9.6-mRNA-1 protein Name:Similar to At5g12110 Elongation factor 1-beta 1 (Arabidopsis thaliana) AED:0.07 eAED:0.07 QI:28|1|1|1|1|6|211|226)'
protein biosynthesis.translation elongation.eEF5 poly-p/G elongation factor activity.poly-p/G elongation factor (eEF5/eIF5A)'	xvis03_208182-pa	poly-P/G elongation factor (eEF5/eIF5A) (original description: processed-gene-16.15-mRNA-1 protein Name:Similar to EIF-5A2 Eukaryotic translation initiation factor 5A-2 (Nicotiana plumbaginifolia) AED:0.11 eAED:0.11

		QI:80|1|1|1|0.8|0.66|6|225|159)'
protein biosynthesis.translation elongation.eEF5 poly-p/G elongation factor activity.poly-p/G elongation factor (eEF5/eIF5A)'	xvis03_214372-pa	poly-P/G elongation factor (eEF5/eIF5A) (original description: processed-gene-6.62-mRNA-1 protein Name:Similar to Eukaryotic translation initiation factor 5A (Manihot esculenta) AED:0.20 eAED:0.20 QI:188|1|1|1|0.8|0.66|6|353|159)'
protein biosynthesis.translation elongation.eEF5 poly-p/G elongation factor activity.poly-p/G elongation factor (eEF5/eIF5A)'	xvis03_221720-pa	poly-P/G elongation factor (eEF5/eIF5A) (original description: augustus-gene-5.43-mRNA-1 protein Name:Similar to EIF-5A2 Eukaryotic translation initiation factor 5A-2 (Nicotiana plumbaginifolia) AED:0.05 eAED:0.05 QI:177|1|1|1|0.8|0.66|6|330|160)'
protein biosynthesis.organelle machinery.plastidial ribosome.large ribosomal subunit proteome.component psRpL18'	xvis03_224660-pa	component psRPL18 of large ribosomal subunit proteome (original description: processed-gene-1.62-mRNA-1 protein Name:Similar to FEN1 Flap endonuclease 1 (Zea mays) AED:0.25 eAED:0.26 QI:20|0.7|0.71|0.95|1|1|21|362|621)'
protein biosynthesis.organelle machinery.translation elongation.elongation factor (EF-Tu)'	xvis03_212520-pa	EF-Tu translation elongation factor (original description: augustus-gene-6.14-mRNA-1 protein Name:Similar to TUFB1 Elongation factor Tu, chloroplastic (Glycine max) AED:0.04 eAED:0.16 QI:0|0|0.5|1|1|1|2|351|455)'
Coenzyme metabolism.iron-sulfur cluster assembly machinery.plastidial SUF system.assembly phase.SUF-SE sulfur transfer complex.cysteine desulfurase component NFS2'	xvis03_220549-pa	cysteine desulfurase component NFS2 of plastidial SUF system assembly phase (original description: processed-gene-6.81-mRNA-1 protein Name:Similar to NFS2 Cysteine desulfurase 1, chloroplastic (Arabidopsis thaliana) AED:0.13 eAED:0.23 QI:55|0.77|0.8|1|1|1|10|0|498)'

Coenzyme metabolism.iron-sulfur cluster assembly machinery.mitochondrial ISC system.transfer phase.assembly factor (IBA57)'	xvis03_224887-pa	assembly factor BA57 of mitochondrial ISC system transfer phase (original description: augustus-gene-0.36-mRNA-1 protein Name:Similar to At4g12130 Putative transferase At4g12130, mitochondrial (Arabidopsis thaliana) AED:0.05 eAED:0.05 QI:50|1|1|1|1|1|5|427|411)'
Coenzyme metabolism.tetrapyrrol biosynthesis.5-aminolevulinic acid formation.glutamate-1-semialdehyde-2,1-aminomutase'	xvis03_216135-pa	glutamate-1-semialdehyde-2,1-aminomutase (original description: augustus-gene-2.5-mRNA-1 protein Name:Similar to GSA Glutamate-1-semialdehyde 2,1-aminomutase, chloroplastic (Oryza sativa subsp. japonica) AED:0.00 eAED:0.00 QI:90|1|1|1|1|1|3|296|478)'
Coenzyme metabolism.tetrapyrrol biosynthesis.chlorophyll metabolism.magnesium-chelatase complex.component CHL-I'	xvis03_222911-pa	component CHL-I of magnesium-chelatase complex (original description: processed-gene-1.35-mRNA-1 protein Name:Similar to CHLI Magnesium-chelatase subunit ChlI, chloroplastic (Oryza sativa subsp. japonica) AED:0.00 eAED:0.00 QI:218|1|1|1|1|1|3|269|418)'
Coenzyme metabolism.tetrapyrrol biosynthesis.chlorophyll metabolism.protochlorophyllide oxidoreductase (pOR) activities.light-dependent pOR'	xvis03_212894-pa	light-dependent protochlorophyllide oxidoreductase (original description: augustus-gene-2.1-mRNA-1 protein Name:Similar to PORB Protochlorophyllide reductase B, chloroplastic (Hordeum vulgare) AED:0.09 eAED:0.09 QI:162|1|1|1|1|1|5|457|393)'
photosynthesis.photophosphorylation.chlororespiration.NADH dehydrogenase-like (NDH) complex.assembly and stabilization.Cpn60 chaperonin heterodimer.subunit beta'	xvis03_205691-pa	subunit beta of Cpn60 chaperonin complex (original description: processed-gene-31.124-mRNA-1 protein Name:Similar to RuBisCO large subunit-binding protein subunit beta, chloroplastic (Pisum sativum) AED:0.20 eAED:0.20 QI:97|0.8|0.81|0.87|0.93|0.87|16|0|678)'

photosynthesis.calvin cycle.ribulose-1,5-bisphosphat carboxylase/oxygenase (RuBisCo) activity.RuBisCo heterodimer.small subunit'	xvis03_223144-pa	small subunit of ribulose-1,5-bisphosphat carboxylase/oxygenase heterodimer (original description: processed-gene-3.56-mRNA-1 protein Name:Similar to RBCS1 Ribulose bisphosphate carboxylase small chain, chloroplastic (Musa acuminata) AED:0.05 eAED:0.05 QI:145|1|1|1|1|3|356|174)'
photosynthesis.calvin cycle.ribulose-1,5-bisphosphat carboxylase/oxygenase (RuBisCo) activity.RuBisCo assembly.CpN60 assembly chaperone complex.component CpN60b'	xvis03_205691-pa	component CPN60b of CPN60 assembly chaperone complex (original description: processed-gene-31.124-mRNA-1 protein Name:Similar to RuBisCO large subunit-binding protein subunit beta, chloroplastic (Pisum sativum) AED:0.20 eAED:0.20 QI:97|0.8|0.81|0.87|0.93|0.87|16|0|678)'
photosynthesis.calvin cycle.phosphoglycerate kinase'	xvis03_201416-pa	phosphoglycerate kinase (original description: processed-gene-12.20-mRNA-1 protein Name:Similar to Phosphoglycerate kinase, chloroplastic (Nicotiana tabacum) AED:0.04 eAED:0.04 QI:190|1|1|1|1|6|289|477)'
photosynthesis.photorespiration.glycine decarboxylase complex.lipoamide-containing component H-protein'	xvis03_220076-pa	lipoamide-containing component H-protein of glycine cleavage system (original description: augustus-gene-4.88-mRNA-1 protein Name:Similar to GDCSH Glycine cleavage system H protein, mitochondrial (Oryza sativa subsp. japonica) AED:0.04 eAED:0.04 QI:127|1|1|1|1|4|484|165)'
Cellular respiration.glycolysis.cytosolic glycolysis. Phosphoglycerate kinase'	xvis03_201416-pa	phosphoglycerate kinase (original description: processed-gene-12.20-mRNA-1 protein Name:Similar to Phosphoglycerate kinase, chloroplastic (Nicotiana tabacum) AED:0.04 eAED:0.04

		QI:190|1|1|1|1|6|289|477)' 0.4267875
Cellular respiration.glycolysis.methylglyoxal degradation. Hydroxy-acyl-glutathione hydrolase (GLX2)'	xvis03_211424-pa	hydroxy-acyl-glutathione hydrolase (GLX2) (original description: augustus-gene-2.30-mRNA-1 protein Name:Similar to GLX2-2 Hydroxyacylglutathione hydrolase cytoplasmic (Arabidopsis thaliana) AED:0.23 eAED:0.23 QI:367|1|1|1|1|0.83|6|257|190)' 1.663941
protein modification.phosphorylation CAMK protein kinase superfamily.SNF1-related protein kinase (SnRK2)'	xvis03_216515-pa	SNF1-related protein kinase (SnRK2) (original description: augustus-gene-8.70-mRNA-1 protein Name:Similar to SAPK7 Serine/threonine-protein kinase SAPK7 (Oryza sativa subsp. japonica) AED:0.12 eAED:0.12 QI:115|0.83|1|1|1|1|7|226|305)' 1.8659521
protein modification.S-glutathionylation.glutaredoxin'	xvis03_218158-pa	glutaredoxin (original description: augustus-gene-3.24-mRNA-1 protein Name:Similar to Glutaredoxin (Ricinus communis) AED:0.01 eAED:0.01 QI:220|1|1|1|1|4|501|106)' 1.1671811
protein modification.protein folding.protein folding catalyst (Cyclophilin)'	xvis03_206458-pa	protein folding catalyst (original description: processed-gene-30.78-mRNA-1 protein Name:Similar to PCKR1 Peptidyl-prolyl cis-trans isomerase (Catharanthus roseus) AED:0.01 eAED:0.01 QI:0|-1|0|1|-1|1|1|0|173)' 0.88642055
protein modification.protein folding.protein folding catalyst (Cyclophilin)'	xvis03_223454-pa	protein folding catalyst (original description: processed-gene-3.78-mRNA-1 protein Name:Similar to PCKR1 Peptidyl-prolyl cis-trans isomerase (Catharanthus roseus) AED:0.02 eAED:0.02 QI:0|-1|0|1|-1|1|1|0|173)' 1.266422
protein translocation.chloroplast.outer envelope insertion system.chaperone (AKR2)	xvis03_217196-pa	chaperone (AKR2) (original description: augustus-gene-1.26-mRNA-1 protein Name:Similar to AKR2

		Ankyrin repeat domain-containing protein 2 (Arabidopsis thaliana) AED:0.11 eAED:0.11 QI:0|0|0|1|1|1|6|0|276)' 1.775295
protein translocation.nucleus.nucleocytoplasmic transport.importin alpha adaptor proteins'	xvis03_215434-pa	importin alpha adaptor proteins (original description: augustus-gene-6.51-mRNA-1 protein Name:Similar to Os01g0253300 Importin subunit alpha-1a (Oryza sativa subsp. japonica) AED:0.21 eAED:0.21 QI:191|0.81|0.75|1|1|1|12|0|614)' 2.079471
protein translocation.nucleus.nucleocytoplasmic transport.GTpase activation accessory protein (RanBp1)	xvis03_204022-pa	GTPase activation accessory protein (RanBP1) (original description: processed-gene-29.69-mRNA-1 protein Name:Similar to RANBP1C Ran-binding protein 1 homolog c (Arabidopsis thaliana) AED:0.01 eAED:0.01 QI:85|1|1|1|1|1|4|338|224)' 1.8266815
RNA processing.RNA chaperone activities.RNA chaperone (CSp)'	xvis03_206453-pa	RNA chaperone (CSP) (original description: processed-gene-29.128-mRNA-1 protein Name:Similar to CSP4 Cold shock domain-containing protein 4 (Arabidopsis thaliana) AED:0.32 eAED:0.32 QI:0|-1|0|1|-1|1|1|0|231)' 1.2821975
RNA processing.RNA chaperone activities.RNA chaperone (CSp)'	xvis03_223451-pa	RNA chaperone (CSP) (original description: processed-gene-3.71-mRNA-1 protein Name:Similar to CSP1 Cold shock protein 1 (Arabidopsis thaliana) AED:0.30 eAED:0.30 QI:0|-1|0|1|-1|1|1|0|215)' 2.1634965
RNA processing.RNA chaperone activities.RNA chaperone (RZ1|GR-RBp)'	xvis03_215153-pa	RNA chaperone (RZ1|GR-RBP) (original description: augustus-gene-12.40-mRNA-1 protein Name:Similar to RZ1B Glycine-rich RNA-binding protein RZ1B (Arabidopsis thaliana) AED:0.25 eAED:0.25

		QI:0|1|1|1|0.5|0.33|3|1599|326)' 1.83855
RNA processing.organelle machinery.RNA editing.RNA editing factor (MORF-type)'	xvis03_221754-pa	RNA editing factor (MORF) (original description: augustus-gene-1.62-mRNA-1 protein Name:Similar to MORF1 Multiple organellar RNA editing factor 1, mitochondrial (Arabidopsis thaliana) AED:0.23 eAED:0.23 QI:47|1|1|1|0.75|0.6|5|384|406)' 1.7289507
External stimuli response. temperature. Heat response.organellar chaperone (Clp-p|Clp-m)'	xvis03_207210-pa	organellar chaperone (Clp-p|Clp-m) (original description: augustus-gene-28.48-mRNA-1 protein Name:Similar to CLPB3 Chaperone protein ClpB3, mitochondrial (Oryza sativa subsp. japonica) AED:0.12 eAED:0.12 QI:139|1|1|1|1|10|182|968)' 1.7187872
External stimuli response.temperature.cold response.mRNA chaperone (CSD)'	xvis03_206453-pa	mRNA chaperone (CSD) (original description: processed-gene-29.128-mRNA-1 protein Name:Similar to CSP4 Cold shock domain-containing protein 4 (Arabidopsis thaliana) AED:0.32 eAED:0.32 QI:0|-1|0|1|-1|1|0|231)' 1.2821975
External stimuli response.temperature.cold response.mRNA chaperone (CSD)'	xvis03_223451-pa	mRNA chaperone (CSD) (original description: processed-gene-3.71-mRNA-1 protein Name:Similar to CSP1 Cold shock protein 1 (Arabidopsis thaliana) AED:0.30 eAED:0.30 QI:0|-1|0|1|-1|1|1|0|215)' 2.1634965
Lipid metabolism.glycerolipid biosynthesis.phosphatidylcholine.CTp:phosphorylcholine cytidylyltransferase'	xvis03_202655-pa	CTP:phosphorylcholine cytidylyltransferase (original description: processed-gene-53.13-mRNA-1 protein Name:Similar to CCT2 Choline-phosphate cytidylyltransferase 2 (Arabidopsis thaliana) AED:0.15 eAED:0.15 QI:50|1|1|1|1|1|8|392|291)' 2.4340105

Lipid metabolism.lipid degradation.phospholipase activities.phospholipase A2 activities.phospholipase A2 (ppLA2-II)'	xvis03_218200-pa	phospholipase A2 (pPLA2-II) (original description: augustus-gene-6.42-mRNA-1 protein Name:Similar to PLP1 Patatin-like protein 1 (Oryza sativa subsp. japonica) AED:0.26 eAED:0.26 QI:72|0.4|0.16|1|1|1|6|0|314)' 1.306471
Lipid metabolism.lipid degradation.fatty acid degradation.core beta-oxidation.3-ketoacyl-CoA thiolase (KAT)'	xvis03_216330-pa	3-ketoacyl-CoA thiolase (KAT) (original description: processed-gene-6.102-mRNA-1 protein Name:Similar to PED1 3-ketoacyl-CoA thiolase 2, peroxisomal (Arabidopsis thaliana) AED:0.14 eAED:0.14 QI:702|0.85|0.93|0.93|1|1|15|1904|479)' 2.3141983
Lipid metabolism.lipid bodies-associated activities.caleosin lipid body surface protein (CLO/pXG)'	xvis03_221236-pa	caleosin (original description: augustus-gene-4.54-mRNA-1 protein Name:Similar to PXG Peroxygenase (Oryza sativa subsp. japonica) AED:0.38 eAED:0.38 QI:85|0.66|0.85|0.85|1|1|7|299|316)' 1.63025

Table S3.7: List of the Bin names, id and description of the downregulated proteins at LRD

BinName	id	Description
photosynthesis.photophosphorylation.photosystem II.LHC-II complex.component LHCb1/2/3'	xvis03_219722-pa	component LHCb1/2/3 of LHC-II complex (original description: augustus-gene-9.73-mRNA-1 protein Name:Similar to CAB36 Chlorophyll a-b binding protein 36, chloroplastic (Nicotiana tabacum) AED:0.36 eAED:0.36 QI:240|1|1|1|1|2|393|264)'
photosynthesis.photophosphorylation.photosystem II.LHC-II complex.component LHCb1/2/3'	xvis03_223077-pa	component LHCb1/2/3 of LHC-II complex (original description: processed-gene-1.89-mRNA-1 protein Name:Similar to CAB13 Chlorophyll a-b binding protein 13, chloroplastic (Solanum lycopersicum) AED:0.07 eAED:0.07 QI:182|1|1|1|1|4|188|263)'
photosynthesis.photophosphorylation.photosystem II.LHC-II complex.component LHCb1/2/3'	xvis03_224654-pa	component LHCb1/2/3 of LHC-II complex (original description: processed-gene-1.9-mRNA-1 protein Name:Similar to CAB21 Chlorophyll a-b binding protein 21, chloroplastic (Nicotiana tabacum) AED:0.11 eAED:0.11 QI:0|0|0|0.5|1|1|2|0|328)'

photosynthesis.photophosphorylation.photosystem II.LHC-II complex.component LHCb4'	xvis03_212711-pa	component LHCb4 of LHC-II complex (original description: processed-gene-16.130-mRNA-1 protein Name:Similar to LHCB4.2 Chlorophyll a-b binding protein CP29.2, chloroplastic (Arabidopsis thaliana) AED:0.05 eAED:0.05 QI:1875|1|1|1|0.5|0.33|3|204|289)'
photosynthesis.photophosphorylation.photosystem II.LHC-II complex.component LHCb5'	xvis03_202336-pa	component LHCb5 of LHC-II complex (original description: augustus-gene-27.98-mRNA-1 protein Name:Similar to LHCB5 Chlorophyll a-b binding protein CP26, chloroplastic (Arabidopsis thaliana) AED:0.08 eAED:0.08 QI:26|1|1|1|1|1|6|330|363)'
photosynthesis.photophosphorylation.photosystem II.LHC-II complex.component LHCb6'	xvis03_217301-pa	component LHCb6 of LHC-II complex (original description: augustus-gene-11.85-mRNA-1 protein Name:Similar to CAP10A Chlorophyll a-b binding protein CP24 10A, chloroplastic (Solanum lycopersicum) AED:0.00 eAED:0.00 QI:77|1|1|1|1|1|2|315|254)'
photosynthesis.photophosphorylation.photosystem II.pS-II complex.oxygen-evolving center (OEC) extrinsic proteins.component OEC33/psbO'	xvis03_219859-pa	component PsbO/OEC33 of PS-II oxygen-evolving center (original description: augustus-gene-3.73-mRNA-1 protein Name:Similar to PSBO Oxygen-evolving enhancer protein 1, chloroplastic (Solanum lycopersicum) AED:0.03 eAED:0.03 QI:216|1|1|1|1|1|2|224|332)'
photosynthesis.photophosphorylation.photosystem I.LHC-I complex.component LHCa1'	xvis03_225147-pa	component LHCa1 of LHC-I complex (original description: augustus-gene-0.41-mRNA-1 protein Name:Similar to CAB6A Chlorophyll a-b binding protein 6A, chloroplastic (Solanum lycopersicum) AED:0.00 eAED:0.00 QI:106|1|1|1|1|1|3|75|204)'
photosynthesis.photophosphorylation.photosystem I.LHC-I complex.component LHCa1'	xvis03_225829-pa	component LHCa1 of LHC-I complex (original description: augustus-gene-0.17-mRNA-1 protein Name:Similar to LHCA1 Chlorophyll a-b binding protein 6, chloroplastic (Arabidopsis thaliana) AED:0.45 eAED:0.45 QI:0|0.44|0.4|0.5|1|1|10|334|459)'
photosynthesis.photophosphorylation.photosystem I.LHC-I complex.component LHCa2'	xvis03_205558-pa	component LHCa2 of LHC-I complex (original description: augustus-gene-14.7-mRNA-1 protein Name:Similar to CAB7 Chlorophyll a-b binding protein 7, chloroplastic (Solanum lycopersicum) AED:0.16 eAED:0.16 QI:0|0.25|0.4|1|0.75|0.8|5|892|278)'
photosynthesis.photophosphorylation.photosystem I.pS-I complex.component psaD'	xvis03_207379-pa	component PsaD of PS-I complex (original description: processed-gene-13.65-mRNA-1 protein Name:Similar to

		psaD Photosystem I reaction center subunit II, chloroplastic (Cucumis sativus) AED:0.32 eAED:0.32 QI:0|-1|0|1|-1|1|1|0|274)'
photosynthesis.photophosphorylation.photosystem I.pS-I complex.component psaF'	xvis03_216014-pa	component PsaF of PS-I complex (original description: processed-gene-5.37-mRNA-1 protein Name:Similar to PSAF Photosystem I reaction center subunit III, chloroplastic (Arabidopsis thaliana) AED:0.24 eAED:0.24 QI:0|-1|0|1|-1|1|1|0|232)'
photosynthesis.photophosphorylation.photosystem I.pS-I complex.component psaH'	xvis03_205319-pa	component PsaH of PS-I complex (original description: processed-gene-30.54-mRNA-1 protein Name:Similar to PSAH1 Photosystem I reaction center subunit VI-1, chloroplastic (Arabidopsis thaliana) AED:0.09 eAED:0.09 QI:15|1|1|1|1|1|3|336|145)'
photosynthesis.photophosphorylation.photosystem I.pS-I complex.component psaL'	xvis03_200779-pa	component PsaL of PS-I complex (original description: processed-gene-89.11-mRNA-1 protein Name:Similar to PSAL Photosystem I reaction center subunit XI, chloroplastic (Spinacia oleracea) AED:0.06 eAED:0.06 QI:217|1|1|1|1|1|2|190|220)'
photosynthesis.calvin cycle.transketolase'	xvis03_207774-pa	transketolase (original description: processed-gene-21.50-mRNA-1 protein Name:Similar to Transketolase, chloroplastic (Solanum tuberosum) AED:0.17 eAED:0.17 QI:154|0.85|0.75|1|1|1|8|0|716)'
photosynthesis.calvin cycle.transketolase'	xvis03_219001-pa	transketolase (original description: processed-gene-2.79-mRNA-1 protein Name:Similar to Transketolase, chloroplastic (Solanum tuberosum) AED:0.04 eAED:0.04 QI:238|1|1|1|1|1|7|473|742)'
Carbohydrate metabolism.starch metabolism.biosynthesis.ADp-glucose pyrophosphorylase'	xvis03_220998-pa	ADP-glucose pyrophosphorylase (original description: augustus-gene-7.121-mRNA-1 protein Name:Similar to ADG2 Glucose-1-phosphate adenylyltransferase large subunit 1, chloroplastic (Arabidopsis thaliana) AED:0.11 eAED:0.11 QI:196|0.92|0.86|1|0.85|0.86|15|136|540)'
Carbohydrate metabolism.starch metabolism.biosynthesis.starch synthase activities.granule-bound starch (amylose) synthase	xvis03_225238-pa	granule-bound starch (amylose) synthase (original description: augustus-gene-0.18-mRNA-1 protein Name:Similar to WAXY Granule-bound starch synthase 1, chloroplastic/amyloplastic (Antirrhinum majus) AED:0.11 eAED:0.11 QI:73|1|1|1|0.92|0.85|14|142|611)'

Carbohydrate metabolism.oxidative pentose phosphate pathway.non-oxidative phase.transketolase'	xvis03_207774-pa	transketolase (original description: processed-gene-21.50-mRNA-1 protein Name:Similar to Transketolase, chloroplastic (Solanum tuberosum) AED:0.17 eAED:0.17 QI:154|0.85|0.75|1|1|1|8|0|716)'
Carbohydrate metabolism.oxidative pentose phosphate pathway.non-oxidative phase.transketolase'	xvis03_219001-pa	transketolase (original description: processed-gene-2.79-mRNA-1 protein Name:Similar to Transketolase, chloroplastic (Solanum tuberosum) AED:0.04 eAED:0.04 QI:238|1|1|1|1|1|7|473|742)'
Carbohydrate metabolism.gluconeogenesis.pyruvate orthophosphate dikinase activity.pyruvate orthophosphate dikinase'	xvis03_201017-pa	pyruvate orthophosphate dikinase (original description: processed-gene-109.26-mRNA-1 protein Name:Similar to PPD Pyruvate, phosphate dikinase, chloroplastic (Mesembryanthemum crystallinum) AED:0.09 eAED:0.09 QI:8|1|1|1|0.89|0.9|20|257|985)'
Carbohydrate metabolism.nucleotide sugar biosynthesis.UDp-L-arabinose biosynthesis.UDp-L-arabinose mutase'	xvis03_224372-pa	UDP-L-arabinose mutase (original description: processed-gene-2.16-mRNA-1 protein Name:Similar to UAM1 UDP-arabinopyranose mutase 1 (Oryza sativa subsp. japonica) AED:0.08 eAED:0.08 QI:87|1|1|1|1|1|4|347|359)'
protein homeostasis.ubiquitin-proteasome system.26S proteasome.20S core particle.beta-type components.component beta type-5'	xvis03_211689-pa	component beta type-5 of 26S proteasome (original description: processed-gene-6.93-mRNA-1 protein Name:Similar to Proteasome subunit beta type-5 (Spinacia oleracea) AED:0.07 eAED:0.07 QI:0|1|0.87|1|1|1|8|489|310)'
protein homeostasis.proteolysis.cysteine-type peptidase activities.C13-class asparaginyl endopeptidase (Legumain)'	xvis03_211268-pa	asparaginyl endopeptidase (Legumain) (original description: processed-gene-9.25-mRNA-1 protein Name:Similar to Vacuolar-processing enzyme (Citrus sinensis) AED:0.07 eAED:0.07 QI:3|1|1|1|1|1|9|417|590)'
protein homeostasis.proteolysis.serine-type peptidase activities.S28-class serine carboxypeptidase'	xvis03_222506-pa	S28-class serine carboxypeptidase (original description: augustus-gene-4.97-mRNA-1 protein Name:Similar to EDA2 Probable serine protease EDA2 (Arabidopsis thaliana) AED:0.31 eAED:0.31 QI:159|0.92|0.92|1|1|1|14|279|488)'
protein homeostasis.proteolysis.metallopeptidase activities.aminopeptidase activities.M1-class neutral/aromatic-hydroxyl amino acid aminopeptidase'	xvis03_210782-pa	M1 neutral/aromatic-hydroxyl amino acid aminopeptidase (original description: augustus-gene-7.64-mRNA-1 protein Name:Similar to Os08g0562700 Puromycin-sensitive aminopeptidase (Oryza sativa subsp. japonica) AED:0.20 eAED:0.20 QI:160|0.75|0.81|0.90|0.84|0.84|33|284|1052)'

Redox homeostasis.hydrogen peroxide removal.ascorbate-glutathione cycle.ascorbate peroxidase (ApX)'	xvis03_214214-pa	ascorbate peroxidase (APX) (original description: processed-gene-11.33-mRNA-1 protein Name:Similar to APX1 L-ascorbate peroxidase, cytosolic (Pisum sativum) AED:0.17 eAED:0.17 QI:131|1|1|1|1|1|7|558|249)'
Redox homeostasis.hydrogen peroxide removal.ascorbate-glutathione cycle.monodehydroascorbate reductase (MDAR)'	xvis03_204322-pa	monodehydroascorbate reductase (MDAR) (original description: processed-gene-9.15-mRNA-1 protein Name:Similar to AFRR Monodehydroascorbate reductase (Solanum lycopersicum) AED:0.13 eAED:0.13 QI:138|0.72|0.83|0.83|1|1|12|368|489)'
Redox homeostasis.hydrogen peroxide removal.ascorbate-glutathione cycle.glutathione reductase (GR)'	xvis03_205102-pa	glutathione reductase (GR) (original description: processed-gene-9.15-mRNA-1 protein Name:Similar to GOR Glutathione reductase, chloroplastic (Fragment) (Nicotiana tabacum) AED:0.14 eAED:0.14 QI:0|1|0.90|1|0.9|0.81|11|639|590)'
Cell wall organisation.pectin.homogalacturonan.modification and degradation.pectin methylesterase'	xvis03_217074-pa	pectin methylesterase (original description: processed-gene-2.49-mRNA-1 protein Name:Similar to PME35 Probable pectinesterase/pectinesterase inhibitor 35 (Arabidopsis thaliana) AED:0.36 eAED:0.36 QI:662|1|1|1|1|1|3|218|442)'
Cell wall organisation.pectin.rhamnogalacturonan I.modification and degradation.beta-galactosidase (BGAL)'	xvis03_221434-pa	beta-galactosidase (BGAL) (original description: processed-gene-2.106-mRNA-1 protein Name:Similar to Beta-galactosidase (Asparagus officinalis) AED:0.13 eAED:0.13 QI:277|1|1|1|1|1|19|418|832)'
Coenzyme metabolism.thiamine pyrophosphate biosynthesis.thiazole biosynthesis.biosynthetic protein (Thi4)'	xvis03_212280-pa	biosynthetic protein (Thi4) (original description: processed-gene-6.79-mRNA-1 protein Name:Similar to THI1-2 Thiamine thiazole synthase 2, chloroplastic (Vitis vinifera) AED:0.02 eAED:0.02 QI:212|1|1|1|1|1|2|483|354)'
Coenzyme metabolism.tetrapyrrol biosynthesis.chlorophyll metabolism.chlorophyll(ide) interconversions.geranylgeranyl reductase (Chlp)'	xvis03_215774-pa	geranylgeranyl reductase (ChlP) (original description: augustus-gene-7.23-mRNA-1 protein Name:Similar to CHLP Geranylgeranyl diphosphate reductase, chloroplastic (Nicotiana tabacum) AED:0.00 eAED:0.00 QI:382|1|1|1|1|1|2|212|364)'
protein biosynthesis.aminoacyl-tRNA synthetase activities.alanine-tRNA ligase'	xvis03_224672-pa	alanine-tRNA ligase (original description: processed-gene-1.89-mRNA-1 protein Name:Similar to ALATS Alanine--tRNA ligase (Arabidopsis thaliana) AED:0.10 eAED:0.10 QI:33|1|1|1|0.90|0.90|22|389|993)'

protein biosynthesis.aminoacyl-tRNA synthetase activities.aspartate-tRNA ligase'	xvis03_205724-pa	aspartate-tRNA ligase (original description: processed-gene-33.32-mRNA-1 protein Name:Similar to IBI1 Aspartate--tRNA ligase 2, cytoplasmic (Arabidopsis thaliana) AED:0.10 eAED:0.10 QI:60|0.77|0.8|1|1|1|10|190|552)'

KEGG pathways

To further identify the *X. schlechteri* proteins and enzymes involved in biological pathways that are active in response to dehydration stress, our proteomic data was analysed using KEGG-Kyoto Encyclopaedia of Genes and Genomes (Kanehisa and Goto, 2000). A total of 3125 protein sequences were mapped to KEGG pathways and a total of 47 maps were identified (Supplementary Table S3.8). Only pathways with large numbers of proteins mapped to pathways were analysed further. Several biological pathways were shown to contain proteins from the *X. schlechteri* dataset (Figure S3.7). The data obtained from the KEGG pathway analysis was also supplemented by the Blast2GO and MapMan results.

Table S3.8: List of pathways, enzymes and corresponding *X. schlechteri* sequences across the drying stages.

Pathway	#Enzs in Pathway	Enzyme	Sequences
Biosynthesis of antibiotics	6	ec:2.5.1.47 - synthase, ec:4.3.1.17 - L-serine ammonia-lyase, ec:4.2.1.3 - hydratase, ec:2.7.1.1 - hexokinase type IV glucokinase, ec:4.2.1.46 - 4,6-dehydratase, ec:3.1.3.3 - phosphatase	Xvis03_208884-PA, Xvis03_216310-PA, Xvis03_202628-PA, Xvis03_212683-PA, Xvis03_210031-PA, Xvis03_208169-PA
Glycine, serine and threonine metabolism	5	ec:5.1.1.10 - racemase, ec:4.3.1.17 - ammonia-lyase, ec:4.3.1.18 - ammonia-lyase, ec:5.1.1.18 - racemase, ec:3.1.3.3 – phosphatase	Xvis03_216310-PA, Xvis03_216310-PA, Xvis03_216310-PA, Xvis03_216310-PA, Xvis03_208169-PA
Purine metabolism	3	ec:3.6.1.3 - adenylpyrophosphatase, ec:3.6.1.15 - phosphatase, ec:2.7.1.20 - kinase	Xvis03_202101-PA, Xvis03_205065-PA, Xvis03_210207-PA, Xvis03_211869-PA, Xvis03_202101-PA, Xvis03_205065-PA, Xvis03_210207-PA,

			Xvis03_211869-PA, Xvis03_210868-PA
Galactose metabolism	3	ec:2.4.1.67 - galactosyltransferase, ec:2.7.1.1 - hexokinase type IV glucokinase, ec:2.4.1.82 - galactosyltransferase	Xvis03_202536-PA, Xvis03_212683-PA, Xvis03_210699-PA
Amino sugar and nucleotide sugar metabolism	3	ec:2.7.1.1 - hexokinase type IV glucokinase, ec:4.1.1.35 - decarboxylase, ec:2.7.1.4 - fructokinase (phosphorylating)	Xvis03_212683-PA, Xvis03_203867-PA, Xvis03_212683-PA
Cysteine and methionine metabolism	3	ec:5.1.1.10 - racemase, ec:2.5.1.47 - synthase, ec:4.3.1.17 - ammonia-lyase	Xvis03_216310-PA, Xvis03_208884-PA, Xvis03_216310-PA
Riboflavin metabolism	2	ec:3.1.3.2 - phosphatase, ec:2.5.1.9 - synthase	Xvis03_204013-PA, Xvis03_203270-PA
Thiamine metabolism	2	ec:3.6.1.15 - phosphatase, ec:3.1.3.2 - phosphatase	Xvis03_202101-PA, Xvis03_205065-PA, Xvis03_210207-PA, Xvis03_211869-PA, Xvis03_204013-PA
Starch and sucrose metabolism	2	ec:2.7.1.1 - hexokinase type IV glucokinase, ec:2.7.1.4 - fructokinase (phosphorylating)	Xvis03_212683-PA, Xvis03_212683-PA
Streptomycin biosynthesis	2	ec:2.7.1.1 - hexokinase type IV glucokinase, ec:4.2.1.46 - 4,6-dehydratase	Xvis03_212683-PA, Xvis03_210031-PA
Porphyrin and chlorophyll metabolism	2	ec:1.1.1.294 - b reductase, ec:6.6.1.1 - chelatase	Xvis03_208904-PA, Xvis03_204983-PA
Fructose and mannose metabolism	2	ec:2.7.1.1 - hexokinase type IV glucokinase, ec:2.7.1.4 - fructokinase (phosphorylating)	Xvis03_212683-PA, Xvis03_212683-PA
D-Arginine and D-ornithine metabolism	1	ec:5.1.1.10 - racemase	Xvis03_216310-PA
Glyoxylate and dicarboxylate metabolism	1	ec:4.2.1.3 - hydratase	Xvis03_202628-PA
Glycolysis / Gluconeogenesis	1	ec:2.7.1.1 - hexokinase type IV glucokinase	Xvis03_212683-PA
Tryptophan metabolism	1	ec:2.3.1.87 - N-acetyltransferase	Xvis03_217143-PA
Lysine degradation	1	ec:2.3.1.32 - N-acetyltransferase	Xvis03_217143-PA
Sulfur metabolism	1	ec:2.5.1.47 - synthase	Xvis03_208884-PA

Caffeine metabolism	1	ec:2.3.1.5 - N-acetyltransferase	Xvis03_217143-PA
Neomycin, kanamycin and gentamicin biosynthesis	1	ec:2.7.1.1 - hexokinase type IV glucokinase	Xvis03_212683-PA
Glycosylphosphatidylinositol (GPI)-anchor biosynthesis	1	ec:2.4.1.198 - N-acetylglucosaminyltransferase	Xvis03_200985-PA
Glycerolipid metabolism	1	ec:3.1.3.4 - phosphatase	Xvis03_203349-PA
Fatty acid elongation	1	ec:1.1.1.330 - 3-oxoacyl-CoA reductase	Xvis03_202071-PA
Nitrotoluene degradation	1	ec:2.3.1.5 - N-acetyltransferase	Xvis03_217143-PA
Methane metabolism	1	ec:3.1.3.3 - phosphatase	Xvis03_208169-PA
Ether lipid metabolism	1	ec:3.1.3.4 - phosphatase	Xvis03_203349-PA
Biosynthesis of unsaturated fatty acids	1	ec:1.1.1.330 - 3-oxoacyl-CoA reductase	Xvis03_202071-PA
One carbon pool by folate	1	ec:6.3.3.2 - cyclo-ligase	Xvis03_201379-PA
Phenylalanine metabolism	1	ec:5.3.2.1 - tautomerase	Xvis03_205857-PA
Sphingolipid metabolism	1	ec:3.1.3.4 - phosphatase	Xvis03_203349-PA
Tyrosine metabolism	1	ec:5.3.2.1 - tautomerase	Xvis03_205857-PA
D-Glutamine and D-glutamate metabolism	1	ec:5.1.1.10 - racemase	Xvis03_216310-PA
Oxidative phosphorylation	1	ec:1.6.99.3 - dehydrogenase	Xvis03_200831-PA
Biosynthesis of vancomycin group antibiotics	1	ec:4.2.1.46 - 4,6-dehydratase	Xvis03_210031-PA
Glycerophospholipid metabolism	1	ec:3.1.3.4 - phosphatase	Xvis03_203349-PA
Inositol phosphate metabolism	1	ec:3.1.3.62 - inositol-polyphosphate phosphatase	Xvis03_210451-PA
Polyketide sugar unit biosynthesis	1	ec:4.2.1.46 - 4,6-dehydratase	Xvis03_210031-PA
Carbon fixation pathways in prokaryotes	1	ec:4.2.1.3 - hydratase	Xvis03_202628-PA
Drug metabolism - other enzymes	1	ec:2.3.1.5 - N-acetyltransferase	Xvis03_217143-PA
Citrate cycle (TCA cycle)	1	ec:4.2.1.3 - hydratase	Xvis03_202628-PA

Acarbose and validamycin biosynthesis	1	ec:4.2.1.46 - 4,6-dehydratase	Xvis03_210031-PA

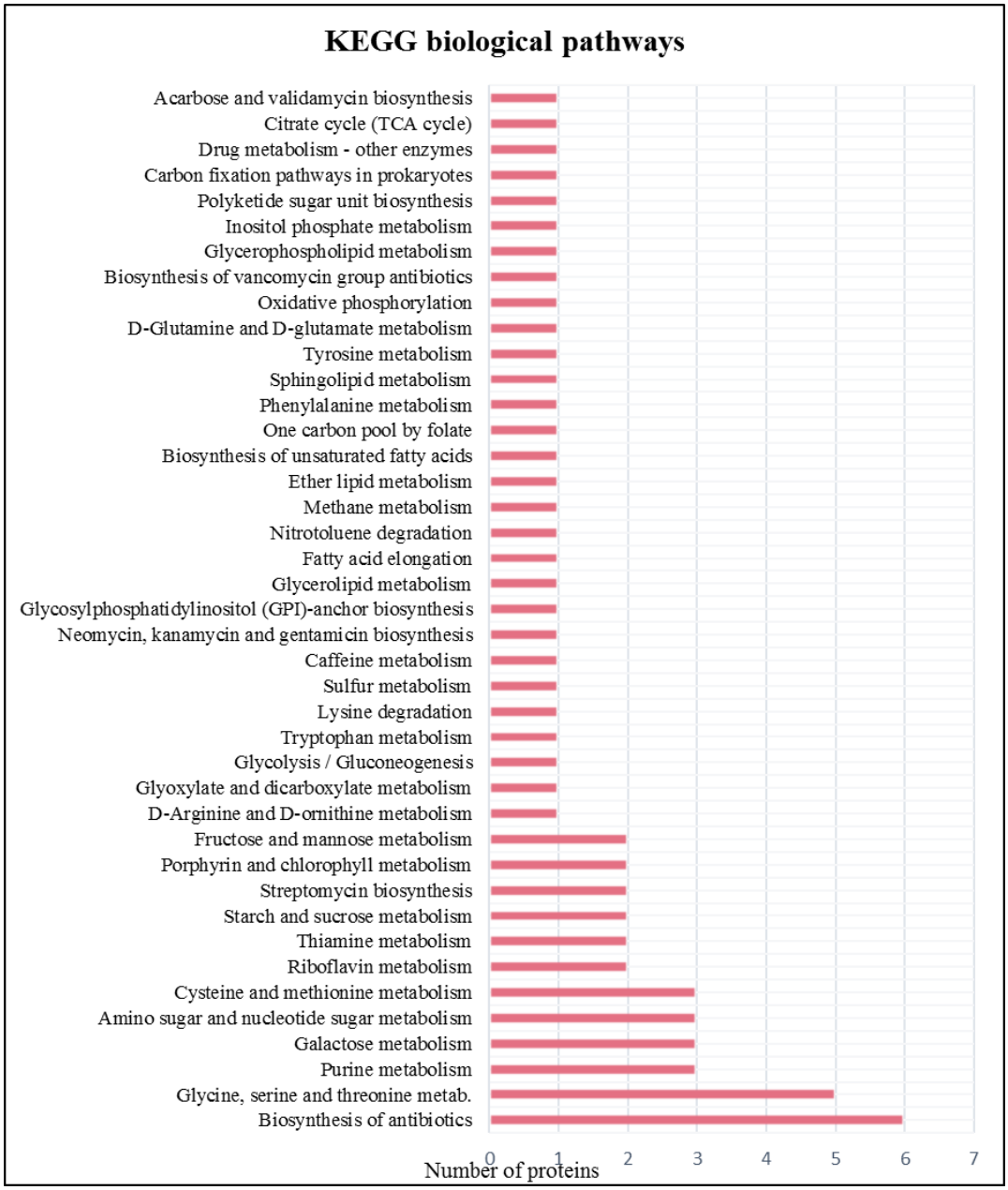

Figure S3.2: Representation of the 42 biological pathways assigned to *X. schlechteri* proteins by KEGG (retrieved by Blast2GO). The X-axis indicates the number of proteins associated with each pathway and the y-axis displays the names of the KEGG pathways.

A general overview of the KEGG data (Figure S 3.7) shows that several pathways were involved in amino acid metabolism, organic compounds and sugar metabolism. The pathways containing the highest number of enzymes were biosynthesis of antibiotics, glycine, serine and threonine metabolism, purine metabolism, galactose metabolism, amino sugar and nucleotide sugar metabolism, cysteine and methionine metabolism, riboflavin metabolism, thiamine metabolism, starch and sucrose metabolism, streptomycin biosynthesis, porphyrin and chlorophyll metabolism and fructose and mannose metabolism. A number of these pathways were found to be involved in sugar regulation such as fructose and mannose metabolism and starch and sucrose metabolism. Apart from sugars, many resurrection plants also accumulate amino acids (Tymms and Gaff, 1978; Gaff and McGregor, 1979; Oliver *et al.,* 2011a), some of which serve as osmoprotectants (Kido *et al.,* 2013). Metabolism of amino acids and nucleotides are also closely related to sugar metabolism (Gaff and McGregor, 1979). Understanding the function of these enzymes and pathways could help elucidate the mechanisms whereby *X. schlechteri* adapts and tolerates desiccation stress. Only pathways with high numbers of proteins and that are known to play a pivotal role in plant stress responses will be briefly discussed below.

Biosynthesis of antibiotics pathway

As plants are restricted to their place of germination, they are highly dependent on their capability to produce chemical signals to protect, promote tolerance and resistance against stressful conditions such as drought and disease respectively. The enzymes (Supplementary Table S3.9 and Figure S3.3) involved in the biosynthesis of antibiotic pathway were synthase (EC:2.5.1.47), ammonia-lyase (EC:4.3.1.17), hydratase (EC:4.2.1.3), hexokinase type IV glucokinase (EC:2.7.1.1), 4,6-dehydratase (EC:4.2.1.46), phosphatase (EC:3.1.3.3). While these enzymes participate in antibiotic formation, but in some instance, they also participate in protection against stresses associated with water loss.

Synthase (EC:2.5.1.47) is a reduced sulfur donor molecule that is involved in the synthesis of defence compounds and essential biomolecules (Romero *et al.,* 2014). It was also reported to play a role in redox signalling which occurs in various cellular compartments (Romero *et al.,* 2014). Hexokinases catalyse the conversion of glucose and to a lesser degree fructose using ATP, resulting in hexose monophosphates (Doehlert, 1989; Schnarrenberger, 1990; Renz and Stitt, 1993). Previous studies suggest that hexokinase is predominantly located in the cytoplasm or the outer envelope of the chloroplast (Baldus *et al.,* 1981; Schnarrenberger, 1990; Wiese *et al.,* 1999). The reactions catalysed by hexokinase are thought to be important during dehydration as there is an increase in hexokinase activity during dehydration where the reaction catalysed by hexokinase is a vital step regulating the entry of hexose sugars for biosynthesis and sucrose storage (Whittaker *et al.,* 2001).

Glycine, serine and threonine metabolism

Glycine, serine and threonine metabolism (Supplementary Table S3.10 and Figure S3.4) are important to protein biosynthesis and participate in the syntheses of several other important metabolites. In this study, the enzymes involved were racemase (EC:5.1.1.10), ammonia-lyase (EC:4.3.1.17), phosphatase (EC:3.1.3.3). Therefore, changes in the regulation of these amino acids could potentially affect overall metabolic processes in plant tissue (Yang *et al*., 2019). Glycine has been reported as an amino acid which promotes the absorption of phosphorous, promotes plant growth and improves plant stress resistance (Wagstaff *et al*., 2002).

Table S3.9: List of enzymes and corresponding *X. schlechteri* sequences involved in the biosynthesis of antibiotics**.** The column with the colour rectangles corresponds to Figure S3.3.

Color	Enzyme	Sequences
	ec:2.5.1.47 - synthase	Xvis03_208884-PA
	ec:4.3.1.17 - ammonia-lyase	Xvis03_216310-PA
	ec:4.2.1.3 - hydratase	Xvis03_202628-PA
	ec:2.7.1.1 - hexokinase type IV glucokinase	Xvis03_212683-PA
	ec:4.2.1.46 - 4,6-dehydratase	Xvis03_210031-PA
	ec:3.1.3.3 - phosphatase	Xvis03_208169-PA

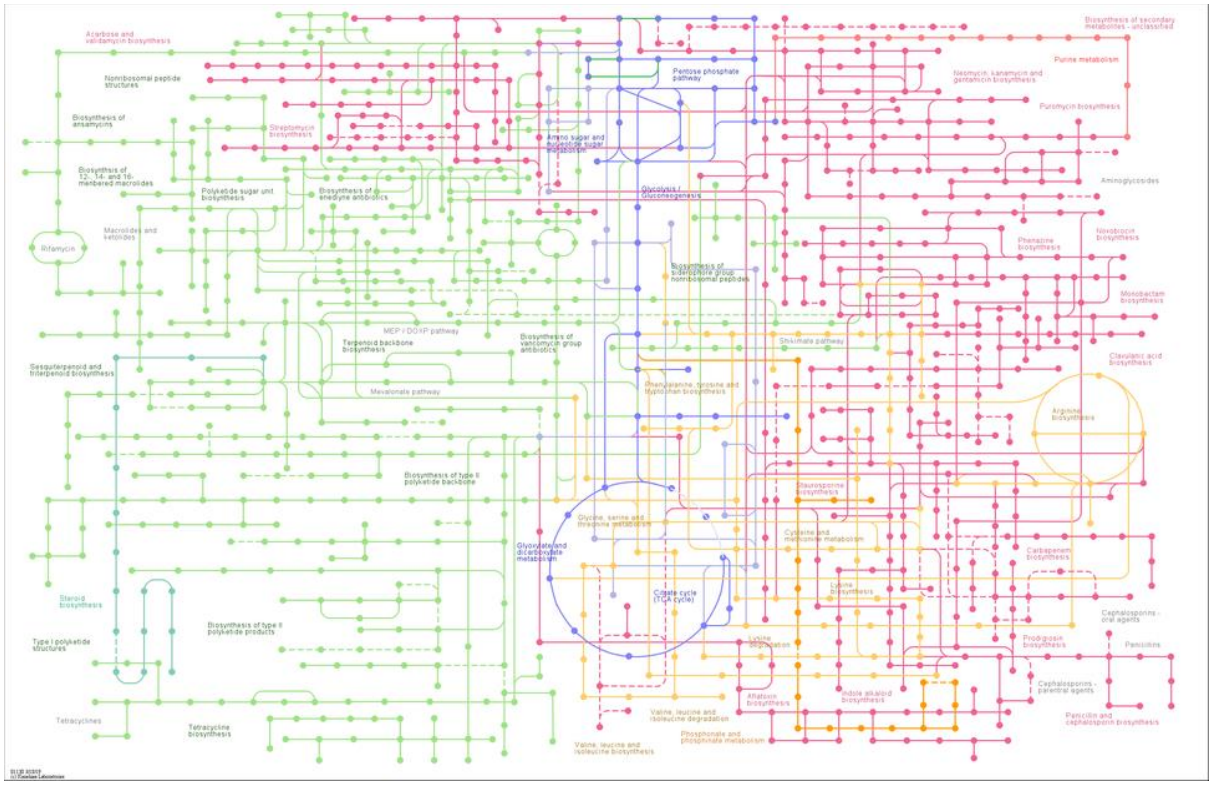

Figure S3.3: Enzymes involved in the biosynthesis of antibiotics of *X. schlechteri.*

Table S3.10: List of enzymes and corresponding *X. schlechteri* sequences involved in the glycine, serine and threonine metabolism The column with the colour rectangles corresponds to Figure S3.4.

Color	Enzyme	Sequences
	ec:5.1.1.10 - racemase	Xvis03_216310-PA
	ec:4.3.1.17 - ammonia-lyase	Xvis03_216310-PA
	ec:4.3.1.18 - ammonia-lyase	Xvis03_216310-PA
	ec:5.1.1.18 - racemase	Xvis03_216310-PA
	ec:3.1.3.3 - phosphatase	Xvis03_208169-PA

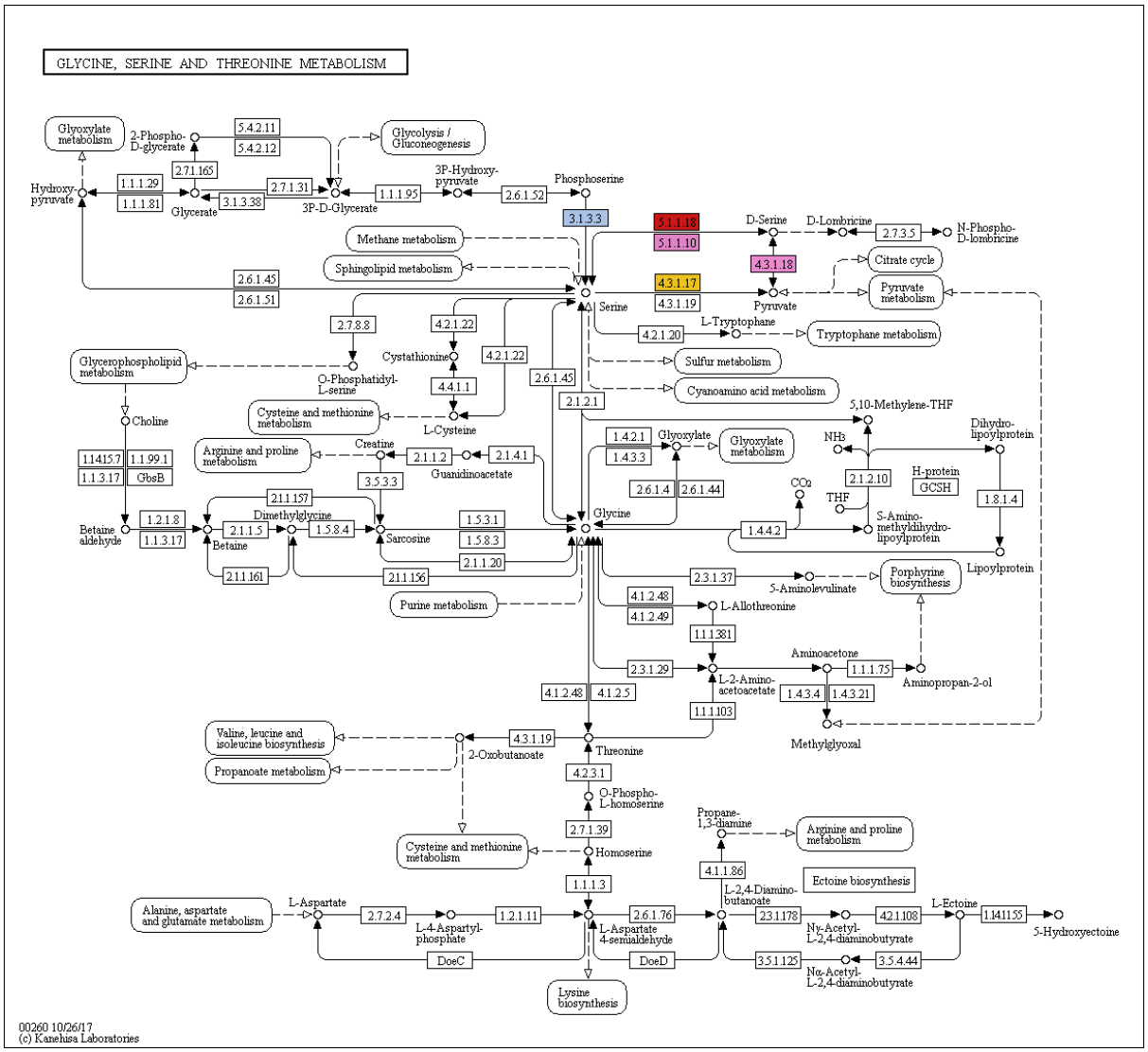

Figure S3.4: Enzymes involved in the glycine, serine and threonine metabolism of *X. schlechteri*.

Supplementary Material-Chapter 4

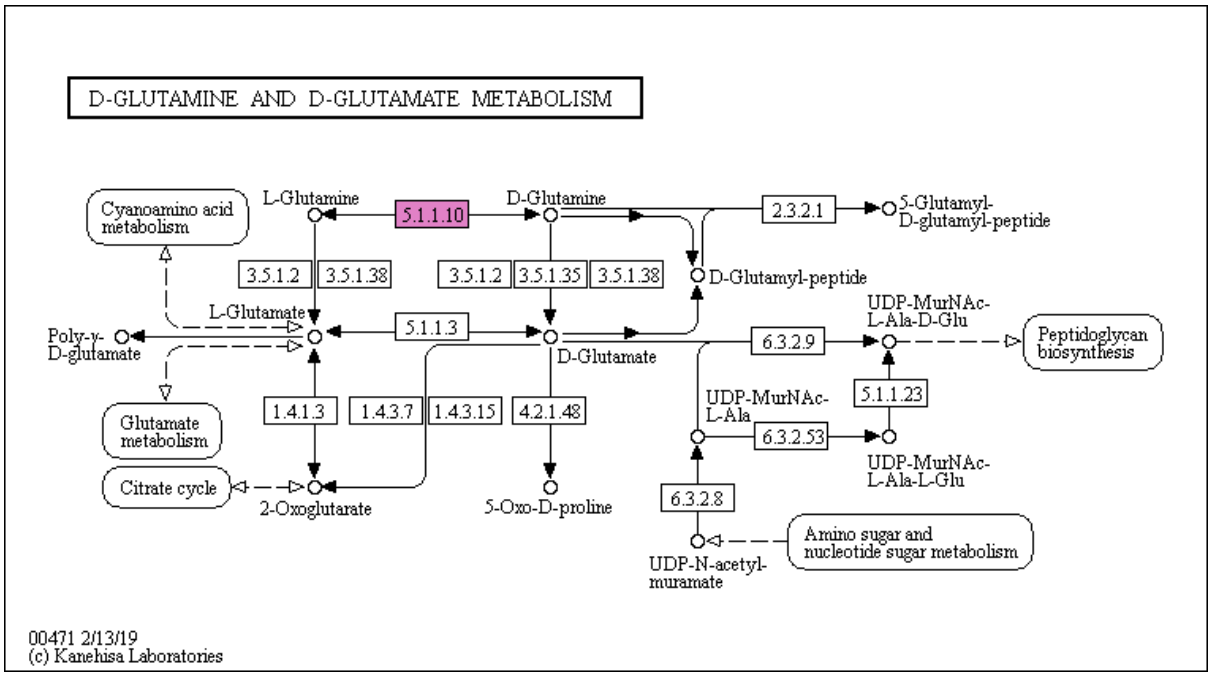

Figure S4.1: Representation of glutamine and glutamate metabolism generated in KEGG

Table S4.2: Overview of the KEGG pathways with high numbers of *X. schlechteri* proteins and that are known to play a role in plant stress responses and the metabolites associated with the pathways.

Proteome and pathways[1]	**Metabolome[2]**
Biosynthesis of antibiotics	Phenylalanine Tyrosine Tryptophan Glucose Sucrose
Glycine, serine and threonine metabolism	Serine Glycine Threonine Aspartic acid
Purine metabolism	Glycine Histidine
Galactose metabolism	Glucose Sorbitol Mannose Myo-inositol Fructose Raffinose
Amino sugar and nucleotide sugar metabolism	Fructose Mannose Glucose
Cysteine and methionine metabolism	Serine Glycine

	Methionine Aspartic acid
Thiamine metabolism	Glycine Tyrosine
Starch and sucrose metabolism	Fructose Sucrose Glucose
Streptomycin biosynthesis	Glucose Myo-inositol
Porphyrin and chlorophyll metabolism	Glycine Threonine
Fructose and mannose metabolism	Glucose Mannitol Sorbitol

[1]Plant stress response pathways identified from the *X. schlechteri* proteomic dataset using KEGG pathway analyses (see Supplementary Chapter 3, Figure S 3.2).
[2]Metabolites that were identified in this study and quantified in *X. schlechteri* across dehydration stages.

References

Abdalla K.O., Baker B., Rafudeen M.S., 2010. Proteomic analysis of nuclear proteins during dehydration of the resurrection plant *Xerophyta viscosa*. Plant Growth Regululation, 1–14.

Abdalla, K.O., Rafudeen, M.S., 2012. Analysis of the nuclear proteome of the resurrection plant *Xerophyta viscosa* in response to dehydration stress using iTRAQ with 2DLC and tandem mass spectrometry. Journal of Proteomics, 75, 2361–2374. https://doi.org/10.1016/j.jprot.2012.02.006.

Agrawal, G.K. and Rakwal, R., 2006. Rice proteomics: A cornerstone for cereal food crop proteomes. Mass Spectrometry Reviews, 25(1):1-53.

Ahrné E, Molzahn L, Glatter T *et al.*, 2013. Critical assessment of proteome-wide label-free absolute abundance estimation strategies. Proteomics 13(17):2567–2578.

Ajithkumar, I.P.; Panneerselvam, R., 2014. ROS scavenging system, osmotic maintenance, pigment and growth status of Panicum sumatrense roth under drought stress. Cell Biochemistry Biophysics, 68, 587–595.

Alaei, Y.; Khabiri, E., 2012. Effects of two biologic fertilizers containing amino acids on leaf chlorophyll index in bread wheat cultivars in greenhouse. Medienwissenschaft: Rezensionen, 2, 1333–1336.

Alamillo, J. M., and Bartels, D., 1996. Light and stage of development in fluence the expression of desiccation-induced genes in the resurrection plant Craterostigma plantagineum. Plant, Cell and Environment, 19, 300–310.doi:10.1111/j.1365- 3040.tb00252.x

Amir, R., 2008. Towards improving methionine content in plants for enhanced biology of heat shock proteins and molecular chaperones. In: The biology of heat shock.

Anjum, S.A.; Xie, X.; Wang, L.; Saleem, M.F.; Man, C.; Lei, W., 2011. Morphological, physiological and biochemical responses of plants to drought stress. African Journal of. Agricultural Research, 6, 2026–2032.

Arbona, V., Manzi, M., Ollas, C., Gómez-Cadenas, A., 2013. Metabolomics as a Tool to Investigate Abiotic Stress Tolerance in Plants. International Journal of Molecular Sciences, 14, 4885–4911. https://doi.org/10.3390/ijms14034885.

Artur, M.A.S., Rienstra, J., Dennis, T.J., Farrant, J.M., Ligterink, W., Hilhorst, H., 2019. Structural Plasticity of Intrinsically Disordered LEA Proteins from *Xerophyta schlechteri* Provides Protection in Vitro and In Vivo. Frontier Plant Sciences, 10, 1272.https://doi.org/10.3389/fpls.2019.01272.

Ashburner, M., Ball, C.A., Blake, J.A., Botstein, D., Butler, H., Cherry, J.M., Davis, A.P., Do-linski, K., Dwight, S.S., Eppig, J.T., Harris, M.A., Hill, D.P., Issel-Tarver, L., Kasarskis, A., Lewis, S., Matese, J.C., Richardson, J.E., Ringwald, M., Rubin, G.M. and Sherlock, G. 2000. Gene ontology: tool for the unification of biology. The Gene Ontology Consortium. Nature Genetics, 25(1):25-29.

Avramova, V., Abd El gawad, H., Zhang, Z., Fotschki, B., Casadevall, R., Vergauwen, L., Knapen, D., Taleisnik, E., Guisez, Y., Asard, H., Beemster, G.T.S., 2015. Drought Induces Distinct Growth Response, Protection, and Recovery Mechanisms in the Maize Leaf Growth Zone. Plant Physiology, 169, 1382–1396.

Baginsky, S. 2009. Plant proteomics: Concepts, applications, and novel strategies for data interpretation. Mass Spectrometry Reviews, 28(1):93-120.

Bailly, C., Benamar, A., Corbineau, F., Come, D., 1996. Changes in malondialdehyde content and in superoxide dismutase, catalase and glutathione reductase activities in sunflower seeds as related to deterioration during accelerated aging. Physiologia Plantarum, 97, 104–110.

Baldus B, Kelly CJ, Latzko E. 1981. Hexokinases of spinach leaves. Phytochemistry, 20, 1181–1814.

Bandurski, R.S., 1979. Chemistry and physiology of myo-inositol esters of indole 3-acetic acid. In: Wells W.W., Eisenberg, F. Jr. Cyclitols and Phosphoinositides. Academic Press, London, New York, 35-54.

Banfi, C., Baetta, R., Gianazza, E., Tremoli, E., 2017. Technological advances and proteomic applications in drug discovery and target deconvolution: identification of the pleiotropic effects of statins. Drug Discovery Today 22, 848–869. https://doi.org/10.1016/j.drudis.2017.03.001.

Barrs, H.D. and Weatherley, P.E. 1962. A Re-Examination of the Relative Turgidity Tech-nique for Estimating Water Deficits in Leaves. Australian Journal of Biological Sciences,15,413-428.https://doi.org/10.1071/BI9620413.

Bartels D., Schneider K., Terstappen G., Piatkowski D., Salamini F., 1990. Molecular cloning of abscisic acid-modulated genes which are induced during desiccation of the resurrection plant *Craterostigma plantagineum*. Planta 181 27–34 10.1007/bf00202321.

Bartels D, Hussain SS., 2011. Resurrection plants: physiology and molecular biology. In: Lüttge U, Beck E, Bartels D, editors. Plant desiccation tolerance. Berlin: Springer; pp. 339–364.

Bartoli C. G., Simontacchi M., Tambussi E., Beltrano J., Montaldi E., Puntarulo S.,1999. Drought and watering-dependent oxidative stress: effect on antioxidant content in Triticum aestivum L. leaves. Journal of Experimental Botany, 50 375–383. 10.1093/jxb/50.332.375.

Beckett M, Loreto F, Velikova V, Brunetti C, Di Ferdinando M, Tattini M, Calfapietra C, Farrant JM 2012. Photosynthetic limitations and volatile and non-volatile isoprenoids in the poikilochlorophyllous resurrection plant *Xerophyta humilis* during dehydration and rehydration. Plant, Cell and Environment, 35: 2061–2074.

Behnke, H.-D., Hummel, E., Hillmer, S., Sauer-Gürth, H., Gonzalez, J., Wink, M., 2013. A revision of African Velloziaceae based on leaf anatomy characters and rbcL nucleotide se-quences: Revision of African Velloziaceae. Botanical Journal of the Linnean Society, 172, 22–94. https://doi.org/10.1111/boj.12018.

Benešová M., Holá D., Fischer L., Jedelský P.L., Hnilička F., Wilhelmová N., Rothová O., Kočová M., Procházková D., Honnerová J., et al., 2012. The physiology and proteomics of drought tolerance in maize: Early stomatal closure as a cause of lower tolerance to short-term dehydration? PLoS ONE. 2012; 7: e38017. doi: 10.1371/journal.pone.0038017.

Benkeblia, N. 2011. Sustainable agriculture and new biotechnologies. CRC Press, Florida, USA.

Berjak P, Farrant JM, Pammenter NW, 2007. Seed desiccation-tolerance mechanisms. In: Jenks MA, Wood AJ, editors. Plant desiccation tolerance. Ames: Blackwell Publishing; pp. 151–192.

Bewley J.D., 1979. Physiological aspects of desiccation-tolerance. Annual Review of Plant Physiology, 30, 195–238.

Bianchi G., Gamba A., Murelli C., Salamini F., Bartels D., 1991. Novel carbohydrate metabolism in the resurrection plant *Craterostigma plantagineum.* Plant Journal, 1 355–359 10.1046/j.1365-313X.1991.t01-11-00999.x

Bieri P, Leibundgut M, Saurer M, Boehringer D, Ban N., 2016. The complete structure of the chloroplast 70S ribosome in complex with translation factor pY. EMBO J. 2017 Feb 15; 36(4):475-486. doi: 10.15252/embj.201695959. Epub 2016 Dec 22. PMID: 28007896; PMCID: PMC5694952.

Blomstedt C. K., Gianello R. D., Hamill J. D., Neale A. D., Gaff D. F., 1998. Drought-stimulated genes correlated with desiccation tolerance of the resurrection grass *Sporobolus stapfianus.* Plant Growth Regulation, 24 153–16110.1023/A: 1005923528109.

Boeckx, T., Winters, A.L., Webb, K.J., Kingston-Smith, A.H., 2015. Polyphenol oxidase in leaves: is there any significance to the chloroplastic localization? Journal of experimental botony, 66, 3571–3579. https://doi.org/10.1093/jxb/erv141.

Bouche N, Fromm H., 2004. GABA in plants: just a metabolite? Trends Plant Science.; 9:110–5.

Bown AW, MacGregor KB, Shelp BJ., 2006. Gamma-aminobutyrate: defence against invertebrate pests? Trends Plant Science, 11:424–7.

Bresson, Justine, Stefan Bieker, Lena Riester, Jasmin Doll, and Ulrike Zentgraf., 2018. A Guideline for Leaf Senescence Analyses: From Quantification to Physiological and Molecular Investigations. Journal of Experimental Botany 69 (4): 769–86.

Campalans, A., Messeguer, R., Goday, A., Pagès, M., 1999. Plant responses to drought, from ABA signal transduction events to the action of the induced proteins. Plant Physiology and Biochemistery, 37, 327–340.

Carpentier, S.C., Panis, B., Vertommen, A., Swennen, R., Sergeant, K., Renaut, J., Laukens, K., Witters, E., Samyn, B. and Devreese, B., 2008. Proteome analysis of non-model plants: A challenging but powerful approach. Mass Spectrometry Reviews. 27(4):354-377.

Carrari F, Baxter C, Usadel B, Urbanczykwochniak E, Zanor MI, Nunesnesi A, Nikiforova V, Centero D, Ratzka A, Pauly M., 2006. Integrated analysis of metabolite and transcript levels reveals the metabolic shifts that underlie tomato fruit development and highlight regulatory aspects of metabolic network behavior. Plant Physiology, 142(4):1380.

Castrillo, M.; Calcagno, A.M., 1989. Effects of water stress and re watering on ribulose-1, 5-bis-phosphate carboxylase activity, chlorophyll and protein contents in two cultivars of tomato. Journal of Horticultural Science and Biotechnology, 64, 717–724.

Chagoyen, M., Pazos, F., 2013. Tools for the functional interpretation of metabolomic experiments. Briefings in Bioinformatics 14, 737–744. https://doi.org/10.1093/bib/bbs055.

Challabathula D, Puthur JT, Bartels D., 2016. Surviving metabolic arrest: photosynthesis during desiccation and rehydration in resurrection plants. Annals of the New York Academy of Sciences; 1365: 89.

Challabathula, Dinakar & Zhang, Qingwei & Bartels, Dorothea., 2018. Protection of photosynthesis in desiccation-tolerant resurrection plants. Journal of Plant Physiology. 227.

Chaves, M.M., 2002. How Plants Cope with Water Stress in the Field? Photosynthesis and Growth. Annals of Botany, 89, 907–916.

Chen Z, Zheng Z, Huang J, Lai Z, Fan B., 2009. Biosynthesis of salicylic acid in plants. Plant Signal Behaviour, 4:493–496.

Choi, Young and van Spronsen, Jaap and Dai, Yuntao and Verberne, Marianne and Hollmann, Frank and Arends, Isabel and Witkamp, Geert-Jan and Verpoorte, Robert, 2011. Are Natural Deep Eutectic Solvents the Missing Link in Understanding Cellular Metabolism and Physiology. Plant physiology, 156. 1701-5. 10.1104/pp.111.178426.

Chong J, Wishart DS, Xia J., 2019. Using MetaboAnalyst 4.0 for comprehensive and integrative metabolomics data analysis. Curr Protoc Bioinformatics. 68(1): e86.

Christ B, Egert A, Süssenbacher I, Kräutler B, Bartels D, Peters S, Hörtensteiner S., 2014. Water deficit induces chlorophyll degradation via the “PAO/phyllobilin” pathway in leaves of homoio- (*Craterostigma pumilum*) and poikilochlorophyllous (*Xerophyta viscosa*) resurrec-tion plants. Plant, Cell and Environment, 37: 2521–2531.

Chu, S., Huang, M., Kelly, R., Benedetti, E., Siddiqui, J., Zeleznik, O., Pereira, A., Herrington, D., Wheelock, C., Krumsiek, J., McGeachie, M., Moore, S., Kraft, P., Mathé, E., Lasky-Su, J., 2019. Integration of Metabolomic and Other Omics Data in Population-Based Study Designs: An Epidemiological Perspective. Metabolites 9, 117. https://doi.org/10.3390/metabo9060117.

Ciereszko I., 2009. Sucrose metabolism in plant tissues under stress conditions: key enzymes, localization and function. In: Maksymiec W, editor. Compartmentation of responses to stresses in higher plants, true or false. Kerala: Transworld Research Network; p193–218.

Ciereszko, I., 2018. Regulatory roles of sugars in plant growth and development. Acta Societatis Botanicorum Poloniae, 13.

Claiborne, A., 1985. Catalase activity. In: Greenwald EA (ed) CRC handbook of methods for oxygen radical research. CRC Press, Bocca Raton, pp 283–284.

Clarke J.M., 1986. Effect of leaf rolling on leaf water loss in *Triticum spp*. Can J Plant Sci. 66:885–891.

Close, D. C., and Beadle, C. L., 2003. The Ecophysiology of Foliar Anthocyanin. Botanical Review, 69(2), 149–161. https://doi.org/10.1663/0006-8101069[0149:TEOFA]2.0.CO;2

Coca MA, Almoguera C, Jordano J., 1994. Expression of sunflower low molecular weight heat shock proteins during embryogenesis and persistence after germination: localization and possible functional implications. Plant Molecular Biology, 25: 479–492.

Coetzee, H., 1974. Anatomy of the leaves of the *Velloziacea*e in South Africa and South West Africa and a key based on leaf anatomy. Diniteria, 10, 19–33.

Colebrook EH, Thomas SG, Phillips AL, Hedden P., 2014. The role of gibberellin signalling in plant responses to abiotic stress. Journal of Experimental Botany, 217:67–75.

Coleman HD, Ellis DD, Gilbert M, Mansfield SD., 2006. Up-regulation of sucrose synthase and UDP-glucose pyrophosphorylase impacts plant growth and metabolism, Plant Biotechnology Journal, vol. 4, pg. 87-101.

Collett, H., 2003. Photosynthetic genes are differentially transcribed during the dehydration-rehydration cycle in the resurrection plant, *Xerophyta humilis*. Journal of Experimental Botany 54, 2593–2595. https://doi.org/10.1093/jxb/erg285.

Conesa, A., Götz, S., García-Gómez, J.M., Terol, J., Talón, M. and Robles, M., 2005. Blast2GO: a universal tool for annotation, visualization and analysis in functional genomics research. Bioinformatics. 21(18):3674-3676.

Cooper K., Farrant J. M., 2002. Recovery of the resurrection plant *Craterostigma wilmsii* from desiccation: protection versus repair. Journal of Experimental Botany, 53 1805–1813 10.1093/jxb/erf028.

Cornic, G.; Massacci, A., 1996. Leaf photosynthesis under drought stress. In Photosynthesis and the Environment; Springer: Berlin/Heidelberg, Germany; pp. 347–366.

Costa, M.-C.D., Artur, M.A.S., Maia, J., Jonkheer, E., Derks, M.F.L., Nijveen, H., Williams, B., Mundree, S.G., Jiménez-Gómez, J.M., Hesselink, T., Schijlen, E.G.W.M., Ligterink, W., Oliver, M.J., Farrant, J.M., Hilhorst, H.W.M., 2017. A footprint of desiccation tolerance in the genome of *Xerophyta viscosa*. Nature Plants 3.

Cote, G.G. and Crain, R.C., 1993. Biochemistry of phosphoinositides. Annual Review of Plant Physiology. 44:333-356.

Crowe, J. H., Carpenter, J. F., and Crowe, L. M., 1998. The role of vitrification in anhydrobiosis. Annual Review of Physiology, 60, 73–103. doi: 10.1146/annurev.physiol.60.1.73.

Cruz de Carvalho MH., 2008. Drought stress and reactive oxygen species: Production, scavenging and signalling. Plant Signaling & Behavior, 3(3):156-165. doi:10.4161/psb.3.3.5536.

Dace, H., Sherwin, H.W., Illing, N., Farrant, J.M., 1998. Use of metabolic inhibitors to elucidate mechanisms of recovery from desiccation stress in the resurrection plant *Xerophyta humilis*.

Dace, H., 2014. The Metabolomics of Desiccation Tolerance in *Xerophyta humilis*, 213.

Dai Y, van Spronsen J, Witkamp GJ, Verpoorte R, Choi YH., 2013. Natural deep eutectic solvents as new potential media for green technology. Analytica Chimica Acta, 766:61-68. doi:10.1016/j. aca. 2012.12.019.

Das, K., Roychoudhury, A., 2014. Reactive oxygen species (ROS) and response of antioxidants as ROS-scavengers during environmental stress in plants. Frontiers of Environmental Science & Engineering, Frontier Environment. Science. 2. https://doi.org/10.3389/fenvs.2014.00053.

Dennison KL, Spalding EP., 2000. Glutamate-gated calcium fluxes in Arabidopsis. Plant Physiology, 124:1511–4.

Díaz-Villanueva, J. F., Díaz-Molina, R., & García-González, V., 2015. Protein Folding and Mechanisms of Proteostasis. International journal of molecular sciences, 16(8), 17193–17230. https://doi.org/10.3390/ijms160817193

Dinakar C, Djilianov D, Bartels D., 2012. Photosynthesis in desiccation tolerant plants: energy metabolism and antioxidative stress defence. Plant Science, 182:29–41.

Dinakar C, Bartels D., 2013. Desiccation tolerance in resurrection plants: new insights from transcriptome, proteome and metabolome analysis. Front Plant Sci.; 4:482. Published 2013 Nov 28. doi:10.3389/fpls.2013.00482.

Ding, W., Wang, L., Zhang, J., Ke, W., Zhou, J., Zhu, J., Guo, X., Long, R., 2017. Characterization of antioxidant properties of lactic acid bacteria isolated from spontaneously fermented yak milk in the Tibetan Plateau. Journal of Functional Foods 35, 481–488. https://doi.org/10.1016/j.jff.2017.06.008

Drennan P.M., Smith M.T., Goldsworthy D., Vanstaden J., 1993. The occurrence of trehalose in the leaves of the desiccation-tolerant angiosperm *Myrothamnus flabellifolius*. Plant Physiology, 142, pp. 493-496.

Doehlert DC. 1989. Separation and characterization of four hexose kinases from developing maize kernels. Plant Physiology, 89, 29–39.

Dubouzet, J. G., Strabala, T. J., & Wagner, A., 2013. Potential transgenic routes to increase tree biomass. Plant Science, 212, 72–101.

Dudek, H.; Datta, S.R.; Franke, T.F.; Birnbaum, M.J.; Yao, R.J.; Cooper, G.M.; Segal, R.A.; Kaplan, D.R.; Greenberg, M.E., 1997. Regulation of neuronal survival by the serine-threonine protein kinase Akt. Science 1997, 275, 661–665.

Ellis, R.J., and van der Vies, S.M., 1991. Molecular chaperones. Annual. Rev. Biochemistry., tolerance: degradation and reactivation of damaged proteins. Annual Review of Genetics, 27:437-496.

Elmore, J. M., Liu, J., Smith, B., Phinney, B. *et al.*, 2012. Quantitative proteomics reveals dynamic changes in the plasma membrane during Arabidopsis immune signalling. Molecular and Cell Proteomics, 11, 1– 13.

ElSayed A, Rafudeen M.S, Golldack D., 2014. Physiological aspects of raffinose family oligosaccharides (RFOs) in plants: Protection against abiotic stress. Plant Biology. 16 (1):1-8.

Erb M., Meldau S., Howe G. A., 2012. Role of phytohormones in insect-specific plant reactions. Trends Plant Science. 17, 250–259. 10.1016/j.tplants.2012.01.003.

Ermakova, M., Lopez-Calcagno, P.E., Raines, C.A., Furbank, R.T., von Caemmerer, S., 2019. Overexpression of the Rieske FeS protein of the Cytochrome b 6 f complex increases C 4 photosynthesis (preprint). Plant Biology. https://doi.org/10.1101/574897.

Fani, E., 2012. Changes chlorophyll b in response to drought stress in alfalfa (vs. Nick Ur-ban) in climatic conditions of the south west Iran. Am. Journal of Biochememistry and Biotechnology, 1, 107–110.

Farooq, M., Wahid, A., Kobayashi, N., Fujita, D., Basra, S.M.A., 2009a. Plant drought stress: effects, mechanisms and management. Agronomy for Sustainable Development, 29, 185–212. https://doi.org/10.1051/agro:2008021.

Farooq, M.; Wahid, A.; Lee, D.-J. 2009 b. Exogenously applied polyamines increase drought tolerance of rice by improving leaf water status, photosynthesis and membrane properties. Acta Physiology Plant, 31, 937–945.

Farrant J.M., 2000. Comparison of mechanisms of desiccation tolerance among three angio-sperm resurrection plants. Plant Ecology 151, 29-39.

Farrant JM, Vander Willigen C, Loffel DA, Bartsch S, Whittaker A., 2003. An investigation into the role of light during desiccation of three angiosperm resurrection plants. Plant, Cell and Environment. 26: 1275–1286.

Farrant, Jill M, Wolf Brandt, and George G Lindsey., 2007. "An Overview of Mechanisms of Desiccation Tolerance in Selected Angiosperm Resurrection Plants." Plant Stress. https://www.semanticscholar.org/paper/An-overview-of-mechanisms-of-desiccation tolerance-Farrant-Brandt/b812c9a1370d125b91af265dbd2f417b4329a9df

Farrant, J. M., Cooper, K., Nell, H., 2012. Desiccation tolerance, in Plant Stress Physiology. Edition. Shabala, S. (Wallingford, CT: CAB International), 238–265. doi: 10.1079/9781845939953.0238.

Farrant, J.M., Cooper, K., Hilgart, A., Abdalla, K.O., Bentley, J., Thomson, J.A., Dace, H.J.W., Peton, N., Mundree, S.G., Rafudeen, M.S., 2015. A molecular physiological review of vegetative desiccation tolerance in the resurrection plant *Xerophyta viscosa* (Baker). Planta 242, 407–426.

Farrant JM, Cooper K, Dace HJW, Bentley J, Hilgart A. 2017. Desiccation tolerance. In Plant Stress Physiology, ed. S Shabala, pp. 217–52.Wallingford, UK: CABI. 2nd edition

Feki, K., Brini, F., 2016. Role of proteins in alleviating drought stress in plants, in Ahmad, P. (Ed.), Water Stress and Crop Plants. John Wiley & Sons, Ltd, Chichester, UK, pp. 165–176. https://doi.org/10.1002/9781119054450.ch12.

Fernandez, D., Castrillo, M., 1999. Maize Leaf Rolling Initiation. Photosynthesis. 37, 493–497. https://doi.org/10.1023/A:1007124214141.

Fernandez O, Ishihara H, George GM, Mengin V, Flis A, Sumner D, *et al*., 2017. Leaf starch; 174:2199–2212.

Fernie AR., 2007. The future of metabolic phytochemistry: larger numbers of metabolites, higher resolution, greater understanding. Phytochemistry 68, 2861–2880.

Forde BG, Lea PJ., 2007 Glutamate in plants: metabolism, regulation, and signalling. Journal of Experimental Botony, 58:2339–58.

Forde BG, Walch-Liu P., 2009. Nitrate and glutamate as environmental cues for behavioural responses in plant roots. Plant, Cell and Environment, 32:682–93.

Foyer, C.H, Noctor, G., 2003. Redox sensing and signalling associated with reactive oxygen in chloroplasts, peroxisomes and mitochondria. Physiologia Plantarum 119, 355–364.

Foyer, C.H., Noctor, G., 2005. Redox Homeostasis and Antioxidant Signalling: A Metabolic Interface between Stress Perception and Physiological Responses. Plant Cell 17, 1866–1875. https://doi.org/10.1105/tpc.105.033589.

Frank, W., 2000. Water deficit triggers phospholipase D activity in the resurrection plant Craterostigma plantagineum. Plant Cell 12, 111–123.

Fu J., Momcilović I., Prasad P.V.V., 2012. Roles of Protein Synthesis Elongation Factor EF-Tu in Heat Tolerance in Plants. Journal of Experimental Botony, 835836:8. doi: 10.1155/2012/835836.

Gaff, D.F; 1977. Desiccation tolerant vascular plants of southern Africa. Oecologia 31, 95–109. https://doi-org.ezproxy.uct.ac.za/10.1007/BF00348713.

Gaff DF, McGregor GR., 1979. The effect of dehydration and rehydration on the nitrogen content of various fractions from resurrection plants, Biologia Plantarum, 1979, vol. 22, pg. 92-99.

Gaff DF., 1989. Responses of desiccation tolerant 'resurrection' plants to water stress. In: Kreeb KH, Richter H, Hinckley TM, eds. Structural and functional responses to environmental stresses. The Hague: SPB Academic Publishing; pp. 255-268.

Gaff, D.F., and Loveys, B.R., 1993. Abscisic acid levels in drying plants of a resurrection grass. Transactions of the Malaysian Society of Plant Physiology 3, 286287.

Gaff D. F., Bartels D., Gaff J. L.,1997. Changes in gene expression during drying in a desiccation-tolerant grass *Sporobolus stapfianus* and a desiccation-sensitive grass *Sporobolus pyramidalis*. Functional Plant Biology, 24 617–622.

Gaff, D. F. and Oliver, M., 2013. The evolution of desiccation tolerance in angiosperm plants: a rare yet common phenomenon. Functional Plant Biology, 40(4), 315 - 328. https://doi.org/10.1071/FP12321.

Gammulla, A. G., Pascovici, D., Atwell, B. J., Haynes, P. A., 2011. Differential proteomics response of rice (*Oryza sativa*) leaves exposed to high- and low-temperature stress. Proteomics, 11, 2839– 2850.

Garrone, A., Archipowa, N., Zipfel, P.F., Hermann, G., Dietzek, B., 2015. Plant Protochlorophyllide Oxidoreductases A and B: catalytic efficiency and initial reaction steps. Journal of Biology and Chemistry, 290, 28530–28539. https://doi.org/10.1074/jbc.M115.663161.

Gechev, Dinakar, Benina, Toneva, Bartels, 2012. Molecular mechanisms of desiccation tolerance in resurrection plants Cell, Molecular and Life Science, 69, pp. 3175-3186.

Gechev TS, Benina M, Obata T, Tohge T, Sujeeth N, Minkov I, Hille J, Temanni MR, Marriott AS, Bergström E, *et al.*, 2013. Molecular mechanisms of desiccation tolerance in the resurrection glacial relic Haberlea rhodopensis. Cell, Molecular and Life Science, 70: 689–709.

Gechev, T.S., Hille, J., Woerdenbag, H.J., Benina, M., Mehterov, N., Toneva, V., Fernie, A.R., Mueller-Roeber, B., 2014. Natural products from resurrection plants: Potential for medi-cal applications. Biotechnology Advances 32, 1091–1101. https://doi.org/10.1016/j.biotechadv.2014.03.005.

Gething, MJ. and Sambrook, J., 1992. Protein folding in the cell. Nature, 355:33-45.

Ghasempour H. R., Gaff D. F., Williams R. P. W., Gianello R. D., 1998. Contents of sugars in leaves of drying desiccation tolerant flowering plants particularly grasses. Plant Growth Regulation, 24 185–191 10.1023/A: 1005927629018.

Ghoumari AM, Ibanez C, El-Etr M, Leclerc P, Eychenne B, O'Malley BW, Baulieu EE, Schumacher M., 2003. Progesterone and its metabolites increase myelin basic protein expression in organotypic slice cultures of rat cerebellum. Journal of Neurochemistry, 86(4):848–859. 10.1046/j.1471-4159. 01881.x

Giarola, V., Hou, Q., Bartels, D., 2017. Angiosperm Plant Desiccation Tolerance: Hints from Transcriptomics and Genome Sequencing. Trends in Plant Science 22, 705–717. https://doi.org/10.1016/j.tplants.2017.05.007.

Good A.G., Zaplachinski S.T., 1994. The effects of drought stress on free amino acid accumulation and protein synthesis in Brassica napus. Physiologia Plantarum 90, 9–Huang T, Jander G. 2017. Abscisic acid-regulated protein degradation causes osmotic stress-induced accumulation of branched-chain amino acids in Arabidopsis thaliana. Planta 246, 737–747.

Götz, S., Garcia-Gomez, J.M., Terol, J., Williams, T.D., Nagaraj, S.H., Nueda, M.J., Robles, M., Talon, M., Dopazo, J. and Conesa, A., 2008. High-throughput functional annotation and data mining with the Blast2GO suite. Nucleic Acids Research. 36(10):3420-3435.

Govender K., 2006. Molecular and biochemical characterisation of a type II peroxiredoxin (XvPrx2) from the resurrection plant *Xerophyta viscosa* (Baker). Dissertation, University of Cape Town.

Gratão PL, Polle A, Lea PJ, Azevedo RA., 2005. Making the life of heavy metal-stressed plants a little easier. Functional Plant Biology, 32, 481–494.

Griffiths, C.A., Gaff, D.F., Neale, A.D., 2014. Drying without senescence in resurrection plants. Front. Plant Sci. 5. https://doi.org/10.3389/fpls.2014.00036.

Griffiths, C. A., Paul, M. J., & Foyer, C. H., 2016. Metabolite transport and associated sugar signalling systems underpinning source/sink interactions. Biochimica et biophysica acta, 1857(10), 1715–1725. https://doi.org/10.1016/j.bbabio.2016.07.007.

Grossmann J, Roschitzki B, Panse C *et al.*, 2010. Implementation and evaluation of relative and absolute quantification in shotgun proteomics with label-free methods. Journal of Proteomics 73:1740–1746.

Gygi, S. P., Rist, B., Gerber, S. A., Turecek, F. *et al.*, 1999. Quantitative analysis of complex protein mixtures using isotopecoded affinity tags. Nature Biotechnology, 17, 994–999.

Hallam N.D. & Luff S.E., 1980. Fine structural changes in the mesophyll tissue of the leaves of *Xerophyta villosa* during desiccation. Botanical Gazette 141, 173–179.

Hartung, W., Schiller, P., and Karl-Josef, D., 1998. Physiology of poikilohydric plants. Prog. Bot. 59, 299–327. doi: 10.1007/978-3-642-80446-5_11.

Hendrickson EL, Xia Q, Wang T *et al.*, 2006. Comparison of spectral counting and metabolic stable isotope labeling for use with quantitative microbial proteomics. Analyst 131:1335–1341.

Hernández JA, Campillo A, Jiménez A, Alarcón JJ, Sevilla F., 1999. Response of antioxidant systems and leaf water relations to NaCl stress in pea plants. New Phytology, l.; 141: 241–251.

Hildebrandt, T.M., Nunes Nesi, A., Araújo, W.L., Braun, H.-P., 2015. Amino Acid Catabolism in Plants. Molecular Plant 8, 1563–1579. https://doi.org/10.1016/j.molp.2015.09.005.

Hoekstra, F. A., Golovina, E. A., and Buitink, J., 2001. Mechanisms of plant desiccation tolerance. Trends Plant Science, 6, 431–438. doi: 10.1016/S1360-1385(01)02052-0.

Hoekstra, F.A., 2005. Differential Longevities in Desiccated Anhydrobiotic Plant Systems.Integrative and Comparative Biology, 45, pp.725-733.

Huang, W., Pi, L., Liang, W., Xu, B., Wang, H., Cai, R., Huang, H., 2006. The Proteolytic Func-tion of the Arabidopsis 26S Proteasome Is Required for Specifying Leaf Adaxial Identi-ty. Plant Cell 18, 2479–2492. https://doi.org/10.1105/tpc.106.045013.

Huang, W., Pi, L., Liang, W., Xu, B., Wang, H., Cai, R., Huang, H., 2017. The Proteolytic Function of the Arabidopsis 26S Proteasome Is Required for Specifying Leaf Adaxial Identity. Plant Cell 18, 2479–2492. https://doi.org/10.1105/tpc.106.045013.

Igamberdiev, A.U., Kleczkowski, L.A., 2018. The Glycerate and Phosphorylated Pathways of Serine Synthesis in Plants: The Branches of Plant Glycolysis Linking Carbon and Nitrogen Metabolism. Front. Plant Science, 9, 318. https://doi.org/10.3389/fpls.2018.00318.

Illing N., Denby K., Collett H., Shen A., Farrant J., 2005. The signature of seeds in resurrection plants: a molecular and physiological comparison of desiccation tolerance in seeds and vegetative tissues. Integrative and Comparative Biology, 45 771–787 10.1093/icb/45.5.771.

Ingle, R.A., Schmidt, U.G., Farrant, J.M., Thomson, J.A., Mundree, S.G., 2007. Proteomic analysis of leaf proteins during dehydration of the resurrection plant *Xerophyta viscosa*. Plant Cell Environ 30, 435–446. https://doi.org/10.1111/j.1365-3040.2006.01631.x.

Ingle RA, Collett H, Cooper K, Takahashi Y, Farrant JM, Illing N.,2008. Chloroplast biogenesis during rehydration of the resurrection plant *Xerophyta humilis*: parallels to the etioplast-chloroplast transition. Plant, Cell and Environment, 31:1813–1824.

Ingle, R.A., 2011. Histidine Biosynthesis. The Arabidopsis Book 9, e0141. https://doi.org/10.1199/tab.0141.

Ingram, J., and Bartels, D., 1996.The molecular basis of dehydration tolerance in plants. Annual Review Plant Physiology Plant Molecular Biology, 47, 377–403.doi: 10.1146/annurev.arplant.47.1.377.

Ishihama Y, Schmidt T, Rappsilber J *et al.,* 2008. Protein abundance profiling of the Escherichia coli cytosol. BMC Genomics 9:102.

Ishihara S, *et al*., 2007. Homologous subunits of 1, 3-beta-glucan synthase are important for spore wall assembly in Saccharomyces cerevisiae. Eukaryotic Cell, 6(2):143-56.

Ishihara, A., Hashimoto, Y., Tanaka, C., Dubouzet, J.G., Nakao, T., Matsuda, F., Nishioka, T., Miyagawa, H., Wakasa, K., 2008. The tryptophan pathway is involved in the defence responses of rice against pathogenic infection via serotonin production. Plant J 54, 481–495. https://doi.org/10.1111/j.1365-313X.2008.03441.x

Jackson, M.A., Gilding, E.K., Shafee, T., Harris, K.S., Kaas, Q., Poon, S., Yap, K., Jia, H., Gua-rino, R., Chan, L.Y., Durek, T., Anderson, M.A., Craik, D.J., 2018. Molecular basis for the production of cyclic peptides by plant asparaginyl endopeptidases. Nature Communications 9, 2411. https://doi.org/10.1038/s41467-018-04669-9.

Jacob, P., Hirt, H., Bendahmane, A., 2017. The heat-shock protein/chaperone network and multiple stress resistance. Plant Biotechnology Journal, 15, 405–414. https://doi.org/10.1111/pbi.12659.

Jäger H.-J., Meyer, H.R., 1977. Effect of water stress on growth and proline metabolism of Phaseolus vulgaris L. Oecologia 30, 83–96. https://doi.org/10.1007/BF00344894.

Jiang GQ, Wang Z, Shang HH, Yang WL, Hu Z, Phillips J, *et al.*, 2007. Proteome analysis of leaves from the resurrection plant *Boea hygrometrica* in response to dehydration and rehydration. Planta; 225:1405–20.

Jiménez-Arias, D., García-Machado, F. J, Morales-Sierra, S., Luis, J. C, Suarez, E., Hernández, M., Valdés, F., & Borges, A. A., 2019. Lettuce plants treated with L-pyroglutamic acid increase yield under water deficit stress. Environmental and experimental botany, 158, 215-222. doi: 10.1016/j.envexpbot.2018.10.034.

Jorge, T.F., Rodrigues, J.A., Caldana, C., Schmidt, R., van Dongen, J.T., Thomas-Oates, J., António, C., 2016. Mass spectrometry-based plant metabolomics: Metabolite responses to abiotic stress: mass spectrometry-based plant metabolomics. Mass Spectrometry Reviews, 35, 620–649. https://doi.org/10.1002/mas.21449.

Joshi, V., Joung, J.-G., Fei, Z., Jander, G., 2010. Interdependence of threonine, methionine and isoleucine metabolism in plants: accumulation and transcriptional regulation under abiotic stress. Amino Acids 39, 933–947.

Journet E.P., Bligny R., Douce R., 1986. Biochemical changes during sucrose deprivation in higher plant cells. J Biol Chem.; 261:3193–3199.

Kaddurah-Daouk R, Krishnan KR., 2009. Metabolomics: a global biochemical approach to the study of central nervous system diseases. Neuropsychopharmacology, 34:173-186.

Kalaji, H.N., Jajoo, A., Oukarroum, A., Brestic, M., Zivcak, M., Samborska, I.A., Cetner, M.D., Łukasik, I., Goltsev, V., and Ladle, R.J., 2016. Chlorophyll a fluorescence as a tool to monitor physiological status of plants under abiotic stress conditions, Acta Physiology Plant., vol. 38: 102.

Kamies, R., Rafudeen, M. S., and Farrant, J., 2010. The use of aeroponics to investigate antioxidant activity in the roots of *Xerophyta viscosa*. Plant Growth Regulation, 62(3), 203–211. https://doi.org/10.1007/s10725-010-9498-1

Kanehisa, M. and Goto, S., 2000. KEGG: Kyoto Encyclopedia of Genes and Genomes. Nucleic Acids Research. 28(1):27-30.

Kaur H, Verma P, Petla BP, Rao V, Saxena SC, Majee M., 2013. Ectopic expression of the ABA-inducible dehydration-responsive chickpea L-myo-inositol 1-phosphate synthase 2 (CaMIPS2) in Arabidopsis enhances tolerance to salinity and dehydration stress. Planta 237: 321–335.

Kavar T, Maras M, Kidric M, *et al.*, 2007. Identification of genes involved in the response of leaves of Phaseolus vulgaris to drought stress. Molecular Breed 21: 159–172.

Khan M.I.R, Fatma M, Pe T.S, Anjum N.A., Khan N.A., 2015. Salicylic acid induced abiotic stress tolerance and underlying mechanisms in plants. Front Plant Science, 6:462.

Kido, E.A., Ferreira Neto, J.R., Silva, R.L., Belarmino, L.C., Bezerra Neto, J.P., Soares-Cavalcanti, N.M., Pandolfi, V., Silva, M.D., Nepomuceno, A.L., Benko-Iseppon, A.M., 2013. Expression dynamics and genome distribution of osmoprotectants in soybean: identifying important components to face abiotic stress. BMC Bioinformatics 14, S7. https://doi.org/10.1186/1471-2105-14-S1-S7

Kim, S. and Pevzner, P.A., 2014. MS-GF+ makes progress towards a universal database search tool for proteomics. Nature Communications, 5, p.5277.

Kitano H., 2002. Systems Biology: a brief overview. Science, 295(5560):1662–1664. 10.1126/science.1069492.

Kleczkowski LA., 1994. Glucose activation and metabolism through UDP-glucose pyrophosphorylase in plants, Phytochemistry, volume, 37. pg. 1507-1515.

Kosová, K., Vítámvás, P., Prášil, I.T. and Renaut, J., 2011. Plant proteome changes under abiotic stress-contribution of proteomics studies to understanding plant stress response. Journal of Proteomics. 74(8):1301-1322.

Kranner, I, Beckett R. P., Wornik S., Zorn, M, and Pfeihofer H. W, 2002. Revival of a resurrection plant correlates with its antioxidant status, Plant Journal, vol. 31, no. 1, pp. 13–24.

Kruger NJ, von Schaewen A., 2003. The oxidative pentose phosphate pathway: structure and organisation. Current Opinion in Plant Biology 6, 236–246.

Larrainzar, E., Wienkoop, S., Weckwerth, W., Ladrera, R., Arrese-Igor, C. et al., 2007. *Medicago truncatula* root nodule proteome analysis reveals differential plant and bacteroid responses to drought stress. Plant Physiol., 144, 1495– 1507.

Larson A., 1988. The antioxidants of higher plants. Phytochemistry 27, 969–978.

Laxa, M., M. Liebthal, W. Telman, K. Chibani, and K.-J. Dietz., 2019. The Role of the Plant Antioxidant System in Drought Tolerance. Antioxidants. 8:94.

Le D.T., Tarrago L., Watanabe Y., Kaya A., Lee B.C., Tran U., Nishiyama R., Fomenko D.E., Gladyshev V.N., Tran L.S.P., 2013. Diversity of plant methionine sulfoxide reductases B and evolution of a form specific for free methionine sulfoxide. PLoS ONE; 8:1706. doi: 10.1371/journal.pone.0065637.

Lea PJ, Miflin BJ., 1974. Alternative route for nitrogen assimilation in higher plants. Nature, 251: 614–6.

Lee, J., Feng, J., Campbell, K. B., Scheffler, B. E. *et al*., 2009. Quantitative proteomic analysis of bean plants infected by a virulent and avirulent obligate rust fungus. Molecular Cell Proteomics, 2009, 8, 19– 31.

Lehner, A., Mamadou, N., Poels, P., Côme, D., Bailly, C., Corbineau, F., 2008. Changes in soluble carbohydrates, lipid peroxidation and antioxidant enzyme activities in the embryo during ageing in wheat grains. Journal of Cereal Science 47, 555–565. https://doi.org/10.1016/j.jcs.2007.06.017.

Lempradl, A., Pospisilik, J.A., & Penninger, J.M., 2015. Exploring the emerging complexity in transcriptional regulation of energy homeostasis. Nature Reviews Genetics, 16, 665-681.

Leopold, A. C., and Vertucci, C. W., 1986. "Physical attributes of desiccated seeds," in Membranes, metabolism and Dry Organisms, ed. A. C. Leopold (New York: Cornell University Press), 22–34.

Li, P. and Ma, F., 2012. Different effects of light irradiation on the photosynthetic electron transport chain during apple tree leaf dehydration, Plant Physiology and Biochemistry, vol. 55, pp. 16–22.

Li, P., Li, Y.-J., Zhang, F.-J., Zhang, G.-Z., Jiang, X.-Y., Yu, H.-M., Hou, B.-K., 2017. The Arabidopsis UDP-glycosyltransferases UGT79B2 and UGT79B3, contribute to cold, salt and drought stress tolerance via modulating anthocyanin accumulation. Plant Journal 89, 85–103. https://doi.org/10.1111/tpj.13324.

Lichtenthaler, H. K., & Wellburn, A. R., 1983. Determinations of total carotenoids and chlorophylls a and b of leaf extracts in different solvents. Liverpool.

Lindquist S. Jarosz DF., 2010. Hsp90 and environmental stress transform the adaptive value of natural genetic variation. Science; 330(6012):1820-1824. doi:10.1126/science.1195487.

Lisec, J., Schauer, N., Kopka, J., Willmitzer, L., Fernie, A.R., 2006. Gas chromatography mass spectrometry–based metabolite profiling in plants. Nature Protocols, 1, 387–396. https://doi.org/10.1038/nprot.2006.59.

Liu J, Zhu JK., 1997. Proline accumulation and salt-stress-induced gene expression in a salt-hypersensitive mutant of Arabidopsis. Plant Physiology, 114(2):591–596. doi: 10.1104/pp.114.2.591.

Liu, H., Sadygov, R. G., Yates, J. R., 2004. A model for random sampling and estimation of relative protein abundance in shotgun proteomics. Analytical Chemistry,76, 4193–4201.

Liu X, Challabathula D, Quan W, Bartels D. 2019. Transcriptional and metabolic changes in the desiccation tolerant plant *Craterostigma plantagineum* during recurrent exposures to dehydration. *Planta*, 249:1017–35.

llakhverdiev S.I., Kreslavski V.D., Klimov V.V, Los D.A., Carpentier R., Mohanty P., 2008. Heat stress: An overview of molecular responses in photosynthesis. Photosynth. Res.98:541–550.

Lohse, M., Nagel, A., Herter, T., May, P., Schroda, M., Zrenner, R., Tohge, T., Fernie, A.R., Stitt, M., Usadel, B., 2014. Mercator: a fast and simple web server for genome scale functional annotation of plant sequence data: Mercator: sequence functional annotation server. Plant, Cell and Environmental, 37, 1250–1258. https://doi.org/10.1111/pce.12231.

Lu SC., 2013. Glutathione synthesis. Biochemistry, Biophysics Acta. 1830:3143–53.

Łukaszuk E., Rys M., Możdżeń K., Stawoska I., Skoczowski A., Ciereszko I., 2017. Photosynthesis and sucrose metabolism in leaves of Arabidopsis thaliana aos, ein4 and rcd1 mutants as affected by wounding. Acta Physiology Plant; 39:17. https://doi.org/10.1007/s11738-016-2309-1.

Ma, Z.Q., Dasari, S., Chambers, M.C., Litton, M.D., Sobecki, S.M., Zimmerman, L.J., Halvey, P.J., Schilling, B., Drake, P.M., Gibson, B.W. and Tabb, D.L., 2009. IDPicker 2.0: Im-proved protein assembly with high discrimination peptide identification filtering. Journal of Proteome Research, 8(8), pp.3872-3881.

Madden CF., 2019. Understanding senescence in a desiccation tolerant African grass: Eragrostis nindensis. PhD thesis. Department of Molecular and Cell Biology, University of Cape Town, South Africa.

Manchandia, A.M., Banks, S.W., Gossett, D.R., Bellaire, B.A., Lucas, M.C., Millhollon, E.P., 1999. The influence of a-amanitin on the NaCl-induced up-regulation of antioxidantenzyme activity in cotton callus tissue. Free Radical Res. 30,429/438.

Martins-de-Souza, D. (Ed.), 2014. Shotgun proteomics: methods and protocols, Methods in molecular biology. Humana Press, New York.

Matsoukas, I.G., 2014. Interplay between sugar and hormone signalling pathways modulate floral signal transduction. Front. Genet. 5. https://doi.org/10.3389/fgene.2014.00218.

Mazelis, M., Pratt, H.M., 1976. In Vivo Conversion of 5-Oxoproline to Glutamate by Higher Plants. Plant Physiology, 57, 85–87. https://doi.org/10.1104/pp.57.1.85.

Megger, D.A., 2013. Label-free quantification in clinical proteomics. Biochimica et Biophysica Acta 10.

Meng, M., Geisler, M., Johansson, H., Harholt, J., Scheller, H.V., Mellerowicz, E.J., Kleczkow-ski, L.A., 2009. UDP-Glucose Pyrophosphorylase is not Rate Limiting, but is Essential in Arabidopsis. Plant and Cell Physiology 50, 998–1011. https://doi.org/10.1093/pcp/pcp052.

Mhlongo Msizi I., Piater Lizelle A., Madala Ntakadzeni E., Labuschagne Nico, Dubery Ian A.,2018.The Chemistry of Plant–Microbe Interactions in the Rhizosphere and the Potential for Metabolomics to Reveal Signaling Related to Defense Priming and Induced Systemic Resistance., Frontiers in Plant Science,Volume 9,112,doi10.3389/fpls.2018.00112;ISSN=1664-462X

Michel, D., Furini, A., Salamini, F., and Bartels, D., 1994. Structure and regulation of an ABA-and desiccation-responsive gene from the resurrection plant *Craterostigma plantagineum*. Plant Molecular Biology, 24, 549–560.doi:10.1007/BF00023553.

Miernyk, J.A., 1999. Protein folding in the plant cell. Plant Physiology, 121:695-703.

Miura K, Tada Y., 2014. Regulation of water, salinity, and cold stress responses by salicylic acid. Front Plant Science, 5:4.

Mohammed, S.A., Ambrosini, S., Lüscher, T., Paneni, F., Costantino, S., 2020. Epigenetic Control of Mitochondrial Function in the Vasculature. Front. Cardiovascular Medicine, 7, 28. https://doi.org/10.3389/fcvm.2020.00028.

Moore, J.P., Farrant, J.M., Lindsey, G.G., Brandt, W.F., 2005. The South African and Namibian Populations of the Resurrection Plant *Myrothamnus flabellifolius* are Genetically Distinct and Display Variation in Their Galloylquinic Acid Composition. Journal of Chemical Ecology, 31, 2823–2834. https://doi.org/10.1007/s10886-005-8396-x.

Moore R.B., Obornik M., Janouskovec J., Chrudimsky T. VM, Green DH, Wright SW *et al.*, 2008. A photosynthetic alveolate closely related to apicomplexan parasites. Nature (Lond) 451:959–963.

Moore, J.P., Le, N.T., Brandt, W.F., Driouich, A., Farrant, J.M., 2009. Towards a systems-based understanding of plant desiccation tolerance. Trends in Plant Science 14, 110–117. https://doi.org/10.1016/j.tplants.2008.11.007

Morano K, Thiele D., 1999. Heat shock factor function and regulation in response to cellular stress, growth, and differentiation signals. Gene Expr. 7:271.

Morimoto, R.I., Tissieres, A., Georgopoulus, C., 1994. Progress and perspectives on the Progress and perspectives on the biology of heat shock proteins and molecular chaperones. 26: 1275–1286.

Mortensen, P., Gouw, J. W., Olsen, J. V., Ong, S. E. et al., 2009. MSQuant, an open source platform for mass spectrometry- based quantitative proteomics. J. Proteome Res., 9, 393–403.

Mowla, S. B., Thomson, J. A., Farrant, J. M., and Mundree, S. G., 2002. A novel stress in-ducible antioxidant enzyme identified from the resurrection plant *Xerophyta viscosa* Baker. Planta 215, 716–726. doi: 10.1007/s00425-002-0819-0.

Moyankova, D., Mladenov, P., Berkov, S., Peshev, D., Georgieva, D., & Djilianov, D., 2014. Metabolic profiling of the resurrection plant *Haberlea rhodopensis* during desiccation and recovery. Physiologia plantarum, 152(4), 675-687.

Mundree, S.G., Farrant, J.M., 2000. Some Physiological and Molecular Insights into the Mechanisms of Desiccation Tolerance in the Resurrection Plant *Xerophyta viscosa* Baker, in: Cherry, J.H., Locy, R.D., Rychter, A. (Eds.), Plant Tolerance to Abiotic Stresses in Agriculture: Role of

Genetic Engineering. Springer Netherlands, Dordrecht, pp. 201–222. https://doi.org/10.1007/978-94-011-4323-3_15.

Mundree S.G, Baker B., Mowla S., Peters S., Marais S., van der Willigen C., Govender K., Maredza A., Farrant J.M., Thomson J.A., 2002. Physiological and molecular insights into drought tolerance. African Journal of Biotechnology 1, 28-38.

Nakashima K, Yamaguchi-Shinozaki K., 2013. ABA signaling in stress-response and seed development. Plant Cell Reports, 32(7):959–70.

Nanjo, Y., Nouri, M.Z. and Komatsu, S., 2011. Quantitative proteomic analyses of crop seedlings subjected to stress conditions; a commentary. Phytochemistry, 72(10):1263-1272.

Narváez-Vásquez J., Florin-Christensen J., Ryan CA., 1999. Positional specificity of a phospholipase A activity induced by wounding, systemin, and oligosaccharide elicitors in tomato leaves Plant Cell., 11 1999, pp. 2249-2260.

Ndima, T., Farrant, J., Thomson, J., and Mundree, S., 2001. Molecular characterization of XVT8, a stress-responsive gene from the resurrection plant *Xerophyta viscosa* Baker. Plant Growth Regulation, 35, 137–145.doi:10.1023/A:1014433821730.

Neilson, K.A., Ali, N.A., Muralidharan, S., Mirzaei, M., Mariani, M., Assadourian, G., Lee, A., van Sluyter, S.C., Haynes, P.A., 2011. Less label, more free: Approaches in label-free quantitative mass spectrometry. Proteomics 11, 535–553. https://doi.org/10.1002/pmic.201000553.

Netzer, W.J., and Hartl, F.U., 1998. Protein folding in the cytosol: chaperonin-dependent and independent mechanisms. Trends in Biochemical Sciences., 23:68-73.

Nishiyama R, Watanabe Y, Leyva-Gonzalez MA, Van Ha C, Fujita Y, Tanaka M, *et al*., 2013. Arabidopsis AHP2, AHP3, and AHP5 histidine phosphor-transfer proteins function as redundant negative regulators of drought stress response. Proceedings of the National Academy of Sciences, U S A. 110(12):4840–5.

Nishizawa A., Yabuta Y., Shigeoka S., 2008. Galactinol and Raffinose Constitute a Novel Function to Protect Plants from Oxidative Damage. Plant Physiology, 147: 1251–1263. doi: 10.1104/pp.108.122465.

Noctor, G.; Foyer, C.H., 1998. Ascorbate and glutathione: keeping active oxygen under con-trol. Annual Review of Plant Physiology and Plant Molecular Biology, v.49, p.249-279, 1998.

Norwood M., Truesdale M., Richter A., Scott P., 2000. Photosynthetic carbohydrate metabolism in the resurrection plant *Craterostigma plantagineum*. Journal of Experimental Botany, 51 159–165 10.1093/jexbot/51.343.159.nutritional quality. Func. Plant Sci. Biotechnol. 2, 36–46.

Obata, T., Witt, S., Lisec, J., Palacios-Rojas, N., Florez-Sarasa, I., Araus, J.L., Cairns, J.E., Yousfi, S., Fernie, A.R., 2015. Metabolite profiles of maize leaves in drought, heat and combined stress field trials reveal the relationship between metabolism and grain yield. Plant Physiology pp.01164.2015. https://doi.org/10.1104/pp.15.01164.

Oikawa, A., Matsuda, F., Kusano, M., Okazaki, Y., and Saito, K., 2008. Rice metabolomics. Rice 1, 63–71. doi: 10.1007/s12284-008-9009-4.

Oliver, M. J., Wood, A. J., and O'Mahony, P., 1998. To dryness and beyond preparation for the dried state and rehydration in vegetative desiccation-tolerant plants. Plant Growth Regulation, 24, 193–201. doi: 10.1023/A:1005863015130.

Oliver M.J., 2007. Lessons on dehydration tolerance from desiccation-tolerant plants. In 'Plant desiccation tolerance'. (Eds MA Jenks, AJ Wood) pp. 11–50. (Blackwell: Ames, Iowa, USA).

Oliver, M.J., Cushman, J.C., Koster, K.L., 2010. Dehydration Tolerance in Plants, in: Sunkar, R. (Ed.), Plant Stress Tolerance, Methods in Molecular Biology. Humana Press, Totowa, NJ, pp. 3–24. https://doi.org/10.1007/978-1-60761-702-0_1.

Oliver, M. J., Guo, L., Alexander, D. C., Ryals, J. A., Wone, B. W., & Cushman, J. C., 2011a. A sister group contrast using untargeted global metabolomic analysis delineates the biochemical regulation underlying desiccation tolerance in *Sporobolus stapfianus*. The Plant Cell, 23(4), 1231-1248.

Oliver, M.J., Farrant, J.M., Hilhorst, H.W.M., Mundree, S., Williams, B., Bewley, J.D., 2020. Desiccation Tolerance: Avoiding Cellular Damage during Drying and Rehydration. Annu. Rev. Plant Biol. 71, annurev-arplant-071219-105542. https://doi.org/10.1146/annurev-arplant-071219-105542.

Ong, S. E., Blagoev, B., Kratchmarova, I., Kristensen, D. B. *et al.*, 2002. Stable isotope labelling by amino acids in cell culture, SILAC, as a simple and accurate approach to expression proteomics. Molecular Cell Proteomics, 1, 376–386.

Pandey V., Ranjan S., Deeba F., Pandey A. K., Singh R., Shirke P. A., et al., 2010. Desiccation-induced physiological and biochemical changes in resurrection plant, *Selaginella bryopteris*. J. Plant Physiology, 167, 1351–1359. 10.1016/j.jplph.2010.05.001

Parida, A., 2018. Advancement of Metabolomics Techniques and Their Applications in Plant Science: Current Scenario and Future Prospective.

Parsell, D.A., and Lindquist, S., 1993. The function of heat-shock proteins in stress proteins and molecular chaperones, Morimoto, R.I., Tissieres, A., Georgopoulos, C., eds., pp1-30. Cold Spring Harbor Laboratory Press, New York.

Parthasarathy, A., Savka, M.A., Hudson, A.O., 2019. The Synthesis and Role of β-Alanine in Plants. Front. Plant Science, 10, 921. https://doi.org/10.3389/fpls.2019.00921.

Patel S., Ahmed S., 2015. Emerging field of metabolomics: big promise for cancer biomarker identification and drug discovery. Journal of Pharmaceutical and Biomedical Analysis, 107:63–74.

Payne, S.H., 2015. The utility of protein and mRNA correlation. Trends in Biochemical Sciences 40, 1–3. https://doi.org/10.1016/j.tibs.2014.10.010.

Peng, B., Li, H., Peng, X.-X., 2015. Functional metabolomics: from biomarker discovery to metabolome reprogramming. Protein Cell 6, 628–637. https://doi.org/10.1007/s13238-015-0185-x.

Peshev D., Vergauwen R., Moglia A., Hideg E., Van den Ende W., 2013. Towards Understanding Vacuolar Antioxidant Mechanisms: A Role for Fructans? Journal of Experimental Biology, 64: 1025–1038. doi: 10.1093/jxb/ers377.

Peters S., Mundree S.G., Thomson J.A., Farrant J.M., Keller F., 2007. Protection mechanisms in the resurrection plant *Xerophyta viscosa* (Baker): both sucrose and raffinose family oligosaccharides (RFOs) accumulate in leaves in response to water deficit. Journal of Experimental Botany, 58, 1947–1956.

Phizicky, E., Bastiaens, P. I., Zhu, H., Snyder, M. and Fields, S., 2003. Protein analysis on a proteomic scale. Nature 422, 208- 215.

Poliakov, A., Russell, C. W., Ponnala, L., Hoops, H. J. *et al*., 2011. Large-scale label-free quantitative proteomics of the pea aphid-Buchnera symbiosis. Molecular Cell Proteomics, 10, 1– 17.

Porembski, S. and W. Barthlott., 2000. Granitic and gneissic outcrops (inselbergs) as centres of diversity for desiccation-tolerant vascular plants. Plant Ecology 151: 19–28.

Porembski, S., 2007. Tropical inselbergs: habitat types, adaptive strategies and diversity patterns. Brazilian Journal of Botany 30: 579–586.

Porra, R.J. 2002. The chequered history of the development and use of simultaneous equations for the accurate determination of chlorophylls a and b. Photosynthesis Research, 73: 149-156.

Radermacher, A.L., du Toit, S.F., Farrant, J.M., 2019. Desiccation-Driven Senescence in the Resurrection Plant *Xerophyta schlechteri* (Baker) N.L. Menezes: Comparison of Ana-tomical, Ultrastructural, and Metabolic Responses between Senescent and Non-Senescent Tissues. Front. Plant Science, 10, 1396. https://doi.org/10.3389/fpls.2019.01396.

Rai VK., 2002. Role of amino acids in plant responses to stresses. Journal of Plant Biology, 45(4):481–487. doi: 10.1023/A:1022308229759.

Ramanjulu S, Bartels D., 2002. Drought- and desiccation induced modulation of gene expression in plants. Plant, Cell and Environment, 25: 141.

Reddy, M.M., Ulaganathan, K., 2015. Nitrogen Nutrition, Its Regulation and Biotechnological Approaches to Improve Crop Productivity. American Journal of Political Science, 06, 2745–2798.

Reggiani R, Nebuloni M, Mattana M, Brambilla I., 2000. Anaerobic accumulation of amino acids in rice roots: role of the glutamine synthetase/glutamate synthase cycle. Amino Acids 18:207-217.

Reis, P. A. A. *et al.*, 2011. The binding protein BiP attenuates stress-induced cell death in soybean via modulation of the N-rich protein-mediated signalling pathway. Plant Physiology, 157, 1853–1865.

Renz A, Stitt M. 1993. Substrate specificity and product inhibition of different forms of fructokinases and hexokinases in developing potato tubers. Planta, 190, 166–175.

Rodrigues, S. P., Ventura, J. A., Aguilar, C., Nakayasu, E. S. *et al.*, 2012. Label-free quantitative proteomics reveals differentially regulated proteins in the latex of sticky diseased Carica papaya L. plants. Journal of Proteomics, 75, 3191– 3198.

Rodriguez, M. C., Edsgard, D., Hussain, S. S., Alquezar, D., Rasmussen, M., Gilbert, T., et al., 2010. Transcriptomes of the desiccation-tolerant resurrection plant *Craterostigma plantagineum*. Plant Journal, 63 (2), 212–228.

Rosa, M., Prado, C., Podazza, G., Interdonato, R., González, J.A., Hilal, M., Prado, F.E., 2009. Soluble sugars: Metabolism, sensing and abiotic stress: A complex network in the life of plants. Plant Signaling & Behavior, 4, 388–393. https://doi.org/10.4161/psb.4.5.8294.

Romero, L.C., Aroca, M.Á., Laureano-Marín, A.M., Moreno, I., García, I., Gotor, C., 2014. Cysteine and Cysteine-Related Signaling Pathways in Arabidopsis thaliana. Molecular Plant 7, 264–276. https://doi.org/10.1093/mp/sst168

Ross, P. L., Huang, Y. N., Marchese, J. N., Williamson, B. *et al*., 2004. Multiplexed protein quantitation in *Saccharomyces cerevisiae* using amine-reactive isobaric tagging reagents. Molecular and Cell Proteomics, 3, 1154–1169.

Roth, R.; Chiapello, M.; Montero, H.; Gehrig, P.; Grossmann, J.; O'Holleran, K.; Hartken, D.; Walters, F.; Yang, S.Y.; Hillmer, S.; *et al.* 2018. A rice Serine/Threonine receptor-like kinase regulates arbuscular mycorrhizal symbiosis at the peri-arbuscular membrane. Nature Communications, 9, 4677.

Ruan Y.L., 2014. Sucrose metabolism: gateway to diverse carbon use and sugar signalling. Annu Rev Plant Biol.; 65:33–67. https://doi.org/10.1146/annurev-arplant-050213-040251.

Ruan, J., Zhou, Y., Zhou, M., Yan, J., Khurshid, M., Weng, W., Cheng, J., Zhang, K., 2019. Jasmonic Acid Signaling Pathway in Plants. IJMS 20, 2479. https://doi.org/10.3390/ijms20102479.

Sairam RK, Rao KV, Srivastava G C., 2002. Differential response of wheat genotypes to long-term salinity stress in relation to oxidative stress, antioxidant activity and osmolyte concentra-tion. Plant Science, 163:1037-1046.

Sami F., Yusuf M., Faizan M., Faraz A., Hayat S., 2016. Role of sugars under abiotic stress. Plant Journal of Physiology and Biochemistry, 109:54–61. https://doi.org/10.1016/j.plaphy.2016.09.005.

Schiller P, Heilmeier H, Hartung W., 1997. Absisic acid (ABA) relations in the aquatic resurrection plant *Chamaegigas intrepidus* under naturally fluctuating environmental conditions. New Phytologist; 136: 603.

Schnarrenberger C. 1990. Characterization and compartmentation, in green leaves, of hexokinases with different specificities for glucose, fructose and mannose and for nucleoside triphosphates. Planta 181, 249–255.

Scott P., 2000. Resurrection plants and the secrets of eternal leaf. Annals of Botany; 85: 159.

Settembre E, Begley TP and Ealick SE., 2003. Structural biology of enzymes of the thiamine biosynthesis pathway. Current Opinion in Structural Biology, 13: 739–747.

Sharma S. Villamor JG. Verslues PE., 2011 Essential role of tissue-specific proline synthesis and catabolism in growth and redox balance at low water potential. Plant Physiology, 157:292–304.

Sharma, P., Jha, A.B., Dubey, R.S., Pessarakli, M., 2012. Reactive Oxygen Species, Oxidative Damage, and Antioxidative Defence Mechanism in Plants under Stressful Conditions. Journal of Botany, 217037. https://doi.org/10.1155/2012/217037.

Sharma, A.; Zheng, B., 2019. Melatonin mediated regulation of drought stress: Physiological and molecular aspects.Plants, 8, and 190

Shavrukov, Y., Kurishbayev, A., Jatayev, S., Shvidchenko, V., Zotova, L., Koekemoer, F., De Groot, S., Soole, K., & Langridge, P., 2017. Early flowering as a drought escape mechanism in plants: How can it aid wheat production? Frontiers in Plant Science, 1–8. https://doi.org/10.3389/fpls.2017.01950.

Shelp BJ, Bown AW, McLean MD., 1999. Metabolism and functions of gamma-aminobutyric acid. Trends Plant Science, 1999; 4:446–52.

Sherwin H.W. & Farrant J.M., 1996 Differences in rehydration of three desiccation-tolerant angiosperm species. Annals of Botany 78, 703–710.

Sherwin HW, Farrant JM., 1998. Protection mechanisms against excess light in the resurrection plants *Craterostigma wilmsii* and *Xerophyta viscosa*. Plant Growth Regulations; 24: 203.

Shivaraj, Y., Barbara, P., Gugi, B., Vicré-Gibouin, M., Driouich, A., Ramasandra Govind, S., Devaraja, A., Kambalagere, Y., 2018. Perspectives on Structural, Physiological, Cellular, and Molecular Responses to Desiccation in Resurrection Plants. Scientifica 2018, 1–18. https://doi.org/10.1155/2018/9464592.

Shulaev V, Diego Cortes, Gad Miller, and Ron Mittler., 2008. Metabolomics for Plant Stress Response. Physiologia Plantarum 132(2):199–208.

Simó, C., Ibáñez, C., Valdés, A., Cifuentes, A., and García-Cañas, V., 2014. Metabolomics of genetically modified crops, International Journal of Molecular Sciences, 15, 18941-18966. doi: 10.3390/ijms151018941.

Smirnoff N., 1993. The role of active oxygen in the response of plants to water deficits and desiccation. New Phytology 125, 27–58.

Smirnoff N., 1995. Antioxidant system and plant responses, In: Smirnoff N. (ed) Environ-ment and Plant metabolism: Flexibility and Acclimation, Bios Scientific Publishers, Oxford. pp. 217-243.

Sousa, C.A.F. de, Sodek, L., 2002. The metabolic response of plants to oxygen deficiency. Braz. J. Plant Physiology. 14, 83–94. https://doi.org/10.1590/S1677-04202002000200002.

Stoop, J. M. H., Williamson, J. D., & Pharr, D. M., 1996. Mannitol metabolism in plants: a method for coping with stress. Trends in Plant Science, 1, 139-144. https://doi.org/10.1016/s1360-1385 (96) 80048-3.

Suguiyama, V. F., da Silva, E. A., Meirelles, S. T., Centeno, D. D. C., & Braga, M.R. , 2014. Leaf metabolite profile of the Brazilian resurrection plant *Barbacenia purpurea* Hook. (Velloziaceae) shows two time-dependent responses during desiccation and recovering. Frontiers in Plant Science, 5, 96.

Szymanska, E., E. Saccenti, AK. Smilde, and JA. Westerhuis, 2012. "Double-Check: Validation of Diagnostic Statistics for PLS-DA Models in Metabolomics Studies." Metabolomics 8 (1, 1):3–16. http://dx.doi.org/10.1007/s11306-011-0330-3.

Tabuchi M, Abiko T, Yamaya T., 2007. Assimilation of ammonium ions and reutilization of nitrogen in rice (Oryza sativa L.). J Exp Bot.; 58:2319–27.

Taiz L, Zeiger E, 2006. Plant Physiology (4th Edn), Sinauer Associates, Massachusetts, 690 pp.

Tanaka, R., Oster, U., Kruse, E., Rüdiger, W., Grimm, B., 1999. Reduced Activity of Geranyl-geranyl Reductase Leads to Loss of Chlorophyll and Tocopherol and to Partially Geranylgeranylated

Chlorophyll in Transgenic Tobacco Plants Expressing Antisense RNA for Geranylgeranyl Reductase. Plant Physiology. 120, 695–704. https://doi.org/10.1104/pp.120.3.695.

Thimm, O., Blasing, O., Gibon, Y., Nagel, A., Meyer, S., Kruger, P., Selbig, J., Muller, L.A., Rhee, S.Y. and Stitt, M., 2004. MAPMAN: a user-driven tool to display genomics data sets onto diagrams of metabolic pathways and other biological processes. The Plant Journal. 37(6):914-939.

Trudgian DC, Ridlova G, Fischer R *et al.,* 2011. Comparative evaluation of label-free SINQ normalized spectral index quantitation in the central proteomics facilities pipeline. Proteomics 11:2790–2797.

Tsai, T.-H., Wang, M., Ressom, H.W., 2016. Pre-processing and Analysis of LC-MS-Based Proteomic Data, in: Jung, K. (Ed.), Statistical Analysis in Proteomics. Springer New York, New York, NY, pp. 63–76. https://doi.org/10.1007/978-1-4939-3106-4_3.

Tshabuse, Freedom, Jill M. Farrant, Lydie Humbert, Deborah Moura, Dominique Rainteau, Christophe Espinasse, Abdelghani Idrissi, *et al.,* 2018. Glycerolipid Analysis during Desiccation and Recovery of the Resurrection Plant Xerophyta humilis (Bak) Dur and Schinz. Plant Cell and Environment41 (3): 533–47. https://doi.org/10.1111/pce.13063.

Tuba, Z., Lichtenthaler, H.K., 2011. Ecophysiology of homoiochlorophyllous and poikilo-chlorophyllous desiccation-tolerant and vegetations. In U Lüttge, E Beck, D Bartels, eds, Plant Desiccation Toler. Springer Berlin Heidelberg, Berlin, Heidelberg, pp 157plants–183.

Tuberosa, R., and Salvi, S., 2006. Genomics-based approaches to improve drought tolerance of crops. Trends Plant Science, 11, 405–412. doi: 10.1016/j.tplants.2006.06.003.

Tunc-Ozdemir, M., Miller, G., Song, L., Kim, J., Sodek, A., Koussevitzky, S., Misra, A.N., Mit-tler, R., Shintani, D., 2009. Thiamin Confers Enhanced Tolerance to Oxidative Stress in Arabidopsis. Plant Physiology, 151, 421–432. https://doi.org/10.1104/pp.109.140046.

Tymms M.J., Gaff D.F., 1978. Proline accumulation during water stress in resurrection plants, Journal of Experimental Botany, vol. 30, pg. 165-168.

Ullah, A., Manghwar, H., Shaban, M., Khan, A.H., Akbar, A., Ali, U., Ali, E., Fahad, S., 2018. Phytohormones enhanced drought tolerance in plants: a coping strategy. Environmental Science and Pollution Research, 25, 33103–33118. https://doi.org/10.1007/s11356-018-3364-5.

UNDP. Transforming our world: The 2030 agenda for sustainable development. New York, USA: United Nations, 2015.

Usadel, B., Nagel, A., Thimm, O., Redestig, H., Blaesing, O.E., Palacios-Rojas, N., Selbig, J., Hannemann, J., Piques, M.C., Steinhauser, D., Scheible, W.-R., Gibon, Y., Morcuende, R., Weicht, D., Meyer, S. and Stitt, M., 2005. Extension of the visualization tool MapMan to allow statistical analysis of arrays, display of corresponding genes, and comparison with known responses. Plant Physiology. 138(3):1195-1204.

Usadel, B., Poree, F., Nagel, A., Lohse, M., Czedik-Eysenberg, A., Stitt, M., 2009. A guide to using MapMan to visualize and compare Omics data in plants: a case study in the crop species, Maize. Plant, Cell & Environment 32, 1211–1229. https://doi.org/10.1111/j.1365-3040.2009.01978.x.

van Agthoven, M.A., Lam, Y.P.Y., O'Connor, P.B., Rolando, C., Delsuc, M.-A., 2019. Two-dimensional mass spectrometry: new perspectives for tandem mass spectrometry. European Biophysics Journal, 48, 213–229. https://doi.org/10.1007/s00249-019-01348-5.

VanBuren, R., Wai, C.M., Ou, S., Pardo, J., Bryant, D., Jiang, N., Mockler, T.C., Edger, P., Michael, T.P., 2018. Extreme haplotype variation in the desiccation-tolerant clubmoss *Selaginella lepidophylla*. Nature Communications, 9: 13.

Vander Willigen C, Pammenter CNW, Jaffer MA, Mundree SG, Farrant JM., 2003. An ultrastructural study using anhydrous fixation of *Eragrostis nindensis*, a resurrection grass with both desiccation-tolerant and sensitice tissues. Functional Plant Biology 2003; 30: 10 10.

Vanderschuren, H., Lentz, E., Zainuddin, I. and Gruissem, W., 2013. Proteomics of model and crop plant species: Status, current limitations and strategic advances for crop improvement. Journal of Proteomics. 93(0):5-19.

Velasco, R., Salamini, F., and Bartels, D., 1994. Dehydration and ABA increase mRNA levels and enzyme activity of cytosolic GAPDH in the resurrection plant *Craterostigma plantagineum*. Plant Molecular Biology, 26, 541–546.doi: 10.1007/BF00039567.

Verbruggen, Hermans, 2008. Proline accumulation in plants: a review Amino Acids, 35, pp. 753-759.

Vertucci, C. W., and Farrant, J. M., 1995. "Acquisition and loss of desiccation-tolerance," in Seed Development and Germination, eds J. Kigel and G. Galili (New York: Marcel Dekker), 237–271.

Vicré M., 2001. Cell Wall Involvement in Desiccation Tolerance in the Resurrection Plant *Craterostigma wilmsii*. PhD Thesis, University of Cape Town, South Africa.

Vicré, M., Farrant J. M., and Driouich D., 2004. Insights into the Cellular Mechanisms of Desiccation Tolerance among Angiosperm Resurrection Plant Species. Plant, Cell and Environment 27(11):1329–40.

Vogel, C., Marcotte, E.M., 2012. Insights into the regulation of protein abundance from proteomic and transcriptomic analyses. Nature Reviews Genetics, 13, 227–232. https://doi.org/10.1038/nrg3185.

Voss-Fels, K.P., Stahl, A., Hickey, L.T., 2019. Q&A: modern crop breeding for future food security. BMC Biology, 17, 18. https://doi.org/10.1186/s12915-019-0638-4.

Wagstaff, C.; Leverentz, M.K.; Griffiths, G.; Thomas, B.; Chanasut, U.; Stead, A.D.; Rogers, H.J., 2002. Cysteine protease gene expression and proteolytic activity during senescence of Alstroemeria petals. Journal of Experimental Botany, 53, 233–240.

Walch-Liu P, Liu L-H, Remans T, Tester M, Forde BG., 2006. Evidence that L-glutamate can act as an exogenous signal to modulate root growth and branching in Arabidopsis thaliana. Plant Cell Physiology, 47:1045–57.

Walford SA, Thomson JA, Farrant JM, Mundree SG, et al., 2003. The HSP90 family of chaperones: a look at the structure, function and mode of action. Current Topics in Plant Biology, 4:1–25.

Walters, L., D. Wade, and D. Lewis, 2002. Transition to nuclear/hydrogen energy system. The Nuclear Engineer, 43, (6), 169-175.

Wang C, Yang A, Yin H, Zhang J. 2008. Influence of water stress on endogenous hormone contents and cell damage of maize seedlings. Journal of Integrative Plant Biology, 50:427–434.

Wang X, Chen S, Zhang H, Shi L, Cao F, Guo L, *et al*., 2010. Desiccation tolerance mechanism in resurrection fernally *Selaginella tamariscina* revealed by physiological and proteomic analysis. Journal Proteome, 3; 9:6561–7.

Wani, S.H., Kumar, V., Shriram, V., Sah, S.K., 2016. Phytohormones and their metabolic engineering for abiotic stress tolerance in crop plants. The Crop Journal 4, 162–176. https://doi.org/10.1016/j.cj.2016.01.010.

Wasternack C., Strnad M., 2016. Jasmonate signalling in plant stress responses and development–active and inactive compounds. New Biotechnology, 25, 604–613. 10.1016/j.nbt.2015.11.001.

Watanabe, M., Balazadeh, S., Tohge, T., Erban, A., Giavalisco, P., Kopka, J., *et al.*, 2013. Comprehensive Dissection of Spatiotemporal Metabolic Shifts in Primary, Secondary, and Lipid Metabolism during Developmental Senescence in Arabidopsis. Plant Physiology, 162 (3), 1290–1310. doi: 10.1104/ pp.113.217380.

Whittaker A., Bochicchio A., Vazzana C., Lindsey G., Farrant J., 2001. Changes in leaf hexokinase activity and metabolite levels in response to drying in the desiccation-tolerant species *Sporobolus stapfianus* and *Xerophyta viscosa*. Journal of Experimental Botany, 52 961–969 10.1093/jexbot/52.358.961.

Wiese A, Gröner F, Sonnewald U, Deppner H, Lerchl J, Hebbeker U, Flügge U-I, Weber A. 1999. Spinach hexokinase I is located in the outer envelope membrane of plastids. FEBS Letters, 461, 13–18.

Williams, B., Njaci, I., Moghaddam, L., Long, H., Dickman, M. B., Zhang, X., and Mundree, S., 2015. Trehalose accumulation triggers autophagy during plant desiccation. PLoS Genetics 11: e1005705. doi: 10.1371/journal.pgen.1005705.

Wilkinson, S., and Davies, W. J., 2002. ABA-based chemical signalling: the co-ordination of responses to stress in plants. Plant, Cell and Environment, 25, 195–210. doi: 10.1046/j.0016-8025.2001.00824.x

Winzor, C.L., Winzor, D.J., Paleg, L.G., Jones, G.P. and Naidu, B.P., 1992. Rationalization of the effects of compatible solutes on protein stability in terms of thermodynamic nonideality. Archives of Biochemistry and Biophysics. 296: 102–107.

Xiong, Y., DeFraia, C., Williams, D., Zhang, X., & Mou, Z., 2009. Deficiency in a cytosolic ribose-5-phosphate isomerase causes chloroplast dysfunction, late flowering and premature cell death in Arabidopsis. Physiologia Plantarum, 137, 249–263.

Yamaguchi K, Subramanian AR., 2000. The plastid ribosomal proteins. Identification of all the proteins in the 50 S subunit of an organelle ribosome (chloroplast). Journal of Biology and Chemistry .September 15; 275 (37):28466-82. doi: 10.1074/jbc.M005012200. PMID: 10874046.

Yang, Vanderbeld, Wan, Huang, 2010. Narrowing down the targets: towards successful genetic engineering of drought-tolerant crops, Molecular Plant, pp. 469.

Yang, L., Fountain, J.C., Ji, P., Ni, X., Chen, S., Lee, R.D., Kemerait, R.C., Guo, B., 2018. Deciphering drought-induced metabolic responses and regulation in developing maize kernels. Plant Biotechnology journal, 16, 1616–1628. https://doi.org/10.1111/pbi.12899.

Yobi A,Wone BWM, Xu W, Alexander DC, Guo L, et al. 2012. Comparative metabolic profiling between desiccation-sensitive and desiccation-tolerant species of *Selaginella* reveals insights into the resurrection trait. Plant Journal, 72:983–99.

Yobi, A., Batushansky, A., Oliver, M.J., Angelovici, R., 2019. Adaptive responses of amino acid metabolism to the combination of desiccation and low nitrogen availability in *Sporobolus stapfianus*. Planta 249, 1535–1549. https://doi.org/10.1007/s00425-019-03105-6

Yoo, H., Widhalm, J.R., Qian, Y., Maeda, H., Cooper, B.R., Jannasch, A.S., Gonda, I., Lewinsohn, E., Rhodes, D., Dudareva, N., 2013. An alternative pathway contributes to phenylalanine biosynthesis in plants via a cytosolic tyrosine: phenylpyruvate aminotransferase. Nature Communications, 4, 2833. https://doi.org/10.1038/ncomms3833.

Yoshiba, Y., Kiyosue, T., Nakashima, K., Yamaguchi-Shinozaki, K., Shinozaki, K., 1997. Regulation of Levels of Proline as an Osmolyte in Plants under Water Stress. Plant and Cell Physiology, 38, 1095–1102. https://doi.org/10.1093/oxfordjournals.pcp.a029093.

Yu SM., 1999. Cellular and genetic responses of plants to sugar starvation. Plant Physiology, 121:687–693.

Zhang, Cui, LI, Wei, and Kirkham, 1995. Protoplasmic factors, antioxidant responses, and chilling resistance in maize. Plant Physiology and Biochemistry, 33, 567-575.

Zhang J, Shen H, XuW, Xia Y, Barr DB, Mu X, Wang X, Liu L, Huang Q, Tian M., 2014. Urinary metabolomics revealed arsenic internal dose-related metabolic alterations: a proof-of-concept study in a Chinese male cohort. Environmental Science & Technology, 48:12265–12274.

Zhang, Q., Song, X., Bartels, D., 2016. Enzymes and Metabolites in Carbohydrate Metabolism of Desiccation Tolerant Plants. Proteomes 4, 40. https://doi.org/10.3390/proteomes4040040.

Zhang Q, Bartels D. 2018. Molecular responses to dehydration and desiccation in desiccation-tolerant angiosperm plants. Journal of Experimental Botany, 69:3211–22.

Zivkovic T., Quartacci M. F., Stevanovic B., Marinone F., Navari-Izzo F., 2005. Low-molecular weight substances in the poikilohydric plant Ramonda serbica during dehydration and rehydration. Plant Science, 168 105–111 10.1016/j.plantsci.2004.07.018.